2019

Surface elevation dynamics across a range of timescales in coastal wetlands of south-eastern Australia

Kirti Kamna Lal
University of Wollongong

UNIVERSITY
OF WOLLONGONG
AUSTRALIA

Surface elevation dynamics across a range of timescales in coastal wetlands of south-eastern Australia

Kirti Kamna Lal

Supervisors:

Kerrylee Rogers, Colin Woodroffe and Carla Bonetti

This thesis is presented as part of the requirement for the conferral of the degree:

Doctor of Philosophy

University of Wollongong

School of Earth, Atmospheric and Life Sciences

August 2019

Abstract

Coastal wetlands are dynamic ecosystems that are threatened by climate change, particularly sea-level rise. Consequently, there is an urgent need to understand the response of coastal wetlands to sea-level rise and apply this knowledge to planning and management. The aim of this thesis is to investigate surface elevation dynamics in coastal wetlands of south-eastern Australia across a range of timescales. The influence of tides on processes contributing to surface elevation change was examined over annual to decadal timescales using the surface elevation table and marker horizon technique (SET-MH). The rate of sediment accumulation in relation to sea-level rise over the past century was quantified using ^{210}Pb dating methods. The distribution of benthic foraminiferal assemblages was examined in surface sediment samples, and this modern analogue was used to reconstruct palaeo-wetland surface elevation and vegetation changes occurring over millennial timescales.

On Comerong Island, deep-rod SETs were paired with shallow-rod SETs and MHs to differentiate processes of mineral sediment accumulation on the surface (vertical accretion) from belowground processes (e.g. such as root additions, decomposition of organic materials, autocompaction and consolidation of substrate) occurring within the shallow substrate and at greater depths. Surface elevation change did not equal vertical accretion, and this was attributed to belowground processes. However, surface elevation change was related to tidal inundation frequency with surface elevation gain greater at mid tidal positions where inundation frequency was higher, negligible at intermediate tidal positions that had a lower inundation frequency, and surface elevation loss was measured at high tidal positions where inundation frequency was low. At the mid tidal positions where mangrove dominate, processes operating in the shallow and deep substrate, such as root addition by mangrove, contributed to surface elevation gain of 4.3 ± 2.0 mm/y was beyond vertical accretions of 2.1 ± 1.7 mm/y. At high tidal positions, little detectable surface elevation change (-1.2 ± 1.4 mm/y) was observed despite

considerable vertical accretion (3.6 ± 0.45 mm/y), which was primarily related to shallow and deep zone autocompaction. In the intermediate tidal positions, shallow zone autocompaction offset vertical accretion resulting in very little change in surface elevation.

The relationship between surface elevation change and tidal inundation frequency at Comerong Island was relatively consistent with the decadal SET-MH study undertaken at Minnamurra River, Cararma inlet and Currambene Creek. At mid tidal positions at Minnamurra River and Cararma Inlet that had higher inundation frequency and where mangrove dominate, mean surface elevation gain of 1.3 ± 0.31 mm/y and 1.9 ± 0.25 mm/y was observed, respectively. Currambene Creek exhibited a different pattern whereby the mid tidal positions were increasing surface elevation at a negligible rate (0.089 ± 0.076 mm/y), which may have been associated with belowground decomposition exceeding rates of organic and mineral sediment additions. Vertical accretion could only be measured for more than a few years in saltmarsh vegetation located at intermediate to high tidal positions. At these intermediate to high tidal positions, vertical accretion directly contributed to an equivalent degree of surface elevation gain (1.2 ± 0.28 mm/y) at Cararma Inlet. Belowground substrate change (-0.44 ± 0.088 mm/y) was offsetting low rates of vertical accretion (0.28 ± 0.078 mm/y) resulting in surface elevation loss at Currambene Creek. Vertical accretion (0.55 ± 0.69 mm/y) may have been contributing to low rate of surface elevation gain (0.52 ± 0.070 mm/y) at Minnamurra River despite negligible rates of belowground substrate change (-0.13 ± 0.69 mm/y). Annual and decadal scale SET-MH measurements indicated that organic matter addition makes an important contribution to surface elevation gain, particularly at tidal position where mangrove is encroaching upon saltmarsh.

Sedimentation rates over decadal to centurial timescales were higher at lower tidal position (1.3 – 2.5 mm/y) where mangrove dominate and there is more vertical space for sediment accumulation than at high tidal positions in the saltmarsh (0.62 – 1.6 mm/y). Sedimentation rates were greater at Comerong Island where

sediments were sourced from the Shoalhaven River catchment (~7000 km^2) in comparison with Cararma Inlet, which had the smallest catchment areas (~7 km^2). Mangrove sedimentation rates exceeded the rate of relative sea-level rise over the past century of 1.0 ± 0.093 mm/y (derived from Fort Denison tide gauge record 1914-2017), whilst saltmarsh accumulated sediments at rates comparable to sea-level rise. This study demonstrated that sediment supply is crucial if coastal wetlands are to maintain their position within a tidal frame that is influenced by sea-level rise.

Spatial distribution of living and dead benthic foraminiferal assemblages provided a suitable proxy for reconstructing palaeo-depositional environments; however, gaps in foraminiferal data in cores limited the application of transfer function models for palaeo-wetland surface elevation reconstructions. Sixteen dominant taxa in modern samples, comprising the most common species found in all study sites, were categorised in a regional training set. Foraminiferal associations based on cluster analysis corresponded to vegetation communities and position in the tidal frame where the *Miliammina – Quinqueloculina* association dominated in mangrove substrates lower in the tidal frame, whilst *Entzia – Trochammina* association dominated in saltmarsh substrates higher in the tidal frame. Consequently, wetland elevation relative to mean sea level was applied as the principal environmental variable in transfer function models. Down-core foraminiferal analysis showed that subtidal and/or lower intertidal positions transitioned to mangrove and subsequently to saltmarsh at higher elevations over the past few millennia.

Surface elevation gain and sedimentation rates were generally found to be greater beneath mangrove than in saltmarsh, irrespective of timescale of analysis. Whilst there is considerable variability both within and between study sites at annual to decadal timescales, sedimentation patterns in mangrove and saltmarsh became increasingly consistent between sites at decadal to centurial timescales. These observations form the foundation for future modelling that is crucial for projecting

the vertical and lateral response of coastal wetlands to anticipated sea-level rise and will assist with management of coastal wetlands.

Acknowledgments

I would like to express my sincere gratitude to Associate Professor Kerrylee Rogers for her constant support, guidance and assistance with this thesis. I very much appreciate the expertise, time and effort that she has dedicated to my research project as well as her patience and faith in me, without which this PhD would not have come to completion. We worked on this project as a team and I am grateful for her initiative in overcoming many of the hurdles along the way.

I would also like to express my heartfelt appreciation to Professor Colin Woodroffe for his assistance and constructive criticism with this project and the quick feedback on my draft chapters. Thank you for your time, expertise and enthusiasm in managing the broad topics of my thesis and valuable assistance in bringing them all together. Many thanks to my third supervisor, Dr Carla Bonetti for her assistance and guidance with benthic foraminiferal analysis and identification.

I would also like to express my heartfelt appreciation to several staff, colleagues and friends in the School of Earth, Atmospheric and Life Sciences (former SEES) for their assistance and guidance, especially with my fieldwork. Special thanks to Brent Peterson for his assistance with fieldwork and surface elevation table installations at Comerong Island. He made many of the tasks possible that would otherwise have been impossible on my own. I would also like to thank other members of the school; Jose Abrantes, John Morrison and Heidi Brown for their professional assistance with sediment and geospatial laboratory related needs I have had throughout the course of my PhD. Thanks to Atun Zawadzki, Patricia Gadd, Jack Goralewski, Brodie Cutmore, Daniela Fierro at the Australian Nuclear Science and Technology Organisation (ANSTO) for their help in ^{210}Pb analysis and advice on interpreting the results.

Special thanks to Christopher Owers for the laughs in the wetlands (and cores we did not need) and the amazing adventure we had in Darwin (poor kangaroo – may its soul rest in peace). A hearty thanks you for the friendship and assistance during

numerous fieldwork (in no particular order) to; Sara Brandolese, Martin Struck, Natasha Phillips, Emma Asbridge, Jessica Welsh, Madeline May, Rafaela Maria, Yvonne Ellis, Maria Schaarschmidt, Kristian Kumbier, Catherine Bowie, and Tsu-You Pan. Not forgetting Varsha Natrajan for lending her ear and the sneaky beers at the unibar.

I owe a lot to my family especially my parents, Vinod and Subhag Lal. Things were difficult with me being away from home, but they held strong and gave me all the love and support I needed to complete this chapter of my life. Special thanks to my sisters, Arti V. and Arti A., and brother-in-law's Arvind and Amitesh for taking such diligent care of my parents back home and paying me regular visits when I needed love and support. Special reference to my nieces, Arishta and Aruhi for their beautiful smiles, chatter and warm hugs when we were near.

Finally, a big thank you to Lukas Bauer. Breakfast at Berry's was an inexpensive bribe to lure you into the wetlands with me for data collection and you did it so chivalrously. Thanks for the constructive criticism, being a great companion, keeping up with the mood swings and suffering the PhD with me. Thank you for existing! This would not have been possible without you.

Certification

I, Kirti Kamna Lal, declare that this thesis submitted in fulfilment of the requirement for the conferral of the degree Doctor of Philosophy, from the University of Wollongong, is wholly my own work unless otherwise referenced or acknowledged. This document has not been submitted for qualifications at any other institute.

_____

Kirti Kamna Lal

20th August 2019

List of Names or Abbreviations

AHD	Australian height datum
ANOVA	Analysis of Variance
ANSTO	Australia's Nuclear Science and Technology Organisation
^{14}C	Radiocarbon
^{137}Cs	Caesium-137
cal BP	Calibrated ^{14}C age
CCA	Canonical correspondence analysis
CIC	Constant initial concentration
CRS	Constant rate of supply
DCA	Detrended canonical analysis
DEM	Digital elevation model
HAT	highest astronomical tide
HHWSS	High high-water solstices springs
LiDAR	Light detection and ranging
MH	Marker horizon
MSL	Mean sea level
MTL	Mean tidal level
HWS	Mean high water
^{210}Pb	Lead-210
p-value	Probability value
PVC	Polyvinyl chloride
r^2	Coefficient of determination
RMSE	Root mean square of error
RMSEP	Root mean square error of prediction
rSET	Rod surface elevation table
RTK-GPS	Real-time kinematic global positioning system
SE	Surface elevation
SEC	Surface elevation change
SET	Surface elevation table
SLR	Sea-level rise
STPI	Standardised Tidal Position Index
VA	Vertical accretion
WA	Weighted averaging
WA_Inv	Weighted averaging, inverse deshrinking
WA-PLS	Weighted averaging partial least squares
WA-TOL	Weighted averaging tolerance downweighted
WA-TOL_Inv	Weighted averaging tolerance downweighted, inverse deshrinking

Table of Contents

List of Figures and Illustrations

Chapter 1

Chapter 2

Chapter 4

Chapter 5

List of Tables

Chapter 1

Chapter 2

Chapter 3

Chapter 4

Chapter 5

Chapter 6

Chapter 7

Chapter 1

Introduction

Coastal wetlands occur at the dynamic interface between the land and the sea, and are typically vegetated communities comprising mangroves, saltmarshes and seagrasses. Many stressors may influence their behaviour and condition because they occur in the coastal zone, where development pressures are high. Climate change adds a new dimension to these stressors, with sea-level rise (SLR) in particular increasing the elevation at which tidal inundation occurs (Adam, 2009; Laegdsgaard et al., 2009; Saintilan and Rogers, 2013). Consequently, SLR is projected to influence the distribution of coastal wetlands and there is an urgent need to understand their response to sea-level changes (Gilman et al., 2008; Rogers et al., 2017). Fortunately, there is an archive of information stored within coastal wetland substrates that can be explored to consider past responses of coastal wetlands to sea-level variation.

This study focuses on describing the response of the upper portion of the intertidal zone that supports mangroves and saltmarshes, henceforth termed coastal wetlands, to sea-level changes across a range of timescales. In south-eastern Australia, the focal area of this study, saltmarshes extend up to highest astronomical tide (HAT), whilst mangroves are typically limited to elevations near mean sea level and grade into saltmarshes on their landward margin (Fig. 1.1). In this region, mangrove are typically dominated by the cold tolerant *Avicennia marina*, whilst saltmarsh forms as mosaics of grasses, sedges, rushes and succulents (Clarke et al., 1995; Rogers et al., 2006).

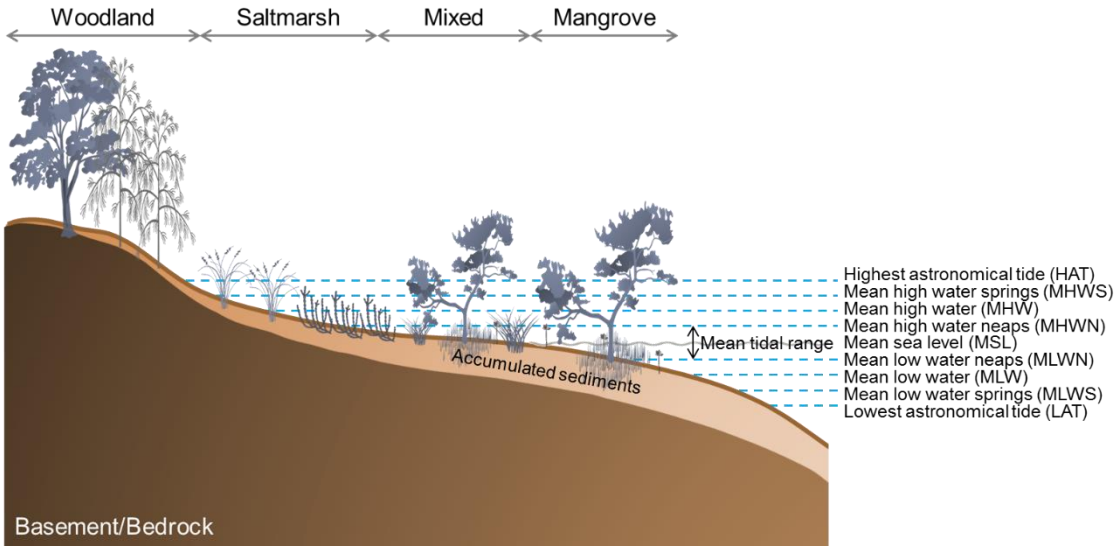

Figure 1.1: Schematic of a typical coastal wetland vegetated by both mangrove and saltmarsh with tidal limits in south-eastern Australia.

Coastal wetlands provide a distinct ecosystem dominated by halophytic plants that protect the shoreline from wave action, reduce the impact of storms and floods, and improve water quality by absorbing pollutants. In recent decades there has been an increasing appreciation of the ecosystem services provided by coastal wetlands including their carbon sequestration capabilities (Barbier et al., 2011; Chmura et al., 2003; Friess et al., 2016; Guo et al., 2009; Howe et al., 2009; Marchio et al., 2016; Rogers et al., 2019a; Saintilan et al., 2013a; Sanders et al., 2010b). The rapid loss of wetland vegetation, particularly due to climate induced SLR, reinforces the importance of assessing the value of coastal wetlands and managing them appropriately in coastal management and planning. As climate change continues to intensify, there is an urgent need for the proper evaluation of coastal wetland services. This will require an effective regional legislative and local-level planning measures to explicitly recognise their services within policy and legislation (Laegdsgaard et al., 2009; Rogers et al., 2016).

1.1. Response of coastal wetlands to sea level

Mangrove and saltmarsh exhibit zonation across the tidal frame that corresponds to tidal inundation patterns; they are, therefore, particularly susceptible to changes

in sea level change as it alters the elevation at which inundation occurs, in which case coastal wetlands must respond accordingly (Fig. 1.2a). The response of coastal wetlands to SLR is dependent upon the relationship between sediment accumulation and tidal inundation frequency. Coastal wetlands can either maintain their elevation within the tidal frame by; (i) increasing substrate elevations through mineral and organic matter accumulations that can promote vertical adjustment of the wetland surface to SLR (Fig. 1.2b); or (ii) translating to higher elevations (Allen, 2000; Cahoon et al., 2000a; Kirwan and Temmerman, 2009; McFadden et al., 2007; Rogers et al., 2013a) (Fig. 1.2c). In the absence of mineral and organic sediment supply, coastal wetlands may become increasingly susceptible to SLR. They can succumb to increased inundation and eventually drowning when tolerance thresholds of the vegetation to inundation and salinity are exceeded (Ball, 1988; Woodroffe et al., 2016) (Fig. 1.2d). Drowning of wetland vegetation is also linked to 'coastal squeeze' where landward translation is limited by tidal impediments, such as buildings, roads and steep geomorphology (Torio and Chmura, 2013; Woodroffe et al., 2014) (Fig. 1.2d).

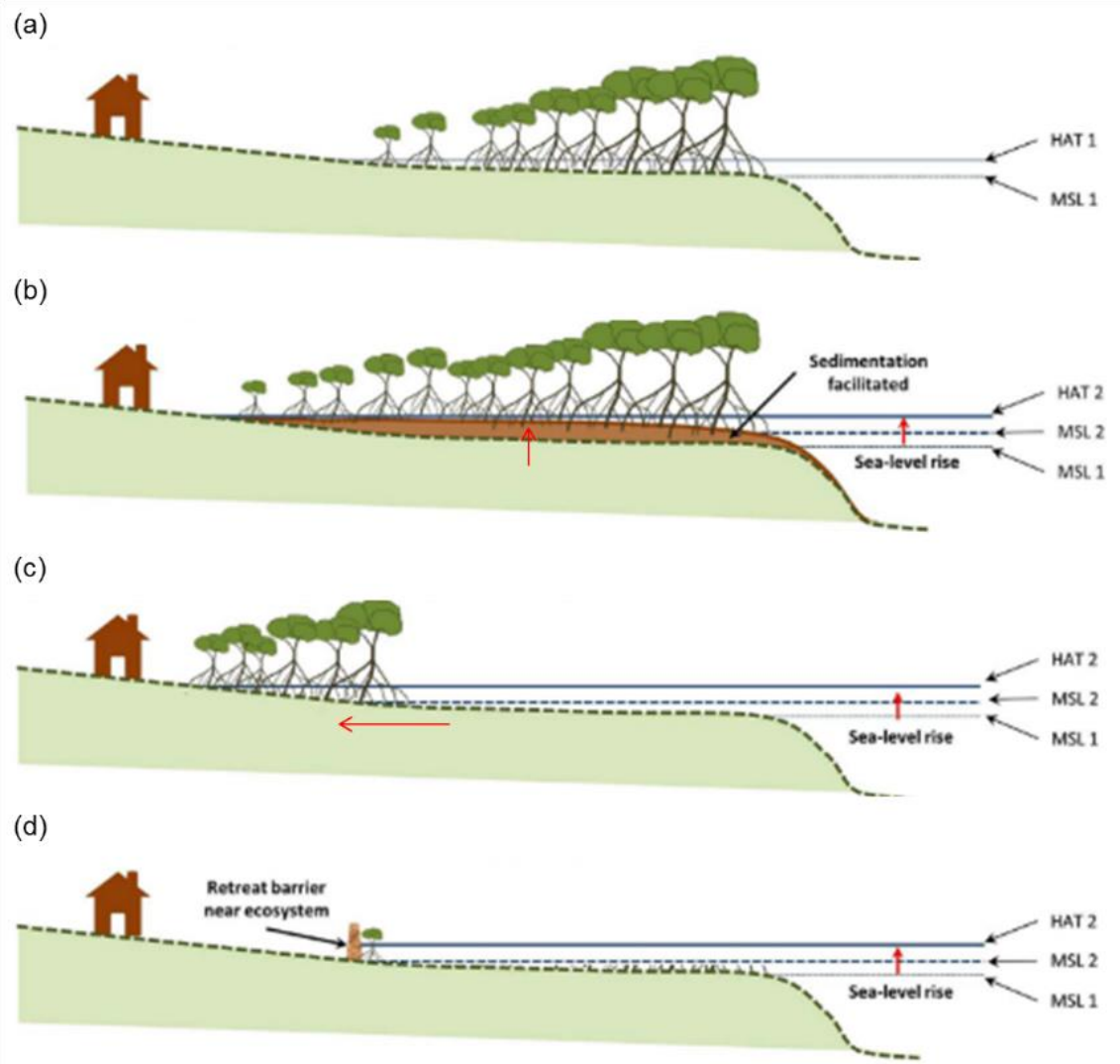

Figure 1.2: Illustrations showing (a) Mangrove and saltmarsh are distributed and their response to sea level rise by (b) increasing substrate elevations; (c) retreating to higher elevation if there are no barriers present; or (d) drowning (adapted from Rogers et al. (2016)).

Mineral and organic sediment supply is therefore crucial for coastal wetlands to adjust to SLR (Allen, 2000; Kirwan and Megonigal, 2013; Krauss et al., 2014; Lovelock et al., 2011; McKee et al., 2007; Mcleod et al., 2011; Rogers et al., 2019a). However, it is not just mineral and organic matters additions but belowground processes, such as decomposition and loss of biomass, sediment shrink/swell and consolidation also has a considerable influence surface elevation dynamics and the capabilities of coastal wetlands to adjust to SLR (Cahoon et al., 2003; Krauss et al., 2014; Lovelock et al., 2015a; McKee et al., 2007; Rogers and Saintilan, 2008;

Whelan et al., 2005). Understanding the relationship between above and belowground processes contributing to surface elevation gain and relative SLR is crucial when gauging the response of coastal wetlands to future SLR.

1.2. Coastal wetland accommodation space

Accommodation space is a term developed by sedimentary geologists to define the space available for mineral and organic matter accumulation to occur along the coast (Jervey, 1988). It integrates the influence of tidal range and wetland position within the tidal frame, which provides a useful framework for considering the response of coastal wetlands to SLR (Kirwan and Guntenspergen, 2010). Accommodation space, however, is restricted by three boundary conditions. These include bedrock or basement geology, sea level that is defined by highest tidal limit (e.g. HAT), and zone where hydrodynamic energy favours sediment deposition rather than transportation (Rogers et al., 2019a). Some of the available accommodation space becomes realised as sediments accumulate, and the available accommodation space diminishes over time (Fig. 1.3). SLR acts to increase available accommodation space by creating vertical and lateral space for the continuation of mineral and organic matter accumulation (Kirwan and Megonigal, 2013; Krauss et al., 2014; Rogers et al., 2019a; Schuerch et al., 2018a).

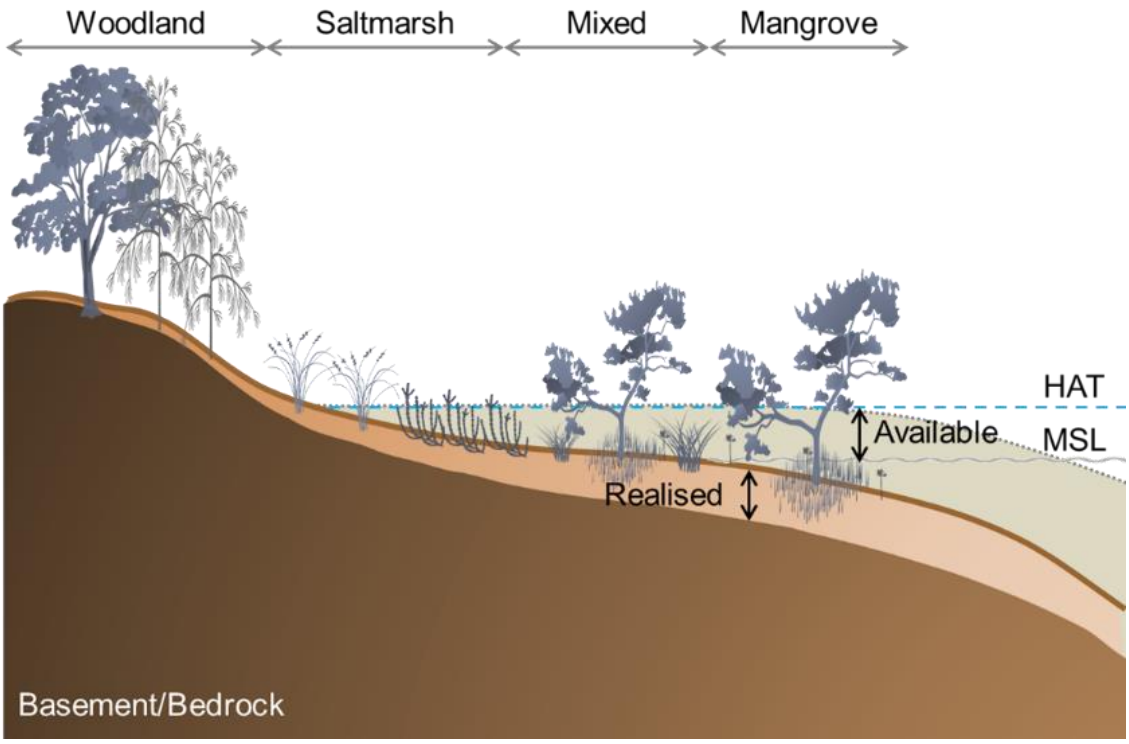

Figure 1.3: Coastal wetland realised, and available accommodation space defined by the highest astronomical tides and mean sea level.

Realised accommodation space is influenced by changes to the boundary conditions, such as eustatic SLR, deep subsidence, tectonism, and hydrological changes along estuaries. Inland wetland migration inhibited by coastal infrastructure and coastal squeeze can also reduce available accommodation space (Mills et al., 2015; Torio and Chmura, 2013). Relationships between wetland accommodation space and sediment accumulation under stable sea level conditions can lead to coastal wetland stability. This is achieved through a negative feedback loop (Pethick, 1981; Saintilan et al., 2009). Sediment accumulation increases wetland surface elevation, which decreases the available accommodation space, thereby decreasing the inundation frequency; consequently, the supply of suspended sediments to wetland surface by tides diminishes, thus lowering sediment accumulation rates (Fig. 1.4).

The negative feedback loop may dismantle if sediment availability or the capacity of wetland vegetation to accumulate organic materials *in situ* exceed the threshold levels. In this situation, wetland elevations become too low in the tidal frame

where vegetation can no longer effectively accumulate sediments and start to lose elevation and drown as the surface will become too deep for vegetation to survive (Fagherazzi et al., 2012).

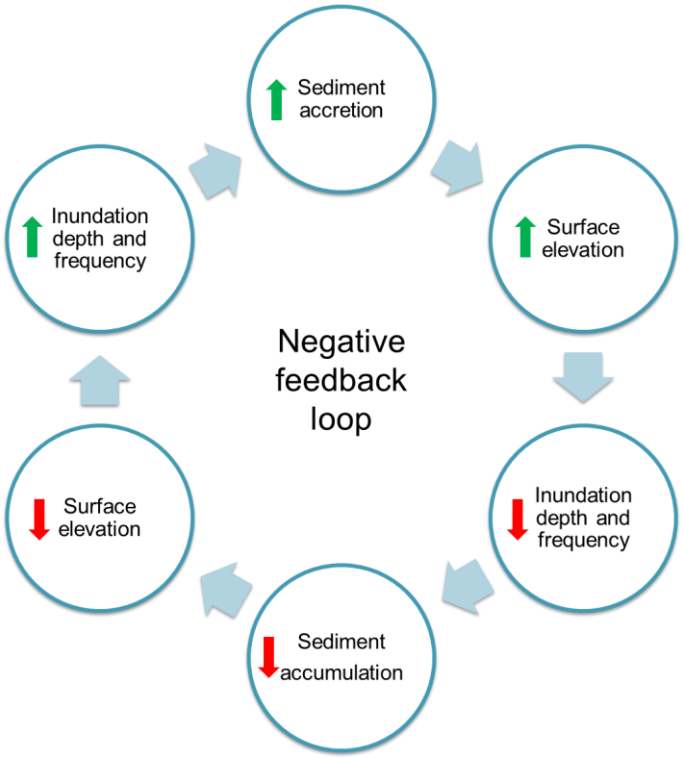

Figure 1.4: Relationships between accommodation space, sedimentation and wetland elevation in a coastal wetlands (adapted from Saintilan et al. (2009)).

1.3. Changing accommodation space over time

Quantifying changes in accommodation space over time, based on relationships between sediment accumulation rates and wetland elevation dynamics and SLR is a means of quantifying changes in vegetation position within a tidal frame, including both vertical increases and lateral expansion (Allen, 2000, 1999; Rogers et al., 2019a; Schuerch et al., 2018b). This can be measured across a range of spatial and temporal scales (Fig. 1.4). Extrapolating this over longer geological and historical timescales comprise evolution processes operating over many fluctuations in boundary conditions. At this timescale, processes responsible for sediment transport can be seen in the form of estuary infill and progradation of

mangrove forests (Woodroffe, 2018a).

At the event scales, processes operate across time spans ranging from that of a single event, such as storms through to seasonal variations. They operate over annual to decadal timescales. For example, storms can lead to episodic sediment erosion and deposition, and slow landward migration of mangroves as tidal inundation patterns change (Kelleway et al., 2016; Rogers et al., 2006, 2005b; Saintilan et al., 2009; Saintilan and Williams, 1999). The instantaneous timescale includes contemporary processes involving the evolution of wetland morphology during a single cycle. This can be regulated by primary forcing agents, such as wave and tides, which can directly relate to physical processes of sediment transportation and deposition, such as particle settling (Cowell and Thom, 1994). These sedimentation rates and rate of surface elevation change can be determined using a range of methods over different timescales (Fig. 1.5).

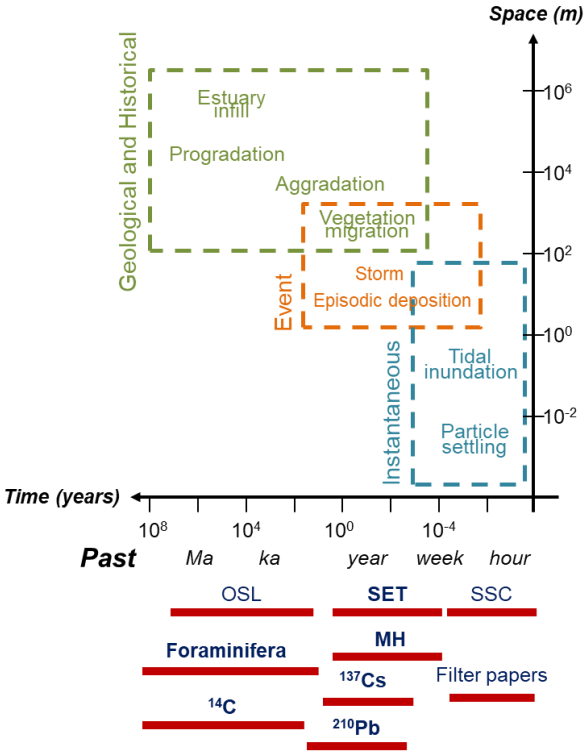

Figure 1.5: An overview of spatial and temporal scale processes in coastal wetlands and techniques that can be used to measure the evolutionary processes occurring at a range of timescales. Techniques in bold were applied in this thesis (adapted from Woodroffe and Murray-Wallace (2012)).

Geological and historical events can be determined using different dating techniques, such as radiocarbon dating (^{14}C) of organic materials applied in this study, and optically stimulated luminescence dating (OSL) of quartz sediments (Walker, 2005). Such reconstructions from coastal wetlands are useful in obtaining longer-term sedimentation rates ranging across decadal to millennial timescales. Benthic foraminiferal assemblages can be used as a proxy for past environmental conditions. Other types of radiometric dating, such as lead dating (^{210}Pb) and caesium dating (^{137}Cs) is applied in this study is used to obtain sediment accumulation rates in coastal wetlands over decades to centurial timescales (Appleby and Oldfield, 1992; Ivanovich and Harmon, 1982; Walker, 2005).

Surface elevation tables (SETs), formerly called the sedimentation-erosion table (Boumans and Day, 1993), which was developed from the sedi-eros table was developed to measure elevation of exposed mudflats during low tides in the Netherlands (Schoot and De Jong, 1982), and provide yearly to decadal rates of surface elevation change in coastal wetlands (Cahoon et al., 2000b). Vertical accretion rates from feldspar marker horizons (MH), typically used in conjunction with SETs, can be used to differentiate vertical accretion from belowground processes, such as root additions, decomposition of organic materials, autocompaction and consolidation of substrate. Other techniques that can be used to measure vertical accretion but were not used in this study include filter papers that are placed on the wetland surface (Reed 1989). Sediments that accumulated on the filter paper are measured by drying and weighing to determine the rate of sediment accumulation. Suspended sediment concentration (SSC) contributing to surface elevation gain can be measured by taking water samples at the beginning and end of tidal cycles, where the collected water samples are usually filtered, dried and weighed to determine sedimentation rates (Kirwan et al., 2010; Nolte et al., 2013).

1.4. Influence of sea-level rise on accommodation space across timescales

Over the past century, advances in science and innovation has enhanced our understanding of spatial and temporal variability of global mean sea level records at historical timescales (thousands of years) (Chappell and Shackleton, 1986; Cuffey and Vimeux, 2001; Long, 2001; Milne, 2014; Murray-Wallace and Woodroffe, 2014; Pirazzoli, 1991). Sea-level histories of different coastlines has been recognized through geophysical models, geomorphological and geological records of shorelines, beaches, and marine terraces (Cann et al., 1988; Chappell et al., 1996; Pirazzoli, 1991). The last known record of sea level being the lowest was during the Last Glacial Maximum (ca. 22,000–20,000 years ago) when sea level was about 125 m below present levels (Fleming et al., 1998; Murray-Wallace et al., 1996). Rising temperatures triggered the melting of ice sheets and sea levels started to increase across the globe, increasing to about 120 m around 8500 years ago. The Holocene sea level and marine transgression is one of the driving factors for the geomorphological evolution and development of the coastal wetlands we see today. Sea level reached a high-stand about 7500 years ago before stabilising (Lambeck, 2002; Lewis et al., 2013; Long, 2001; Sloss et al., 2007). The time of the mid-Holocene high-stand varied along different coastlines due to relative glacio-hydro-isostatic adjustment processes, the vertical movement of the Earth's crust due to ice offloading (Lambeck and Nakada, 1990). Along south-eastern coastline of Australia, the Holocene sea-level curve derived by Sloss et al. (2007) indicates that sea level may have been between +1 and +1.5 m above present levels between 7700 and 7400 years ago, which lasted for about 2000 years before gradually falling to present levels (Fig. 1.6).

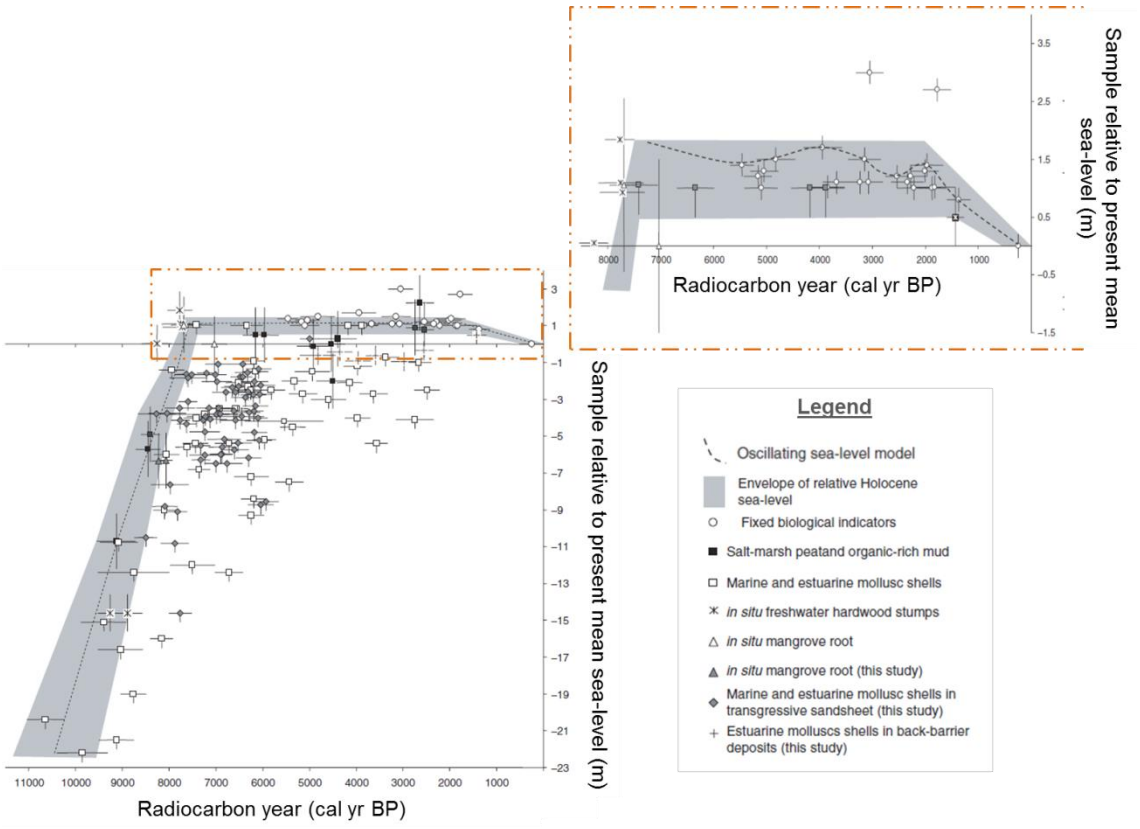

Figure 1.6: Holocene sea-level curve for the southeast Australian coastline. Dates are based on radiocarbon ages and aspartic acid racemization-derived ages (Sloss et al., 2007).

Currently, sea level is rising due to anthropogenic global warming, with global mean sea level increasing by approximately 210 mm from January 1880 to December 2009 (Church and White, 2011). This was largely associated with increasing global temperatures and ice melts, and thermal expansion of the oceans, with the former having a greater contribution to global SLR (Church et al., 2004). Various techniques, such as tide gauges and satellite altimetry (since 1993) have been used to observe variations in sea level over the past century. Sea level data from the two longest tide-gauge records at Sydney (1886 – 2010) and Fremantle (1897 – 2010) showed that sea level increased at relatively high rates in the 1940s, remained relatively stable between 1960 and 1990, before accelerating once more in the early 1990s (White et al., 2014). The satellite altimeter record indicates that the volume of the oceans remains constant, but there have been distribution changes with time, largely influenced by the movement of atmospheric pressure cells and oceanic currents across the Pacific Ocean (Church and White, 2011).

There were significant step changes in the rates of SLR around the Australian coastline where SLR occurred at a rate of 1.4 ± 0.3 mm/y between 1966 and 2009 and 4.5 ± 1.3 mm/y between 1993 and 2009 (White et al., 2014). The recent rate of SLR for Australia is markedly higher than the global sea level trends over the same time periods was estimated at 2.0 ± 0.3 mm/y from tide gauges and 3.4 ± 0.4 mm/y from satellite altimetry (White et al., 2014). This discrepancy has arisen from variability in historical tide gauge records within the Indo-Pacific region due to inter-annual fluctuations in sea level related to El Niño Southern Oscillation (ENSO) events (Church et al., 2006). However, when ENSO and glacial isostatic adjustment were accounted for, the Australian sea level trend for the period 1993 – 2009 was about 2.1 ± 0.2 mm/y and 3.1 ± 0.6 mm/y, which corresponded to global-mean sea level trends.

Sea level is anticipated to continue increasing over the twenty-first century (IPCC, 2014). Global scale projections have demonstrated that in response to future SLR, coastal wetlands can gain up to 60 % of their current area provided they have sufficient accommodation space, and sediment supply remains at present levels (Schuerch et al., 2018b). Feedbacks between plant growth and geomorphology can assist coastal wetlands to actively adapt to the adverse effects of SLR (Kirwan and Megonigal, 2013). Inland wetland migration may be inhibited by coastal infrastructure that reduces the available accommodation space (Mills et al., 2015; Torio and Chmura, 2013). Removing barriers that inhibit the lateral expansion of wetland vegetation may create additional accommodation space for coastal wetlands. Implementation of nature-based adaptation and coastal management can also increase the capacity of coastal wetlands to adapt to SLR (Temmerman et al., 2013). As sea level is never stable and varies over time, analyses of the response of coastal wetlands to sea level change must occur across a range of timescales. This is a crucial data requirement prior to developing generalisations about the response of coastal wetlands to accelerating SLR (Adame et al., 2010; Breithaupt et al., 2018; Woodroffe et al., 2016).

1.5. Thesis rationale

Coastal wetlands provide a range of ecosystem services and it is highly contested as to how they will respond to future SLR. Improved assessment strategies will provide a greater confidence and better understanding of the relationship between coastal wetland surface elevations and SLR. This information can then be incorporated into models and accommodated within plans, policy and management. Empirical data on the rates of surface elevation adjustment across a range of timescales therefore provides crucial information for conceptualising the response of coastal wetlands to SLR.

1.6. Aims and Objectives

The aim of this thesis is to quantify surface elevation dynamics within coastal wetlands of south-eastern Australia across a range of timescales. This was achieved by:

1. Investigating the influence of tides on processes contributing to surface elevation gain over a two-year period;
2. Establishing relationships between surface elevation, vertical accretion, and belowground processes over approximately two decades;
3. Quantifying sediment accumulation rates relative to the rate of SLR over the past century; and
4. Reconstructing environmental conditions and palaeo-wetland surface elevations over the past few millennia using a foraminifera-based regional training set.

1.7. Study region and sites

Four barrier estuaries along the New South Wales coast in south-eastern Australia were selected in this study. They have been classified as wave-dominated barrier

estuaries described to be at a mature stage of infilling (Roy, 1984; Roy et al., 2001). They occur between latitudes of 34.63 to 35.05 °S, namely Minnamurra River, Comerong Island, Cararma Inlet and Currambene Creek (Fig. 1.7). These sites were selected because three of them (Minnamurra River, Cararma Inlet and Currambene Creek) have existing surface elevation tables (SETs) as this study builds on the surface elevation change dynamics work undertaken by Rogers et al. (2006).

At all study sites, sediment infilling has been occurring within each estuary behind the sandy barrier at the estuary entrance, which creates low energy conditions suitable for sediment deposition and wetland development. The temperate climate and geomorphic similarity between study sites that supports both mangrove and saltmarsh vegetation in the upper intertidal zones that are confined to the estuaries and not exposed to the open coast. Within the intertidal frame, mangroves typically occur at lower elevations, while saltmarsh are present at higher elevations (Saintilan et al., 2009). The two species of mangroves present are *Avicennia marina* and *Aegiceras corniculatum*. Saltmarsh vegetation replaces mangroves around mean high water levels and the ecotonal zone has the species *Sueada australis*, and *Tecticornia* (formerly *Sclerostegia*) *arbuscula* (Clarke et al., 1995). Saltmarsh areas reached by only spring tides are dominated by *Sarcocornia quinqueflora*, *Samolus repens*, *Sporobolus virginicus*, and *Wilsonia backhousei*, while at the upper intertidal limits *Juncus kraussii* and *Baumea juncea* occur. The woodland area between the upper tidal limits and non-tidal zones has *Melaleuca ericifolia* on the sandy soils together with swamp oak, *Casuarina glauca* (Clarke et al., 1995; Rogers et al., 2006).

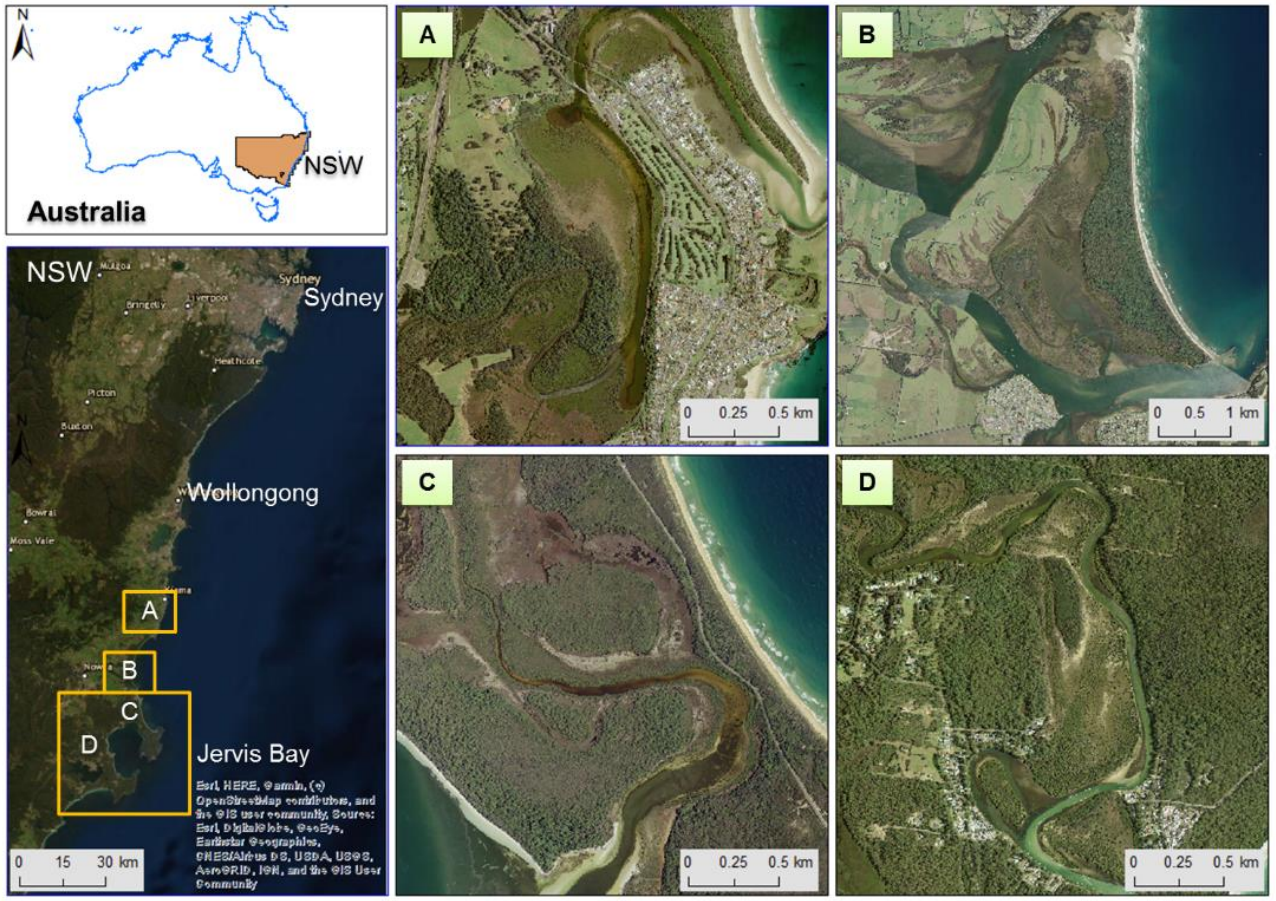

Figure 1.7: Maps created in ArcMap showing the location of the study sites along the south-eastern coastline of Australia; (A) Minnamurra River, (B) Comerong Island, (C) Cararma Inlet, and (D) Currambene Creek.

1.7.1. Study sites

Although the study sites are geomorphologically similar and microtidal (tidal range of about 2 m), they differ in catchment size. The northern-most site occur adjacent to Minnamurra River, which has a catchment size of 117 km^2 and is a mature barrier estuary that has infilled its central mud basin creating extensive alluvial plans and floodplains that now support large areas of mangrove and saltmarsh (Panayotou et al., 2007) (Table 1.1). The Minnamurra River coastline is embayed and experiences an energetic wave climate that has resulted in a series of sand barriers between the prominent headlands (Fig. 1.7). In 2011, Minnamurra River catchment was reported to have about 0.9 km^2 of mangrove and 0.3 km^2 of saltmarsh (Roper et al., 2011).

Table 1.1: Catchment area of the study sites (adapted from (Roper et al., 2011)).

Study site	Area (km^2)		
	Catchment size	Mangrove	Saltmarsh
Minnamurra River	117	0.879	0.327
Comerong Island (Shoalhaven River)	7086	4.180	2.058
Cararma Inlet	7	0.993	1.089
Currambene Creek	160	0.943	0.266

Comerong Island is located at the mouth of the Shoalhaven River, which is part of the Shoalhaven Estuary and has largest catchment area of 7086 km^2 (Fig. 1.7). Comerong Island formed after the construction of the Berry's canal in 1822 that diverted the fluvial base flows so that water exited at Crookhaven Heads. The deposition of fluvial sediments at the southern end of Comerong Island provides ideal habitat for wetland vegetation, shorebirds and waders and in 1986 was declared a Nature Reserve by the NSW National Parks and Wildlife Service (Chafer, 1998a; NPWS, 1998). An advanced version of SET known as the deep and shallow rod-surface elevation tables (rSETs) were installed at Comerong Island for the first time on the Island as the wetland vegetation established recently on the Island. This was done to quantify annual-scale surface and subsurface processes that

influence surface elevation dynamics in coastal wetland vegetation.

Cararma Inlet and Currambene Creek both drain into Jervis Bay (Fig. 1.7). Cararma Inlet is the smaller of the two catchments having a catchment area of about 7 km^2 and has a higher proportion of saltmarsh (1.1 km^2) to mangrove (0.99 km^2). The major source of sediment delivery into the catchment is from Jervis Bay. Cararma Inlet was disconnected from the sea by formation of the Beecroft barrier, inhibiting the deposition of wave-dominated sediments to the system (Taylor et al., 1995). Currambene Creek provides a significant amount of freshwater into Jervis Bay as it is the largest creek draining into the Bay, having a catchment area of about 160 km^2. In 2011 it was reported to have about 0.9 km^2 area of mangrove and 0.3 km^2 of saltmarsh.

1.8. Thesis Structure

This thesis has been prepared in the monograph format, consisting of five experimental chapters detailing original research carried out as part of this study (Chapters 2 – 6), and the general discussion and conclusion chapter (Chapter 7). Each experimental chapter contains a literature review section and a study site and design section providing necessary information for the context of the experiment.

Chapter 2 specifically deals with objective one of this thesis where the effect of tidal inundation on surface elevation dynamics was investigated using the shallow and deep-rod-surface elevation table and marker horizon (rSET-MH) technique (Cahoon et al., 2002b) at Comerong Island over a 2-year study period. The shallow- and deep-rod SET-MH technique was used to differentiate short-term surface processes, such as vertical accretion from belowground processes occurring in the shallow zone from processes occurring deeper in the substrate and their effect on surface elevation dynamics in different tidal positions mangrove and saltmarsh vegetation.

In Chapter 3, surface elevation, vertical accretion, and autocompaction dynamics were investigated in different tidal positions dominated by either mangrove, saltmarsh or mixed mangrove and saltmarsh vegetation over approximately two decades. This was achieved by using and extending the surface elevation table and marker horizon (SET-MH) approach at existing study sites (Rogers et al., 2006).

Chapter 4 aimed to quantify sediment accumulation rates in mangrove and saltmarsh over the past century using the ^{210}Pb dating technique in relation to relative SLR over the longest tide gauge record in the southern Hemisphere located at Fort Denison in Sydney, Australia. ^{137}Cs radioisotope and rates of surface elevation change from SETs were used to validate sedimentation rates.

Chapter 5 characterises the spatial distribution and abundance of benthic foraminiferal assemblages in surficial samples from the four study sites to develop a regional training set. This model was used to interpret past environmental conditions in Chapter 6, which addresses objective four of this thesis. Palaeo-environmental and wetland surface reconstruction was based on two techniques; foraminifera-based clusters and transfer function models.

Chapter 7 provides an overall synthesis of processes occurring at annual-, decadal-, centurial-, and millennial-timescales, determined from the techniques mentioned above, that contribute to surface elevation dynamics in coastal wetlands of south-eastern Australia. It is anticipated that this information would improve our capacity to connect processes influencing wetland elevation changes with the response of coastal wetlands to sea-level rise and improve the capacity to accommodate wetlands and the ecosystem services they provide within plans, policy and management.

Chapter 2

Surface elevation dynamics in coastal wetland vegetation over annual timescales

2.1. Introduction

Coastal wetlands are dynamic ecosystems that are constantly changing because of their proximity to the sea. Tides have an important short-term influence on wetland substrate and vegetation distribution in upper intertidal zones. For instance, in south-eastern Australia, the lower elevation zone of the upper intertidal zone is dominated by mangroves that are inundated for longer periods, whilst the higher position that has a lower inundation frequency are dominated by saltmarsh. Tides influence mineral sedimentation and vegetation distribution across the upper intertidal zone, and accordingly, also influences organic matter addition from vegetation as well as subsurface processes that are hydrologically influenced, such as organic matter de composition and shrink-swell of substrates (Cahoon et al., 2011, 1995; Cahoon and Lynch, 1997; Ford et al., 1999; McKee et al., 2012). Processes, such as vertical accretion (VA), autocompaction and belowground substrate compaction and/or consolidations of materials also contribute to the changes in surface elevation (SE) relative to mean sea level. Surface elevation dynamics in coastal wetland vegetation is therefore related to tidal inundation and sea-level variability over different time periods. As sea-level rise (SLR) will influence tidal propagation and inundation frequency across the wetland surface, it is important to understand short-term variabilities in surface elevation to conceptualise the influence of SLR on surface elevation change.

The aim of this chapter was to investigate the influence of tides on processes contributing to surface elevation gain in coastal wetlands of SE Australia dominated by mangrove and saltmarsh. This chapter specifically focussed on

processes that operate over short time scales, including mineral and organic matter addition at the surface and within the root zone, and substrate shrink-swell. In addition, as this chapter focussed on processes, it intentionally analysed surface elevation changes over a 2-year time period. The specific objectives of this chapter were to;

i. Quantify the variable position of the wetland substrate within the tidal frame by analysing inundation patterns;
ii. Investigate deep and shallow surface elevation change, and vertical accretion in different tidal positions using deep- and shallow-rod surface elevation tables (rSETs) and marker horizons (MHs);
iii. Identify belowground processes contributing to surface elevation dynamics, including total, shallow and deep autocompaction;
iv. Examine belowground substrate characteristics of the different tidal positions;
v. Establish relationships between surface elevation dynamics, vertical accretion, belowground processes (total, shallow and deep autocompaction) and substrate characteristics in different tidal positions; and
vi. Establish relationship between SE change and wetland elevation as an indicator of the influence of inundation on SEC.

This chapter addresses and presents results of each objective. Central to this analysis was accounting for variation in tides across the intertidal zone. This was achieved by quantifying the position of the wetland substrate within the tidal frame in the form of tidal inundation frequency using water level loggers relative to the localised tidal datum. Deep and shallow-rSETs was used to establish deep and shallow surface elevation dynamics across the tidal frame. Marker horizons (MH) were used to quantify mineral sediment additions on the wetland surface. Specific attention was placed on processes operating at different depths including total, shallow and deep within wetland substrates influencing surface elevation

change. To account for the varying substrate depth (autocompaction) over which processes that influence surface elevation operate, deep-rSETs were couple with shallow-rSETs. Relationships between surface elevation dynamics, vertical accretion and autocompaction, and substrate characteristics, such as organic matter content and grainsize was established. Finally, to quantify the overall influence of tides on SE, relationships were established between spatial patterns of surface elevation change and wetland elevation as an indicator of position within the tidal frame.

2.2. Literature Review

2.2.1. Influence of position on the tidal frame

In upper intertidal coastal vegetation of south-east Australia exhibit vertical zonation across the tidal frame, where mangroves are typically limited to elevations near mean sea level (MSL), whilst saltmarsh extend up to the highest astronomical tide (HAT) (Fig. 1.1). This distribution pattern of mangrove and saltmarsh correspond to tidal inundation patterns (Rogers and Krauss, 2018; Saintilan and Rogers, 2013). Mangrove lower in the tidal frame have a higher inundation frequency than saltmarsh that are located higher in the tidal frame. Tides have a significant influence on sediment delivery and deposition within wetlands as established in numerous studies (Pethick, 1981; Rogers et al., 2012, 2005a). Relationships between inundation frequency and duration and sediment accumulation show that the longer a wetland surface is inundated the greater the time over which sediments can to settle in the wetland surface (Kirwan et al., 2016; Lovelock et al., 2011; Rogers et al., 2006). Tidal inundation regime and sediment accumulation has also been linked to vegetation growth, organic matter accumulation and substrate biomass within coastal wetlands that influence surface elevation dynamics in relation to relative sea-level conditions (McKee et al., 2012; Mudd et al., 2004; Rogers and Krauss, 2018; Temmerman et al., 2003).

2.2.2. Sediment dynamics in coastal wetlands

Sediment dynamics in coastal wetlands vary spatially and in response to sediment proximity, the tidal inundation regime, and the local wind-wave system (Pratolongo et al., 2009; Rogers and Woodroffe, 2014; Woodroffe, 2002). The type of sediments in coastal wetlands can range between organic (biotic) or mineral (abiotic) that can either be produced *in situ* (autochthonous) by the wetland vegetation or it can be supplied to the system through hydrological processes (allochthonous) (Cahoon et al., 2002b, 1999, 1995; Callaway et al., 2013).

Autochthonous organic inputs can influence sediment volume and/or sediment strength through the accumulation of decaying organic matter (like wrack and plant litter). Benthic mats (microbial, algal, and roots) can make the sediments resistant to compaction and erosion (Barbier et al., 2011; Cahoon, 2015; Cahoon et al., 2006; McKee, 2011). Algal and microbial mats are highly productive and can also promote vertical accretion and surface elevation gain in saltmarsh vegetation (McKee, 2011; Rogers and Woodroffe, 2014).

Allochthonous materials, derived from terrigenous sources, such as rivers and streams, and offshore marine sediments, transported to wetlands by waves and tides are particularly important for wetland vegetation growth and nutrient enrichment (Allen, 2000; Rogers and Woodroffe, 2014). Sediment supply to coastal wetlands can also be enhanced by anthropogenic processes, whereby wetlands adjacent to industrial or urban centres can accumulate materials, such as sewage and particulate industrial waste.

Mineral sedimentations can also be promoted by wetland vegetation acting as sediment traps (Cahoon and Guntenspergen, 2010). Tidal water containing suspended particles loses velocity as it passes through mangrove and saltmarsh. Aerial roots of mangrove plants, such as the pneumatophores of *Avicennia*, and dense saltmarsh vegetation are able to trap the suspended particles in the slow moving water, which can promote vertical accretion (Krauss et al., 2003; McKee et

al., 2007). Organisms living in the water or on the surface of the intertidal zone, such as, foraminifera and diatoms are also a source of mineral sediments on wetland surface (Allen, 2000).

In addition to mineral sediment delivery and deposition by tides to wetland surfaces, wetland vegetation also adds organic matter to surface and subsurface substrate (Cahoon et al., 2006; Kirwan and Megonigal, 2013; Lovelock et al., 2015a, 2011; McKee et al., 2007). Together mineral sediments and organic matter additions allow wetland elevations to increase with respect to rising water levels and contribute to stability (Cahoon et al., 1999; McKee et al., 2007; Rogers et al., 2013b). However, there are other processes occurring on the surface and belowground that can either promote or inhibit elevation change meaning that surface processes of mineral and organic matter accumulation do not convert directly to an increase in surface elevation. For example, above and belowground mineral and organic matter additions can increase substrate volume, whilst erosion, decomposition or bioturbation can remove sediments from the wetland, and belowground processes, such as autocompaction, consolidation of materials and sediment shrink can reduce substrate volume (Allen, 2000; Cahoon et al., 1995; Krauss et al., 2003; Lovelock et al., 2011; Mudd et al., 2004; Rogers and Woodroffe, 2014; Woodroffe et al., 2016). These processes influence the surface elevation dynamics of coastal wetlands in relation to SLR.

2.2.3. Surface elevation dynamics

The processes controlling coastal wetland surface elevation dynamics are complex and may be divided into geomorphic, biological and hydrological factors (Fig. 2.1). These processes operate in response to regional-scale climatic conditions, relative sea level change and geomorphology control surface elevation of coastal wetlands (Adam, 2009; Adame et al., 2010; Woodroffe et al., 2016). Climatic parameters, such as temperature, precipitation and storms events, long and short-term variations in sea level, and hydrodynamics can influence sediment supply and

substrate geochemical properties. Mangrove and saltmarsh, after establishment can develop surface elevation through vertical accretions but processes, such as autocompaction and consolidation of sediments can reduce substrate volume and decrease surface elevation. Autocompaction of mangrove and saltmarsh substrate occurs when sediment particles can no longer sustain their weight and collapse as sedimentation rates continue (Allen, 2000, 1999). Storm events have been recorded to increase the rate of autocompaction and decrease wetland elevation, even though new sediments are added on the surface (Cahoon et al., 1995).

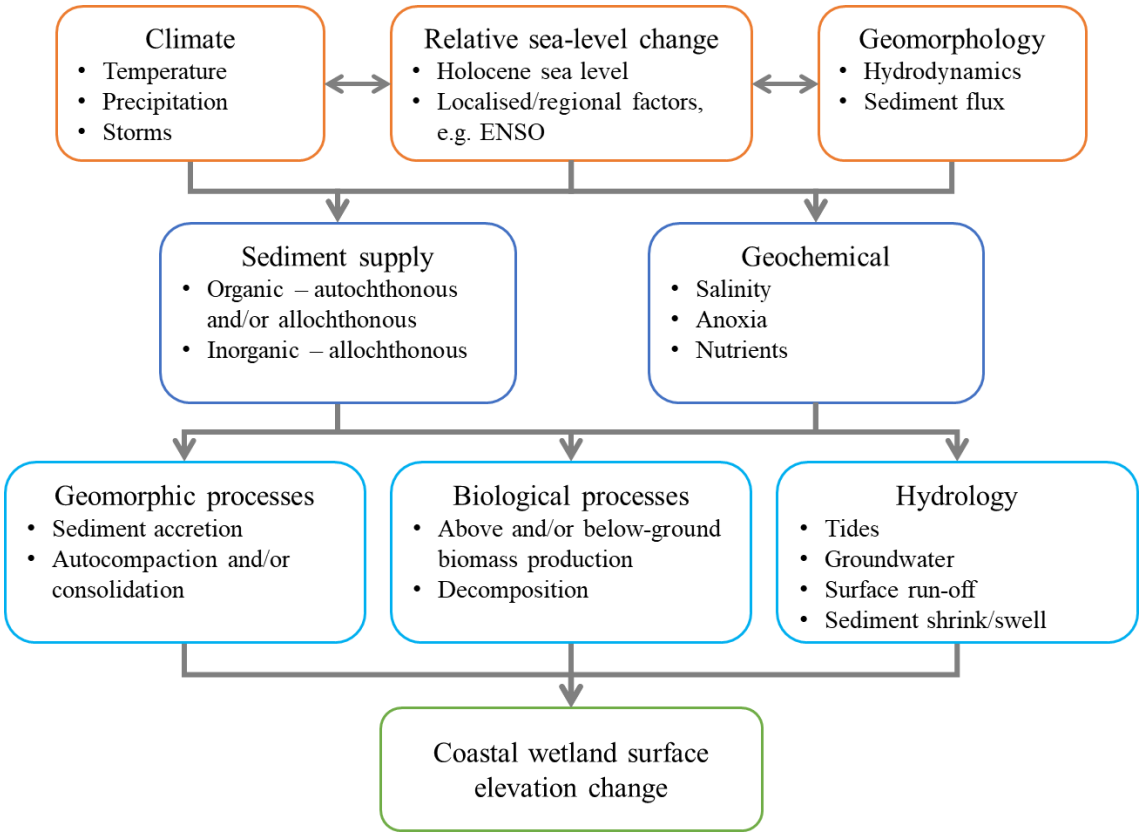

Figure 2.1: Conceptual model representing regional to site-specific interactions that influence coastal wetland surface elevation change.

Mangrove and saltmarsh can develop and gain surface elevation through primary production and increase substrate volume in belowground sediments through root growth, but processes, such as decomposition of biomass that reduce substrate volume and decrease wetland elevation (Cahoon et al., 2006; Lovelock et al., 2015a; McKee et al., 2012, 2007; Rogers and Woodroffe, 2014). Hydrological

properties, such as tides, groundwater, surface run-off and sediment shrink/swell properties also has a strong influence on surface elevation dynamics of coastal wetlands (Cahoon et al., 2011, 1995; Nuttle et al., 1990; Rogers and Saintilan, 2008; Whelan et al., 2005). Water in wetlands ecosystem is controlled by two storage mechanisms; saturation storage and dilation storage that regulate sediment shrink/swell properties (Cahoon et al., 2006; Nuttle et al., 1990). For instance, during the high tidal cycle, water infiltrates and increases the water storage capacity in belowground sediments swelling the substrate (Cahoon et al., 2006; Nuttle et al., 1990; Rogers and Saintilan, 2008). Sediment swell increases substrate volume displacing overlying sediments and increase surface elevation.

It has been established that vertical accretion does not always result in elevation gain (Kaye and Barghoorn, 1964). Consequently, there has been a need to identify belowground processes contributing to wetland surface elevation change over time. For coastal wetlands to maintain elevation with respect to SLR, the rate of sediment accumulation (both mineral and organic) must equal the decomposition, autocompaction and/or consolidation of materials in shallow and deep substrate (Kaye and Barghoorn, 1964). Autocompaction of belowground substrate can affect sedimentation rates by increasing accommodation space for more sediments to accumulate, thus allowing wetland surface to maintain elevation relative to SLR (Haslett et al., 1998).

Coastal wetlands have been reported to keep pace with SLR through the accumulation of sediments (both allochthonous and autochthonous) over longer timescales (Krauss et al., 2014; Saintilan et al., 2013a). Hydrodynamic models show that increased tidal inundation due to SLR will increase rates of mineral and organic sediment accretion on wetland surfaces (Fagherazzi et al., 2012; Kirwan et al., 2010; Kirwan and Guntenspergen, 2010; Temmerman et al., 2004, 2003). However, coastal wetland resilience to SLR is dependent on the relationship between wetland elevation change, sedimentation, and relative sea-level change.

As SLR imposes a threat to the sustainability of mangrove and saltmarsh

ecosystems, an accurate assessment of coastal vegetation response to SLR requires high resolution measurement of five important sediment profile characteristics as argued by Cahoon (2000b). These include the elevation change occurring in the top 1cm of the surface, the accumulation of small quantities of sediments on the surface (vertical accretion), rates of belowground change (commonly termed shallow subsidence) occurring in the zone 5 cm below the surface, rates of compaction of newly deposited sediments, and rates of compaction of the underlying sediments (Cahoon et al., 2000b). Surface elevation table (SET) was designed to provide high-resolution measures of small–scale (microscale) changes in elevation of loose, unconsolidated sediments in vegetated wetland ecosystems (Cahoon et al., 2002a, 2002b, 2000b; Lynch et al., 2015). The original SET was developed by Boumans and Day in 1993 (Fig. 2.2). The design was later modified to rod-SET (rSET) and largely promoted by Cahoon et al. (2002a) at the United States Geological Survey (USGS).

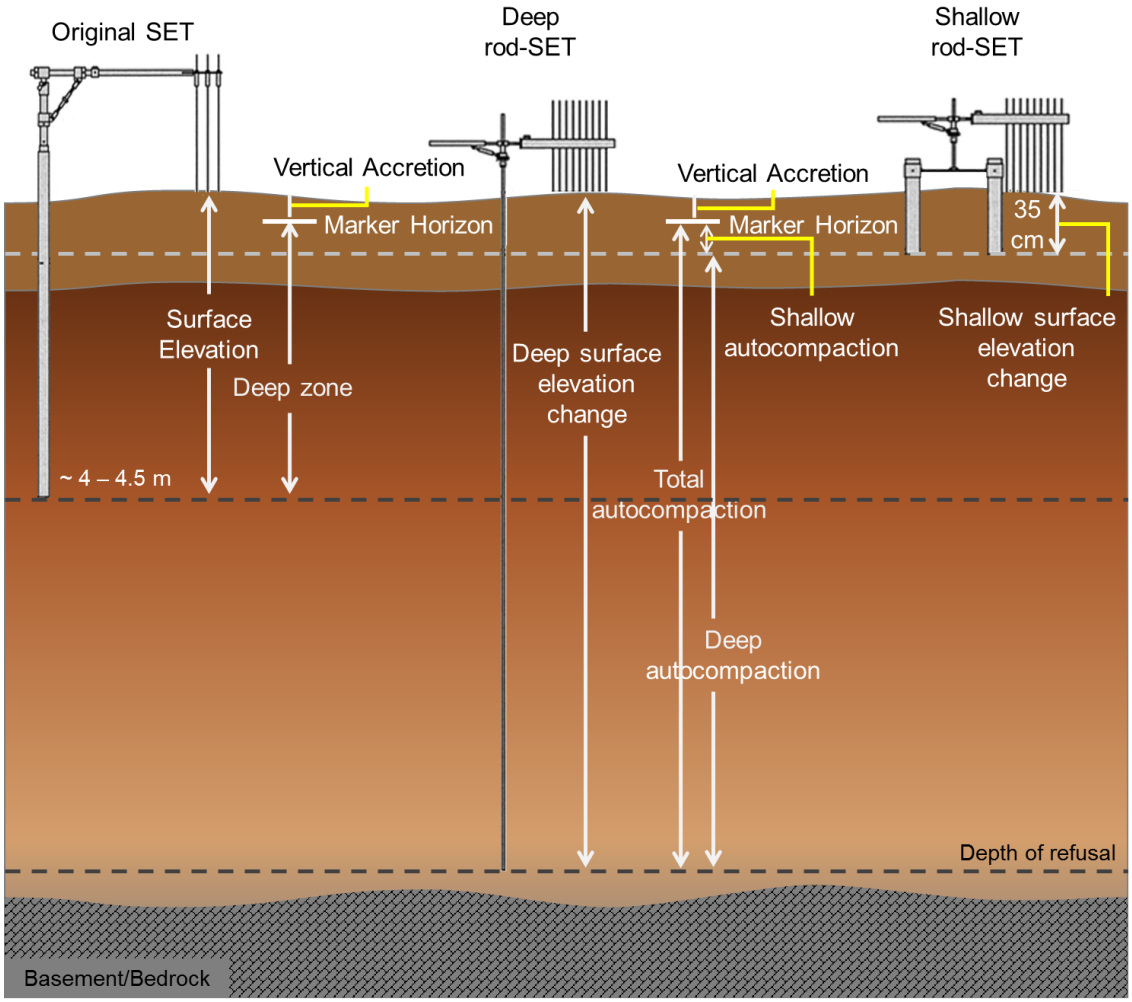

Figure 2.2: Schematic of the original SET, deep-rod-SET and shallow-rod-SET used to determine processes occurring in the intertidal wetland profile including vertical accretion using marker horizons, surface elevation dynamics, and the various sub-surface processes.

2.2.4. Surface elevation table and marker horizon

In comparison to the original SET that weighed about 6.5 kg, the rSET design is more ideal for taking elevation measures in wetland environments as it is lightweight making it less likely to sink the benchmark while taking measurements. The rSET comes with improved fittings to stabilize the rods (also referred to as pins) and reduce measurement errors. Nine fiberglass rods are carefully lowered through the SET arm when taking measurements, and the height of the rods protruding above the arm is recorded. These rods are flexible, are

lighter and so there is less chance that the bottom of pins would pierce the surface if they are accidently dropped on the surface.

The SET technique, irrespective of the version, is usually paired with a technique for measuring vertical accretion at the same timescale. There are a few techniques that could be used, however an artificial MH of feldspar, sand or glitter are some of the most commonly used materials. The MH technique has been problematic in the past as it does not work well in highly erosive sites, such as mangroves where feldspar usually disappears very quickly due to mineral weathering and bioturbation by burrowing crabs and other organisms (Lovelock et al., 2011; Lynch et al., 2015; Rogers et al., 2013b). One way of dealing with this issue is establishing a new MH adjacent to the former plots and not on top of the old plot. Other substances such as, sand and coloured sand, brick dust, glitter, feldspar clay, solid layer of polyester resin, and filter paper have also been previously used as MH (Lynch et al., 2015). Graduated sediment pins and rods were also used to see the amount of accretion that had occurred over time. This method however, was not very effective as the presence of pins and rods can affect the flow of sediments in and around the wetland and cause localised sedimentation as well as scouring around the pin base (Krauss et al., 2003). Tiles made of metal and ceramic were also used in the past. They can be buried beneath the ground and needs to be installed into the ground, and so they are immobile and are fixed in space. This technique, however, disrupts the vegetation and would not really work for mangroves as wave energy is greater in the lower intertidal zones where they might easily get washed away (Callaway et al., 2013).

Generally, replicates of three MH are typically coupled with individual SETs, which are usually established adjacent to SETs at the time of baseline measurements, a month after installations (Cahoon et al., 2000b). A small section of the MH is cored (making efforts to avoid compaction) every time SET measurements are taken to determine the rate of vertical accretion relative to elevation change considering the potential differential compaction. Collectively, the surface elevation table and

marker horizon (SET-MH) approach can be used to delineate belowground substrate expansion and contraction (Fig. 2.2). Change in belowground substrate is the difference between surface elevation change and vertical accretion (Fig. 2.2).

The rSET design comes in two forms, the deep and shallow-rSET (Fig. 2.2). The shallow-r-SET was designed to identify processes that occur in the top 0.35 m of the surface. Typically, the bottom of original SET is usually deployed to a depth of 4 m below the surface; the deep-rSET is deployed to the point of refusal (i.e. the depth at which friction prevents deeper penetration of the rod into the substrate), and the shallow-rSET to a depth of 0.35 m below the surface. Coupling the multi-depth SETs can provide a comprehensive understanding of the relationship between surface and sub-surface processes (expansion and contraction) occurring at different depths of the sediment profile (Cahoon et al., 2002b; Lynch et al., 2015; Whelan et al., 2009, 2005). Processes occurring at four different zones can be identified using the original and rod-SET-MH technique; vertical accretion, depths 0 – 0.35 m (shallow zone), 0.35 – 4 m (middle zone), and 4 – 6 m or depth of refusal (bottom zone). The application of surface elevation measures from the three different benchmarks (0.35 m, 4 m, and depth of refusal) (Cahoon et al., 2002b; Whelan et al., 2009, 2005).

The installation of deep and shallow-rSET benchmarks on a wetland surface requires selecting a suitable site where the surface elevation measurements are to be recorded as they are fixed and assumed to be stable benchmarks for the duration of the study. The spatial distribution of the benchmarks (or stations) depends on the research questions being answered. Stations can be replicated, there could be three in the mangroves and other three in saltmarsh, to capture for instance, the elevation change in different species of mangrove and saltmarsh with respect to their distance from the channel and source of sediment into the system (Lynch et al., 2015).

A global network of mangrove and saltmarsh SET-MH showed considerable variation in surface elevation change, but generally exhibiting the 'keep-up'

behaviour relative to SLR (Cahoon et al., 2006). Vertical accretion was greater if tidal range was greater but high rates of vertical accretion did not always result in elevation gain as a result of decomposition and autocompaction of the recently deposited sediments (Cahoon et al., 1995). Studies have shown that local site-specific tidal variability, root production and substrate expansion can offset high rates of organic matter decomposition and compaction and/or consolidation of sediments that can decrease wetland surface elevation (Lovelock et al., 2015a, 2011). Surface elevation gain can also occur as a result of vegetative regrowth and regeneration of mangroves after a dieback event in the early 1980s was a result of belowground biomass production (Rogers et al., 2005a). Rainfall and storm events can increase vertical accretions but tend to have little impact on the longer-term surface elevation change (Lovelock et al., 2015a; Rogers et al., 2013b, 2005a; Whelan et al., 2009) as surface elevation dynamics may be more closely related to longer-term climatic perturbations, such as the El Niño Southern Oscillation in this region (Rogers et al., 2013b).

The (r) SET-MH is a low-cost and simple method of qualifying above and belowground processes and its influence on surface elevation dynamics of coastal wetlands in relation to SLR. The instrument has a confidence interval of for the measured height of an individual pin ranged between ± 1.3 mm in mangrove substrate and ± 4.3 mm in saltmarsh vegetation (Cahoon et al., 2002b). Studies have demonstrated that expanding the network of SETs across the region can provide a better understanding of coastal wetland response to SLR (Webb et al., 2013). Site-specific and regional models will increase the confidence in identifying coastal wetland vulnerability to SLR.

2.3. Methods

2.3.1. Study design

Surface elevation dynamics was measured in different coastal wetland vegetation

communities at Comerong Island (Fig. 2.3a). Surface elevation change (SCE) was characterised using deep- and shallow-rod surface elevation tables (rSET), vertical accretion (VA) using MH and belowground shallow and deep autocompaction the difference between the degree of shallow/deep SEC and VA. Deep and shallow-rSETs were installed in three different sites. The southern-most site is dominated by tall *Avicennia marina* trees and is close to the entrance of Crookhaven River (Fig. 2.3a). This zone was classified as the mangrove zone based on the dominant vegetation type. The second site is located about 2.2 km north of the Comerong Bay entrance, dominated by saltmarsh *Sporobolus virginicus* with scattered tall *Avicennia marina* trees and termed the saltmarsh zone (Fig. 2.3b and c). The northern-most site is dominated by shrub *Avicennia marina* with some *Sarcocornia quinqueflora* and classified as mixed zone is located 3.3 km from the Bay entrance. Deep-rSETs were installed in replicates of three and shallow-rSETs were installed in replicates of two in between two deep-rSETs in the mangrove, saltmarsh and mixed vegetation zones.

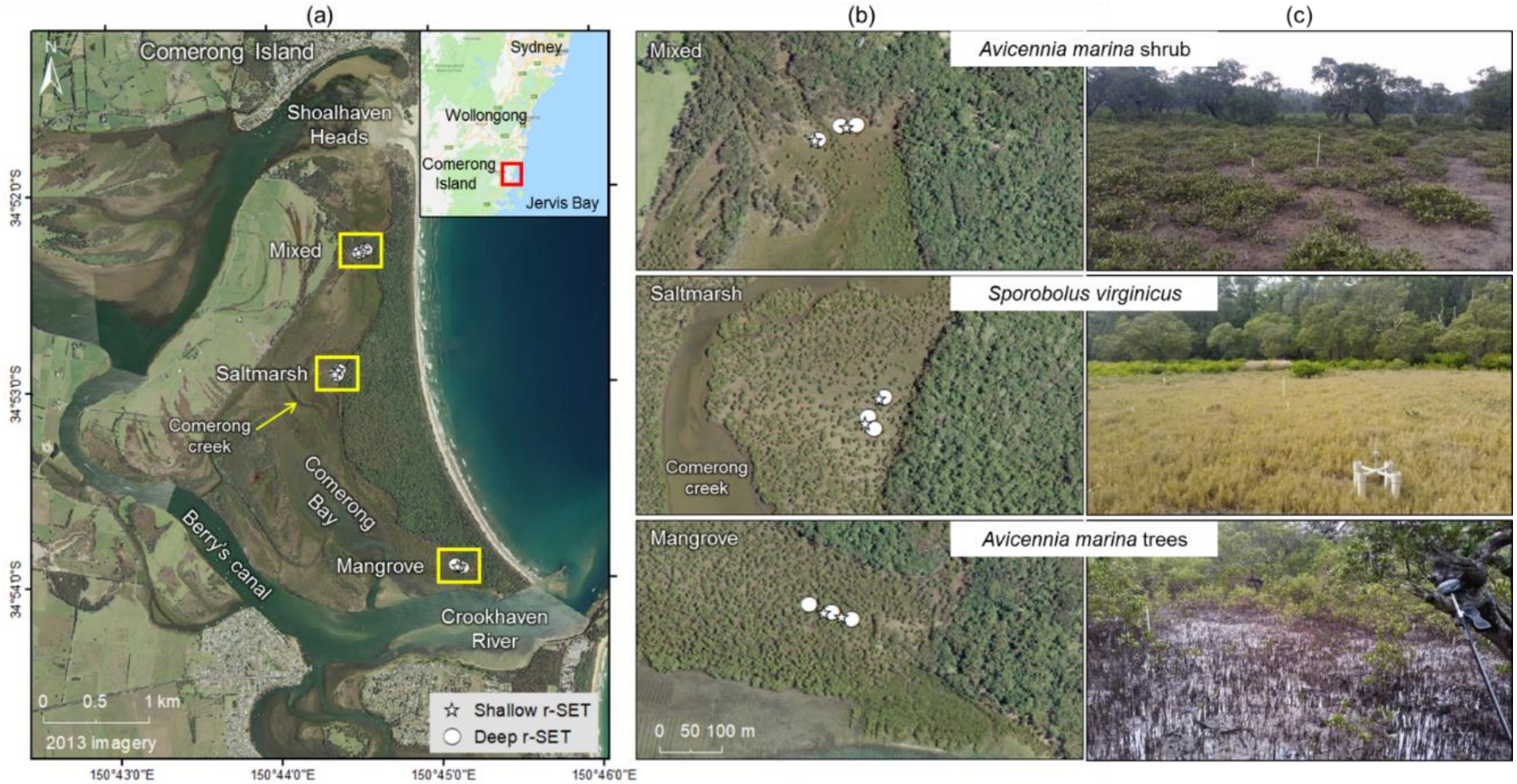

Figure 2.3: (a) Map of Comerong Island created in ArcMap with inset map of NSW; (b) aerial imagery showing the deep and shallow-rSETs in the mixed vegetation site dominated by shrub *Avicennia marina*, saltmarsh site dominated by *Sporobolus virginicus* and mangrove site dominated by *Avicennia marina* tree; and (c) oblique image of the dominant vegetation type in each zone.

As this study used both shallow and deep-rSETs in combination with MH, a suite of analyses could be undertaken to differentiate the zone where changes processes contribute to SEC (Fig. 2.4). More specifically:

i. Surface elevation change (SEC) was determined using deep SETs (deep SEC) to indicate the change in substrate volume occurring between the base of the benchmark and the surface;
ii. Root zone SEC was determined using shallow SETs (shallow SEC) to indicate the change in substrate volume occurring in the rooting zone, thereby indicating the combined contribution of root addition/decomposition and vertical accretion to substrate volume and surface elevation change;
iii. Vertical accretion (VA) was determined using MH to indicate the amount of sediment delivered to the wetland surface by tides;
iv. Total autocompaction associated with consolidation of sediments and organic material dynamics over the substrate profile from the base of the deep-rSET to the surface was determined by excluding the contribution of vertical accretion measured from MH;
v. Shallow autocompaction or expansion primarily associated with root addition/decomposition and sediment consolidation in the root zone was determined by excluding the contribution of vertical accretion measured from MH to root zone surface elevation change; and
vi. Deep autocompaction, primarily caused by consolidation of deeper sediments can be inferred by the difference between the total autocompaction and shallow autocompaction.

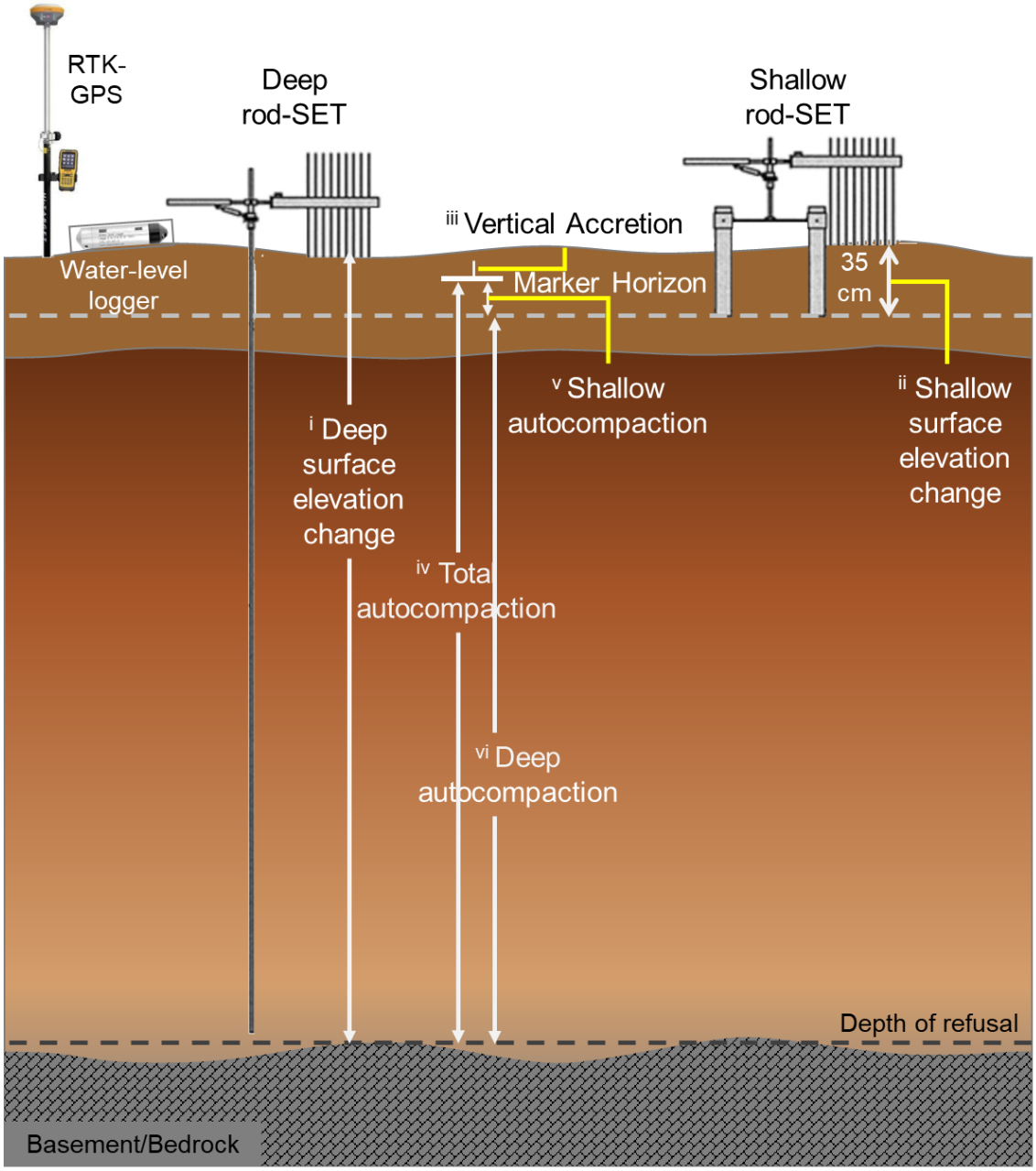

Figure 2.4: Overview of wetland vertical profile properties measured at Comerong Island. Surface elevation change was determined by deep and shallow-rSET, vertical accretion was determined from MH, and total, shallow and deep autocompaction determined from rSET-MH technique. Wetland elevation was determined form RTK-GPS and inundation frequency of the different vegetation zones was determined from water-level loggers.

2.3.2. Position of the tidal frame

Tidal inundation frequency of different sites was used as a proxy for tidal position of the different vegetation groups in the tidal frame. Inundation frequency of the

different sites was determined using water-level loggers. Water-level loggers (Fig. 2.5b) were housed in polyvinyl chloride (PVC) tubes for protection from physical damage, secured with cable ties to a mangrove tree or to a star picket at the wetland surface and deployed next to a deep-r-SET within each of the three different sites (Fig. 2.5a, Fig. 2.6). The wetland elevation and x, y position of each water level logger was determined using a real-time kinematic global positioning system (RTK-GPS) which was referenced to the localised height datum for the region, the Australian Height Datum (AHD). Water-level loggers recorded pressure measurements every 15 minutes over a period of 7 months (March 2016 to October 2016). The period of analysis did not include all phases of the various tidal constituents, it did include both spring and neap tides, as well as the highest astronomical tides that occurred on 5 July 2016, and was regarded to generate a reasonable representation of tidal dynamics of each study site.

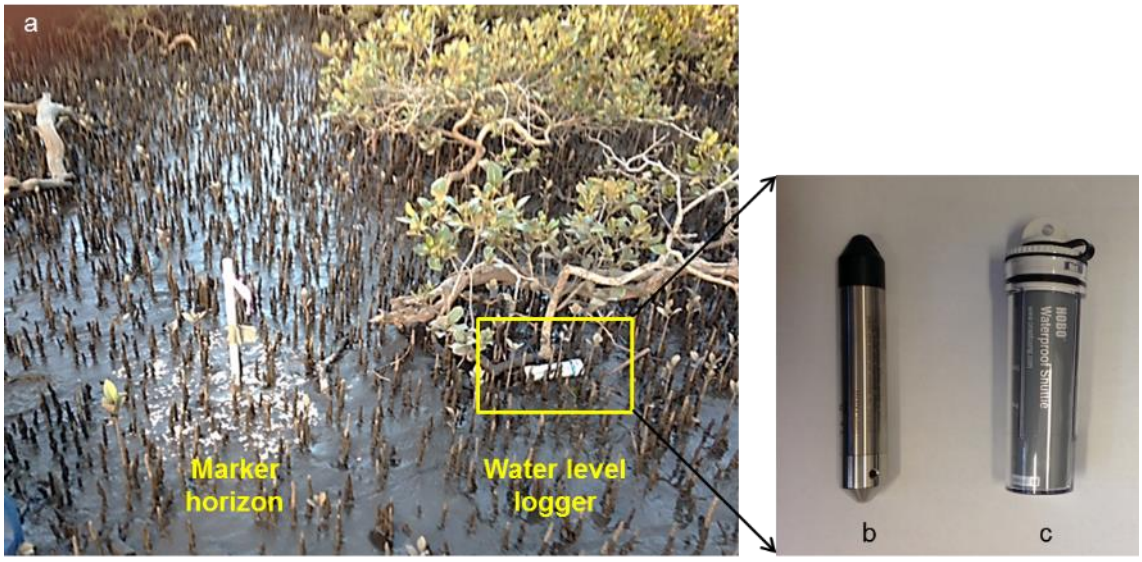

Figure 2.5: (a) Typical set-up of water-level logger on the wetland surface, in this case attached to a mangrove trunk on the surface; (b) the HOBO logger that is housed in PVC pipe; and (c) waterproof shuttle that was used to get the data off the logger.

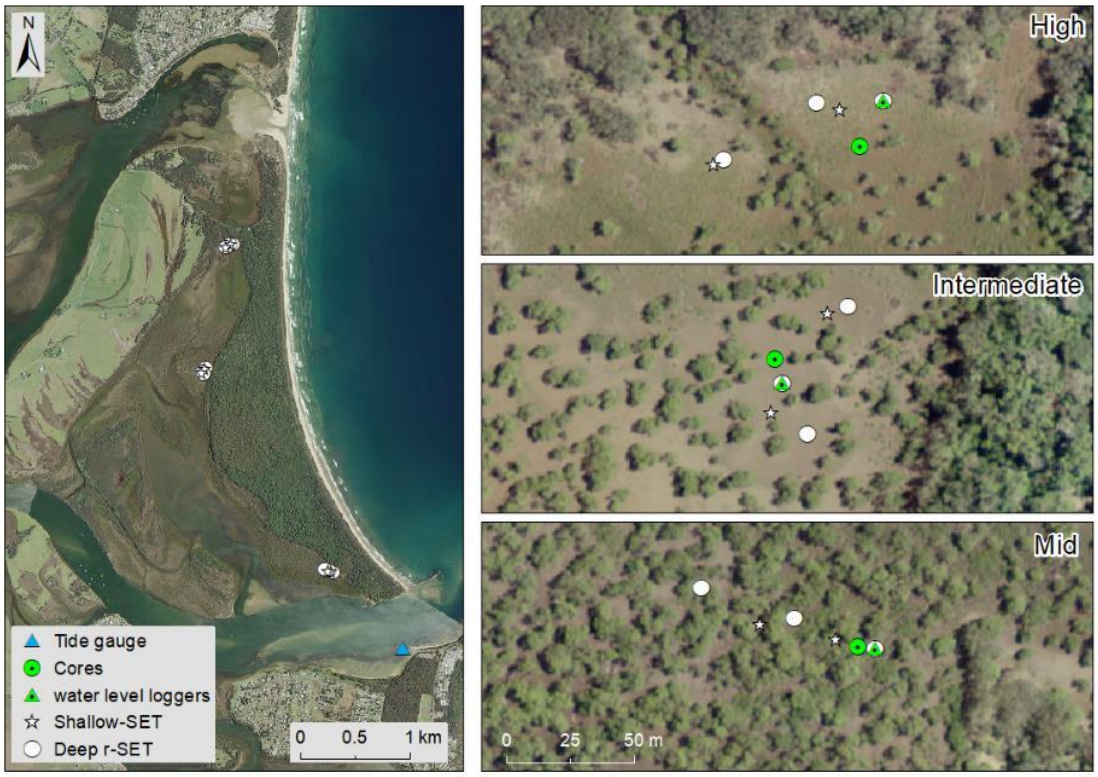

Figure 2.6: Map showing the location of water-level loggers, deep and shallow-rod-SETs, and sediment cores in Comerong Island at Mid, Intermediate and High tidal positions.

Data was transferred to the shuttle (Fig. 2.5c) and downloaded using the HOBOware Pro software. The logger data was corrected to water level or sensor depth measurements by calibrating it against atmospheric pressure measurements from the Nowra station (station number 68072). Data was checked for accuracy and calibrated to ensure that inundation depths were 0 cm when the wetland surface was not inundated. Sensor depth was adjusted to AHD using RTK-GPS elevations.

Inundation frequency of the different sites was quantified as the number of 15-minute time increments that the logger was submerged relative to the total number of 15-minute time increments and expressed as percentage inundation frequency. Water level data for each tidal position was adjusted to the m AHD and plotted against water level data from the nearest tide gauge station at Crookhaven Heads (station number 215408) (Fig. 2.6).

Statistical differences in inundation frequency at different wetland elevations derived from RTK-GPS was identified using ANOVA (analysis of variance) in JMP. Additional values were included in the data set to define the tidal boundary conditions. In Australia, heights above mean sea level (MSL) are referenced to the Australian Height Datum (AHD) (Brown, 2010). As the tidal range for the region is 2 m and centred around MSL or 0 m AHD, tidal inundation was delimited to elevation ranges of -1 m and 1 m AHD, and 0 m AHD was defined to have 50 % inundation frequency (Table 2.1). A relationship between inundation frequency and wetland elevation was developed using a logistic model as this model accommodated the tidal patterns defined by the boundary conditions. More specifically, a logistic model, unlike a linear model, allowed inundation to be absent at elevations > 1 m and to equal 100 % at elevations < -1 m AHD.

Table 2.1: Boundary conditions used to develop the linear inundation model.

Location	Surface elevation	% inundation	Position
Boundary 1	-1	100	Low tidal limit
Boundary 2	0	50	Inflection point
Boundary 3	1	0	Upper tidal limit

Model suitability was assessed based on the coefficient of determination (r^2), RMSE, AICc and BIC, and was subsequently used to predict the inundation frequency of individual rSETs. Tidal inundation analysis confirmed that position within the tidal frame varied according to distance from the bay entrance and corresponded to vegetation cover and so the different rSET locations are classified as mid, intermediate or high tidal position.

2.3.3. Deep and shallow surface elevation change

Deep-rSET

Deep-rSETs were installed in September 2014 using the guidelines of Lynch et al. (2015). The installation of rSET benchmark was made via a platform placed above the wetland surface to minimise disturbance of the sediments (Fig 2.7a). The deep-

rSET benchmark comprises of solid stainless steels rods of 1 m lengths, which were driven into the wetland surface with a hammer (Fig 2.7a). A driving point was attached on the leading edge of the first rod to allow the rod to cut through root material and move more freely through the thick substrate. Upon reaching point of refusal (point when the rod no longer moved) or substantial resistance (came to an abrupt stop), the remaining top-most rod if not completely driven into the substrate was cut at about 30 cm above the surface. A custom-built rSET threaded receiver was bolted to the rod and was encased in a 15-cm diameter PVC pipe (about 50 – 60 cm long) leaving the receiver top exposed. The PVC pipe was then cemented with concrete to make the benchmark permanent (Fig. 2.7b) and the length of the rods to the basement and/or bedrock for each deep benchmark noted (Table 2.2).

Figure 2.7: Installation and surface elevation measurement taken with the deep-r-SET.

Table 2.2: Deep-rod-SET location, depth of rod and surface elevation above MSL at Comerong Island.

Deep-rod-SET benchmark	Location		Approximate depth of rod (m)	Surface elevation (m AHD)
	Latitude	Longitude		
Mid_1	-34° 52' 18.41832''	150° 44' 35.48327''	6	0.390
Mid_2	-34° 52' 18.42457''	150° 44' 34.44301''	6.4	0.468
Mid_3	-34° 52' 19.12513''	150° 44' 32.99729''	7.8	0.380
Intermediate_1	-34° 52' 54.93662''	150° 44' 24.46541''	12.7	0.441
Intermediate_2	-34° 52' 55.90829''	150° 44' 23.43450''	18	0.440
Intermediate_3	-34° 52' 56.55434''	150° 44' 23.80837''	15	0.460
High_1	-34° 53' 56.29249''	150° 45' 8.85186''	11	0.517
High_2	-34° 53' 55.88282''	150° 45' 7.60161''	12.5	0.530
High_3	-34° 53' 55.47661''	150° 45' 6.17888''	12	0.492

Initial measurements were taken in October 2015, a month after benchmark installation, to allow some time for settling of the benchmarks. Measurements were undertaken by placing the portable rSET instrument, with horizontal arm from which nine pins are lowered, onto the inset pipe. Pins were lowered to the wetland surface and the direction of the horizontal arm was recorded. This process was repeated in four arm directions to generate a total of 36 measurements per rSET station. Repeated measurements were subsequently taken in March and August of 2016, and January and November 2017, with arm directions corresponding to the arm direction used when baseline measurements were taken. This ensured that the pin measurements measured changes in wetland surface for the same location at each visit.

Corresponding pins were placed into the holes of the horizontal arm and held with clips. The arm was levelled using the bubble-level (Fig. 2.7d) after which pins were lowered carefully on the wetland surface (Fig. 2.7e and 2.8d). The pins returned to the same bearing positions and measurement of the same surface points was taken every time. The height of the pins protruding above the arm was measured using a ruler and recorded as millimetres (mm) (Fig. 2.7f and 2.8e). When taking surface elevation measurements, any obstacles such as, pins landing on vegetation roots (e.g. mangrove pneumatophores) and/or crab hole or crab mounds were excluded from the data matrix. The change in the measured pin length above the horizontal

arm reflected relative change in surface elevation over the study period.

Shallow-rSET

Shallow-rSETs were strategically positioned between each of the deep-rSETs within each zone. Installations were made via a platform placed above the wetland surface to minimise disturbance of the sediments (Fig 2.8a, Table 2.3). The shallow-rSETs are designed to quantify changes in the substrate volume of the active root zone of wetland vegetation. In this case we targeted the upper 35 cm as the active root zone (Cahoon et al., 2002b). The custom-made frame has a readymade insert collar attached to it and has four hollow openings (or legs) through which 7-cm diameter aluminium pipes was inserted and pushed into the sediments to a depth of 35 cm (Fig. 2.8b and c). Once all shallow-rSET legs were installed to the same depth, each pipe was bolted to the hollow legs to secure the shallow benchmark (Fig. 2.8c). As the legs of shallow-rSET only extend 35 cm into the wetland substrate, their stability may be compromised; some of this instability was anticipated to be offset using four benchmarks per rSET that have a larger diameter, and the stability of shallow-rSETs was later assessed.

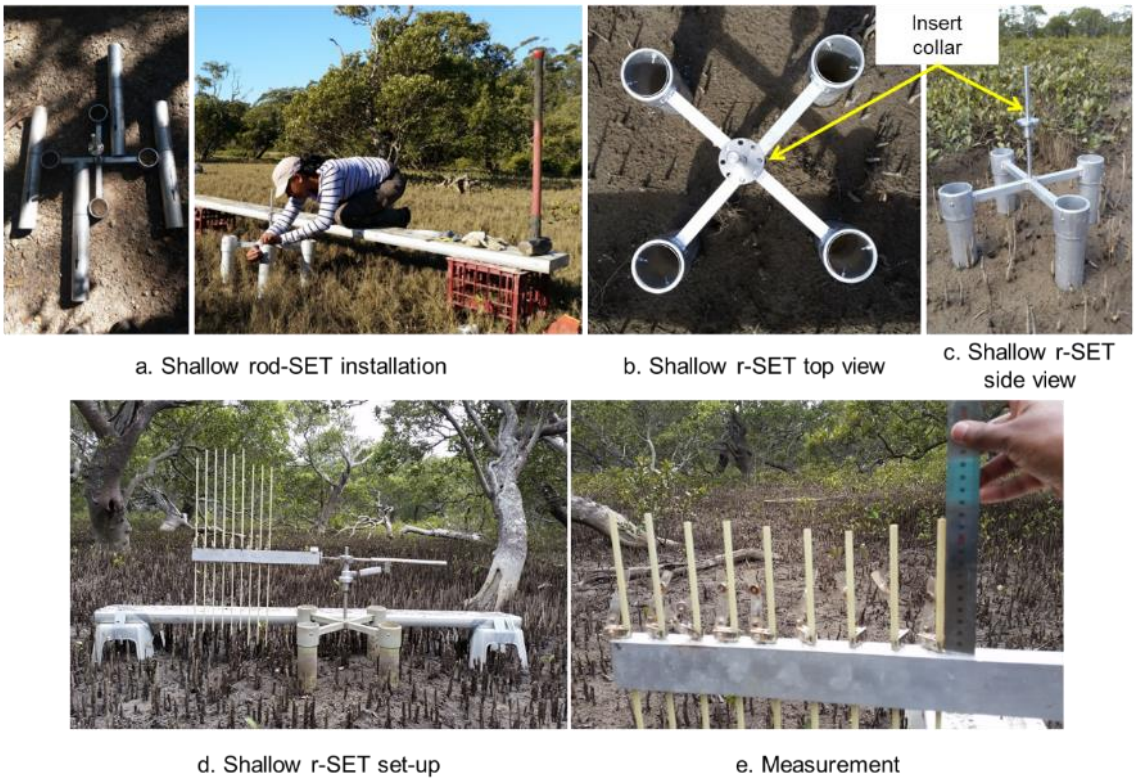

Figure 2.8: Installation and surface elevation measurement taken with the shallow-r-SET.

Table 2.3: Shallow-rod-SET location and elevation above MSL at Comerong Island.

Deep-rod-SET benchmark	Location		Altitude (m AHD)
	Latitude	Longitude	
Mid_A	-34° 52' 18.52294''	150° 44' 34.80099''	0.452
Mid_B	-34° 52' 19.17819''	150° 44' 32.83277''	0.446
Intermediate_A	-34° 52' 55.02156''	150° 44' 24.15132''	0.446
Intermediate_B	-34° 52' 56.27593''	150° 44' 23.24610''	0.441
High_A	-34° 53' 56.17175''	150° 45' 8.23413''	0.547
High_B	-34° 53' 55.95881''	150° 45' 7.07617''	0.509

Shallow-rSETs were taken at the same time as deep-rSET measurements. All measurements were undertaken in a similar manner to the deep-rSET with the portable SET arm being position on the insert. The steps used to take surface elevation measurements were identical for both deep and shallow benchmarks.

2.3.4. Vertical accretion

Feldspar was used as the marker horizon for this study to determine vertical

accretion occurring in the different tidal positions of Comerong Island. Feldspar was used because of its fine texture, bright white colour that can be easily identified in the field, and colloidal properties (insoluble and evenly dispersed on the sediment surface) (Callaway et al., 2013). Marker horizons were installed in replicates of three at each deep-rSET at the time baseline surface elevation measurement (Cahoon et al., 2000b) (Fig. 2.9a). Vertical accretion was measured at the time that surface elevation measurements. When feldspar was seen on the wetland surface, VA was identified to have not occurred to a measurable degree since the last measurement (Fig. 2.9b); when feldspar was not seen on the surface then a small core was extracted from the MH plot (making efforts to avoid any compaction of the sediments) (Fig. 2.9c), and the depth of sediment accumulated above the MH was measured (Fig. 2.9d). Due to bioturbation, feldspar was sometimes not recovered, and in this case a measurement was not recorded.

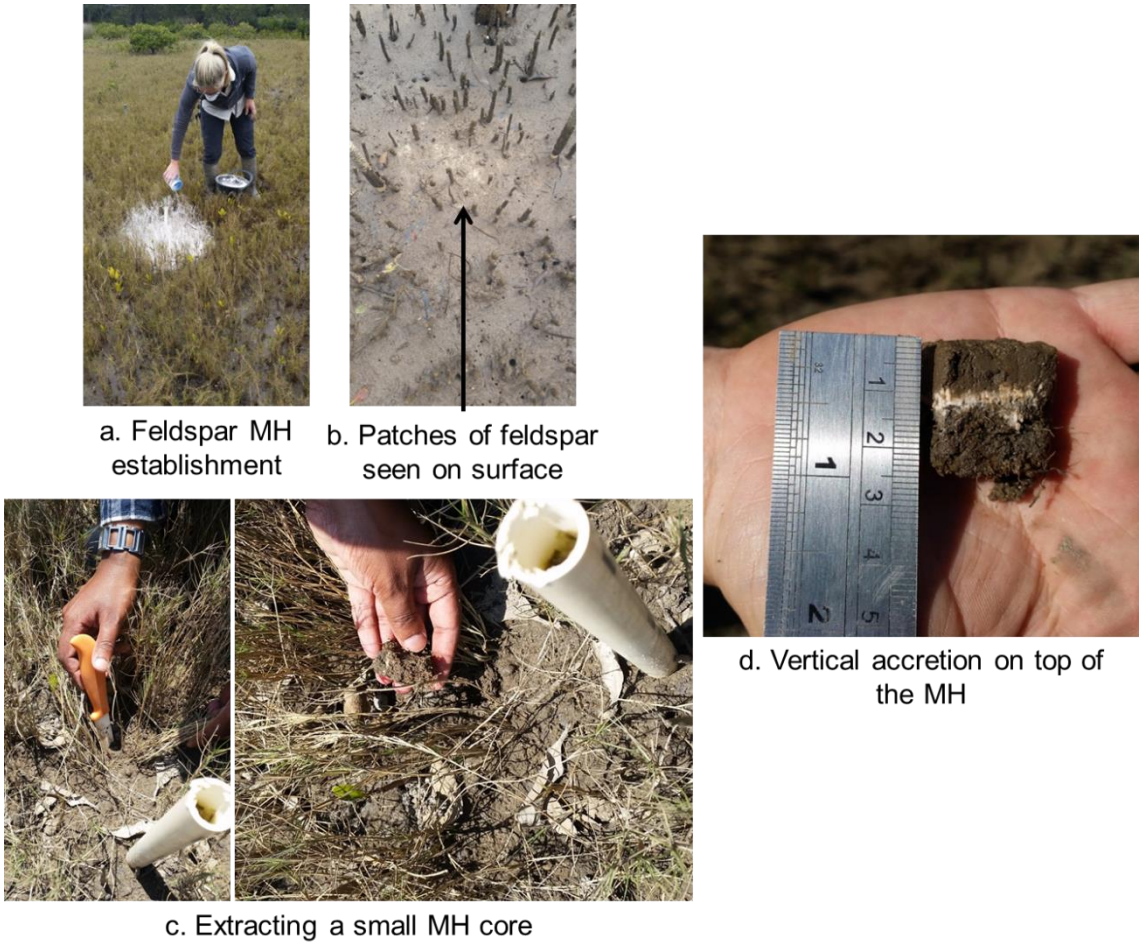

Figure 2.9: Marker horizon measurements at Comerong Island.

2.3.5. Characterising belowground processes and sediment characteristics

Belowground processes divided into changes observed in the total, shallow and deep zone. Total zone change was the difference between deep SEC and VA. Shallow zone change was the difference between shallow SEC and VA (from the nearest MH station). Deep zone change was the difference between total and shallow zone.

Belowground substrate characteristics, such as organic matter content and grainsize were analysed to determine their influence on SEC processes at different tidal positions. Sediment cores were extracted adjacent to an rSET at each tidal

position. Cores of approximately 1.5 m were collected by manually hammering aluminium pipes into the ground as described in detail in Chapter 4. 2-cm sediments were subsampled at every 10-cm interval to analysed for organic matter content using the loss-on-ignition (LOI) technique (Ball, 1964). About 3 g of air-dried sediment was finely ground and oven-dried at 105 °C overnight then combusted in a furnace at 375 °C for 16 hours to oxidise the organic matter content. Percentage organic matter content was determined based on the proportional change in mass of the sample after oxidising. Sediment grainsize was analysed by laser diffraction using a Malvern Mastersizer-X and represented as percentage of sand and mud (silt plus clay). Substrate organic matter content and grainsize in belowground substrate was presented as compaction corrected depths by multiplying the compaction factor with average sub-sample depth and reported with respect to AHD based on the surface elevation of the core.

2.3.6. Relationships between surface elevation change, vertical accretion, and belowground processes

Surface elevation data (deep and shallow) for each rSET arm direction was averaged to generate a mean value for each arm direction. The mean values for each arm direction within a zone was pooled to generate a mean and standard error value for each rSET at each time step. VA generated from each MHs was pooled to generate a mean and standard error for each MH at each time step. SEC and VA plots were generated by adjusting the SE and VA increments based on the starting elevation of the wetland surface. The deep and shallow-rSET data was reduced and combined with MH to determine total, shallow and deep autocompaction. Total, shallow and deep zone change was pooled from each rSET and across a tidal position and analysed in a similar manner as deep and shallow SEC. Statistical analyses was carried out to determine whether differences occurred within and between tidal positions for each measure using ANOVA in JMP. Probability factor (p-value) of interaction over time, between zone and within a zone, and between and within tidal positions over time from ANOVA were

reported on the three most common univariate tests. If the univariate chi-square sphericity test was significant (< 0.05) then f-test or Wilks' lambda p-values were reported, but if it not significant then univariate unadjusted epsilon values were reported. All ANOVA test results are presented in supplementary data (Appendix 1). Based on some degree of confidence that there were no differences within a tidal position, but reasonable differences between positions undertake, linear regression analyses were used to determine rates of SEC, VA and autocompaction.

2.3.7. Relationships between surface elevation change and wetland elevation

Relationship between SEC and tidal position was investigated using linear regression analysis. Wetland elevation was used as a proxy of tidal position (independent variable) versus the rate of SEC. The relationship was assessed based on minimising error (RMSE) and maximising r^2, which was used to develop a surface elevation model to consider the influence of tidal inundation on wetland SEC over longer time scales. As it is unreasonable to extrapolate a short-term data set (2-year rSET data set) forward for an extended period, the model extrapolation was limited to 20 years so it could be correlated with SETs from other study sites in the region (see Chapter 3). The 20-year prediction provided a means to consider the influence tidal inundation alone on SEC across the tidal frame, irrespective of the starting elevation.

2.4. Results

2.4.1. Position of the tidal frame

Water level data from the different tidal positions at Comerong Island shows a semi-diurnal tidal cycle. Water depth and inundation frequency at each site was greatest during the spring tidal cycle and a lag of approximately 2 hours to

completely inundate the site (Fig. 2.10). This lag meant that the timing of the tidal peak at lower elevations corresponded more closely to the tidal peak on the tide gauge than the tidal peak at higher wetland elevations. In combination, the elevation and the lag in the tidal peak influenced the inundation duration and frequency with mangrove having an inundation frequency of 33.2 %, saltmarsh was inundated 23.9 % of the time, and the mixed vegetation zone had an inundation frequency of 18.8 %.

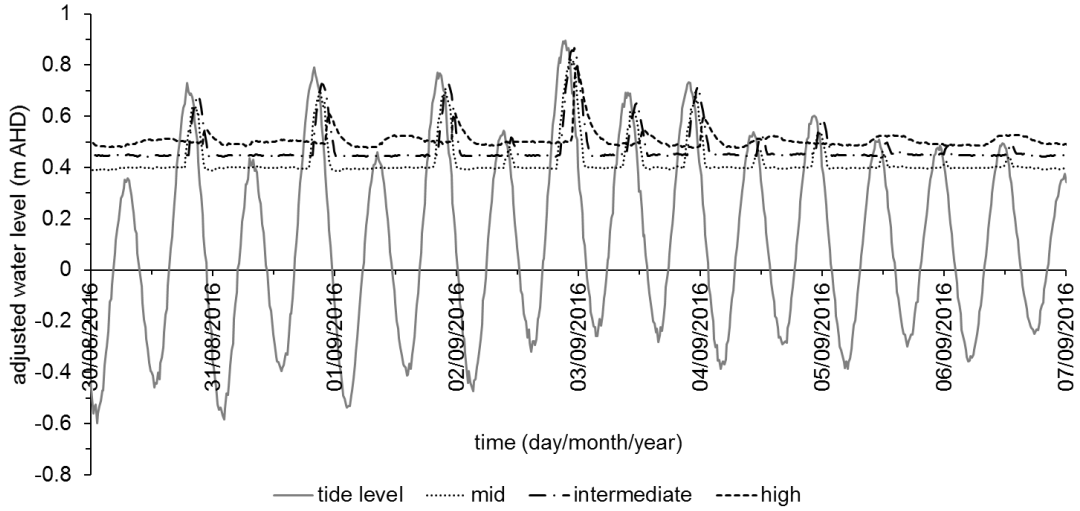

Figure 2.10: Water level (m AHD) at mid, intermediate and high tidal positions in relation to Crookhaven Heads tide gauge data over an 8-day period in 2016.

The logistic relationship between inundation frequency and wetland elevation had an r^2 of 0.9848 (Fig. 2.11) indicating that inundation frequency is influenced by wetland elevation and had the form of Eq. 2.1. The predicted inundation frequency for the mangrove rSET monitoring stations was between 22.4 and 26.7 %. The saltmarsh was inundated between 22.7 and 23.7 % of the time, and the mixed vegetation had an inundation frequency of 18.9 and 21.3 % (Table 2.4). Since mangrove had the highest elevation frequency it is classified as mid tidal position. The mixed vegetation zone had the lowest inundation frequency and is located higher in the tidal frame is classified as high tidal position. The saltmarsh zone having an elevation and inundation frequency in between mid and high is classified as intermediate tidal position.

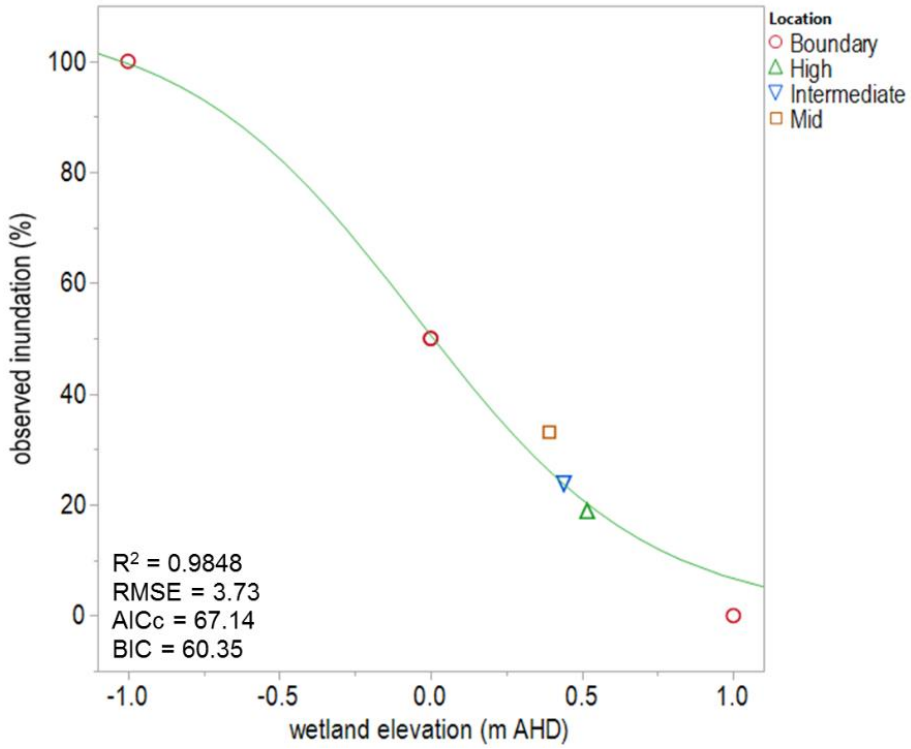

Figure 2.11: Relationship between wetland elevation and observed inundation frequency at all study areas.

$$y = \frac{\mathbf{108.02}}{\mathbf{1} + \boldsymbol{Exp}\left(\mathbf{2.6} \times \left(\boldsymbol{E} - \left(-\mathbf{0.0485}\right)\right)\right)} \qquad \text{Eq. 2.1}$$

Table 2.4: Predicted inundation frequency and tidal position of the rSET monitoring stations.

rSET	Surface elevation (m AHD)	Observed inundation (%)	Predicted inundation (%)	Tidal position
Mangrove 1	0.390	33.2	26.2	Mid
Mangrove 2	0.468		22.4	Mid
Mangrove 3	0.380		26.7	Mid
Shallow mangrove A	0.452		23.1	Mid
Shallow mangrove B	0.446		23.4	Mid
Saltmarsh 1	0.441		23.6	Intermediate
Saltmarsh 2	0.440	23.9	23.7	Intermediate
Saltmarsh 3	0.460		22.7	Intermediate
Shallow saltmarsh A	0.446		23.4	Intermediate
Shallow saltmarsh B	0.441		23.6	Intermediate
Mix 1	0.517	18.8	20.2	High
Mix 2	0.530		19.6	High
Mix 3	0.492		21.3	High
Shallow Mix A	0.547		18.9	High
Shallow mix B	0.509		20.5	High

2.4.2. Surface elevation change

Deep surface elevation change

Surface elevation gain was observed at mid zone rSETs, surface elevation remained stable within the intermediate zone, whilst elevation decline was observed in the high zone rSETs (Fig. 2.12a). SE dynamics varied based on tidal positions ($p = 0.0117$) and over time ($p < 0.0001$); and within a tidal position and over time ($p < 0.0001$). Most of the variation in SEC over time was associated with the high tidal position rSETs, where significant differences were identified between rSETs ($p = 0.0021$), over time ($p < 0.0001$) and within rSETs over time ($p = 0.0006$) (Fig. 2.10d). Significant differences were observed between rSETs despite relatively low changes in surface elevation over time with the mean rate of SEC of -1.2 ± 1.4 mm/y. By contrast, differences were not identified between and within mid rSETs over time ($p = 0.2108$) (Fig. 2.12b), despite significant variation between mid tidal position rSET. At this site rSET1 exhibited a high rate of elevation gain of 11.8 ± 3.0 mm/y and rSET3 increased elevation at a low rate of 0.43 ± 1.4 mm/y. The

intermediate rSETs exhibited an intermediary response where significant differences in the rate of elevation gain was identified over time ($p < 0.0001$), but not between r-SETs (Fig. 2.12c).

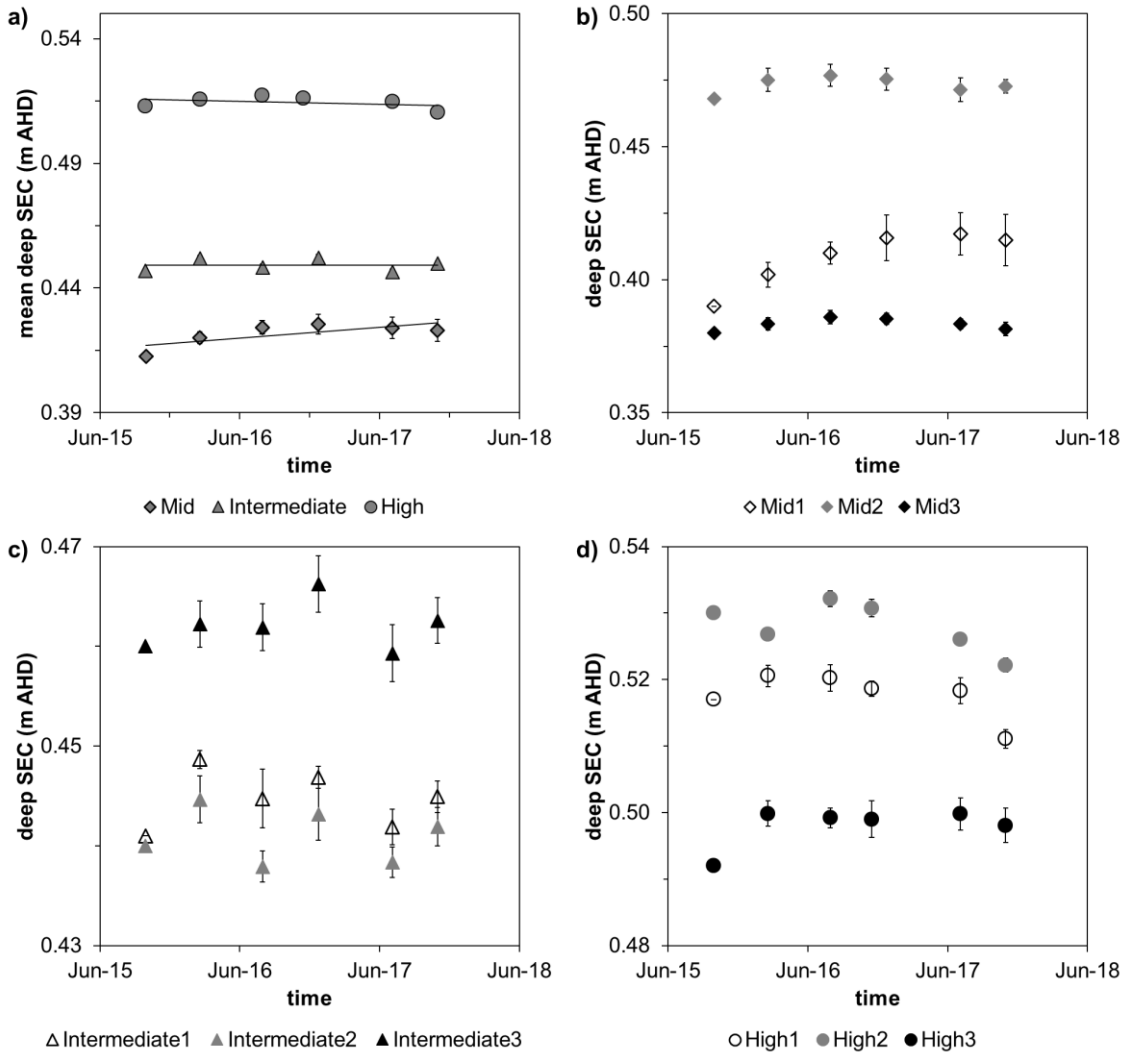

Figure 2.12: (a) Mean deep surface elevation change at each tidal position over the two-year study period. Deep-rSET SEC at (a) mid, (b) intermediate and (c) high tidal positions.

The absolute change in surface elevation was not consistent between rSETs within a tidal position due to the variability observed within a tidal position. For example, mid rSET1 increased 25 ± 3.8 mm, whilst the remaining rSET at this zone increased by less than 2 mm over the study period. Similarly, in the high tidal position, rSET3 increased elevation by approximately 4.1 ± 0.64 mm, whilst the remaining rSETs decreased elevation by more than 5 mm over the study period

(Table 2.5, only the deep-rSETs). There was, however, a relatively consistent pattern in surface elevation change at the intermediate rSETs with little change in surface elevation detected.

Table 2.5: Deep and shallow surface elevation change (rate and absolute ± standard error of mean) at each mid, intermediate (int.) and high rSET.

Deep-rSET	Depth (m)	Deep SEC		Shallow-rSET	Shallow SEC	
		Rate (mm/y)	Absolute (mm)		Rate (mm/y)	Absolute (mm)
Mid 1	6.65	12 ± 3.0	25 ± 3.8			
Mid 2	6.05	0.65 ± 2.0	1.4 ± 0.21	Mid A	4.0 ± 3.2	8.4 ± 1.3
Mid 3	7.45	0.43 ± 1.4	0.90 ± 0.14	Mid B	2.4 ± 1.7	5.1 ± 0.79
Mean	6.7	4.3 ± 2.0	8.9 ± 1.4	Mean	3.2 ± 2.2	6.7 ± 1.0
Int. 1	12.35	-0.03 ± 1.8	-0.07 ± 0.011			
Int. 2	17.65	-0.39 ± 1.7	-0.81 ± 0.13	Int. A	0.92 ± 0.72	1.9 ± 0.30
Int. 3	14.65	0.45 ± 1.5	0.94 ± 0.15	Int. B	-0.80 ± 2.1	-1.7 ± 0.26
Mean	15.2	0.0087 ± 1.5	0.02 ± 0.0028	Mean	0.06 ± 1.4	0.12 ± 0.02
High 1	10.65	-2.5 ± 1.8	-5.3 ± 0.83			
High 2	12.15	-3.0 ± 1.8	-6.2 ± 0.96	High A	-1.4 ± 2.5	-3.0 ± 0.46
High 3	11.65	2.0 ± 1.6	4.1 ± 0.64	High B	4.7 ± 1.7	9.9 ± 1.5
Mean	11.8	-1.2 ± 1.4	-2.5 ± 0.38	Mean	1.7 ± 1.8	3.4 ± 0.52

Shallow surface elevation change

An increasing pattern in shallow surface elevation gain was identified at the mid shallow-rSETs, variable change in shallow SEC was measured at the high s-rSETs, whilst shallow surface elevation was stable at the intermediate zone (Fig. 2.13). There was no difference identified in shallow SE dynamics between tidal positions ($p = 0.2771$), but there was significant difference over time ($p < 0.0001$) and within a tidal position over time ($p = 0.0025$) (Fig. 2.13a). Differences in shallow-rSETs over time was only identified at high tidal position ($p = 0.0210$) (Fig. 2.13d), whilst no difference in shallow SEC was identified between rSETs at mid and intermediate tidal positions (Fig. 2.13b and c). Shallow SEC varied over time when considering all tidal positions ($p < 0.0001$), which was attributed to differences in SEC in the mid tidal position ($p = 0.0008$).

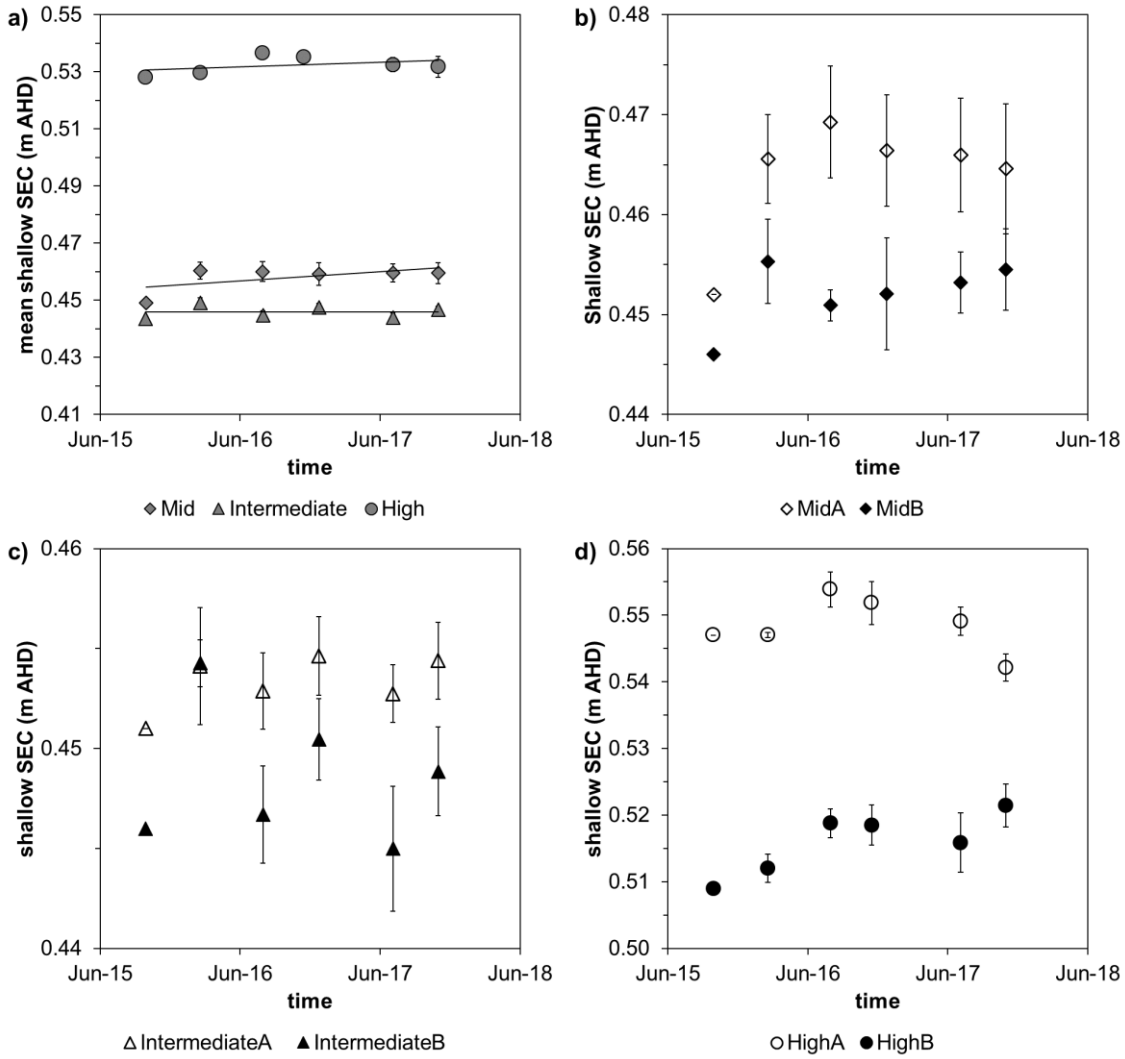

Figure 2.13: (a) Mean shallow surface elevation change at each tidal position over the two-year study period. Shallow-rSET SEC at (a) mid, (b) intermediate and (c) high tidal positions.

The variability between shallow-rSETs at high tidal position meant that the absolute change in surface elevation was not consistent at this site as rSETA decreased 3.0 ± 0.46 mm of elevation, while rSETB increased elevations at 9.9 ± 1.5 mm. Despite the variability between shallow SEC, high and mid tidal positions increased surface elevation at a rate of 1.7 ± 1.8 mm/y and 3.2 ± 2.2 mm/y, respectively (Table 2.5, only the shallow-rSETs). All the shallow-rSETs are behaving like their corresponding deep-rSETs indicating consistent pattern in SEC, irrespective of the sediment depth over which changes are measured.

2.4.3. Vertical accretion

Vertical accretion increased with distance from the entrance of Comerong Bay, with the highest mean rate of vertical accretion occurring in high tidal positions, estimated at 3.6 ± 0.45 mm/y, while the intermediate zone had the lowest rate of VA of 1.9 ± 1.0 mm/y (Fig. 2.14, see Table 2.6 for values). VA varied between tidal positions ($p = 0.0025$), over time ($p < 0.0001$), and within tidal positions over time ($p = 0.0207$) (Fig. 2.14a). Comparable VA rates were measured between MHs at mid tidal positions ($p = 0.2428$), despite different starting elevations of MHs at this site (i.e. elevation ranged between 0.38 and 0.47 m AHD) and mean rate of VA of 2.1 ± 1.7 mm/y (Fig. 2.14b). This contrasted with the patterns in VA at intermediate and high tidal positions where little variation in VA was found between MHs within these zones ($p = 0.3161$, 0.3589, respectively), but significant differences were identified over time in the intermediate ($p = 0.302$, Fig. 2.14c) and high tidal positions ($p = 0.0038$, Fig. 2.14d).

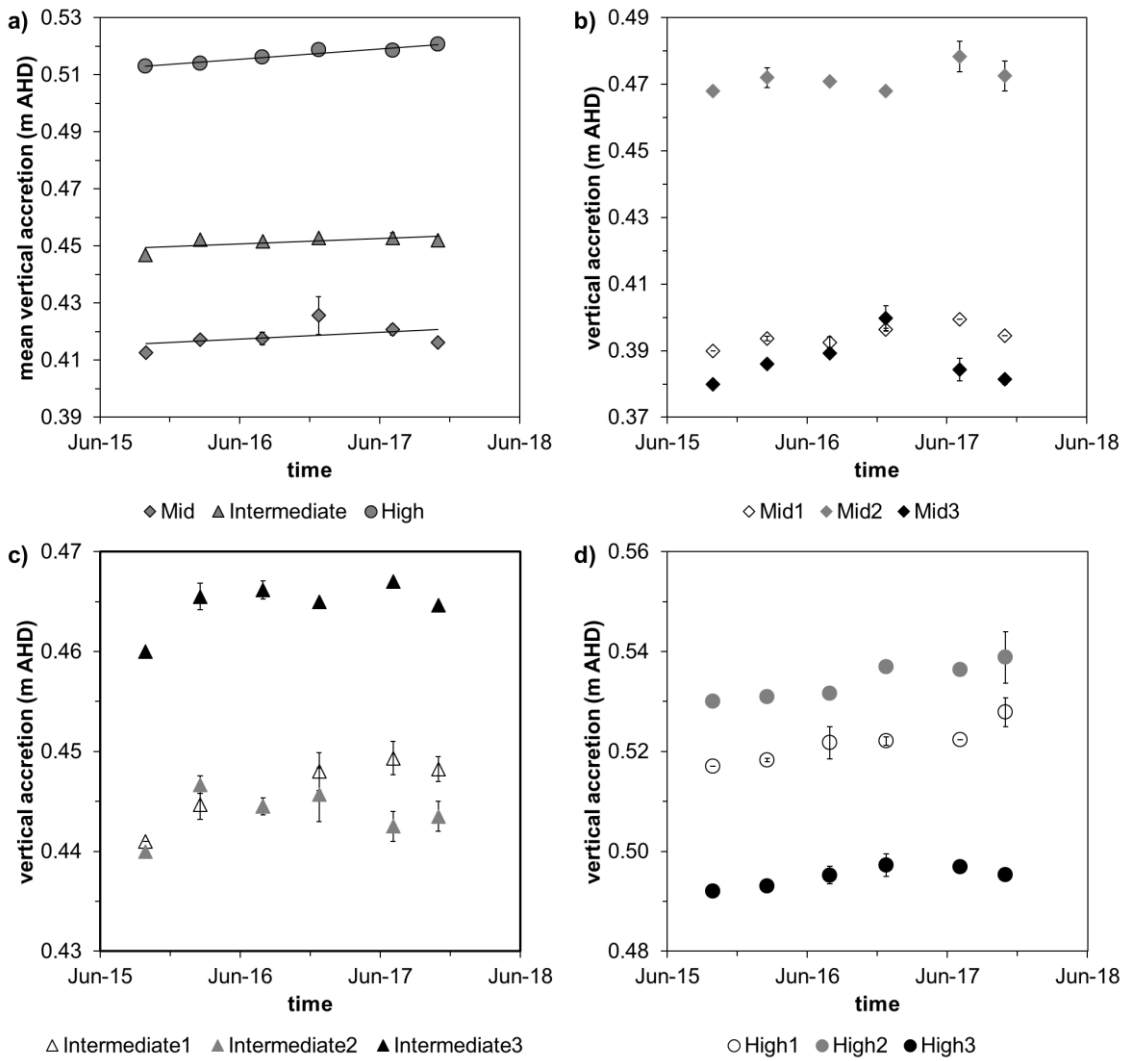

Figure 2.14: (a) Mean MH vertical accretion at different tidal positions over the two-year study period. MH VA at (b) mid, (c) intermediate and (d) high tidal positions.

Table 2.6: Marker horizon vertical accretion (rate and absolute ± standard error of mean) observed at individual rSETs in the different tidal positions.

Tidal Position	Vertical accretion	
	Rate (mm/y)	Absolute (mm)
Mid 1	3.0 ± 1.4	6.2 ± 0.98
Mid 2	2.7 ± 2.0	5.7 ± 0.85
Mid 3	0.68 ± 4.4	1.4 ± 0.22
Mean	2.1 ± 1.7	5.0 ± 0.78
Intermediate 1	3.6 ± 0.77	7.5 ± 1.2
Intermediate 2	0.33 ± 1.5	0.69 ± 0.11
Intermediate 3	1.8 ± 1.2	3.7 ± 0.59
Mean	1.9 ± 1.0	4.0 ± 0.62
High 1	4.4 ± 0.89	9.2 ± 1.4
High 2	4.3 ± 0.77	9.1 ± 1.4
High 3	2.0 ± 0.81	4.3 ± 0.67
Mean	3.6 ± 0.45	7.5 ± 1.2

2.4.4. Belowground processes

Total autocompaction

Deep-rSET surface elevation change at high tidal positions was the only measure that varied within a tidal position ($p = 0.0021$). VA corresponded to SE over time at mid tidal positions ($p = 0.4853$) but varied over time at intermediate ($p = 0.0002$) and high tidal positions ($p = 0.0034$) (Fig. 2.15). When all measures were pooled, VA and SEC were not statistically different ($p = 0.7035$), and a relationship was not established between the two variables ($r^2 = 0.013$, Fig. 2.15). At the high tidal position, the deviation in the degree of SEC and VA increased over time resulting in rates of SEC being less than the rate of VA (Fig. 2.15). A similar pattern was observed at the intermediate tidal positions, however at mid tidal position the observed increase in surface elevation could not be accounted for by VA alone (Fig. 2.15). In all tidal positions, processes other than VA contribute to SEC with an increase in substrate volume beyond that related to VA occurring at mid tidal positions, whilst autocompaction of the substrate contributed to deviations between the degree of VA and SEC at intermediate and high tidal positions. Over

the study period, the degree of autocompaction at high and intermediate tidal positions was in the order of -9.9 ± 1.5 mm and -4.0 ± 0.62 mm respectively. The degree of substrate expansion beyond that attributed to VA was in the order of 4.0 ± 0.62 mm at high tidal positions (Table 2.7, only total autocompaction).

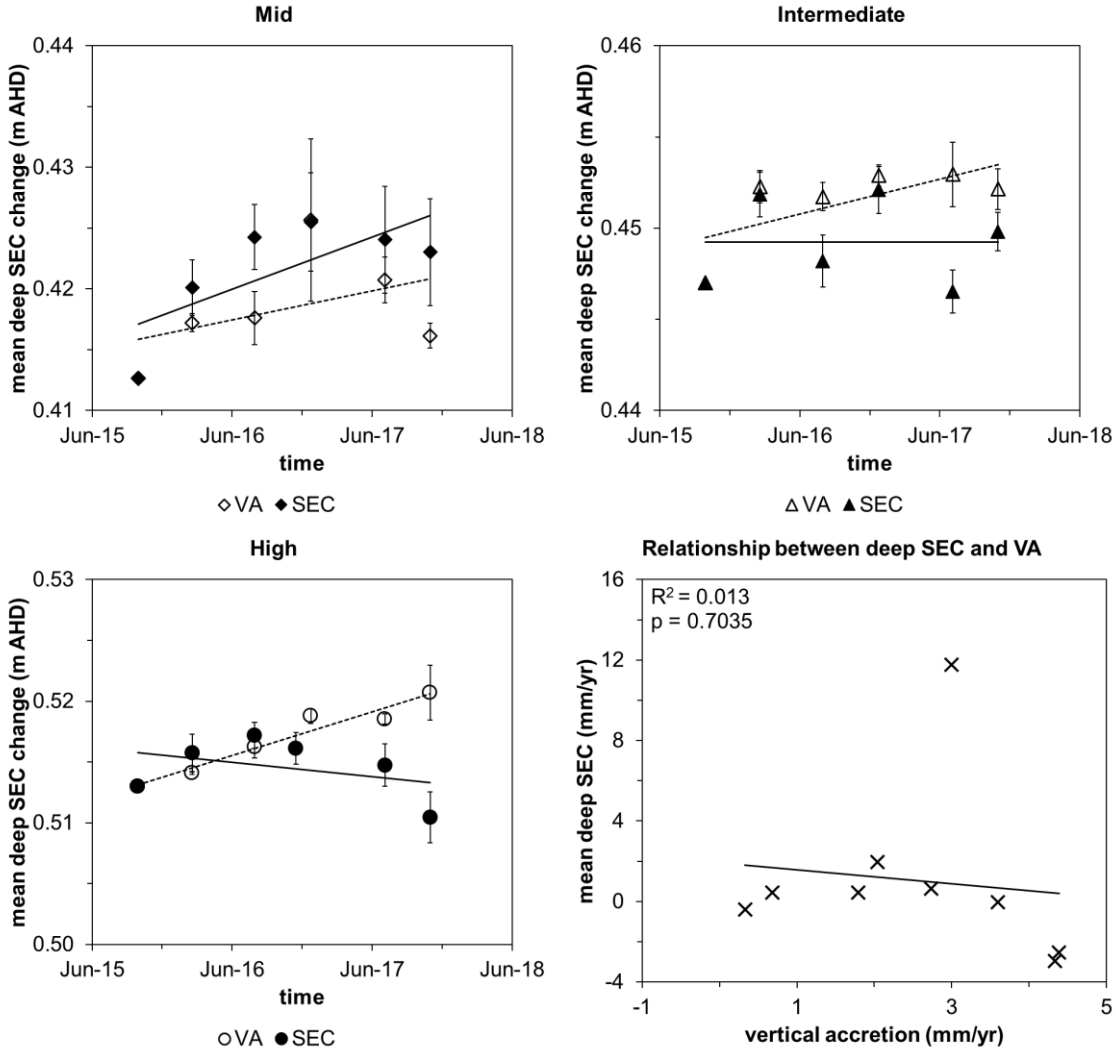

Figure 2.15: Changes in mean deep SEC and VA over the study period at mid, intermediate and high tidal position; and relationship between mean deep SEC and VA in all tidal positions.

Table 2.7: Total, shallow and deep autocompaction (rate and absolute ± standard error of mean) at individual rSETs in mid, intermediate (int.) and high tidal positions.

Deep-r-SET	Total Autocompaction		Deep Autocompaction		Shallow-r-SET	Shallow Autocompaction	
	Rate (mm/y)	Absolute (mm)	Rate (mm/y)	Absolute (mm)		Rate (mm/y)	Absolute (mm)
Mid 1	8.8 ± 2.5	18 ± 2.9	7.8 ± 1.6	16 ± 2.5			
Mid 2	-2.1 ± 3.0	-4.4 ± 0.68	-1.8 ± 1.7	-3.7 ± 0.58	Mid A	1.0 ± 3.1	2.1 ± 0.33
Mid 3	-0.25 ±.4	-0.5 ± 0.083	0.1 ± 5.0	0.1 ± 0.02	Mid B	-0.30 ± 2.2	-0.64 ± 0.10
Mean	2.1 ± 1.2	4.5 ± 0.70	2.0 ± 1.5	4.2 ± 0.66	Mean	0.35 ± 2.3	0.74 ± 0.095
Int. 1	-3.6 ± 1.6	-7.6 ± 1.2	-1.0 ± 1.1	-2.0 ± 0.31			
Int. 2	-0.72 ± 1.4	-1.5 ± 0.23	0.42 ± 0.83	0.87 ± 0.14	Int. A	-2.7 ± 0.74	-5.6 ± 0.88
Int. 3	-1.3 ± 1.9	-2.8 ± 0.44	-0.21 ± 1.7	-0.45 ± 0.07	Int. B	-1.1 ± 1.2	-2.4 ± 0.37
Mean	-1.9 ± 1.2	-4.0 ± 0.62	-0.25 ± 0.64	-0.52 ± 0.08	Mean	-1.9 ± 0.82	-4.0 ± 0.62
High 1	-6.9 ± 2.4	-15 ± 2.3	-1.2 ± 2.0	-2.6 ± 0.40			
High 2	-7.2 ± 1.9	-15 ± 2.4	-1.5 ± 1.0	-3.2 ± 0.50	High A	-5.6 ± 2.7	-12 ± 1.8
High 3	-0.019 ± 1.4	-0.040 ± 0.0063	-2.8 ± 1.9	-5.9 ± 0.92	High B	2.8 ± 1.6	5.7 ± 0.90
Mean	-4.7 ± 1.4	-9.9 ± 1.5	-1.9 ± 1.2	-3.9 ± 0.61	Mean	-1.4 ± 1.6	-3.0 ± 0.47

Shallow autocompaction

At intermediate and high tidal positions, the deviation in the degree of shallow SEC and VA increased over time resulting in rates of SEC being less than rates of VA (Fig. 2.16). Shallow surface elevation gain at mid tidal position was greater than VA indicating substrate expansion at this tidal position (Fig 2.16). The mean rate of shallow substrate expansion exceeds the mean rate of VA by 0.35 ± 2.3 mm/y at mid tidal position. The mean rate of shallow autocompaction was in the order of 1.4 ± 1.6 mm/y at the high tidal position (Table 2.7, only shallow autocompaction).

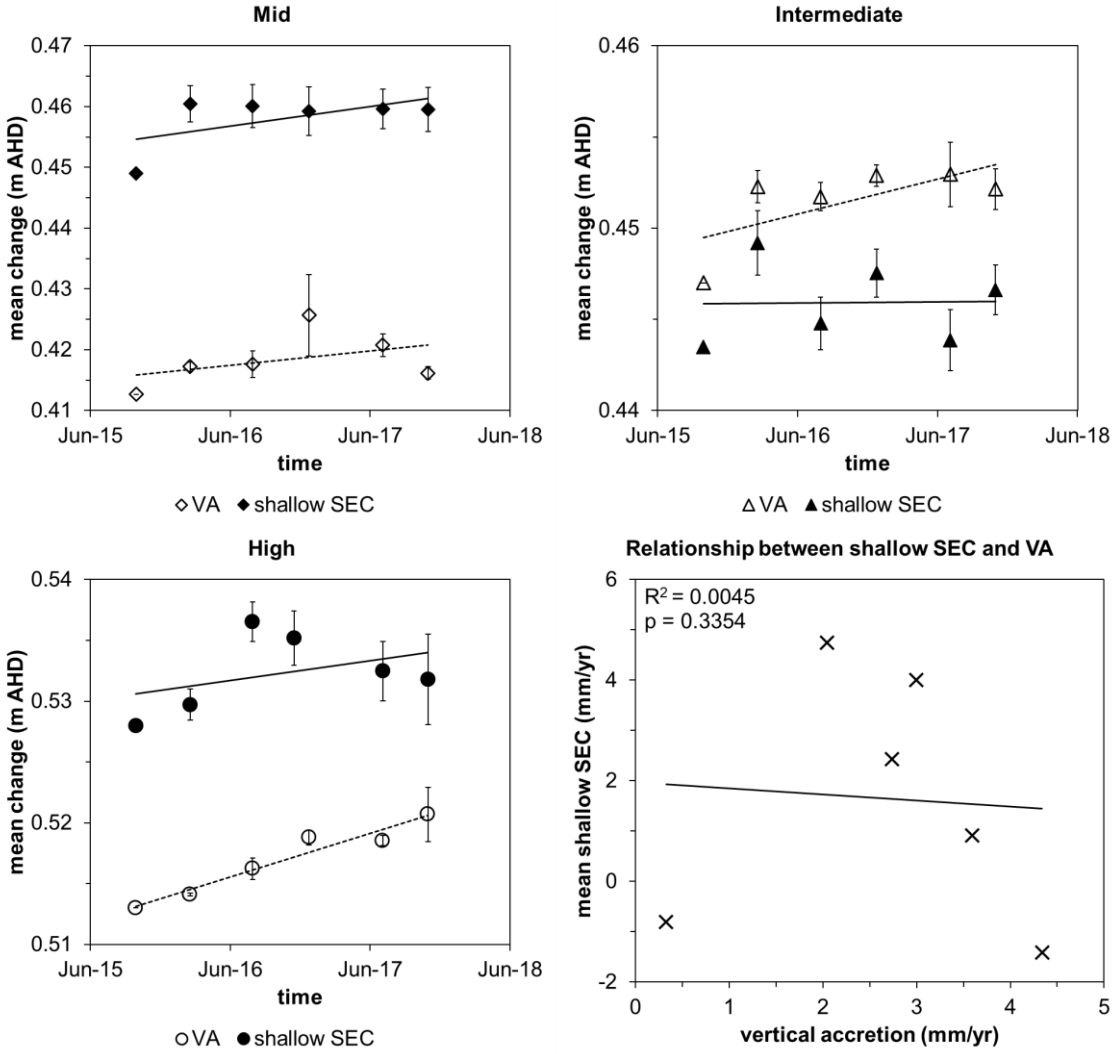

Figure 2.16: Changes in mean shallow SEC and VA over the study period at mid, intermediate and high tidal position; and relationship between mean shallow SEC and VA in all tidal positions.

The intermediate tidal position exhibited the highest rate of autocompaction of 1.9 ± 0.82 mm/y. Rates of shallow autocompaction varied over time ($p = 0.0412$) and within tidal positions over time ($p = 0.0137$), but not between tidal positions ($p = 0.2660$). Within tidal positions, significant difference between shallow-rSETs was identified only at the high tidal position ($p = 0.0158$). In general, the degree of shallow SEC and VA was not found to be significantly different ($p = 0.3354$) and a linear relationship could not be established between SEC and VA ($r^2 = 0.0045$ Fig. 2.16).

Deep autocompaction

Comparison of the deep and shallow-r-SETs indicated that there was no difference between measurement techniques ($p = 0.7218$) or the interaction effect over time ($p = 0.7412$), but a consistent pattern of variability was identified between the two measures over time ($p < 0.0001$) (Fig. 2.17). In the mid tidal position, 95 % of total zone expansion occurred in the deep zone at a magnitude of 2.0 ± 1.5 mm/y, while much of total autocompaction in the intermediate tidal position was associated with shallow autocompaction (Fig. 2.17 and Table 2.7, only deep autocompaction). Shallow autocompaction accounted for total autocompaction in the intermediate tidal position and very little deep zone change was detected over the study period (Fig. 2.17). Deep zone autocompaction occurred at a magnitude of 1.9 ± 1.2 mm/y accounting for about 40 % of total autocompaction of 4.7 ± 1.4 mm/y in the high tidal position (Fig. 2.17).

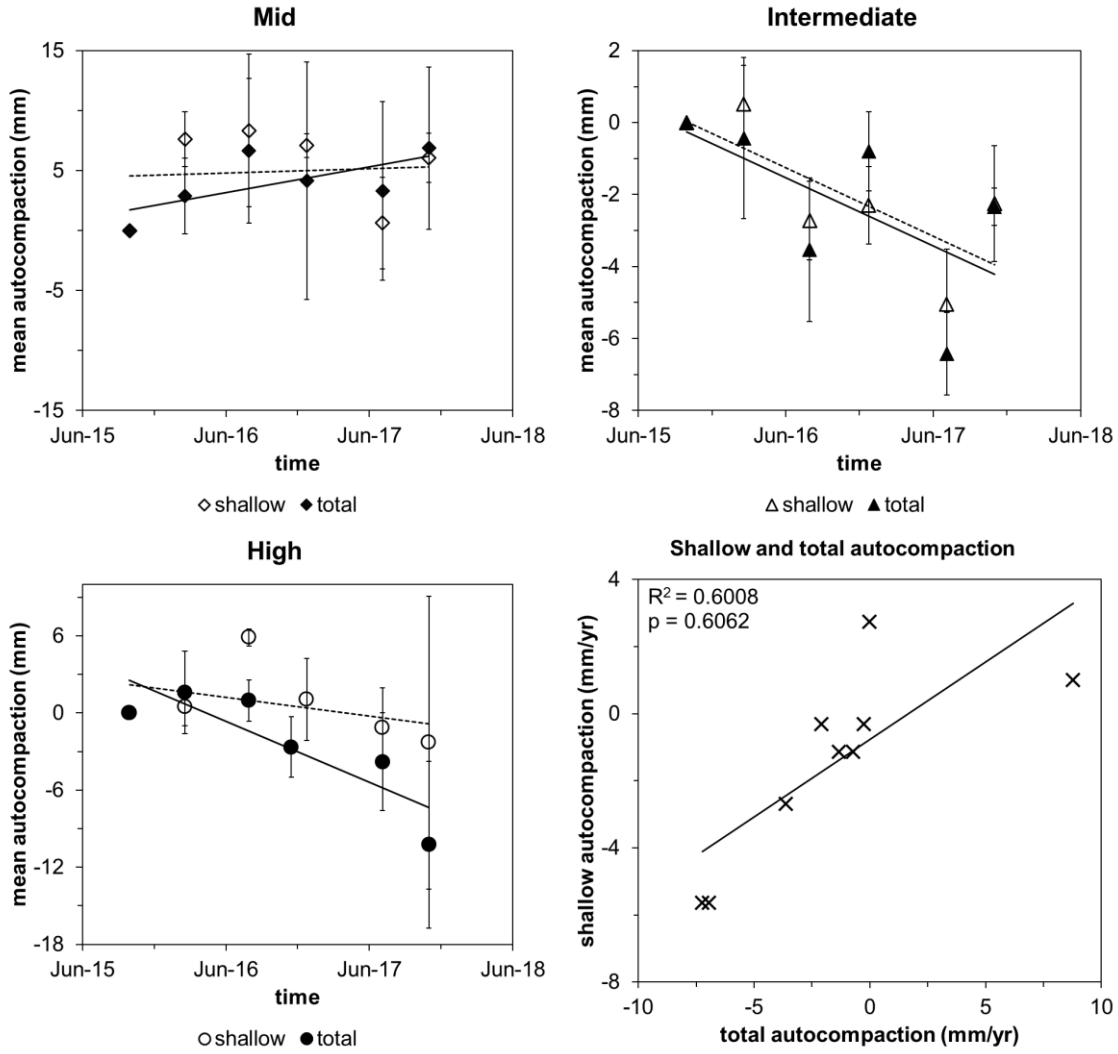

Figure 2.17: Changes in mean total and shallow autocompaction over the study period at mid, intermediate and high tidal position; and relationship between mean total autocompaction and shallow autocompaction in all tidal positions.

Statistical analysis further verified significant differences in deep autocompaction over time ($p = 0.0014$) and between high tidal position rSETs over time ($p < 0.0001$). In high tidal position half of the SE loss detected by d-rSETs 1 and 2 appeared to occur in the upper 35 cm as was detected by s-rSET A, while SE gain in the s-rSET B was approximately double detected by d-rSET 3, indicating that substantial deep zone subsidence occurred (Fig. 2.17). In general, shallow autocompaction contributed to 60 % ($r^2 = 0.6008$) of the total autocompaction and rates of change between the two were statistically similar over the period of analysis ($p = 0.6062$, Fig. 2.17). Therefore, autocompaction over the total sediment

profile primarily occurred in the upper 35 cm of the substrate (i.e. shallow autocompaction).

2.4.5. Sediment characteristics

Relatively high organic matter was measured in the shallow substrate of all tidal positions, but most prominently in the active root zone of the mid tidal position, which is dominated by mangroves (Fig. 2.18a). Organic matter content gradually decreased in all cores with depth, except in the high tidal position core where the amount of organic material in sediments 50 to 70 cm below the surface was at relatively high level compared to surface sample, and like that observed in the shallow substrate of the active root zone (Fig. 2.18a).

Belowground substrate was highly sandy, but high variation in sediment grainsize from 0 cm AHD to 70 cm AHD in all the cores was indicative of changing environmental conditions (Fig. 2.18a). Organic matter content was higher in muddy (silt and clay particles) substrates (Fig. 2.18c).

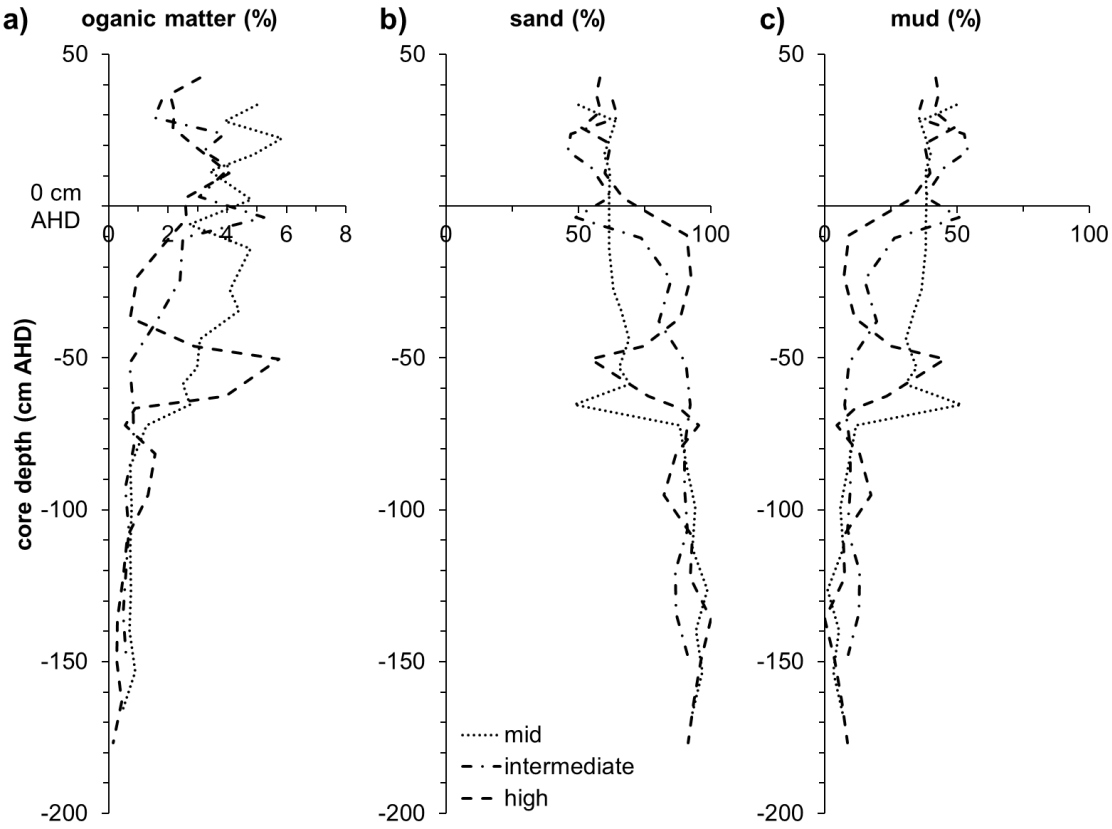

Figure 2.18: Belowground substrate (a) organic matter content, (b) percent sand composition; and (c) percent mud (silt and clay) composition in mid, intermediate and high tidal position.

Autocompaction correlated with substrate organic matter content and the sand to mud ratio. Little autocompaction (and some expansion) was observed in the mid tidal position where organic content was relatively high (Fig. 2.19a and b), which may be contributing to surface elevation gain at this site facilitated by deep zone root expansion by *Avicennia marina* roots. Increased autocompaction was associated with muddy substrates that had a low proportion or organic material (Fig. 2.19c), more specifically the shallow zones of intermediate and high tidal position. Very little autocompaction was observed in the deep zone of the intermediate tidal position that was very sandy and had very little organics (Fig. 2.19b and d) and elevation loss could be due to low organic contributions in the shallow zone of intermediate tidal position. The high autocompaction and associated loss of surface elevation at the high tidal position may be facilitated by consolidation and decomposition of organic matter detected at 60 cm AHD, despite

the high sand content at other depths within the substrate (Fig. 2.19b and d), which may have contributed to elevation loss in the high tidal position.

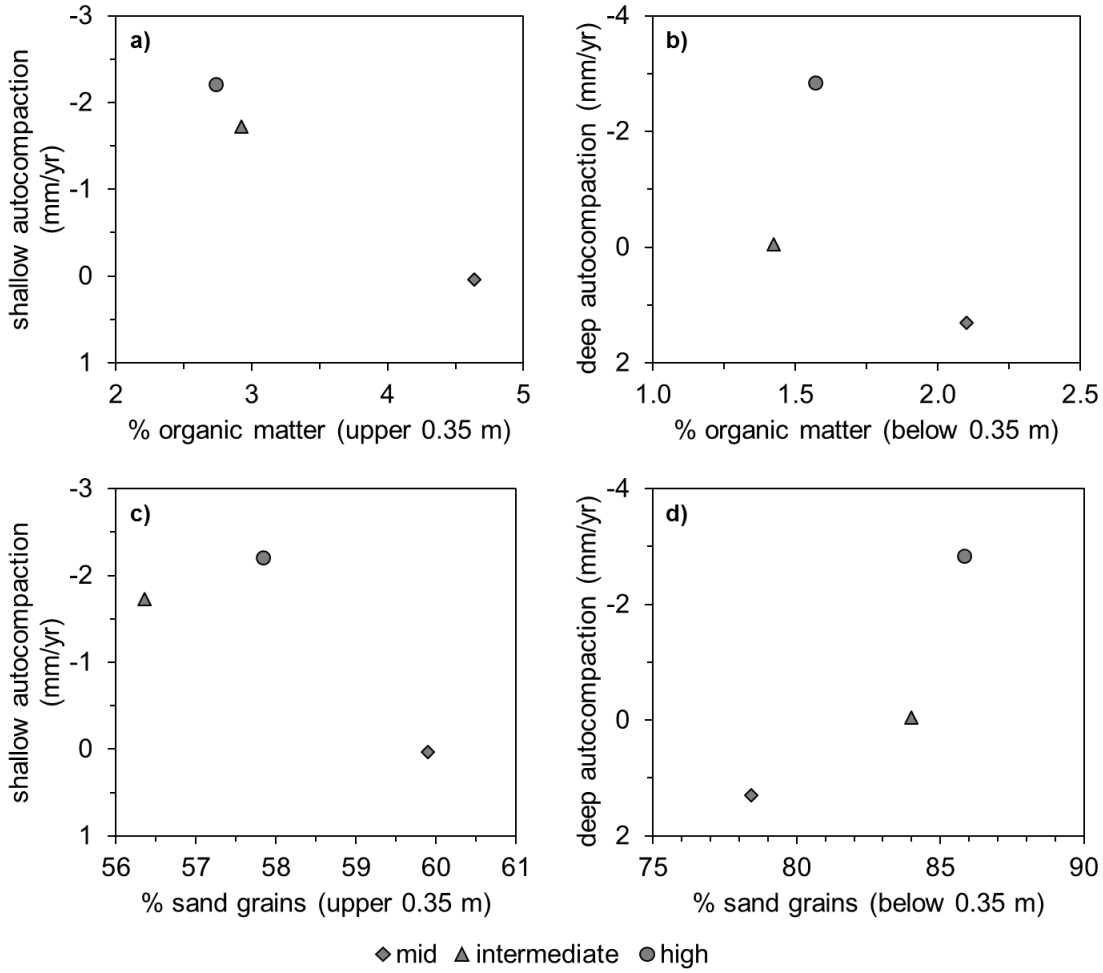

Figure 2.19: Relationship between organic matter content in the (a) upper 0.35 m substrate and shallow autocompaction, and (b) below 0.35 m substrate and deep autocompaction. Relationship between sandy substrate in the (c) upper 0.35 m and shallow autocompaction, and (d) below 0.35 m sandy substrate and deep autocompaction.

2.4.6. Relationships between surface elevation change, vertical accretion and belowground processes

SE dynamics of the different tidal positions was variably influenced by surface sediment additions, subsurface substrate expansion and/or autocompaction. Subsurface expansion was likely associated with root zone expansion. Autocompaction may be a result of decomposition of organic materials throughout

the total substrate profile (Fig. 2.20). In the high tidal position, deep and shallow autocompaction estimated at 1.9 ± 1.2 mm/y and 1.4 ± 1.6 mm/y, respectively, are collectively offsetting VA of 3.6 ± 0.45 mm/y, resulting in surface elevation fall of 2.5 ± 0.38 mm over the study period (see Table 2.8 for mean rates of change). At the mid tidal position, VA of 2.1 ± 1.7 mm/y and deep substrate expansion of 2.0 ± 1.5 mm/y contributed to SE gain of 8.9 ± 1.4 mm in two years. At intermediate tidal positions, shallow autocompaction offset VA, resulting in no net wetland surface elevation change over the study period. More specifically, the mid tidal position is increasing surface elevation with respect to MSL (m AHD), the high tidal position is losing elevation, and the intermediate tidal position is in a stable state with no net surface elevation change over the study period (Fig. 2.21).

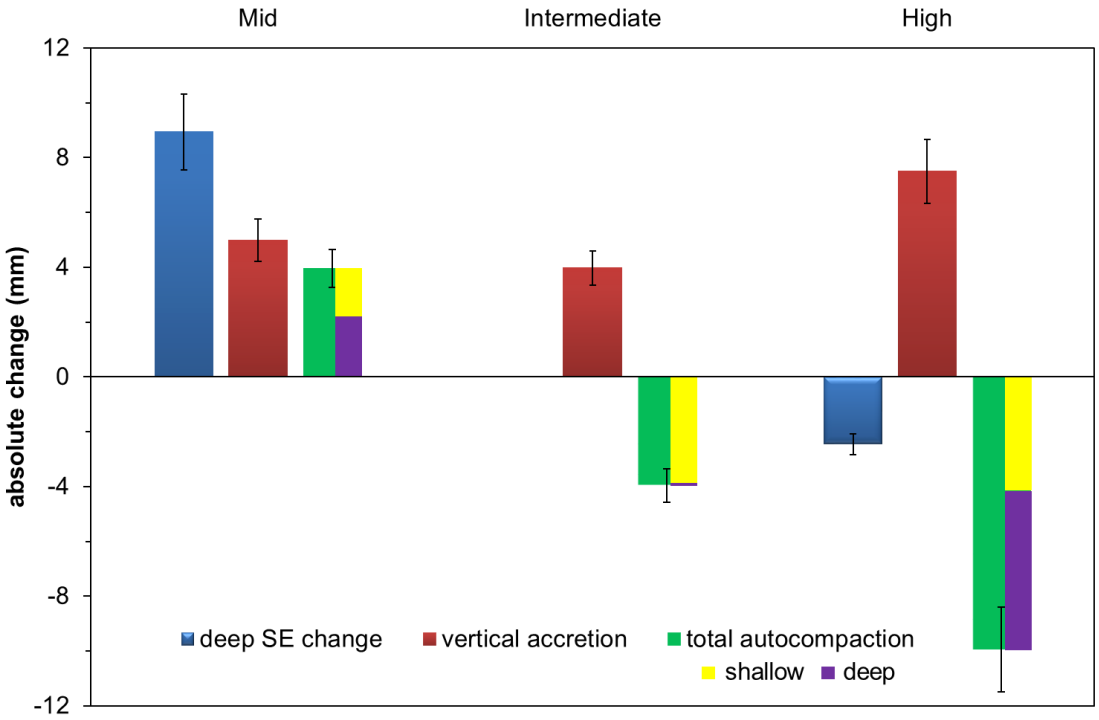

Figure 2.20: Surface elevation change in relation to VA, shallow and deep autocompaction.

Table 2.8: Mean rates of change observed in the wetland profile at mid, intermediate and high tidal positions.

Tidal position	Wetland profile	Deep SEC	Shallow SEC	Vertical accretion	Autocompaction		
					Total	Shallow	Deep
Mid	Depth (m)	0 - 6.7	0 - 0.35	surface	6.7	0.35	6.35
	Rate (mm/y)	4.3	3.2	2.1	2.1	0.35	2.0
	Error (± mm/y)	2.0	2.2	1.7	1.2	2.3	1.5
Intermediate	Depth (m)	15.2	0 - 0.35	surface	15.2	0.35	14.9
	Rate (mm/y)	0.0087	0.057	1.9	-1.9	-1.9	-0.3
	Error (± mm/y)	1.5	1.4	1.0	1.2	0.824	0.64
High	Depth (m)	11.8	0 - 0.35	surface	11.8	0.35	11.5
	Rate (mm/y)	-1.2	1.7	3.6	-4.7	-1.4	-1.9
	Error (± mm/y)	1.4	1.8	0.45	1.4	1.6	1.2

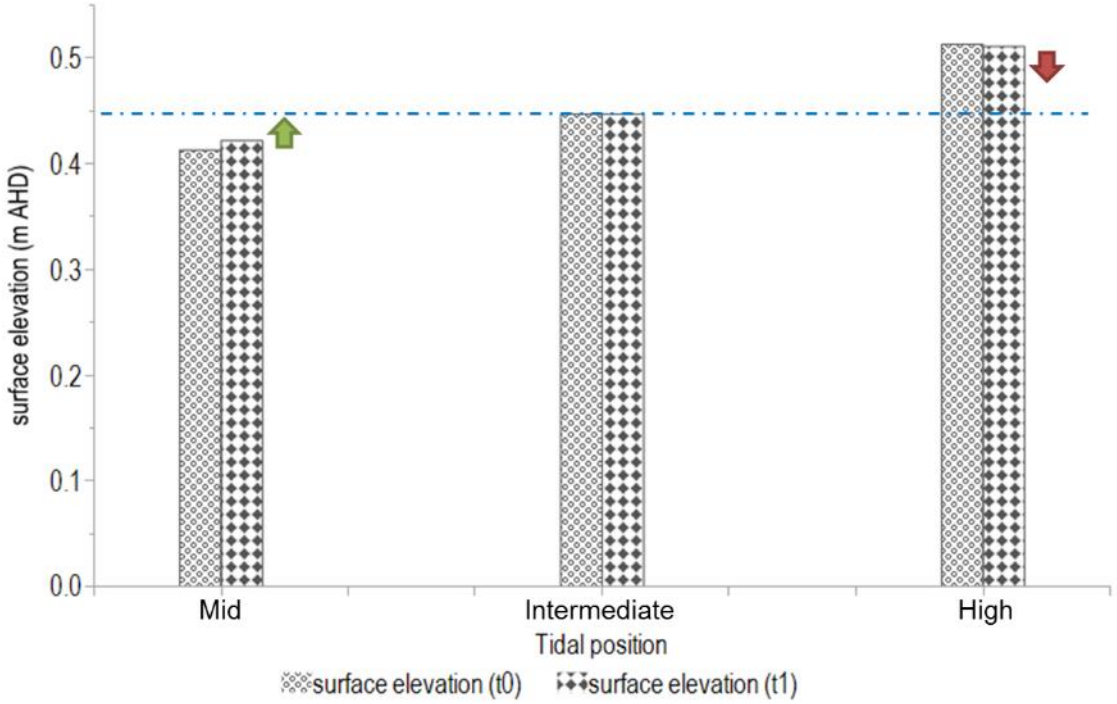

Figure 2.21: Surface elevation relative to MSL at approximately 0 m (AHD) in the different tidal positions at the time baseline measurements (t0) and after 2 years (t1).

Surface elevation change in the upper intertidal wetland environments of is a function of surface and subsurface processes. Surface elevation is increasing in the mid tidal position which has higher inundation frequency and SEC appears to be

driven by expansion of belowground substrate through mangrove root expansion. Sediment analyses confirm that the substrates are more organic then other tidal positions, in the order of 0.4 to 5.9 %, and characterised by fine-grained sediments. SE gain occurred at mid tidal positions despite lower rates of VA than other tidal positions and contrasted SEC observed in the high tidal position, where surface elevation was being lost, primarily due to high rate of autocompaction. Despite high rates of VA in this zone, organic matter content was lower in the substrate and sediments were dominated by coarse-grained sands. The intermediate tidal position exhibited an intermediary response with stable surface elevations over the study period as VA corresponded to the degree of autocompaction.

2.4.7. Relationship between surface elevation change and wetland elevation

SEC was related to tidal position with SE gain at mid tidal positions and SE loss at high tidal positions. A significant and negative relationship was established between SEC and wetland elevation ($r^2 = 0.3901$, $p = 0.0721$) (Fig. 2.22). SEC projection based on Eq. 2.2 for the next 18 years show that under current tidal conditions, mid tidal positions will continue to increase surface elevation, the high tidal position will continue decreasing surface elevation relative to MSL. The intermediate tidal position elevation remaining consistent in the first two years will start gaining elevation before flattening the wetland profile (Fig. 2.23). The model projects surface elevations will transition towards an elevation of approximately 0.47 – 0.48 m AHD across all zones, corresponding to the optimal elevation for mangrove vegetation.

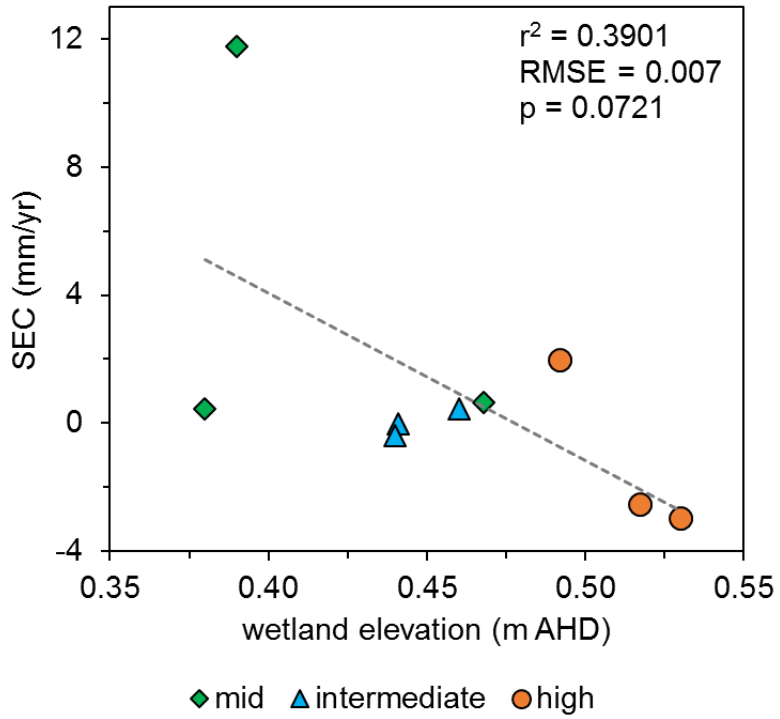

Figure 2.22: Relationship between SEC and wetland elevation (m AHD).

$$\textbf{predicted SEC} = \mathbf{0.0521} - \mathbf{0.1090} \times \mathbf{E} \qquad \text{Eq. 2.2}$$

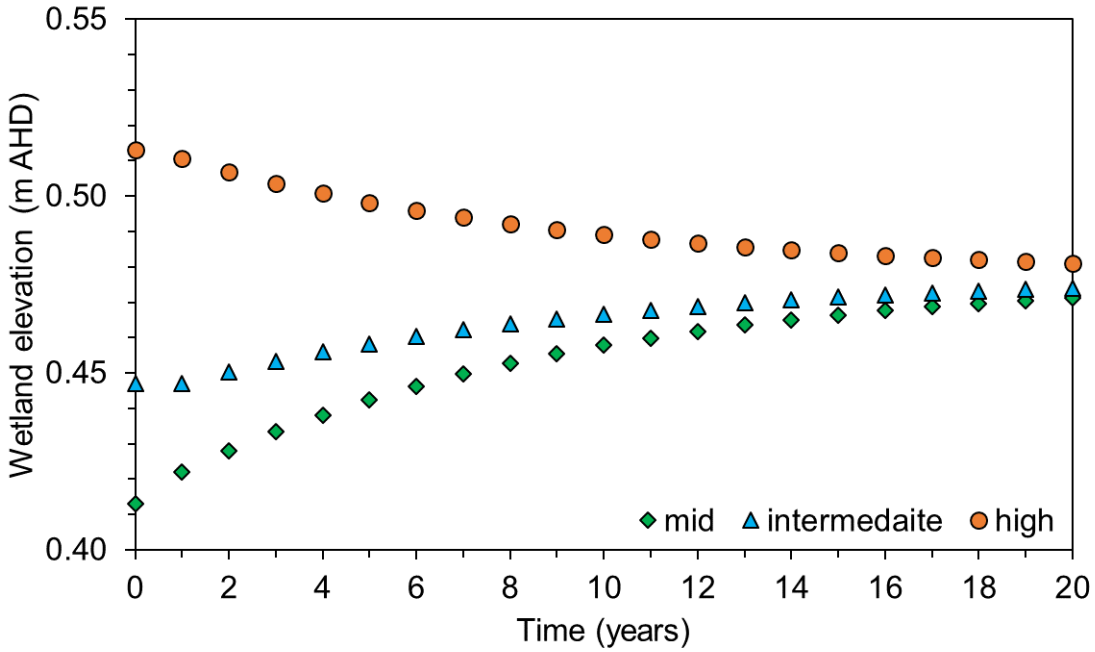

Figure 2.23: 20-year prediction of surface elevation change in the mid, intermediate and high tidal positions at Comerong Island.

2.5. Discussion

2.5.1. Surface elevation and vertical accretion dynamics

VA was not related to tidal position over this study period, which is different to other studies that have demonstrated that accretion equals inundation frequency because the longer a wetland surface is inundated, the more time there is for sediments to settle on the wetland surface (Fagherazzi et al., 2012; Kirwan et al., 2010; Pethick, 1981; Temmerman et al., 2004, 2003). SEC, however, was related to tidal position, and did not correlate with VA as SEC gain at lower elevations exceeded rates of VA, while SE loss occurred despite high rates of VA higher in the tidal frame. This relationship between VA and SEC was initially identified by Kaye and Barghoorn (1964). The increasing use of coupled SET-MH approaches means that it is now widely accepted that VA does not accurately indicate wetland elevations and cannot be solely used to project the response of coastal wetlands to SLR and that belowground processes should be further investigated to establish

relationships between surface elevation change and wetland processes (Cahoon et al., 2000b, 1995).

SE dynamics were positively related to tidal inundation frequency over the two-year study period. SE gain was highest at mid tidal positions located lower in the tidal frame dominated by mangroves (4.3 ± 2.0 mm/y). Very little SEC occurred at intermediate tidal position currently dominated by saltmarsh. SE loss was observed at tidal positions located higher in the tidal frame where mangrove has recently encroached upon saltmarsh (1.2 ± 1.4 mm/y). VA did not exhibit a strong relationship with patterns of inundation. VA corresponding to tidal position has been established for some time for saltmarshes (Allen, 2000; Pethick, 1981) and studies have demonstrated that VA tends to be higher where inundation occurs more frequently, corresponding to lower elevations within coastal wetlands (Lovelock et al., 2011; Rogers et al., 2006). However, in this study, relatively high amounts of VA were measured at high tidal positions. The source of this additional sediment was not established in this study, but two hypotheses are proposed. The additional sediment at high tidal positions may be terrigenous and delivered by overland flows near the wetland margin and onto the wetland surface. Terrigenous sediment sources have been identified in other studies and known to alter relationships between VA and sedimentation (Allen, 2000). Alternatively, the tidal energy along Comerong Bay may be pushing sediments along the funnel-like tidal creek that drains water up towards higher positions at the end of the tidal creek. This mechanism of sediment movement is similar to the modulation of VA on the basis of distance to tidal creeks, and has been incorporated into various models developed from empirical data (Temmerman et al., 2003).

2.5.2. Relationship between surface elevation dynamics and belowground processes

At mid tidal positions where inundation frequency was higher SEC was facilitated by both mineral and organic matter sediment addition. Mineral sediment addition

alone did not account for the SE gain observed and belowground root additions complemented mineral sediment addition in the mid tidal position. Mangrove, and in particular *Avicennia marina*, the dominant mangrove species at mid tidal positions, is known to accumulate organic material within substrates as they have extensive root systems (Adame et al., 2010; McKee, 2011). Expansion in belowground sediments was documented in Rogers et al. (2005a) in Homebush Bay, NSW in Australia where mangrove recovery in a regenerated mangrove forest resulted in substrate volume increase and an increase in surface elevation gain beyond what was related to vertical accretion alone.

Coupling the multi-depth rSETs provided an opportunity to explore relationships between surface and belowground processes occurring at different depths of the sediment profile as was demonstrated by Cahoon et al. (2011, 2002b), Lynch et al. (2015), and Whelan et al. (2009, 2005). VA was offset by shallow autocompaction in the intermediate tidal position where there would have been additions that equalled the losses and resulted in no net gain in shallow root zone volume. Cahoon et al. (2011, 1995) and Whelan et al. (2009) demonstrated that shallow zone substrate volume change as a result of hydrological shrink and swell can have a considerable influence on surface elevation dynamics. In this research little autocompaction was observed in the sandy substrate of the deep zone, as sandy sediments are less compressible, it did not contribute to any SEC in the intermediate tidal position. No autocompaction was observed in the shallow sandy substrate of the mid tidal position but root growth in this zone likely contributed to SE gain, as demonstrated by other studies (Cahoon, 2006; Cahoon and Lynch, 1997).

At the high tidal position, SE decline was observed despite higher rates of VA. This was attributed to autocompaction modulating VA. This may be a mechanism, as proposed by Rogers et al. (2019), that ensures that wetland elevations remain within the tidal frame for as long as possible until all the vertical space has been filled with mineral sediments that are no longer compactable/compressible.

Autocompaction high tidal position may have been facilitated by decomposition of older organic material, such as mangrove roots preserved beneath the saltmarsh vegetation, as consolidation of larger grainsizes would be limited in highly sandy substrate. The decomposition of mangrove roots preserved beneath saltmarsh vegetation has been proposed in other studies (Saintilan et al., 2009). The low inundation frequency at high tidal positions creates more aerobic conditions that can also facilitate decomposition of organic materials in belowground sediments (McKee et al., 2012; Rogers et al., 2019a).

2.5.3. Relationship between surface elevation change and wetland elevation

Modelling of the wetland surface under stable sea level conditions indicated that the relationship between SEC and inundation frequency contributes to the development of broad intertidal wetland surface, with all initial tidal positions transitioning towards a similar wetland elevation over time. The SEC predictive model showed that surface elevation transitions towards a stable elevation based on inundation conditions documented in this study. Interestingly, the predicted elevations of 0.47 – 0.48 m AHD correspond to the current vertical distribution of mangrove (approximately 0.3 – 0.6 m AHD). The projected pattern of wetland elevation transitioning towards an elevation suitable for mangrove corresponds to a regional trend of saltmarsh converting to mangrove. In addition, mangrove expansion into saltmarsh has been observed at this study location in a previous study (Chafer, 1998a).

The mid tidal position with mangrove increased elevation at a faster rate than wetland vegetation higher in the tidal frame. This indicates that the mid tidal position has a greater capacity to increase elevations, which can contribute to the flattening of the intertidal platform. In addition, mangrove movement into saltmarsh may therefore be an adaptation to increase tidal inundation frequency at higher tidal positions that comes about as the tidal platform flattens over time.

Recent studies have also demonstrated elevation gain properties of mangrove over a 20-year SET record and encroachment into saltmarsh as a consequence of relative SLR (Rogers et al., 2019b).

SLR was not included as a variable within the model, however SLR alters the negative feedback relationship between SEC and tidal inundation by altering inundation frequencies as demonstrated in other studies (Fagherazzi et al., 2012; Pethick, 1981; Saintilan et al., 2009). Inferring the effect of SLR can be achieved by considering the projected SEC where inundation frequency is higher. In this study, both mineral and organic matter additions significantly contributed to SEC where inundation frequency was high. This mechanism of SE gain may be triggered when SLR increases inundation frequencies, until the rate of SEC corresponds to the rate of SLR. A balance between rates of SLR and SEC or VA has been proposed as a crucial requirement for wetland stability (Allen, 2000; Cahoon et al., 1999; Woodroffe, 2018a). Over time VA and SEC will decline as wetland surfaces progressively increase in the tidal frame (Cahoon et al., 2006). Results from this study indicate that tidal positions supporting mangrove have a higher capacity to adjust to SLR and imply that mangrove expansion into saltmarsh is a crucial adaptation mechanism that is triggered by SLR.

2.6. Conclusion

Coupling of deep- and shallow-rSET-MH revealed that belowground processes, both deep and shallow, had a significant influence on surface elevation dynamics across upper intertidal zones of Comerong Island. Consequently, VA was not related to SE gain or inundation frequency indicating that belowground processes had a significant influence on SE dynamics over very short timescales at Comerong Island. Root additions in belowground sediments increased wetland elevation beyond that attributed by VA as VA alone could not maintain wetland elevation at this site. Shallow zone autocompaction in intermediate tidal position was offsetting VA and resulted in no net change in SE at this site, whereas shallow and deep zone

autocompaction and/or consolidation of materials offset VA at high tidal positions contributing to SE loss.

SEC showed a positive relationship to inundation frequency. SE increased at mid tidal positions where mangrove dominate, intermediate tidal positions showed very little change in SEC, high tidal positions lost elevation, even though VA was relatively high over the study period. Projection of the relationships between SEC and tidal inundation indicated transition towards a stable elevation, corresponding to the current vertical distribution of mangrove vegetation in the next 18 years. The next chapter explores if this relationship between SEC and inundation frequency exists over decadal-scale SET-MH and provides the opportunity to assess the projections of SEC in this chapter.

Chapter 3

Surface elevation dynamics in coastal wetland over decadal timescales

3.1. Introduction

Surface elevations dynamics of coastal wetlands is a consequence surface and subsurface processes. Over long timescales and under the influence of sea-level rise (SLR), coastal wetlands vegetated by mangrove and saltmarsh can adjust their position in the tidal frame vertically (by building elevation upwards) or horizontally (translating landwards) (Kirwan and Temmerman, 2009; Rogers et al., 2013b). Wetland vegetation can vertically adjust wetland surface through mineral sedimentation, organic matter addition from vegetation and subsurface processes, such as organic matter decomposition and shrink-swell of substrates. These processes influencing surface elevation dynamics is regulated by the tidal inundation frequency (Chapter 2), where surface elevation change is proportional to inundation frequency over very short timescales. The 15-year prediction model further suggested that under stable tidal conditions the wetland elevation will evolve towards a relatively flat surface in the tidal frame, where additions to substrate balances the loss in substrate volume, particularly at high tidal positions.

SLR will alter this relationship between surface elevation change and tidal inundation and influence surface elevation adjustment capabilities of coastal wetlands to SLR as suggested by various models that indicate that coastal wetlands can develop a relatively flat surface if sedimentation rates promoting surface elevation gain occurs at a higher rate than relative SLR (Allen, 2000; Morris et al., 2002; Mudd et al., 2004; Woodroffe, 2018a). If mineral sedimentation is higher than organic matter additions and the rates are higher than relative SLR, the wetland surface will adjust more rapidly to relative SLR (Fagherazzi et al., 2012;

Mudd et al., 2004). This study provides the opportunity to consider whether tidal inundation remains the dominant control on surface elevation change and identify whether the influence of SLR on tidal patterns has influenced patterns of surface elevation dynamics over decadal timescales using a network of SET-MHs that has been in place for almost 20 years. This was useful in understanding the processes contributing to coastal wetland stability across the tidal frame at a given time, and when wetland vegetation may move to higher elevations or maintain their position within the tidal frame.

The aim of this chapter was to establish relationships between surface elevation (SE), vertical accretion (VA) and belowground processes, such as autocompaction in different tidal positions over approximately two decades using SET-MH technique. The outcome of this work will be an indication of the spatial controls on surface elevation dynamics in mangrove and saltmarsh over decadal timescales. The above aim was achieved through;

i. Quantifying decadal scale surface elevation, vertical accretion and belowground autocompaction dynamics within mangrove, mixed and saltmarsh vegetation;
ii. Measuring variable position of the wetland substrate within the tidal frame by analysing inundation patterns;
iii. Establishing relationships between surface elevation change and wetland substrate within the tidal frame; and
iv. Identify relationships between temporal variations in surface elevation change and mean monthly sea levels.

Surface elevation dynamics promoting wetland stability relative to mean sea level and spatial distribution patterns of wetland vegetation in the tidal frame over longer timescales can be useful when planning wetland response to future SLR. As tides influence surface elevation dynamics across the tidal frame (Chapter 2), its effect on vertical accretion and belowground autocompaction was quantified based on the inundation regime of the wetland surface relative to the localised

tidal datum using water level loggers was established over decadal timescales. This chapter provides the opportunity to identify whether the stable tidal conditions modelled in Chapter 2 is evident at decadal timescale using the longer-term SET-MHs in southeast Australian coastal wetlands.

3.2. Methods

3.2.1. Site selection and study design

A network of SET-MH have been installed at Minnamurra River, Cararma Inlet and Currambene Creek (Fig. 3.1) since 2000-2001 (Rogers et al., 2006). This study builds upon the surface elevation change (SEC), vertical accretion (VA) and autocompaction dynamics in coastal wetlands dominated by mangrove and saltmarsh using the SET-MH technique work undertaken by Rogers et al. (2006). The near-annual measurements since then make them amongst the longest records of surface elevation (SE) and VA in Australia. The SET benchmarks were established in replicates of three in mangrove and saltmarsh at Minnamurra River and Cararma Inlet, and an additional set was installed in mixed mangrove and saltmarsh vegetation at Currambene Creek (Table 3.1). SETs were installed in different vegetation zones to capture the vertical accretion rates, SE dynamics and belowground substrate expansion/consolidation processes based on vegetation type and their position in the landscape.

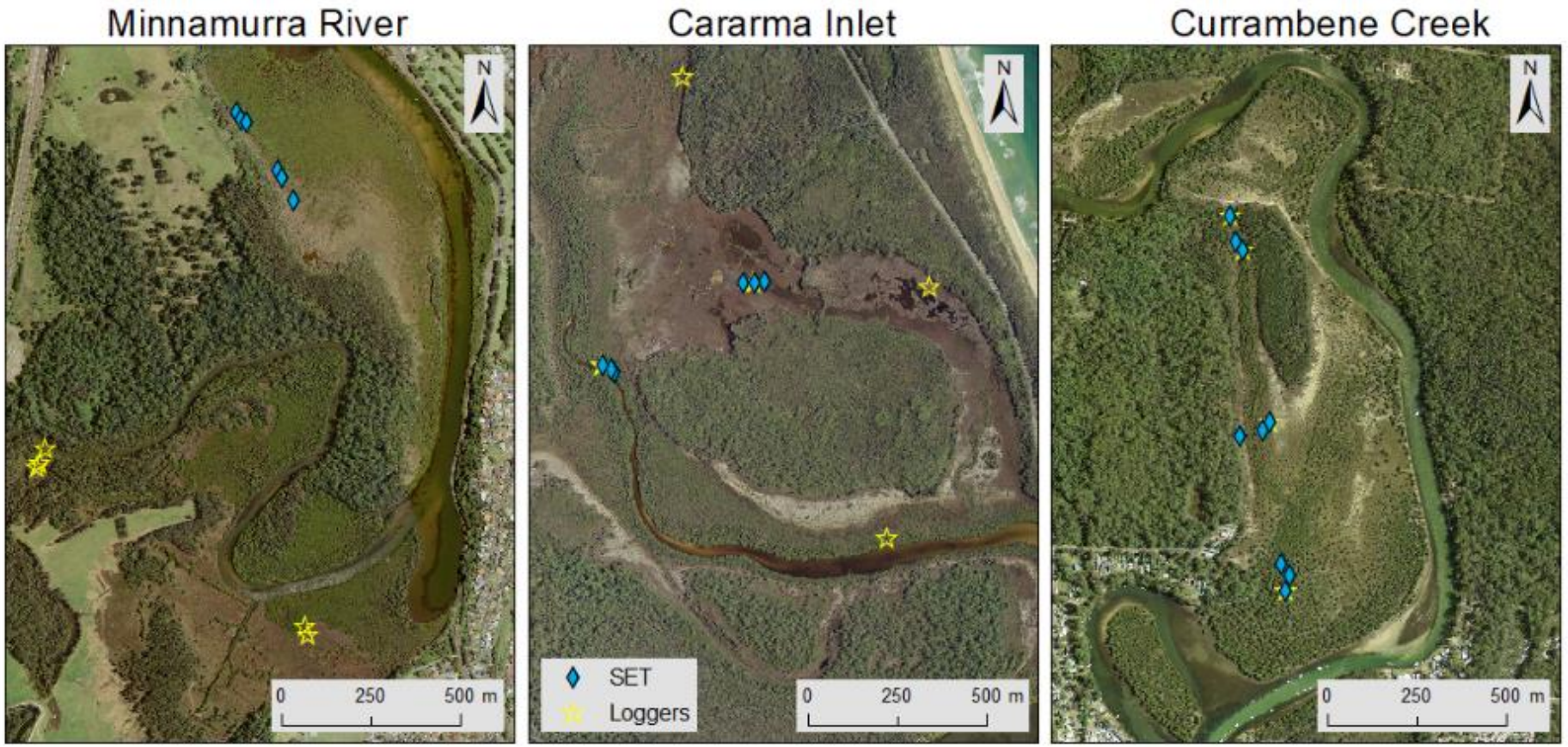

Figure 3.1: Location of the original-SETs and water level loggers at Minnamurra River (a), Cararma Inlet (b) and Currambene Creek (c).

Table 3.1: SET tidal position and vegetation type in Cararma Inlet, Currambene Creek and Minnamurra River.

Site	SET	Location		Former vegetation type	Present vegetation type
		Latitude	Longitude		
Minnamurra River	Mangrove 1	-34° 37' 29.81121''	150° 50' 35.13227''	*Avicennia marina* (tall)	*Avicennia marina* (tall)
	Mangrove 2	-34° 37' 30.50760''	150° 50' 35.59639''		
	Mangrove 3	-34° 37' 30.78881''	150° 50' 36.07574''		
	Saltmarsh 1	-34° 37' 35.19150''	150° 50' 39.40756''	Mixed saltmarsh (*Sporobolus virginicus, Juncus kraussii*/ *Sarcocornia quinqueflora*)	Mixed vegetation (*Sporobolus virginicus, Juncus kraussii*/ *Avicennia marina*)
	Saltmarsh 2	-34° 37' 35.83863''	150° 50' 39.96654''		
	Saltmarsh 3	-34° 37' 37.93477''	150° 50' 41.11732''		
Cararma Inlet	Mangrove 1	-34° 59' 14.80685''	150° 46' 15.81920''	*Avicennia marina* (tall)	*Avicennia marina* (tall)
	Mangrove 2	-34° 59' 14.52839''	150° 46' 15.37759''		
	Mangrove 3	-34° 59' 14.09675''	150° 46' 14.51186''		
	Saltmarsh 1	-34° 59' 6.77826''	150° 46' 32.51597''	*Sarcocornia quinqueflora*	*Sarcocornia quinqueflora*
	Saltmarsh 2	-34° 59' 6.96347''	150° 46' 31.43007''		
	Saltmarsh 3	-34° 59' 6.88908''	150° 46' 30.24039''		
Currambene Creek	Mangrove 1	-35° 1' 8.96393''	150° 40' 1.47418''	*Avicennia marina* (tall)	*Avicennia marina* (tall)
	Mangrove 2	-35° 1' 7.54778''	150° 40' 2.12498''		
	Mangrove 3	-35° 1' 6.54205''	150° 40' 1.16820''		
	Mixed 1	-35° 0' 54.82446''	150° 39' 56.94484''	Mixed mangrove/ saltmarsh	Dominated by *Avicennia marina*
	Mixed 2	-35° 0' 53.63311''	150° 40' 0.22667''		
	Mixed 3	-35° 0' 34.78972''	150° 39' 56.40026''		
	Saltmarsh 1	-35° 0' 54.82446''	150° 39' 56.94484''	Mixed saltmarsh (*Sarcocornia quinqueflora*/ *Juncus kraussii*)	Mixed mangrove/ saltmarsh (*Sarcocornia quinqueflora*/ *Avicennia marina)*
	Saltmarsh 2	-35° 0' 53.63311''	150° 40' 0.22667''		
	Saltmarsh 3	-35° 0' 34.78972''	150° 39' 56.40026''		

Wetland elevation of each SET relative to the localised tidal datum (Australian Height Datum) was measured using RTK-GPS, and inundation frequency was measured using water level loggers.

3.2.2. Surface elevation change, vertical accretion and autocompaction

The network of SET-MHs were installed using the procedure of the installation

outlined in Rogers ((2004), Section 5.2.1). Wooden frames were constructed around each benchmark for access during installation and ensured minimum disturbance to the surface surrounding the benchmark. At each benchmark, a 6 m aluminium pipe was driven into the ground using a hammer to a depth of about 4 – 4.5 m (depth of refusal). The remaining pipe was cut leaving about 25 cm above the surface. A readymade insert pipe was attached to the top of the aluminium pipe to which the SET arm attached to when taking SE measurements. Since their instalment, the mixed vegetation zone SETs at Currambene Creek are now dominated by mangroves, whereas the saltmarsh SETs at Minnamurra River now has a mixed mangrove and saltmarsh vegetation type. Mangrove invading saltmarsh has been reported at many other sites in SE Australia, including these (Kelleway et al., 2016; Rogers et al., 2006, 2005b; Saintilan et al., 2009; Saintilan and Williams, 1999; Saintilan and Wilton, 2001).

Surface elevation change

Surface elevation change (SEC) is determined using the SETs to indicate the change in substrate volume occurring between the base of the benchmark and the surface (Fig. 3.2). SE measurement was carried out by attaching the SET mechanical arm to the receiver and re-occupying each of N, E, S, W orientations of the existing measurement. Pins were placed into the corresponding holes of the horizontal arm and held with clips to ensure the rods did not pierce the wetland surface. The mechanical arm was levelled using the bubble-level on the horizontal bar after which the pins are carefully lowered onto the surface. The pins returned to the same orientation and measurement of the surface at the same points was taken every time. The height of the pins protruding above the arm was measured and recorded in millimetres (mm). When taking SE measurements, any obstacles such as, pins landing on vegetation roots (e.g. mangrove pneumatophores) and/or crab hole or crab mounds were excluded from the data. The change in the measured pin length above the horizontal arm reflected relative change in SE over the study period.

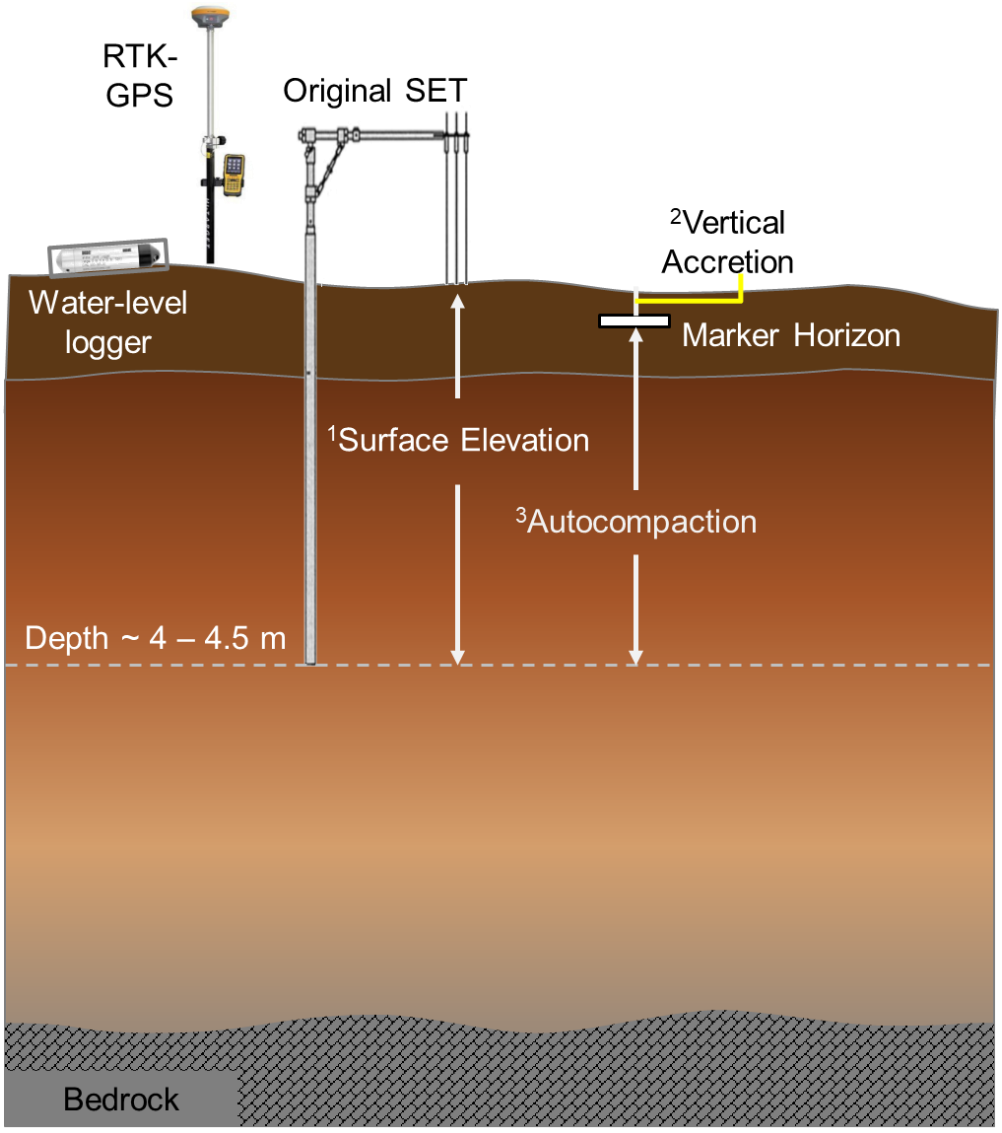

Figure 3.2: Overview of wetland vertical profile determined by an original SET-MH and other hydrological properties considered for this study. The SET was used to measure [1]SE change, MH was used to determine [2]vertical accretion and collectively the SET-MH technique was used to determine belowground [3]autocompaction. Wetland SE relative to the localised tidal datum (m AHD) measured using an RTK-GPS. Water -level loggers was used to determine the inundation regime of wetland surface at the location of the different SET and vegetation zones.

Vertical accretion

Vertical accretion is determined using MH to indicate the amount of sediment delivered to the wetland surface by tides (Fig. 3.2). Feldspar marker horizons were used to determine vertical accretion occurring in the different vegetation

communities in all the three study sites. MHs were placed in replicates of three at each SET monitoring station at the time initial SE measurement (Cahoon et al., 2000b). Vertical accretion was measured at the same time as SE measurements. Any feldspar was seen on the surface was recorded as 0 amount of vertical accretion since the last measurement, but if no feldspar was seen on the surface then a small section of the MH was extracted with a knife within the area marked out as MH location (making efforts to avoid any compaction of the sediments), in hope MH might be found below the surface. Thickness of sediment accumulated on top of the feldspar was measured using a ruler and recorded as vertical accretion in millimetres. If no feldspar was retrieved, then no measurement was recorded for that time.

The feldspar was not an ideal MH particularly in the mangrove sites at some of the sites, particularly at Minnamurra River and Cararma Inlet as it is highly erosive in mangroves due to mineral weathering and bioturbation (Lovelock et al., 2011; Lynch et al., 2015; Rogers et al., 2013b). At these sites, MH had to be replaced over the years, hence consecutive VA measurements could not be achieved over the study period. At Minnamurra River, VA in the saltmarsh vegetation was reported between 11/09/2001 and 12/05/2011, but in the mangrove only between 11/09/2001 and 5/08/2003. At Cararma Inlet, saltmarsh VA was recorded for the whole study period (02/08/2001 to 08/03/2017), but in mangrove VA was recorded only between 2/08/2001 and 14/08/2003. Likewise, mixed and saltmarsh VA was reported for the whole study period (3/02/2001 and 07/03/2017) at Currambene Creek, whilst mangrove VA was reported only between 3/02/2001 and 4/02/2004.

3.2.3. Surface elevation, vertical accretion and autocompaction

SE data for each SET was averaged to generate a mean value for each arm direction. Values for each orientation within a zone were pooled to generate a mean and standard error for each SET at each time step. VA data were pooled from

each MH station and across a vegetation zone. Linear regression analysis was subsequently undertaken to determine the 'best fit' rate of SEC and VA over the study period). Plots were generated by adjusting SE increments based on wetland elevation corrected to AHD.

Belowground autocompaction was the difference between SEC and VA. Autocompaction data was also pooled from each SET and across a zone. Linear regression analyses were subsequently undertaken to determine the 'best fit' rates of autocompaction change for each SET and across each zone.

Statistical differences in SEC and VA between different SET zones and over the study period were determined using ANOVA of repeated measurements in JMP statistical software. Probability factor (p-value) of interaction over time, between zone and within a zone, and between and within tidal positions over time from ANOVA were reported on the three most common univariate tests. If the univariate chi-square sphericity test was significant (< 0.05) then f-test or Wilks' lambda p-values were reported, but if it not significant then univariate unadjusted epsilon values were reported. All ANOVA test results are presented in supplementary data (Appendix 2). A relationship was sought between SEC and VA and SET zones and was correlated to inundation frequency, which was used as a proxy for position in the tidal frame, to establish whether tidal position or sea level had an influence on SEC and VA. ANOVA was used to establish relationships between SEC and VA over time and correlated with sea level data from the nearest tide gauge.

3.2.4. Tidal position

Tidal inundation frequency of the different vegetation communities was used as a proxy for tidal position of SETs in the tidal frame. Inundation frequency of the vegetation zones at Minnamurra River, Cararma Inlet and Currambene Creek was determined using water-level loggers using the procedure described in Section 2.3.2. Five water level loggers were deployed in different locations at Cararma Inlet

including SET benchmarks, and four water level loggers were deployed adjacent to mangrove, mixed and saltmarsh SETs at Currambene Creek. At Minnamurra River water level loggers (eight) were placed strategically in different vegetation zones to measure inundation frequency across the intertidal zone (Fig. 3.1).

Water level data was collected over a few months from each study site. Data was checked for accuracy and calibrated to ensure that inundation depths were 0 cm when the wetland surface was not inundated. Sensor depth was adjusted to AHD using RTK-GPS elevations. Percent inundation was quantified as the number of times the logger was submerged in relation to the times the sensor was exposed.

Table 3.2: Water level loggers used to collect inundation frequency data from Minnamurra River, Cararma Inlet and Currambene Creek.

Study area	Logger	SET Location	Vegetation type	Wetland elevation (m)	Sensor depth threshold (m)	Period of analysis
Minnamurra River	Min_WL2		Mangrove	0.395	0.002	14/07 – 30/08/2018
	Min_WL3		mixed vegetation	0.556	0.012	
	Min_WL5		mixed vegetation	0.460	0.015	
	Min_WL8		Mangrove	0.306	0.02	
	Min_WL9		Saltmarsh	0.670	0.04	
	Min_WL10		mixed vegetation	0.509	0.01	
	Min_WL11		mixed vegetation	0.557	0.012	
Cararma Inlet	WL2	Mangrove3 Saltmarsh2	mixed vegetation	0.408	0	08/2014 – 02/2015
	WL3		Mangrove	0.366	0.01	
	WL4		Saltmarsh	0.786	0.005	
	WL5		Saltmarsh	0.778	0.04	
	WL6		mixed vegetation	0.677	0.005	
	WL3	Mangrove3	Mangrove	0.326	0.02	7/04 – 19/11/2016
	WL4	Saltmarsh2	Saltmarsh	0.803	0.01	
Currambene Creek	CC_WL1	Mangrove1	Mangrove	0.302	0.015	14/05 – 26/12 2015
	CC_WL2	Saltmarsh2	Mangrove	0.648	0.007	
	CC_WL3	Mix2	Saltmarsh	0.656	0.01	
	CC_WL4	Saltmarsh3	Saltmarsh	0.795	0.005	

Water level data for each tidal position was adjusted to m AHD and plotted against water level data from the nearest tide gauge station (Fig. 3.1). For Minnamurra River the Minnamurra tide gauge (station number 214442) was used, whilst for

Cararma Inlet and Currambene Creek the Jervis Bay HMAS Creswell (station number 214470) was used.

Statistical differences in inundation frequency at different wetland elevations derived from RTK-GPS was identified using ANOVA in JMP. Additional values were included in the data set to define the tidal boundary conditions (Table 2.1). A relationship between inundation frequency and wetland elevation was developed using a logistic model as this model accommodated the tidal patterns defined by the boundary conditions. Model suitability was assessed based on the coefficient of determination (r^2), RMSE, AICc and BIC, and was subsequently used to predict the inundation frequency of individual study sites. The logistic model was used to predict the inundation frequency of each SET, which was used to classify their position in the tidal frame into mid, intermediate and high tidal position.

3.2.5. Influence of tidal position on surface elevation dynamics

SEC was correlated with predicted tidal inundation frequency of the SETs to establish relationships between SE dynamics in coastal wetland and tidal position. VA rates were not considered in this relationship as it was only measured in intermediate and high tidal positions. Tidal positions of SETs whose predicted inundation frequency did not correlate with the observed inundation frequency were excluded from this analysis as the variation in observed and predicted inundation frequencies indicated unusual patterns in the hydrological properties of the study sites. SETs that has undergone considerable vegetation change (Table 3.1) were also excluded from this analysis. Average rate of SEC was used to create relationships between predicted inundation frequency for SETs that showed significant differences between within individual tidal positions (for example, Cararma Inlet mangrove SETs).

3.2.6. Influence of sea level on surface elevation dynamics

Temporal variation in SEC was correlation to mean monthly sea level data from the nearest tide gauge for each study site. For Minnamurra River, the Minnamurra tide gauge (station number 214442) was used, whilst for Cararma Inlet and Currambene Creek the Jervis Bay HMAS Creswell (station number 214470) was used (Table 3.3). Sea level data was converted to Australian Height Datum (AHD) and plotted against mean SEC in different tidal positions. For correlation purposes, SEC data for Minnamurra River were reduced to mean value per year due to the high frequency of measurements at this site between 2010 and 2011.

3.3. Results

3.3.1. Surface elevation change, vertical accretion and autocompaction

Minnamurra River

An increase in surface elevation was observed in the mangrove and saltmarsh SETs at Minnamurra River over the 15-year study period (Fig. 3.3a). However, SEC varied between zones ($p = 0.0159$), over time ($p < 0.0001$), and within zones over time ($p < 0.0001$). The mangrove zone has been increasing surface elevation at a mean rate of 1.31 ± 0.31 mm/y (Fig. 3.3b), whilst the saltmarsh zone has been increasing surface elevation at only about 0.52 ± 0.07 mm/y (Fig. 3.3c, see Table 3.3 for rates and absolute SEC). The mangrove SETs behaved like each other ($p = 0.4049$) but showed variation over time ($p = 0.0004$) with a mean surface elevation gain of 20 ± 1.3 mm in almost 16 years. Similarly, variation in saltmarsh SEC was observed over the study period ($p = 0.0094$) but SEC between SETs remained relatively consistent ($p = 0.2496$), despite SET1 increasing SE at 1.3 ± 0.11 mm/y, whilst the rate of SEC remained relatively low and increased at about

0.13 mm/y over the same period (Table 3.3). The mangrove SETs behaved different to each other, but there was a higher mean rate of SEC, whilst the saltmarsh SETs behaved more consistently and with a lower mean rate of SEC. In all zones, the rate of SEC varied over time, indicating that there was a not a consistent process contributing to SEC at Minnamurra River.

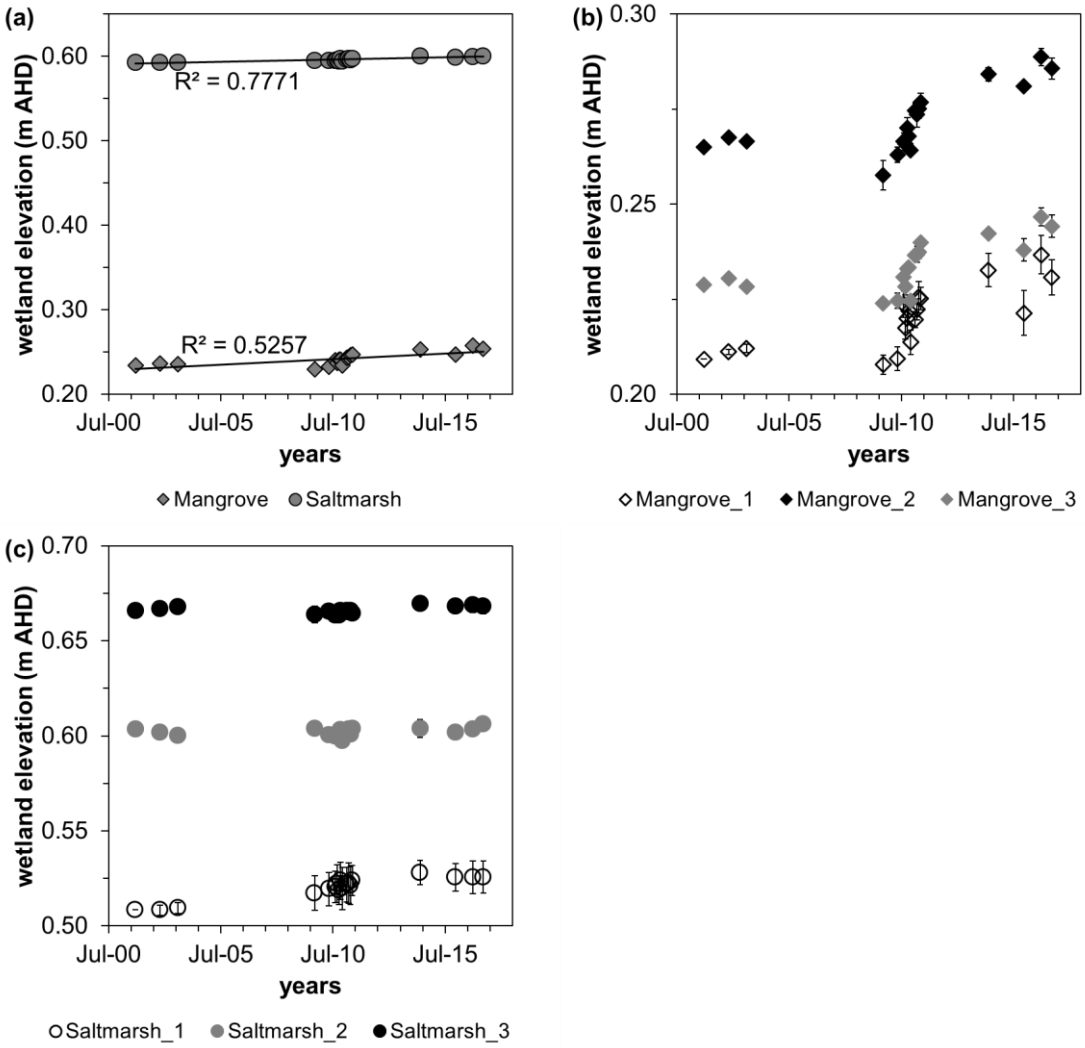

Figure 3.3: (a) Average surface elevation change in mangrove and saltmarsh vegetation at Minnamurra River between 2001 and 2017. SEC measured at each SET in (b) mangrove and (c) saltmarsh zone.

Table 3.3: Absolute (mm) and rate of change (mm/y) (± standard error of the mean) of surface elevation change quantified at individual SETs and mean for mangrove and saltmarsh zone (11/09/2001 to 15/03/2017), and vertical accretion and autocompaction change at individual saltmarsh SETs and mean for saltmarsh zone (11/09/2001 to 12/05/2011) at Minnamurra River. MH was not detectable after 3 years in the mangrove zone and are not reported.

Vegetation	Surface elevation change		Vertical accretion		Autocompaction	
	Absolute	Rate	Absolute	Rate	Absolute	Rate
Mangrove 1	23 ± 1.5	1.5 ± 0.32				
Mangrove 2	22 ± 1.4	1.4 ± 0.36				
Mangrove 3	16 ± 1.1	1.0 ± 0.30				
Mean	20 ± 1.3	1.3 ± 0.31				
Saltmarsh 1	20 ± 1.3	1.3 ± 0.11	7.8 ± 0.75	0.80 ± 0.79	11 ± 1.0	1.1 ± 0.80
Saltmarsh 2	2.0 ± 0.13	0.13 ± 0.12	3.7 ± 0.36	0.39 ± 0.78	-0.29 ± 0.028	-0.030 ± 0.80
Saltmarsh 3	1.9 ± 0.13	0.13 ± 0.10	3.1 ± 0.30	0.32 ± 0.42	-3.5 ± 0.34	-0.36 ± 0.41
Mean (2001 – 2011)	4.0 ± 0.39	0.41 ± 0.09	5.3 ± 0.51	0.55 ± 0.69	-1.3 ± 0.12	-0.13 ± 0.69
Mean (2001 – 2017)	8.1 ± 0.53	0.52 ± 0.07				

The mean rate of VA in the saltmarsh over the period (i.e. 2001 – 2011) remained relatively consistent over the study period ($p = 0.3902$), between SET-MHs ($p = 0.3010$) and within MHs over time ($p = 0.5197$) (Fig. 3.4a). A mean rate of saltmarsh accretion of 0.55 ± 0.69 mm/y was observed over the study period (see Table 3.3 for VA in saltmarsh). As MH were readily dispersed in the mangrove zone, VA is not reported for the mangrove zone. Autocompaction in the saltmarsh zone, however, did vary over the analysis period ($p = 0.0167$), but the rate of VA remained relatively consistent between SET-MHs ($p = 0.3594$) and within SET-MHs over time ($p = 0.6830$) was reported (Fig. 3.4b). Despite no significant difference between SET-MHs, SET-MH1 was increasing belowground substrate volume at a rate of 1.1 ± 0.80 mm/y, whilst relatively stable rates of autocompaction occurring SET-MH2 and 3 (Table 3.3).

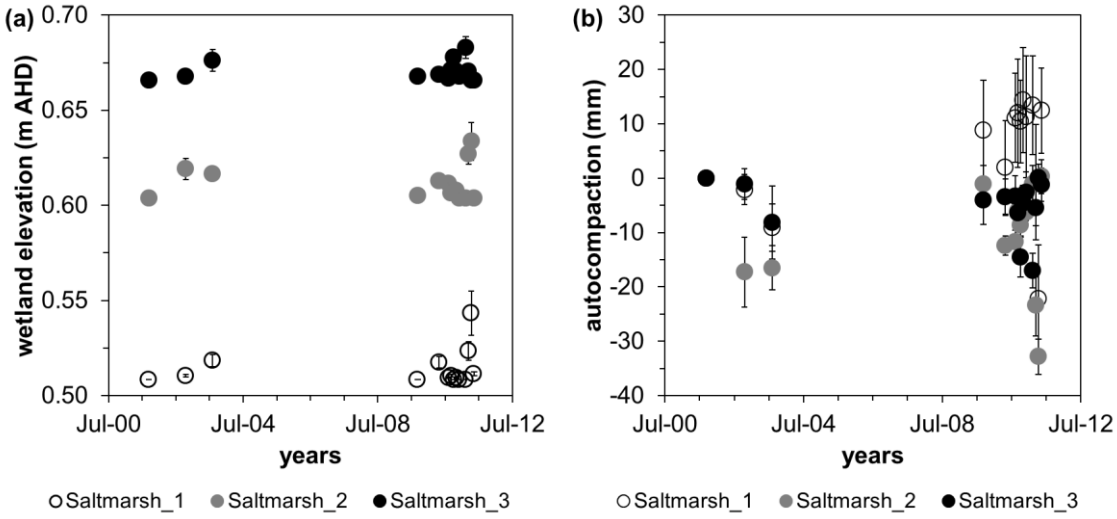

Figure 3.4: (a) Vertical accretion and (b) autocompaction at Minnamurra River in saltmarsh.

SEC in the mangrove zone increased at a higher rate than the saltmarsh zone (Fig. 3.5). In the saltmarsh, the degree of SEC and VA was different between 2001 and 2011 ($p = 0.0099$), over time ($p = 0.0059$) and interaction between the variables over time ($p = 0.0188$) (Fig. 3.5). The variability in VA and SEC remained relatively consistent over this period, where SEC of 0.41 ± 0.09 mm/y was a product of VA that occurred at a mean rate of 0.55 ± 0.69 mm/y (Fig. 3.5). Autocompaction of 0.13 ± 0.69 mm/y was offsetting VA by about 24 % but resulted in an overall surface elevation gain in the saltmarsh zone of 8.1 ± 0.53 mm over the whole study period (2001 – 2017).

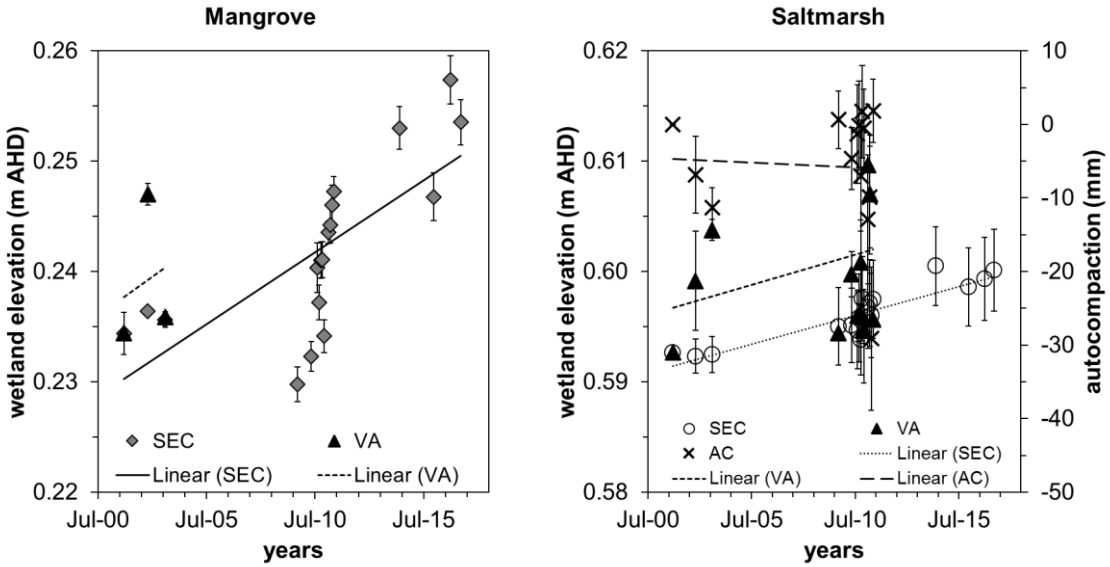

Figure 3.5: Mean SEC in relation to initial VA in the mangrove zone. Relationship between SEC, VA, and autocompaction in the saltmarsh zone at Minnamurra River.

Cararma Inlet

Mangrove was increasing SE at a rate of 1.9 ± 0.25 mm/y that is higher than the rate at which saltmarsh is increasing SE of 1.2 ± 0.28 mm/y (Fig. 3.6a). Statistical analysis showed no significant difference between vegetation zones ($p = 0.3689$ Fig. 3.8b and c). However, differences in SEC were identified over time ($p < 0.0001$) and within a zone over time ($p = 0.0002$, Table 3.4). SEC in the mangrove zone SETs was highly variable ($p < 0.0001$). In this site, SET 2 increased surface elevation at a rate of 4.0 ± 0.44 mm/y over the study period, whilst very little change was observed in SET1 and 3 (Table 3.6). SEC remained comparatively consistent between the saltmarsh SETs but variation was observed over time ($p = 0.0136$) with a mean surface elevation gain of 19 ± 2.3 mm over 15 years.

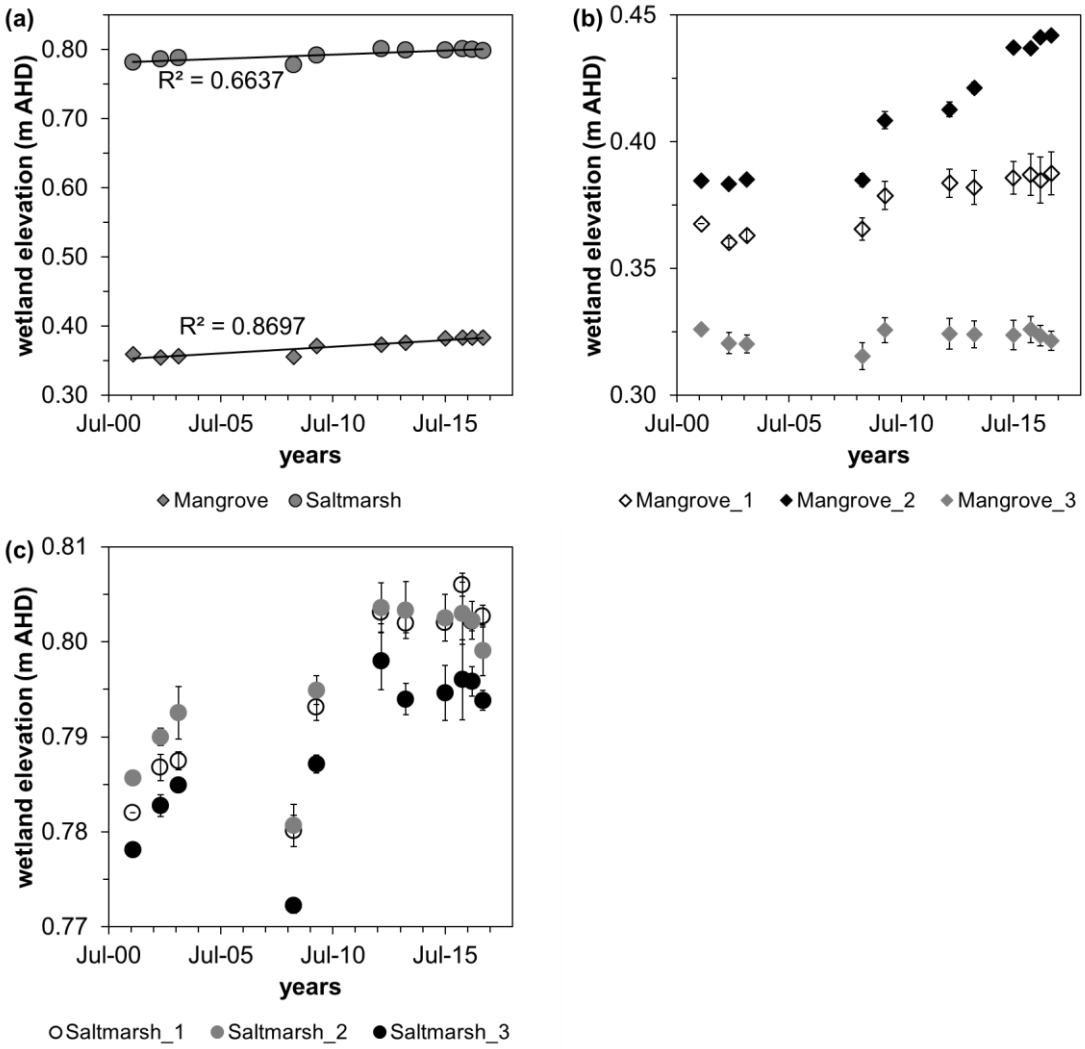

Figure 3.6: (a) Mean surface elevation change in mangrove and saltmarsh vegetation at Cararma Inlet. SEC measured at each SET in (b) mangrove and (c) saltmarsh zone.

Table 3.4: Absolute (mm) and rate of change (mm/y) (± standard error of the mean) of surface elevation, vertical accretion and autocompaction change quantified at individual Cararma Inlet SETs (02/08/2001 to 08/03/2017). MH was not detectable after 3 years in the mangrove zone and are not reported.

Vegetation	Surface elevation change		Vertical accretion		Autocompaction	
	Absolute	Rate	Absolute	Rate	Absolute	Rate
Mangrove 1	24 ± 3.2	1.7 ± 0.22				
Mangrove 2	57 ± 7.7	4.0 ± 0.44				
Mangrove 3	1.7 ± 0.23	0.12 ± 0.18				
Mean	28 ± 3.7	1.9 ± 0.25				
Saltmarsh 1	22 ± 2.8	1.4 ± 0.26	23 ± 2.7	1.5 ± 0.24	-1.5 ± 0.18	-0.096 ± 0.37
Saltmarsh 2	16 ± 2.0	1.0 ± 0.29	15 ± 1.8	0.98 ± 0.10	0.70 ± 0.086	0.045 ± 0.36
Saltmarsh 3	17 ± 2.1	1.1 ± 0.31	19 ± 2.3	1.2 ± 0.19	-1.9 ± 0.24	-0.012 ± 0.31
Mean	19 ± 2.3	1.2 ± 0.28	19 ± 2.3	1.2 ± 0.12	-0.90 ± 0.11	-0.058 ± 0.31

VA in the saltmarsh zone occurred at a rate of 1.2 ± 0.12 mm/y and accreted at a rate of 19 ± 2.3 mm of sediments over the study period (Table 3.4 and Fig. 3.7a). As Variation between SEC and VA was not identified (p= 0.2095), but significant differences were identified over time (p <0.0001) and within SETs over time (p <0.0001). Autocompaction of 0.90 ± 0.11 mm was observed in the saltmarsh zone with little change between the SET-MH monitoring stations (Fig. 3.7b, p = 0.9649), but it was statistically significant over time (p = 0.0737).

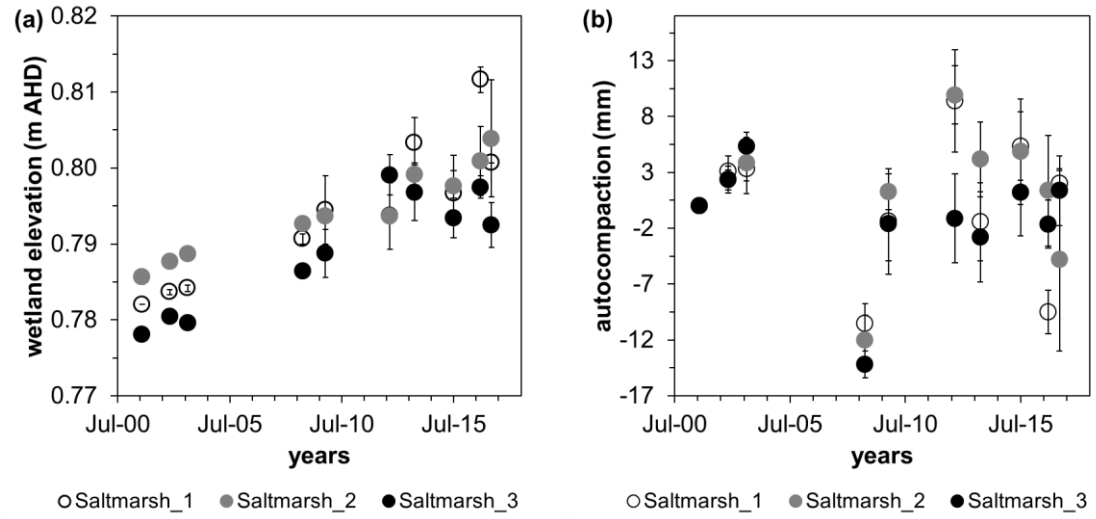

Figure 3.7: (a) vertical accretion and (b) autocompaction at Cararma Inlet saltmarsh zone.

Surface elevation in mangrove increased at a higher rate than saltmarsh and was estimated to be in the order of 1.9 ± 0.25 mm/y. The early VA measurements

showed an increasing pattern of VA in this zone that may have contributed to surface elevation gain in this zone (Fig. 3.8). There was no significant difference between VA and SEC in saltmarsh (p = 0.3501) and SEC of 1.2 ± 0.31 mm/y was a product of VA occurring at a rate of 1.2 ± 0.12 mm/y (Fig. 4.8). Autocompaction was undetectable (p = 0.5285) indicating that belowground processes had very little impact on the surface elevation dynamics in the saltmarsh zone of Cararma Inlet which may be associated with sandy substrate.

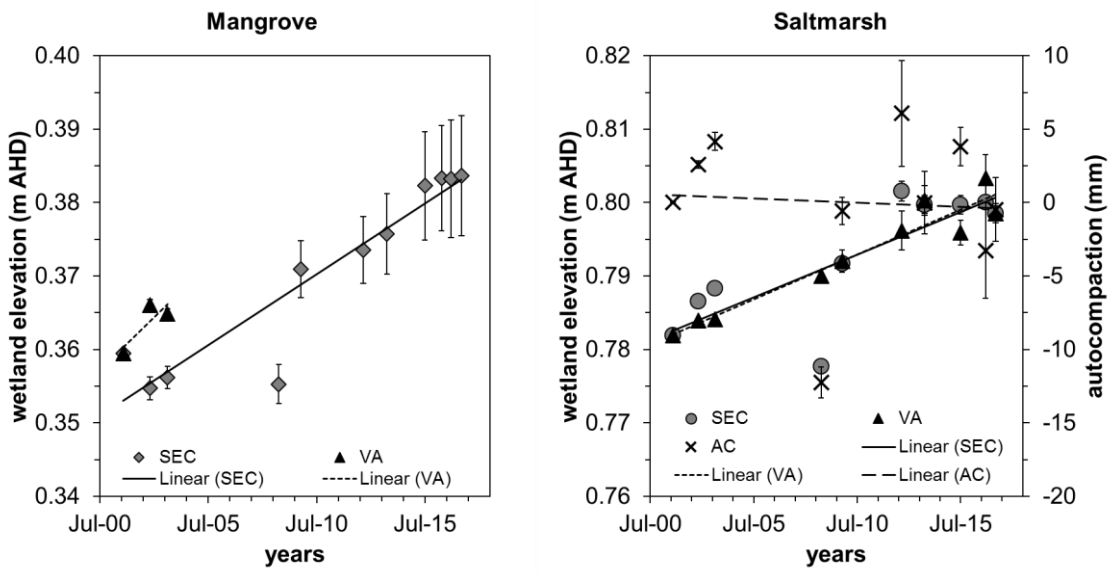

Figure 3.8: Mean SEC in relation to initial VA in the mangrove zone. Relationship between SEC, VA, and autocompaction in the saltmarsh zone at Cararma Inlet.

Currambene Creek

SEC was highly variable between vegetation zones at Currambene Creek, where very little SEC was observed in mangrove SETs, SE gain was measured in mixed SETs and some elevation decline for SETs in saltmarsh (Fig. 3.9a). The variation in SEC over time was observed in all zones (p = 0.0005), within zones over time (p = 0.0003) and between vegetation zones (p = 0.0102). Variation in the rate of SEC within zones was mainly associated with the mangrove SETs (Fig. 3.9b, p = 0.0230). These differences occurred despite relatively low changes in surface elevation in the mangrove SETs, where SET1 was gaining elevation at 0.35 ± 0.12

mm/y, SET2 was losing elevation at a rate of 0.12 ± 0.08 mm/y, whilst very little change was observed at SET3 (Table 3.5).

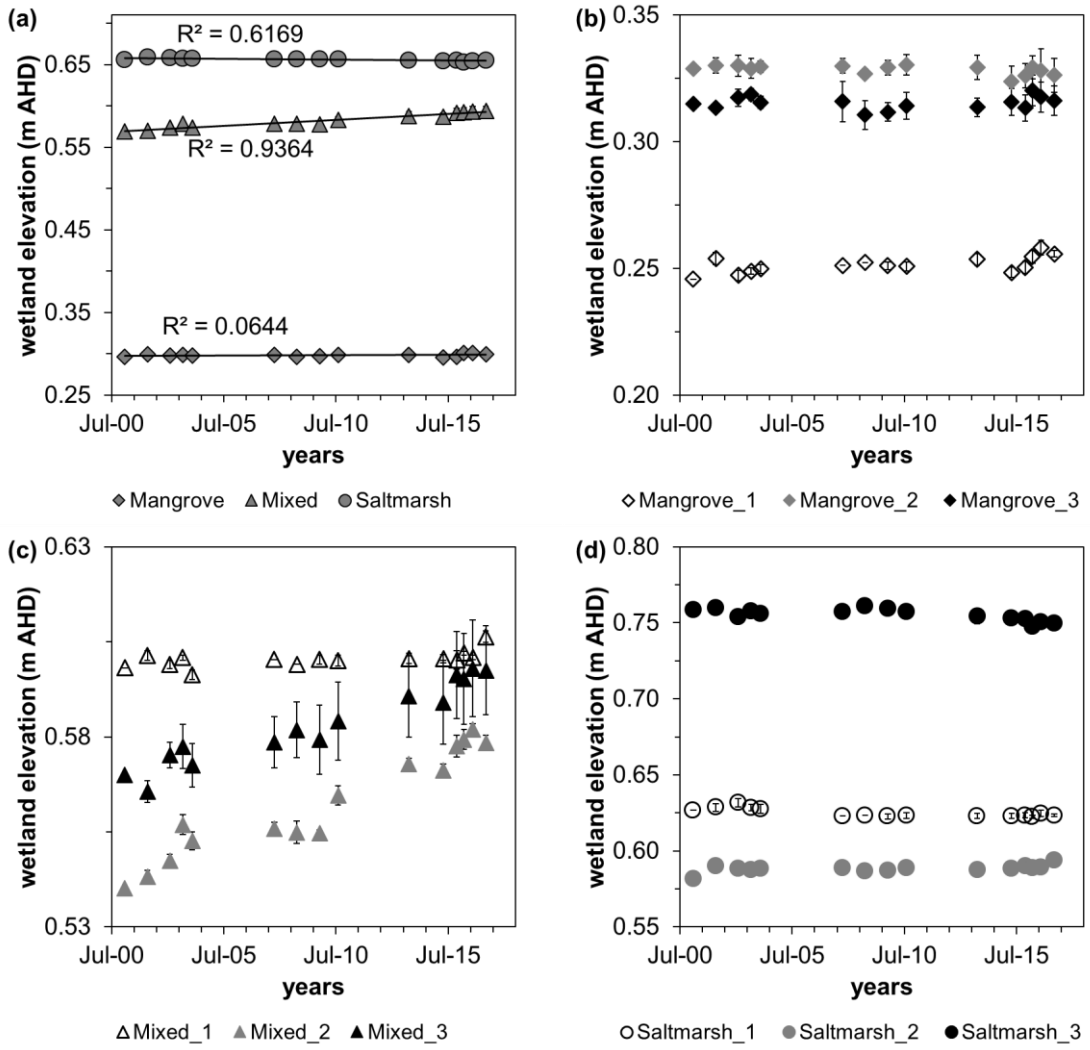

Figure 3.9: (a) Mean surface elevation change in mangrove, mixed and saltmarsh vegetation zones at Currambene Creek. SEC measured at each SET in (b) mangrove, (c) mixed and (d) saltmarsh zone.

Table 3.5: Absolute (mm) and rate of change (mm/y) (± standard error of the mean) of surface elevation change quantified at individual SETs and mean for mangrove, mixed and saltmarsh zone, and vertical accretion and autocompaction change at individual SETs and mean for mixed and saltmarsh zone Currambene Creek (from 03/02/2001 and 07/03/2017). MH was not detectable after 4 years in the mangrove zone and are not reported.

Vegetation	Surface elevation change		Vertical accretion		Autocompaction	
	Absolute	Rate	Absolute	Rate	Absolute	Rate
Mangrove 1	5.7 ± 0.53	0.35 ± 0.12				
Mangrove 2	-1.9 ± 0.18	-0.12 ± 0.08				
Mangrove 3	0.55 ± 0.052	0.034 ± 0.10				
Mean	1.4 ± 0.13	0.089 ± 0.076				
Mixed 1	3.3 ± 0.31	0.21 ± 0.083	4.8 ± 0.48	0.30 ± 0.20	-0.7 ± 0.07	-0.042 ± 0.20
Mixed 2	37 ± 3.4	2.3 ± 0.19	7.1 ± 0.71	0.44 ± 0.062	37 ± 3.7	2.3 ± 0.23
Mixed 3	28 ± 2.6	1.7 ± 0.13	14 ± 1.4	0.89 ± 0.26	28 ± 2.8	1.8 ± 0.33
Mean	23 ± 2.1	1.4 ± 0.10	5.5 ± 0.55	0.34 ± 0.18	22 ± 2.2	1.3 ± 0.24
Saltmarsh 1	-6.0 ± 0.57	-0.37 ± 0.082	4.5 ± 0.45	0.28 ± 0.12	-11 ± 1.1	-0.66 ± 0.16
Saltmarsh 2	3.7 ± 0.35	0.23 ± 0.10	6.5 ± 0.65	0.40 ± 0.14	-1.5 ± 0.15	-0.093 ± 0.18
Saltmarsh 3	-8.2 ± 0.77	-0.51 ± 0.13	4.8 ± 0.48	0.30 ± 0.15	-9.2 ± 0.92	-0.57 ± 0.22
Mean	-3.5 ± 0.33	-0.22 ± 0.048	4.5 ± 0.45	0.28 ± 0.078	-7.1 ± 0.71	-0.44 ± 0.088

The mixed zone SET2 and 3 were increasing elevation at a relatively high rate of 2.3 ± 0.19 mm/y and 1.7 ± 0.13 mm/y, respectively, whilst SET1 increased at only 0.21 ± 0.083 mm/y (Fig. 3.9c, Table 3.5). Statistical difference between SETs was detected over time ($p=0.0020$) and within SETs over time ($p<0.0001$). The saltmarsh zone SET2 increased elevation at 0.23 ± 0.10, whilst SET1 and 3 were losing elevation by more than 0.3 mm/y (Fig. 3.9c). Even though SEC in this zone remained statistically consistent between the SETs at this site ($p = 0.3058$), significant differences in SEC were observed over time ($p = 0.0156$) and within SETs over time ($p <0.0001$).

The mixed and saltmarsh vegetation zones accumulated sediments at a similar rate (Fig. 3.10a). Variability in VA was mainly associated with the mixed zone MHs ($p = 0.0152$), where SET3-MH accumulated 14 ± 1.4 mm of sediments, whilst less than half of this amount was observed at SET1 and SET2 (Fig. 3.10b, Table 3.5). In contrast, very little variation in accretion was observed within the saltmarsh zone (Fig. 3.10c).

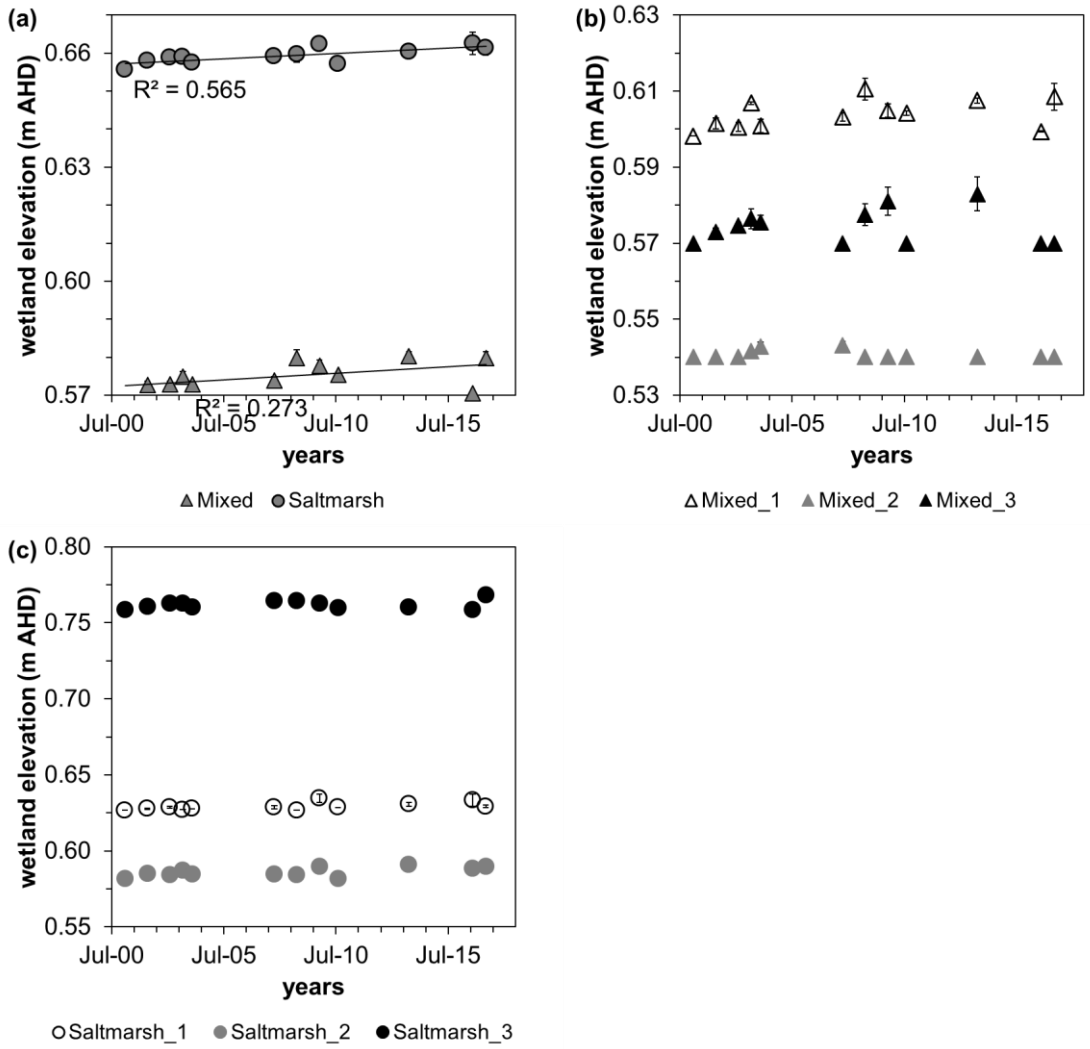

Figure 3.10: (a) Mean vertical accretion measured at mixed and saltmarsh vegetation zone at Currambene Creek. VA at individual MH at (b) mixed and (c) saltmarsh zone.

An average autocompaction of 22 ± 2.8 mm was observed in mixed zone over the study period (Fig. 3.11a, Table 3.5). No variation was identified between SETs in the mixed zone (Fig. 3.11b, $p = 0.1801$), however, belowground substrate expansion was observed at SET2 and 3 and little autocompaction was measured at SET1. Significant variation in autocompaction was identified over time ($p < 0.0001$) and within SETs over time ($p < 0.0001$), which was mainly associated with belowground substrate composition in the saltmarsh SETs (Fig. 3.11c, $p = 0.0312$).

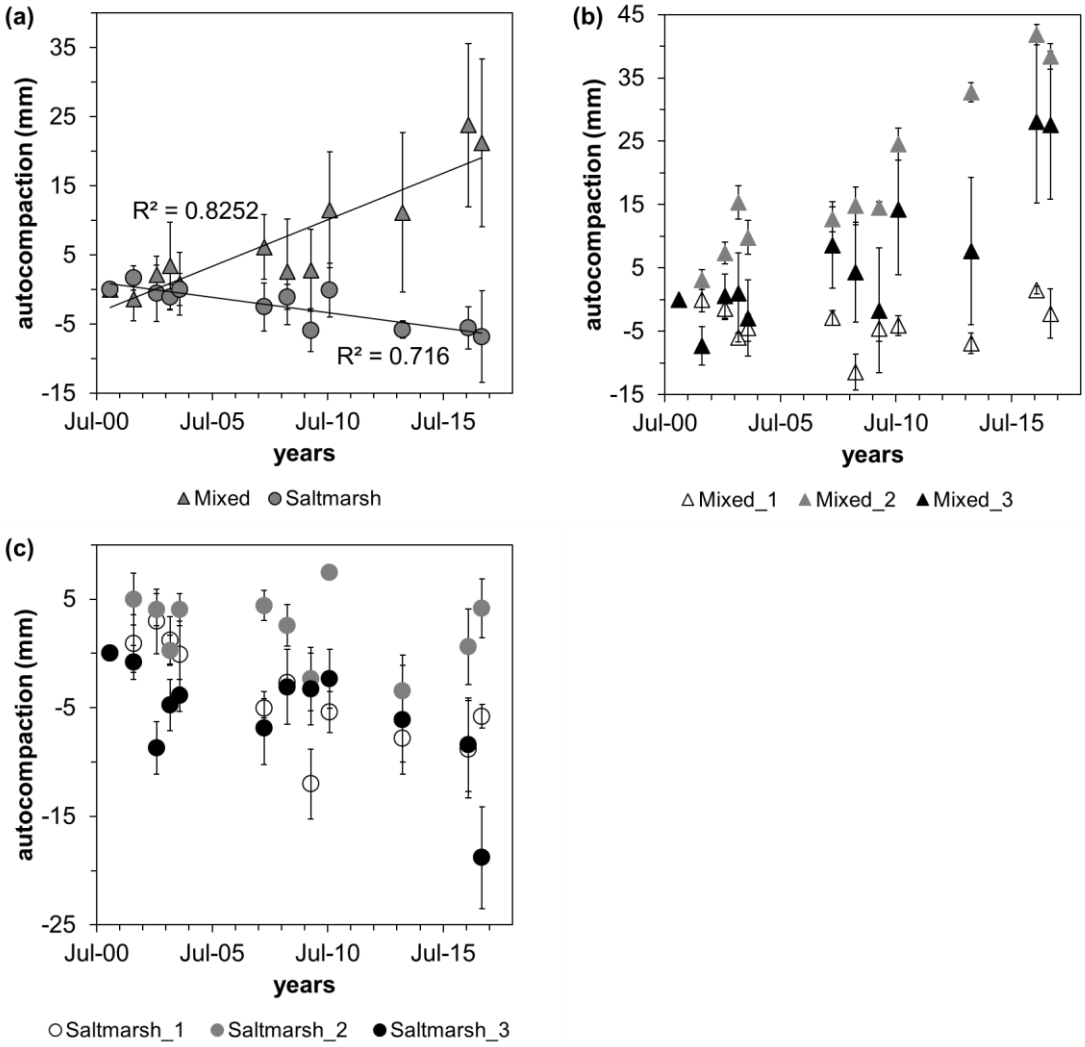

Figure 3.11: Autocompaction at (a) mixed and (b) saltmarsh zone, and (c) mean autocompaction at Currambene Creek.

At Currambene Creek, the mixed vegetation zone is increasing SE at a relatively high rate, whilst very little change was measured in mangrove and SE fall was measured in the saltmarsh zone (Fig. 3.12). VA measurements at the start of the study was very high in mangrove indicating that perhaps belowground autocompaction is offsetting VA in this zone resulting in very little SEC. However, this cannot be assumed for the whole study period. In the mixed zone, the variability in the degree of SEC and VA decreased over time (0.2633), whilst SEC and autocompaction remained consistent ($p = 0.6208$), indicating that SEC was facilitated by both VA and belowground substrate expansion (Fig. 3.12). In saltmarsh, despite VA autocompaction was offsetting sediment accretion resulting

in surface elevation deficit in this zone.

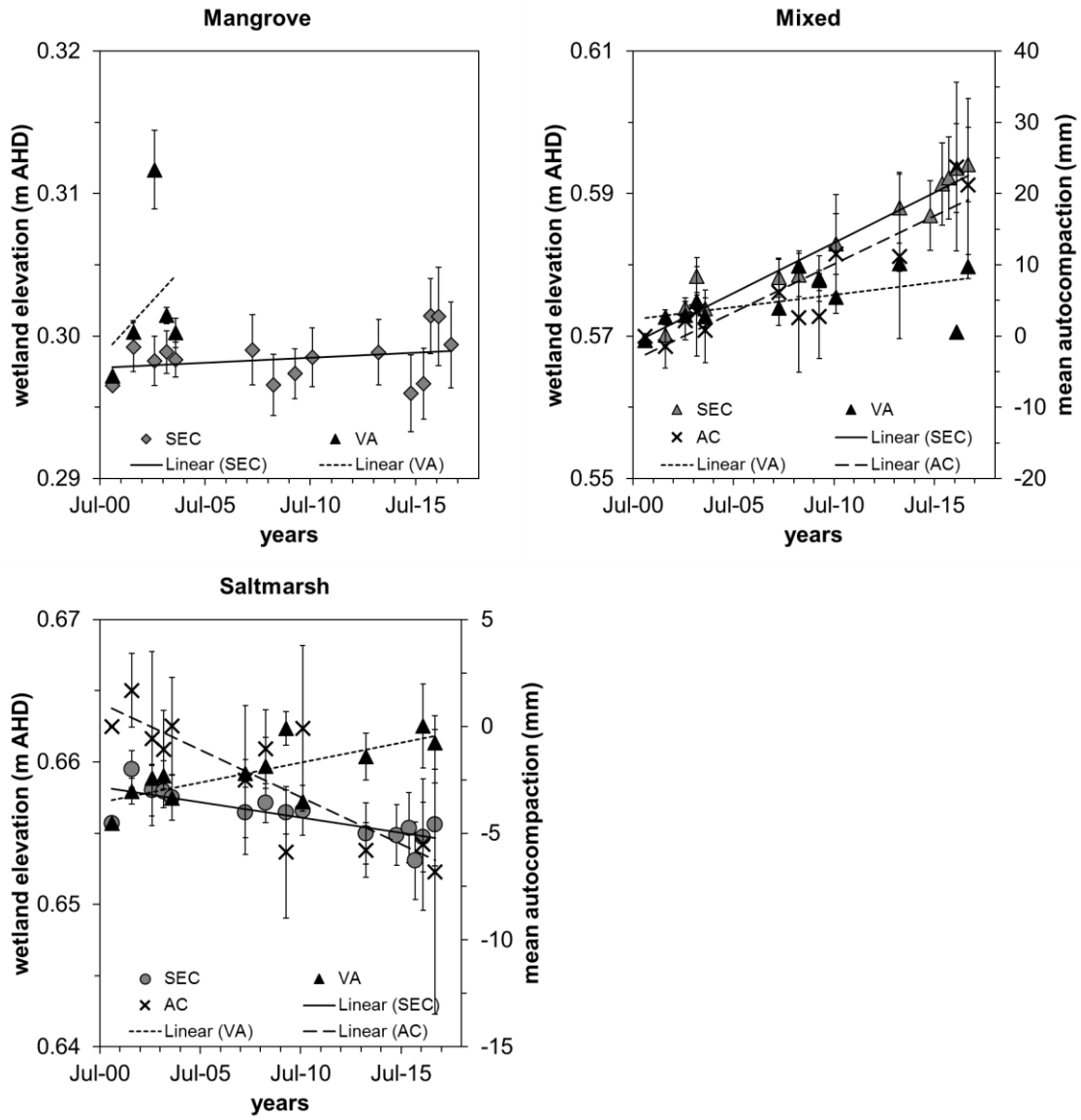

Figure 3.12: Mean SE, VA and AC change at mangrove, mixed and saltmarsh zones at Currambene Creek.

Summary of regional processes

Surface elevation increased by about 20 mm in mangrove zones of Minnamurra River and Cararma Inlet, whereas similar trends of SEC were observed in the mixed vegetation zone of Currambene Creek. The Currambene Creek mangrove zone remained relatively stable with very little change over the study period.

Significant difference between SETs indicated that even within a vegetation zone, variable processes can influence the surface elevation dynamics. VA in the saltmarsh zones of Minnamurra River and Cararma Inlet contributed to SE gain, however in Currambene Creek saltmarsh VA was offset by autocompaction resulting in a decline in SE. Whilst mangrove surface remained stable and saltmarsh was losing elevation at Currambene Creek, VA and belowground substrate volume expansion were collectively contributing to SE gain of 23 ± 2.1 mm in the mixed zone. Overall, the mangrove zones of Cararma Inlet and Minnamurra River were increasing surface elevation at a higher rate than saltmarsh, whilst SEC gain was limited to the mixed zone at Currambene Creek.

3.3.2. Tidal position

Water level logger data from Minnamurra River, Cararma Inlet and Currambene Creek showed that the wetlands are inundated by the semi-diurnal tides typical of the region. The Minnamurra River tidal times and water height water level loggers coincided closely with the water level recorded at the Minnamurra tide gauge (Fig. 3.13). Water depth and inundation frequency at Cararma Inlet and Currambene was greatest during the spring tidal cycle and a lag of approximately 2 hours to completely inundate the site (Fig. 3.14 and 3.15). This lag meant that the timing of the tidal peak at lower elevations corresponded more closely to the tidal peak on the tide gauge than the tidal peak at higher wetland elevations. In combination, the elevation and the lag in the tidal peak influenced the inundation duration and frequency, whereby zones dominated by tall *Avicennia marina* had an inundation frequency between 29 and 45 % (Table 3.5). The mixed mangrove and saltmarsh vegetation zone were inundated 15 to 30 % of the time, whilst the saltmarsh zone located in the higher position of the upper intertidal was inundated only about 13 to 22 % of the time.

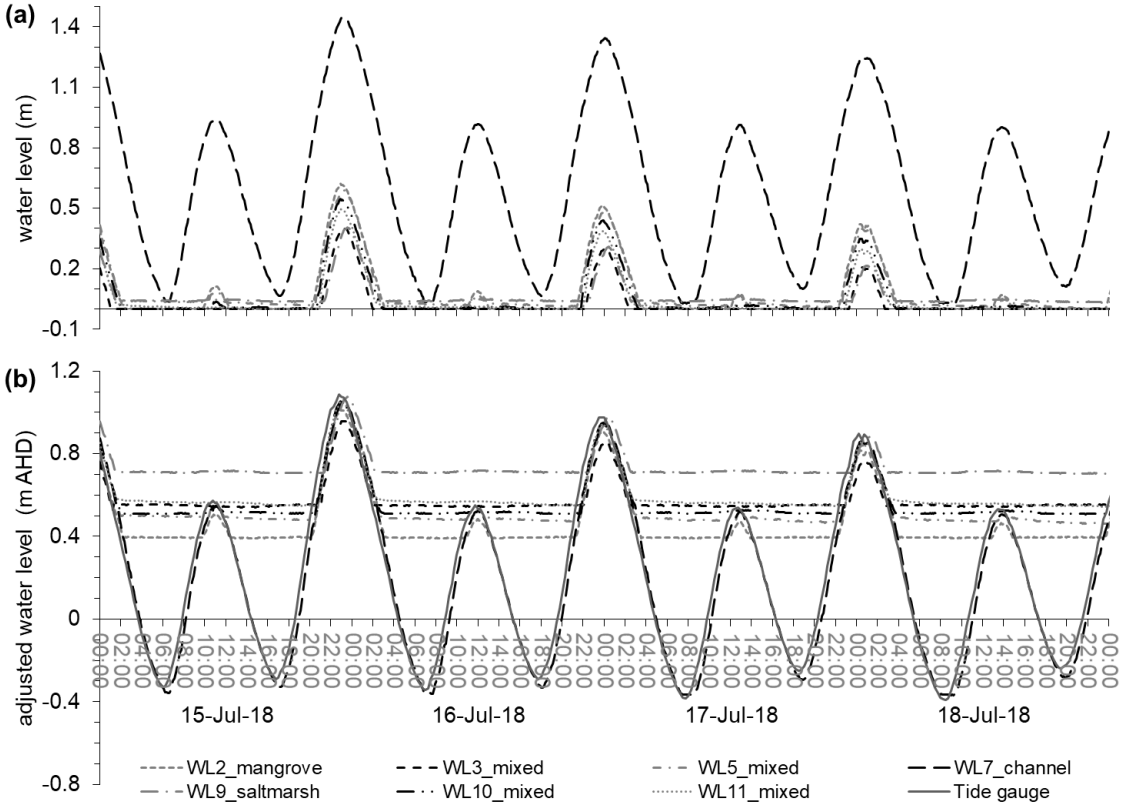

Figure 3.13: Water logger water depth at Minnamurra River (a) above the surface indicating the height of inundation; and (b) adjusted to MSL in relation to water level recorded at the Minnamurra tide gauge.

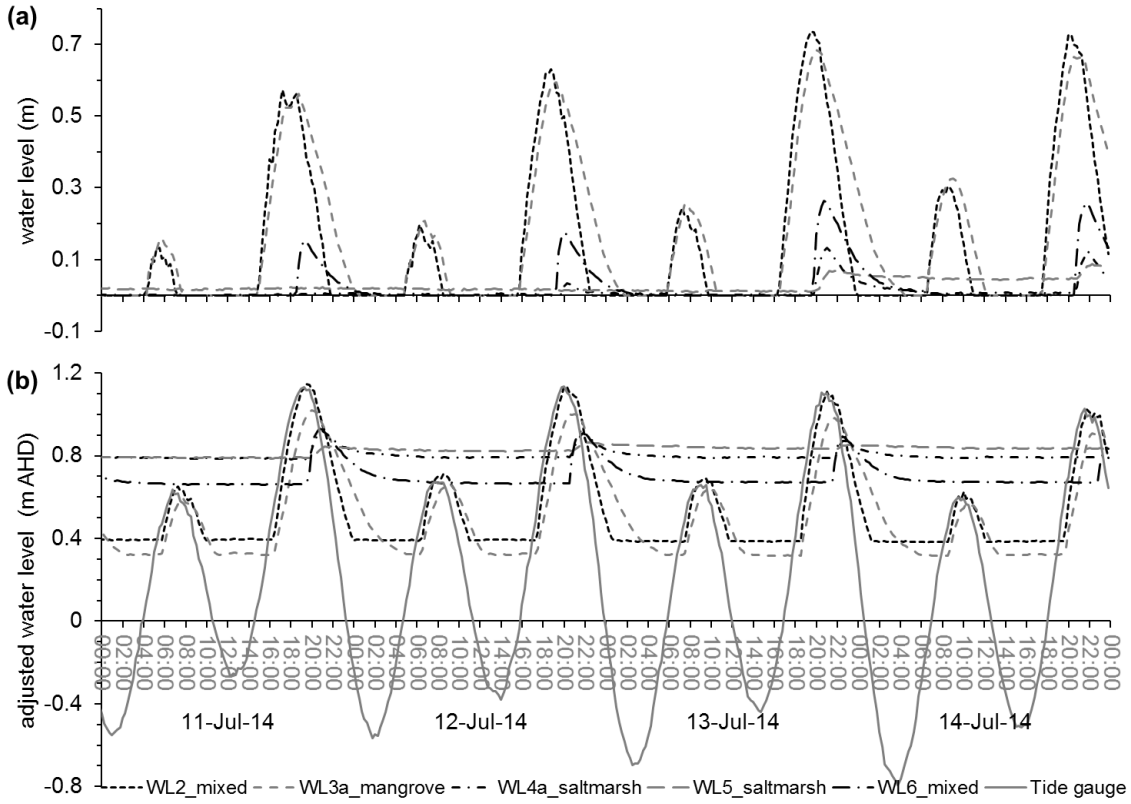

Figure 3.14: Water level logger water depth at Cararma Inlet (a) above the surface indicating the height of inundation; and (b) adjusted to MSL in relation to water level recorded at the Jervis Bay tide gauge.

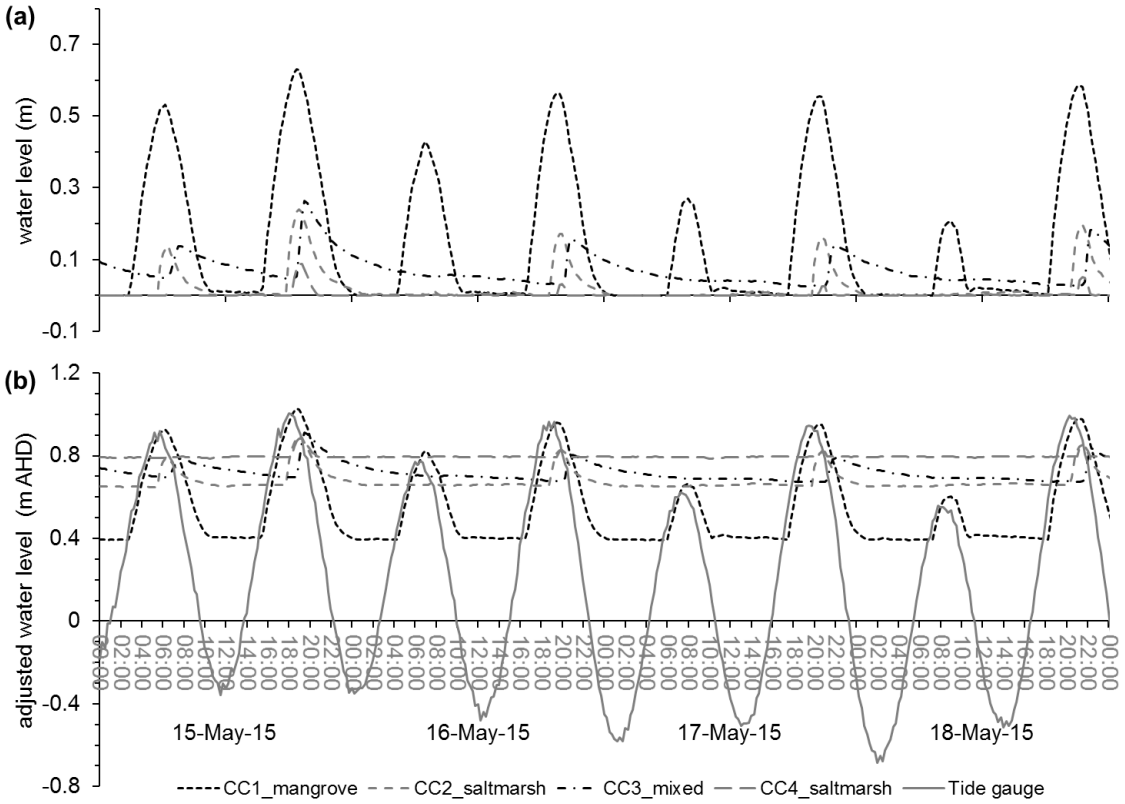

Figure 3.15: Water level logger water depth at Currambene Creek (a) above the surface indicating the height of inundation; and (b) adjusted to MSL in relation to water level recorded at the Jervis Bay tide gauge.

The logistic relationship between inundation frequency and wetland elevation in each study site was very similar and individual models for each study site was used to predict the inundation frequency of SETs (Table 3.6). The parameter estimates for each study site was used to predict the inundation frequency of SETs showed that the mangrove zones across all study sites occurred between an elevation range of 0.237 and 0.437 m AHD and had an inundation frequency between 27.7 and 36.2 % (Table 3.7). These low elevation and high inundation frequency zones were categorised as mid tidal position (Fig. 3.16). The mixed vegetation zone SETs were positioned between 0.526 – 0.669 m AHD and was inundated 16.6 to 22.1 % of the time and was classified as intermediate tidal position. The saltmarsh zone SETs were located higher in the tidal frame between an elevation range of 0.656 and 0.806 m AHD, had an inundation frequency ranging between 12.2 to 16.4 % and was categorised as high tidal position.

Table 3.6: Logistic models of predicted tidal inundation frequency for each study site.

	Summary of fit				Parameter estimates		
Models	r^2	RMSE	AICc	BIC	a	b	c
Regional	0.9576	4.49	141.39	143.71	-2.16	-0.073	112.49
Minnamurra River	0.9785	3.99	82.43	79.69	-2.30	-0.085	111.84
Cararma Inlet	0.9602	5.39	95.98	94.09	-2.10	-0.079	113.33
Currambene Creek	0.9879	3.42	65.40	58.61	-2.40	-0.072	110.49

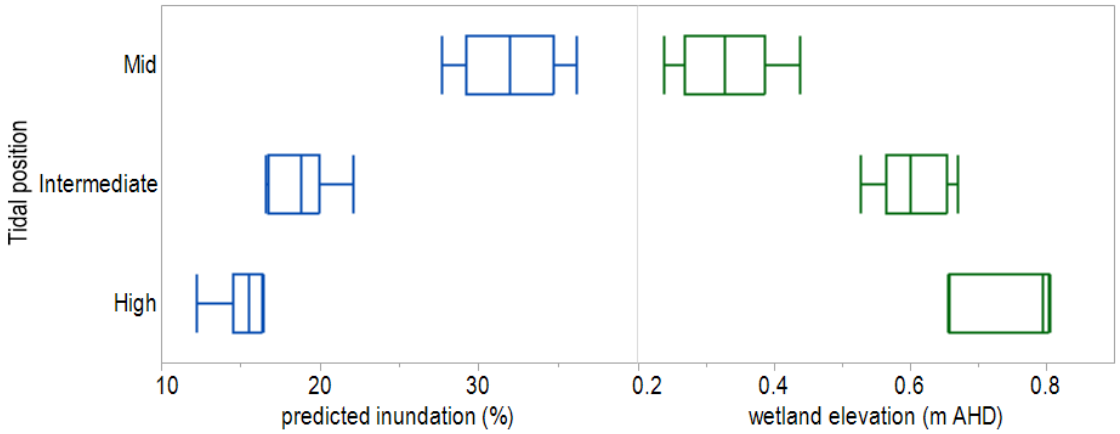

Figure 3.16: Box plot showing the predicted inundation frequency (%) and surface elevation range for the different vegetation categories at all study areas. Box type is quantile.

Table 3.7: Predicted inundation frequency and tidal position of the SETs in all study areas.

Study site	SET #	Surface elevation (m AHD)	Observed inundation frequency (%)	Predicted inundation frequency (%)	Tidal position
Minnamurra River	Mangrove 1	0.237		36.2	Mid
	Mangrove 2	0.289		33.3	Mid
	Mangrove 3	0.247		35.6	Mid
	Saltmarsh 1	0.526		22.1	Intermediate
	Saltmarsh 2	0.603		19.1	Intermediate
	Saltmarsh 3	0.669		16.8	Intermediate
Cararma Inlet	Mangrove1	0.387		31.0	Mid
	Mangrove2	0.437		28.6	Mid
	Mangrove3	0.326	37.6	33.9	Mid
	Saltmarsh1	0.806		15.3	High
	Saltmarsh2	0.803	17.0	15.4	High
	Saltmarsh3	0.796		15.6	High
Currambene Creek	Mangrove_1	0.302	34.7	32.0	Mid
	Mangrove_2	0.384		27.7	Mid
	Mangrove_3	0.342		29.8	Mid
	Mix_1	0.596		18.5	Intermediate
	Mix_2	0.648	66.2	16.6	Intermediate
	Mix_3	0.577		19.2	Intermediate
	Saltmarsh_1	0.658		16.3	High
	Saltmarsh_2	0.656	18.1	16.4	High
	Saltmarsh_3	0.795	15.4	12.2	High

3.3.3. Relationship between surface elevation change and tidal position

Rates of SEC showed a relatively strong positive relationship to tidal inundation frequency at Minnamurra River ($r^2 = 0.8941$), Cararma Inlet ($r^2 = 0.8319$) and Currambene Creek ($r^2 = 0.8791$) over the study period (Fig. 3.17). Overall the mid tidal positions dominated by mangrove was increasing SE at a higher rate than the lower inundation frequency intermediate and high tidal positions. A general pattern between SEC and inundation frequency could be established when SETs that were showing variable vegetation, SE dynamics within tidal positions and inundation frequencies were excluded. Minnamurra River saltmarsh SET1 is now

dominated by mangrove is showing comparable SEC to the mangrove SETs (Table 3.3). Currambene Creek saltmarsh SET2 is dominated by mangroves, whilst the mixed SETs are now dominated by mangrove showed very different predicted inundation frequency from the observed inundation frequency (Table 3.7). The Cararma Inlet mangrove SET showed significant differences over the study period ($p < 0.0001$) but the overall were increasing SE at a higher rate than saltmarsh SETs.

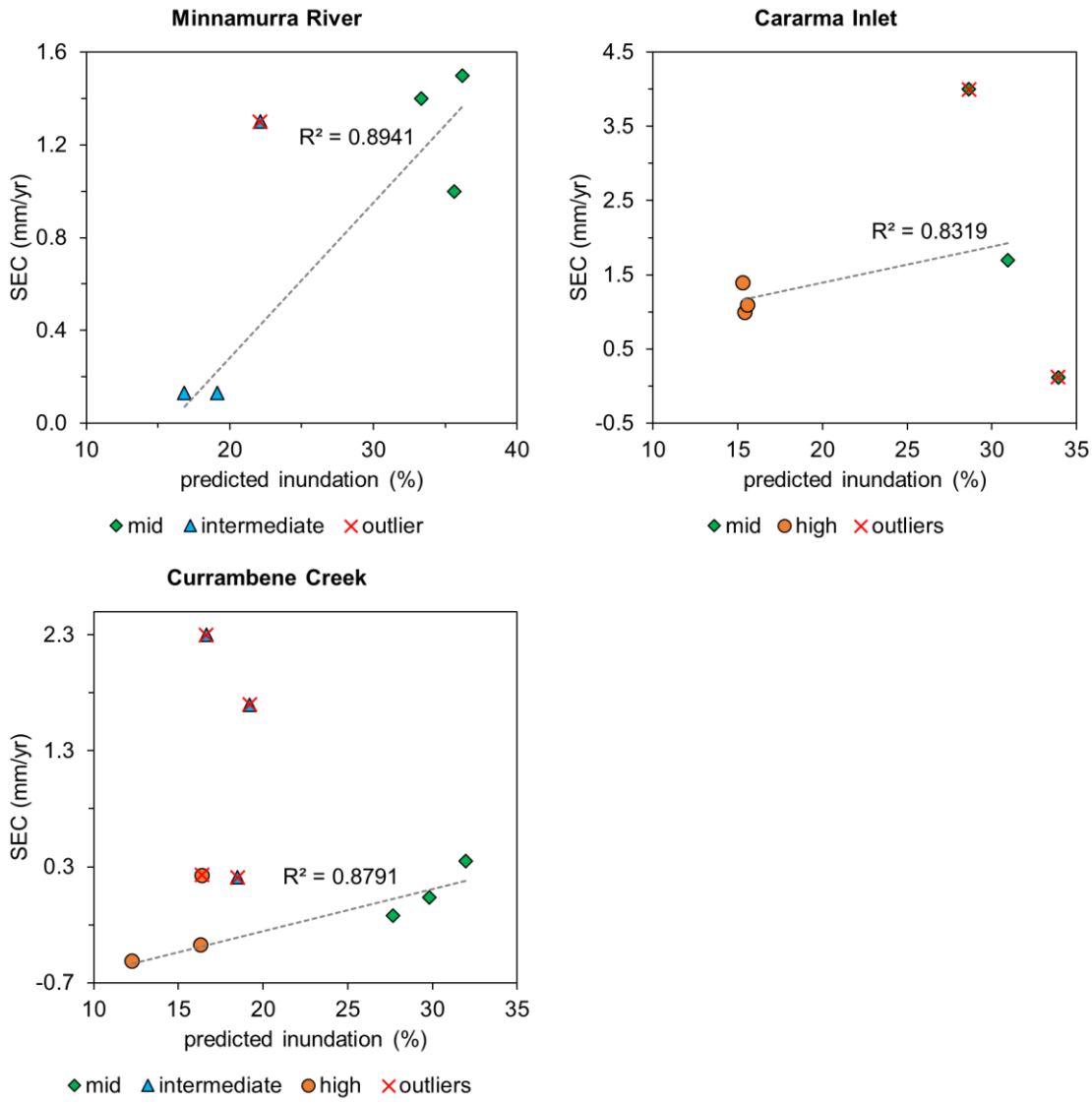

Figure 3.17: Relationship between SEC and inundation frequency at Minnamurra River and Currambene Creek when outliers are removed.

3.3.4. Relationship between surface elevation change and mean sea level

The Minnamurra tide gauge and Jervis Bay tide gaueg are showing an increasing trend in mean monthly sea level over the tide gauge record (Fig. 3.18). Relative sea level rise of 5.4 ± 0.97 mm/y was observed at the mean monthly Minnamurra tide gauge data between 03/2002 to 12/2017, whilst relative SLR of 2.9 ± 0.45 mm/y was measured at the Jervis Bay tide gauge between 09/1989 and 12/2017. The Minnamurra River mid and intermediate tidal positions SETs are both increasing surface elevation at about 1.3 and 0.52 mm/y, respectively over the study period and are correlating to the SLR trend (Fig. 3.19).

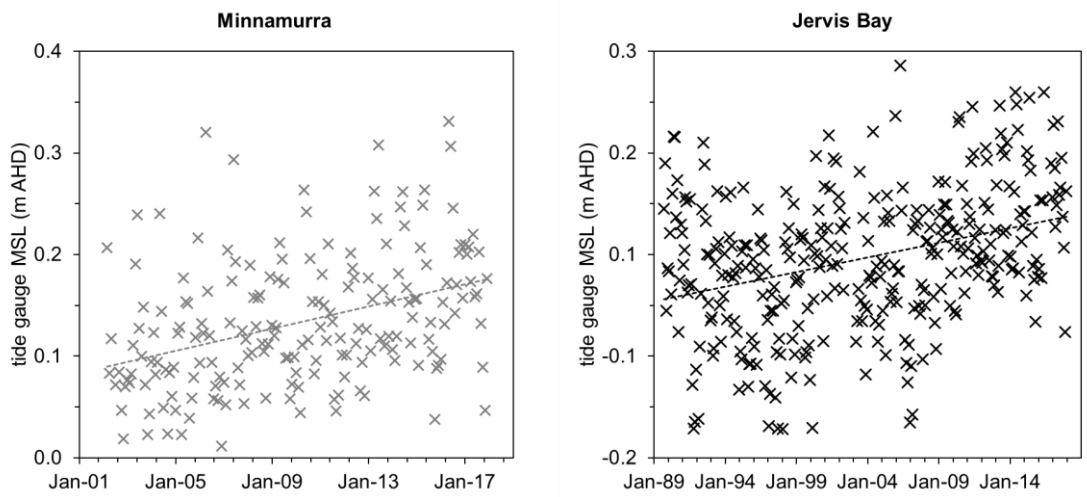

Figure 3.18: Temporal change in tide gauge MSL at Minnamurra and Jervis Bay.

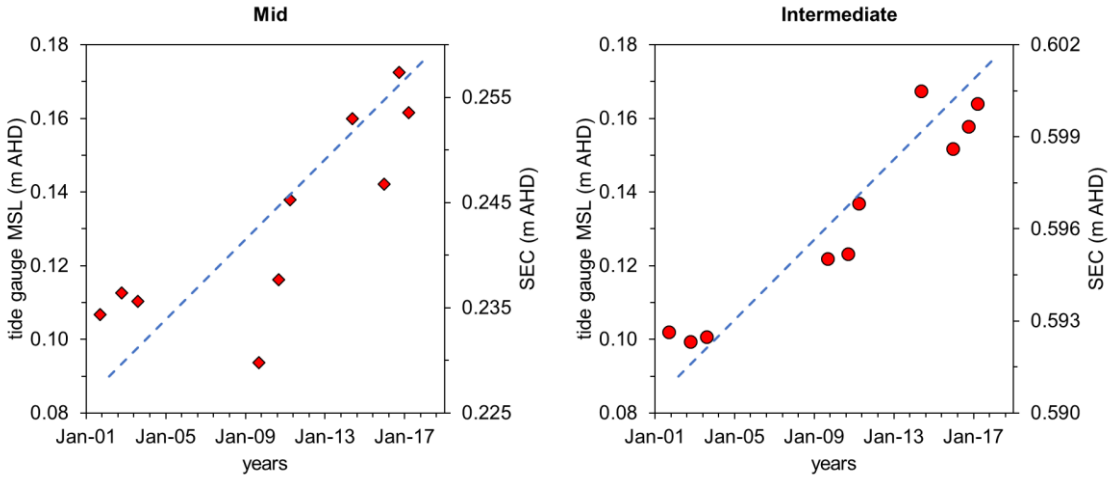

Figure 3.19: Relationship between SEC at mid and intermediate tidal positions at Minnamurra River and MSL trend from Minnamurra tide gauge.

Cararma Inlet mid and high tidal positions are increasing SE and a mean rate of 1.9 and 1.2 mm/y, respectively over the study period and correlating with the MSL trend from Jervis Bay (Fig. 3.20). The Currambene Creek mid tidal position SETS are showing variable SEC over the study period and no apparent relationship could be established relative to the SLR trend from Jervis Bay tide gauge record. The intermediate tidal position SETs are increasing SE at a mean rate of 1.4 mm/y corresponding to the rate of relative SLR, whilst the high tidal position SETs have been losing elevation at an average rate of 0.22 mm/y showing a negative correlation to SLR (Fig. 3.21). At decadal timescales, the increasing SE trend in the mid, intermediate and high tidal positions may be associated with SLR increasing inundation frequency and creating more accommodation space for wetland vegetation to vertically increase elevations, except for Currambene Creek high tidal position that is losing elevation relative to SLR.

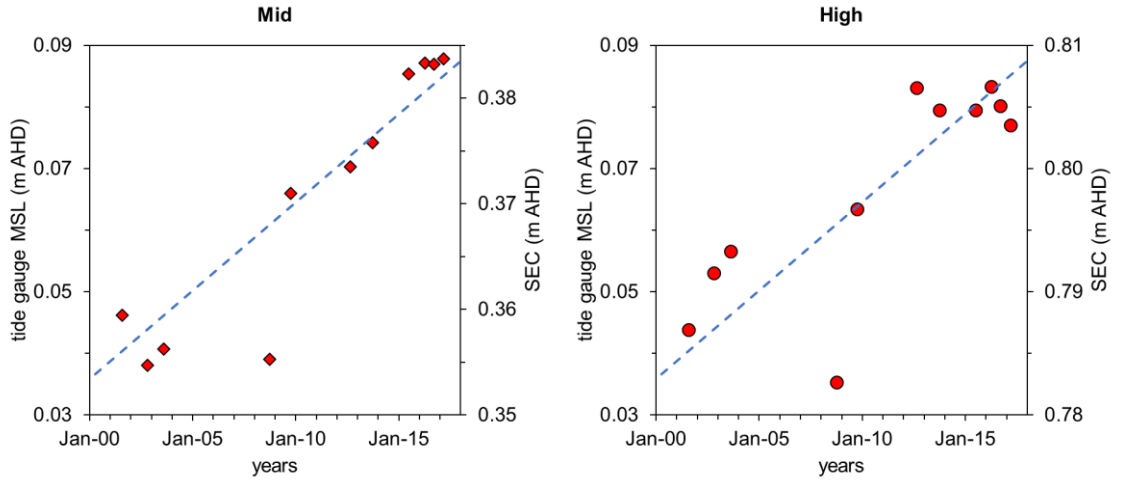

Figure 3.20: Relationship between SEC at mid and high tidal positions at Cararma Inlet and MSL trend from Jervis Bay tide gauge.

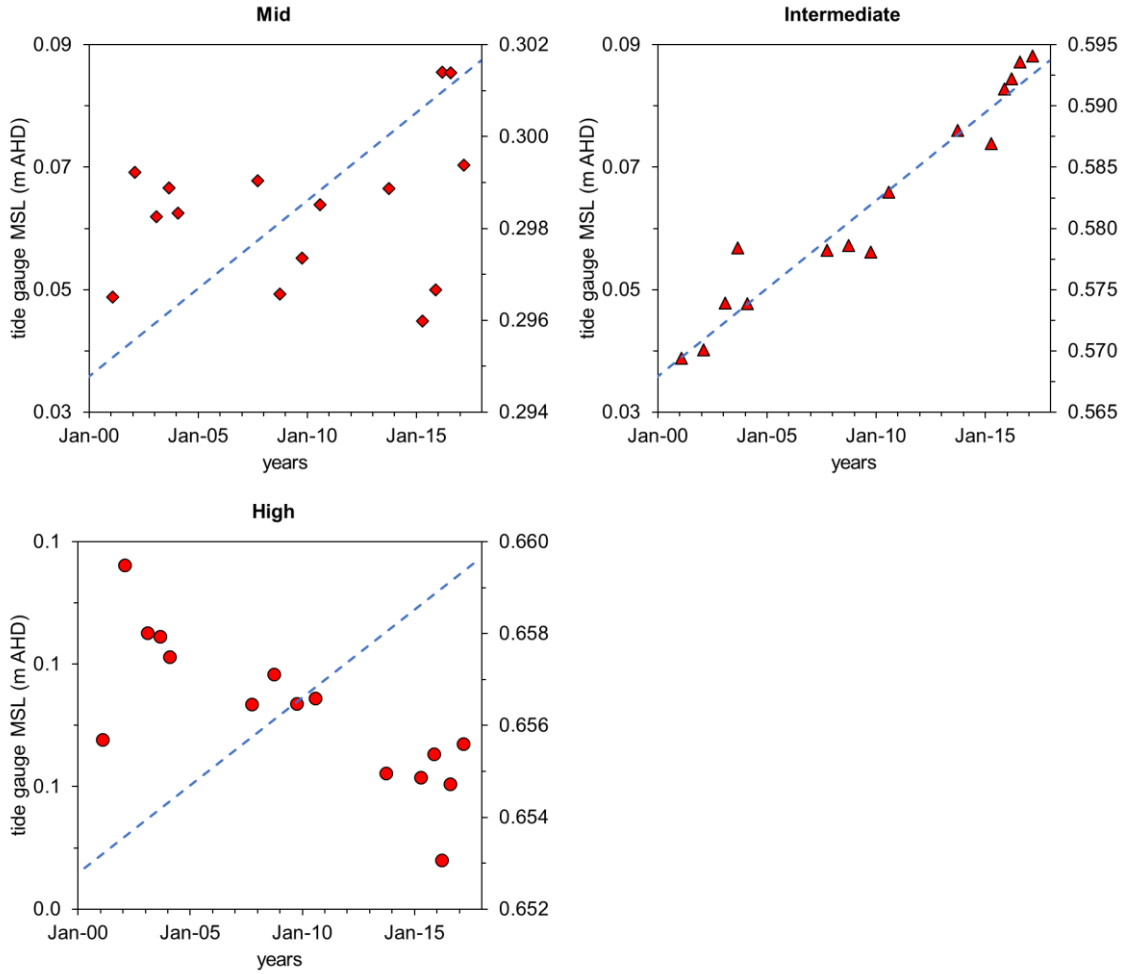

Figure 3.21: Relationship between SEC at mid, intermediate and high tidal positions at Currambene Creek and MSL trend from Jervis Bay tide gauge.

3.4. Discussion

3.4.1. Relationship between vertical accretion and surface elevation dynamics at decadal timescales

SEC did not equal VA even at decadal timescales as was established in the 2-year rSET-MH record in Chapter 2. Within a tidal frame, VA could only be measured in the intermediate and high tidal positions of Currambene Creek over the study period where VA was proportional to inundation frequency in the tidal frame. VA rates were higher in the intermediate tidal position that had a higher inundation frequency in relation to high tidal position. VA corresponding to inundation frequency has been established in other studies (e.g. Kirwan and Guntenspergen, 2010; Lovelock et al., 2011; Rogers et al., 2006), whereby the longer a wetland surface is inundated, the more time there is for sediments to settle on the wetland surface (Fagherazzi et al., 2012; Kirwan et al., 2010; Pethick, 1981; Temmerman et al., 2004, 2003).

SEC related to tidal inundation frequency and position in the tidal frame as was also established in Chapter 2. Surface elevation change showed a positive relationship to tidal inundation frequency at Minnamurra River and Cararma Inlet. SE gain of 1.3 ± 0.31 mm/y and 1.9 ± 0.25 mm/y in these two study sites, respectively, in the mid tidal positions where mangrove dominate was greater than SEC of 0.52 ± 0.07 mm/y in intermediate tidal position at Minnamurra River and 1.2 mm/y in high tidal position at Cararma Inlet.

This trend in SEC was not clear at Currambene Creek as the mid tidal position dominated by mature mangrove trees exhibited very little SEC over the study period. Other studies have also shown significant variation in SE gains, particularly in mangrove forests (Lovelock et al., 2015a). SEC in the intermediate and high tidal positions at Currambene Creek did exhibit relationship to tidal inundation frequency where the intermediate tidal position that had a relatively higher

inundation frequency was gaining SE at 1.4 ± 0.10 mm/y, whilst the high tidal position SE at -0.22 ± 0.048 mm/y over the study period. The decoupling of SEC from high tidal position at Currambene Creek may relate to the proximity of SETs to a smaller tidal creek that is incising further across the tidal frame and funnels water to higher elevations within the wetland as has also been modelled by others (Temmerman et al., 2003).

3.4.2. Influence of belowground processes on surface elevation change

In all study sites, VA could only be measured in the saltmarsh classified as either intermediate or high tidal position. Differences between SEC and VA indicated that belowground processes were occurring and still detectable at this timescale in these study sites, which has also been recognised in other coastal wetlands (Krauss et al., 2003; Lovelock et al., 2011; McKee, 2011; Rogers and Saintilan, 2008). Belowground substrate change can be related to various processes (Cahoon et al., 2006), such as decomposition of organic matter (Cahoon et al., 2003; Lovelock et al., 2015a; McKee et al., 2007), loss of biomass (Krauss et al., 2014; Rogers et al., 2013b), reduction in groundwater (Rogers and Saintilan, 2008; Whelan et al., 2005), and consolidation of minerals sediments (Allen, 2000).

There was no significant difference between the degree of SEC and VA at high tidal positions at Cararma Inlet indicating that VA was directly contributing to SE gain and there was very little consolidation of the belowground sandy substrate occurred over the study period. At Minnamurra River, SE gain was greater than VA at intermediate tidal positions as result of belowground root additions contributing to SE gain at this location. Similarly, belowground root additions were contributing to SEC gain beyond VA alone at the intermediate tidal positions of Currambene Creek. Organic matter addition to substrates was likely related to mangrove expansion into saltmarsh at these study sites. The lateral expansion of mangrove into saltmarsh has been documented at Currambene Creek (Saintilan

and Wilton, 2001) and Minnamurra River (Chafer, 1998b), which corresponded to SET locations at intermediate positions at Currambene Creek and high tidal positions at Minnamurra River. Mangrove expansion into saltmarsh SETs has not occurred at Cararma Inlet, thereby providing more evidence that SEC beyond VA is related to organic matter addition by mangrove as they move into saltmarsh.

SE loss despite VA in high tidal position of Currambene Creek demonstrated that belowground decomposition of organic matter, autocompaction and/or consolidation of substrate was offsetting VA. Studies have demonstrated that autocompaction of substrates at high tidal positions may relate to lower inundation frequencies which can facilitate decomposition of organic matter (Rogers et al., 2019a).

3.4.3. Relationship between surface elevation change and SLR

SE gain is corresponding to relative SLR over the tide gauge record, through VA and belowground organic matter accumulations. The mangrove zones of Minnamurra River and Cararma Inlet both exhibited relatively high rates of SE gain coinciding with the trend of SLR over the past few decades. Studies have also demonstrated that mangrove forests have the capacity to maintain wetland elevation with respect to relative SLR, which they can do this through processes, such as organic matter additions in above and belowground sediments in addition to trapping suspended particles in water brought in by tides (Cahoon et al., 2006; Krauss et al., 2003; Lovelock et al., 2015b; McKee, 2011; McKee et al., 2007). These processes directly contributed to SE gain in lower tidal position mangroves despite belowground substrate autocompaction as demonstrated in this study and others (Cahoon et al., 2000a; Lovelock et al., 2015a).

Organic matter addition was also important to substrates offsetting lower rates of VA is an important mechanism contributing to SE gain in zones in wetland areas where mangroves are expanding into saltmarsh. Wetland vegetation transition is

permitting wetland surface to maintain elevation relative to SLR (Cahoon et al., 2004; McKee, 2011). The exception was high tidal positions at Currambene Creek, where despite relatively high amounts VA, SE loss occurred as a result of autocompaction and/or decomposition of belowground substrate. The rate of SE loss at this site was significantly less than the degree of SLR occurring over the same timescale, indicating that the high tidal positions are transitioning towards a lower position in the tidal frame. The lag between SEC and SLR, however, is not concerning as there is considerable vertical elevation at high tidal positions before vegetation loss can occur. Conversely, this lag may be an important component of the negative feedback loop (Pethick, 1981; Saintilan et al., 2009). SE rates at high tidal position might continue decreasing and transition towards a lower position in the tidal frame creating conditions favourable for mineral and organic matter additions and consequently contribute to SE gain in future (Kirwan and Mudd, 2012).

The lack of SE gain in the mangrove at Currambene Creek in concerning as it indicates that the mangrove is transitioning to a lower position in the tidal frame and that processes contributing to SE gain are not being triggered. This suggests that site-specific conditions, such as decomposition and/or autocompaction of belowground substrate has a stronger influence on SE dynamics of wetland vegetation. This relationship between surface elevation dynamics and belowground processes demonstrate the importance of geomorphic conditions on long term surface elevation variability on coastal wetlands (Cahoon et al., 2006; Woodroffe et al., 2016) and generalisations on regional surface trends should be based on the timescale and location of study. There was, however, substantial SE gain at intermediate elevations, where invasion of mangrove into saltmarsh has occurred over the past few decades (Saintilan and Williams, 1999; Saintilan and Wilton, 2001). Monitoring of mangrove SE changes at Currambene Creek should remain a priority to determine the longer-term resilience of low elevation mangrove at this site.

3.5. Conclusion

SE gain related to inundation frequency in most study sites over decadal timescales, where mangrove that had a higher inundation frequency was increasing SE at a greater rate than saltmarsh that had a relatively lower inundation frequency. Belowground organic matter additions by mangrove plants effectively contributed to SE gain beyond VA alone in areas where mangroves are expanding into saltmarshes. This demonstrated a greater capacity for mangrove to contribute to substrate elevation gain at decadal timescales in maintaining surface elevations relative to SLR. SE loss despite VA indicated that belowground decomposition and/or autocompaction is contributing to loss of substrate volume. The above scenarios are an important transition of higher elevation saltmarsh to lower elevations in the tidal frame before mineral and organic matter additions are triggered, which can contribute to SE gain relative to future SLR. However, SEC corresponded to VA where there was little opportunity for organic matter additions and decompositions in belowground substrate that was highly sandy. Discrepancies in above and belowground processes between and within study sites indicate that site-specific characteristics have a relatively strong influence on SE dynamics of coastal wetlands.

The general pattern of SEC at decadal timescales was to increase SE at tidal positions that have a higher inundation frequency and maintaining elevation relative to SLR, whilst SE loss is an important characteristic of the negative feedback loop in saltmarsh located higher in the tidal frame. The next chapter explores the influence of sea-level variability on surface elevation change across the tidal frame over decadal to centurial timescales in the context of relative SLR over the past century.

Chapter 4

Sediment accumulation rates in coastal wetland vegetation over the past century

4.1. Introduction

The long-term development and evolution of mangrove and saltmarsh has been a consequence of mineral and organic sediment accumulation through geomorphological, biological and hydrological processes. For example, in Australia, where sea level has increased by approximately 2 mm/y between 1966 and 2010 (White et al., 2014), there has been a relatively consistent pattern of mangrove moving into saltmarsh (Saintilan and Williams, 1999), which has been related to sea-level rise (SLR) (Rogers et al., 2006). In particular, Rogers (2004) demonstrated that mangrove expansion into saltmarsh was greater when rates of surface elevation gain in the saltmarsh lagged behind the degree of sea level rise. Projections of accelerating SLR has heightened concerns about the distribution of mangrove and saltmarsh. Accordingly, there is a need to understand whether rates of vertical growth of mangrove and saltmarsh have been able to offset the degree of SLR that has occurred in the past, and whether this pattern will be maintained as sea level rise accelerates.

Results from this study quantify sediment accumulation rates in mangrove and saltmarsh vegetation over the past century in the context of SLR over the same time period. The above aim was achieved through the following objectives;

i. Determine rates of sediment accumulation based on the activity of supported and unsupported ^{210}Pb in sediments;

ii. Validate sediment accumulation rates and validate them using rates of surface elevation change from SETs and/or ^{137}Cs activity in the sediments; and
iii. Establish whether sedimentation rates have accelerated as SLR has accelerated over the past few decades.

This study focuses on developing relationships between sediment accumulation and SLR over the past century based on the Fort Denison tide gauge record, which is the longest tide gauge record in southern Australia. Sedimentation rates were quantified and validated in different vegetation zones and considers whether sediment accumulation varied according to position within the tidal frame. Attention was directed towards establishing whether sedimentation rates varied based on changes in sea level over the ^{210}Pb dating record, particularly as SLR has accelerated over the recent decades.

4.2. Literature Review

4.2.1. ^{210}Pb dating technique

The development of coastal wetland vegetation depends on the type of sediment supplied to the system, tidal range and regime, wind-wave climate, and relative sea level conditions (Woodroffe, 2002). Mangrove and saltmarsh are able to maintain elevations with respect to SLR by either adjusting elevation vertically or horizontally (Kirwan and Temmerman, 2009; Saintilan and Rogers, 2013). As the upper limit of intertidal vegetation is defined by the tidal limit, sea level rise and its influence on elevation of the tidal frame will increase the elevation of this boundary. However, the degree of landward expansion that occurs, and loss at the seaward boundaries is offset by vertical adjustment achieved through mineral and organic matter accumulation on substrates. When vertical adjustment exceeds the degree of sea level rise that is occurring, wetlands prograde seaward, if it lags behind the degree of SLR, than lateral transgression will occur (Cahoon and

Guntenspergen, 2010; Fagherazzi et al., 2012; Kirwan and Temmerman, 2009).

The rate at which sediment accumulates on a wetland surface is useful for understanding whether wetland will prograde sea ward or transgress landward. Shorter-term surface elevation change was determined in chapters 2 and 3 using the (r) SET-MH approach, and as this chapter is focussed on the decadal to centurial timescale of change, radiometric techniques become increasingly useful in measuring longer-term surface elevation dynamics in coastal wetlands. In this regard, dating using radionuclides of ^{210}Pb and ^{137}Cs can provide an indication of wetland vertical adjustment at this timescale.

^{210}Pb is a naturally occurring radionuclide that is part of the Uranium-238 (^{238}U) decay series. It has a half-life of 22.2 years and can provide rates of sediment accumulation for timescales ranging from 1 to 150 years (Appleby and Oldfield, 1992; Ivanovich and Harmon, 1982; Walker, 2005). ^{210}Pb isotope can be found in sediments but due to their instability in nature, ^{210}Pb can undergo time-dependent radioactive decay, where they emit particles of energy to achieve a stable state (Appleby and Oldfield, 1992; Chanton et al., 1983). It gets incorporated in sediments through atmospheric fall-out and has two components; the supported ^{210}Pb activity and the unsupported ^{210}Pb activity (Fig. 4.1).

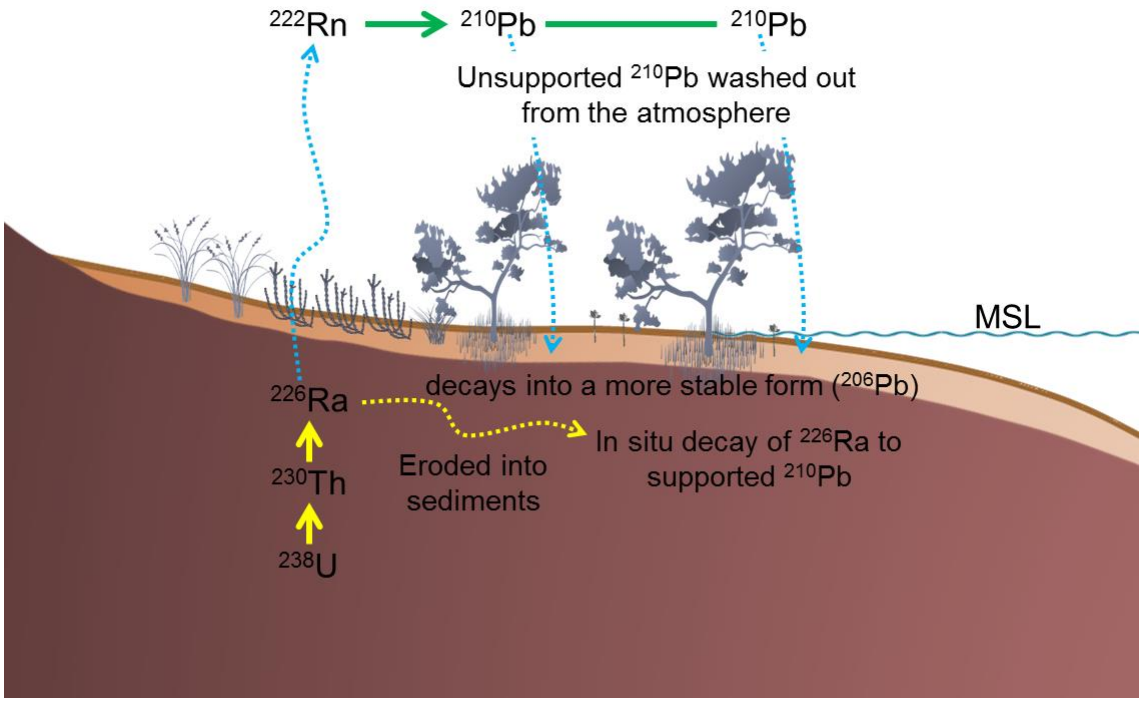

Figure 4.1: ^{210}Pb cycle and specific activity profile in coastal sediments.

The supported ^{210}Pb activity is derived from the decay of *in situ* radioisotope Radium-226 (^{226}Ra). Supported ^{210}Pb can be measured indirectly by measuring ^{226}Ra radionuclides in sediments using alpha spectrometry. A small fraction of ^{210}Pb activity in wetland sediment deposits could originate from particles containing ^{226}Ra, usually in water flowing on the surface (Brenner and Kenney, 2013) but this amount has been found to be negligible. The unsupported ^{210}Pb is derived from Radon-222 (^{222}Rn) gas that decays to form particulate ^{210}Pb, which gets removed from the atmosphere through precipitation. As particulate ^{210}Pb falls to the surface of the Earth, it gets embedded in surface sediments where it subsequently decays to a more stable form of lead, ^{206}Pb. ^{210}Pb dates are based on the vertical distribution of unsupported ^{210}Pb in the top 20 – 30 cm of the sediment cores. The unsupported ^{210}Pb activity in sediments is estimated by subtracting the supported ^{210}Pb from the total amount of ^{210}Pb in sediments.

As ^{210}Pb bonds to sediments, sediment characteristics, particularly grainsize can influence the capacity to which these radionuclides could be used to develop a chronology. ^{210}Pb isotopes are mostly concentrated in finer grained sediments,

such as clay particles therefore, analysing the isotope in smaller grain size fraction (<63 μm) increases the probability of detecting the isotope and developing a chronology (Hollins et al., 2011). Once a chronology is established for individual sediment cores, sediment accumulation rates can be calculated.

4.2.2. CIC vs CRS models

There are two different models of ^{210}Pb dating that are used to construct chronologies, the Constant initial concentration (CIC) model and constant rate of supply (CRS) model following Appleby and Oldfield (1978). The CIC model assumes that the concentration of supported ^{210}Pb on surface deposits display the same activity with time, showing that in an undisturbed sediment core the supported ^{210}Pb concentrations monotonically decreases (constantly decreasing or remaining constant) (Appleby, 2008; Walker, 2005). The CRS model assumes that surface sediments have accumulated constantly through time. It is largely applicable to sediments that have had a constant rate of sediment supply but also in sediments that have a highly variable supply (Brenner and Kenney, 2013).

If no significant migration of ^{210}Pb has taken place within the sediment profile, then the unsupported ^{210}Pb activity will decline down the sediment profile in conformity with its natural radioactive decay (Appleby 1978). However, age determinations from ^{210}Pb dating can be complicated if the concentration of unsupported ^{210}Pb increases with depth because of dilution effect of reworked sediments. The dilution effect reduces the concentration of unsupported ^{210}Pb by labile organic matter that has not yet reduced to the stable residues that are part of mature sediments (Appleby and Oldfield, 1978). Discrepancies such as this creates doubts on the dates derived from CIC model. The CRS model, on the other hand accommodates the dilution effect (Appleby and Oldfield, 1978).

In marine/aquatic ecosystems, including coastal wetlands, sediment deposition and erosional processes varies through tidal inundation, flooding from the

rivers/creeks, and groundwater fluctuations. Sediment variability on the surface can give variable ^{210}Pb isotopic signatures suggesting that the CRS model would provide a more comprehensive chronology of open ecosystems, such as coastal wetlands than the CIC model as there cannot be a constant supply of sediment due to the relationship with tides and sea level (Appleby, 2008; Brenner and Kenney, 2013).

4.2.3. Validating decadal-scale chronologies

^{210}Pb age/depth profiles can be validated using ^{137}Cs. ^{137}Cs is an anthropogenic fall-out radionuclide, which deposits onto the soil surface after being released into the atmosphere as a by-product of nuclear testing in the 1960s (Appleby and Oldfield, 1978; Chanton et al., 1983; Walker, 2005). It has relatively short half-life of 30.5 years and can become increasingly difficult to detect in sediment layers over time as the concentration diminishes. ^{137}Cs activity concentrations in the soil profile that have relatively constant sedimentation rates, such as coastal wetland environments correlate with ^{210}Pb chronology. ^{137}Cs dating can be complicated by bioturbation and the downward migration of the isotope making it difficult to identify specific peak in the core profile and so should be checked with and independent radiometric dating method, such as ^{210}Pb (Tyler et al., 2001). In recent years, surface elevation table (SET) surface elevation gains can be compared with rates of sedimentation inferred from ^{210}Pb dating of sediment cores over decadal timescales from sites where sediment dating and SET data are available (Cahoon and Lynch, 1997; Lovelock et al., 2015b; Swales et al., 2015).

4.3. Methods

4.3.1. Sampling technique and study design

The ^{210}Pb sediment dating technique was the primary technique used to determine

variation in sediment accumulation across the tidal frame at decadal to centurial timescales. ^{210}Pb sedimentation rates were validated by comparison with ^{137}Cs sediment dating techniques but in samples in which ^{137}Cs activity was low, sedimentation rates were validated against SET-MH data. That is why sediment cores for dating were collected adjacent to SET monitoring stations at Minnamurra River, Cararma Inlet and Currambene Creek, and rSET monitoring stations at Comerong Island (Fig. 4.2). Sediment cores of up to 1 to 1.5 m lengths were collected from respective SET vegetation communities in the four study areas. The top 20-30 cm of cores were sub-sampled and taken to the Environmental Radioactivity Measurement Centre at Australia's Nuclear Science and Technology Organisation (ANSTO) for ^{210}Pb dating using alpha spectrometry.

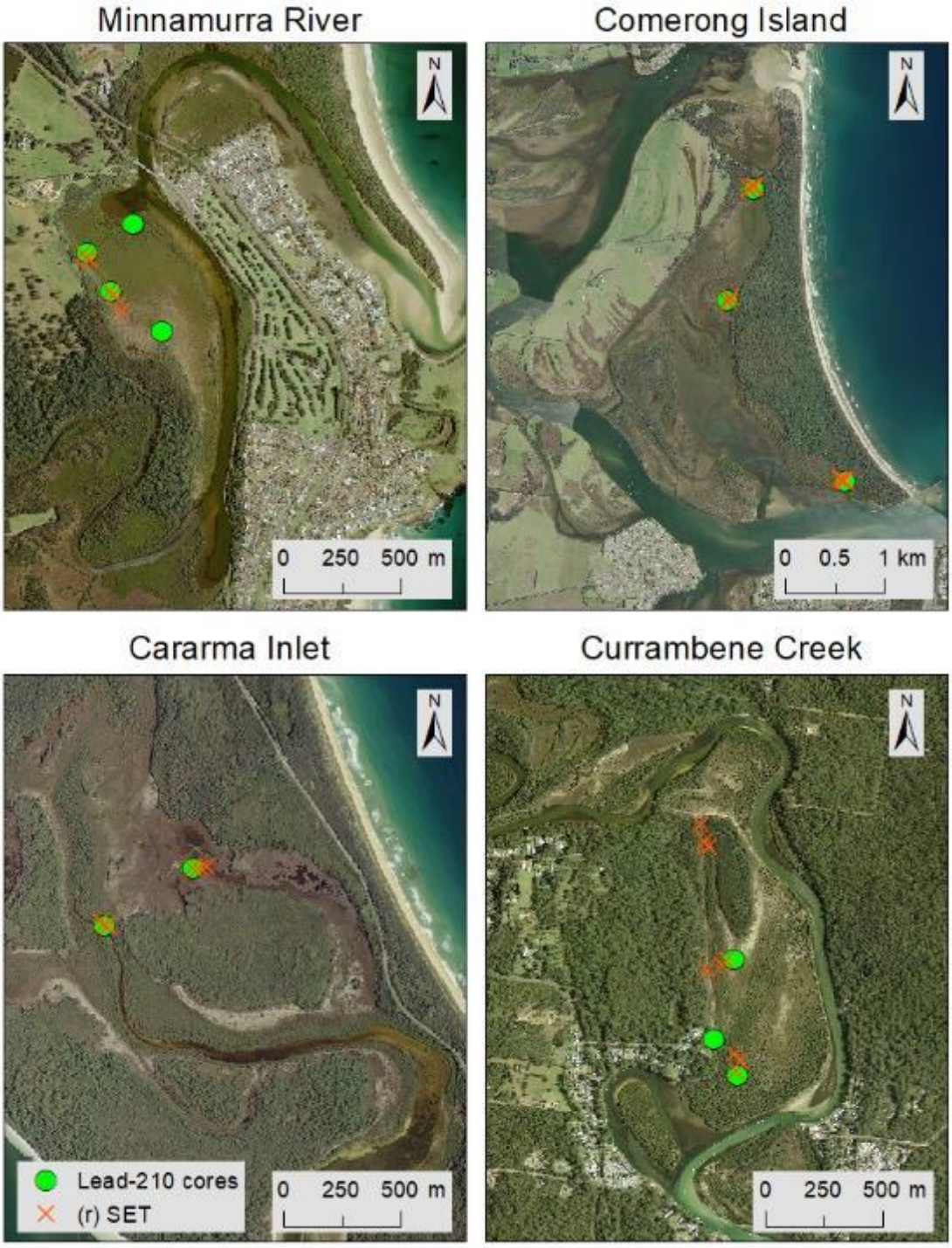

Figure 4.2: Location of ^{210}Pb dated cores in relation to SET monitoring stations and Minnamurra River, Cararma Inlet and Currambene Creek, and rSET monitoring stations at Comerong Island.

Sediment coring and sub-sampling

Sediment cores were collected by manually hammering approximately 2.5 m length (L_p) (7-cm diameter) aluminium pipe into the substrate with the aid of a weight and a sledgehammer (Fig. 4.3a). Insertion of tubes was ceased when ~0.5 m of pipe remained above the surface as this length was required to fix a brace for removal of the cores. Compaction of sediments following insertion of the pipe was typically in the order of 0.2 – 0.6 cm, meaning that a minimum of 1 m length of compacted core was collected.

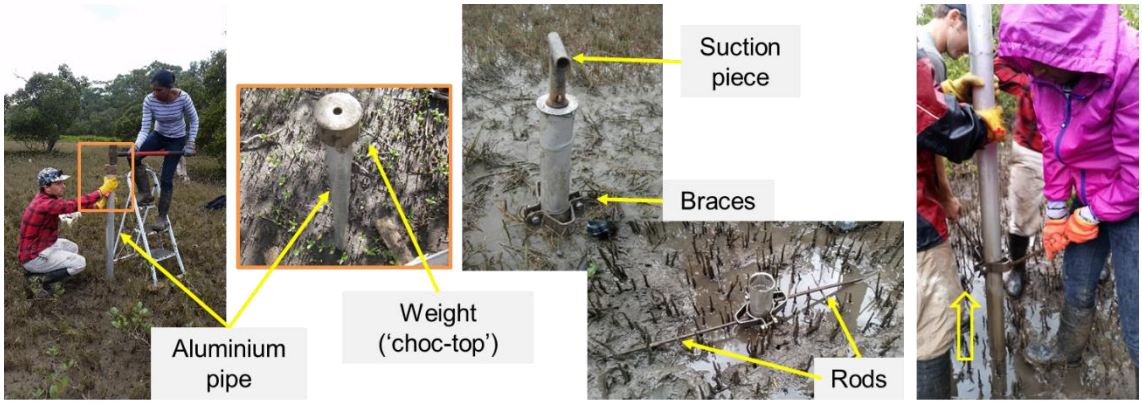

a. Sediment coring

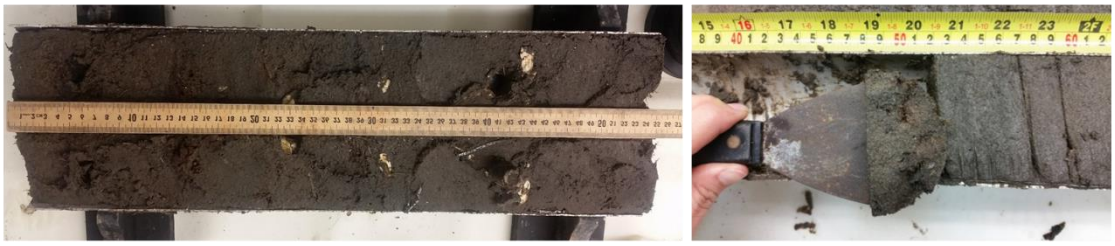

b. Sub-sampling

Figure 4.3: (a) Sediment coring in the field; and (b) sub-sampling in the laboratory.

Before removing the core from the ground, the degree of compaction in each core was measured. This was done by measuring the length of the pipe, the length of pipe empty on the inside (l_{inside}) and the length above the surface ($l_{outside}$) using a measuring tape. These values were later used to determine the compaction factor of each core as in Eq. 4.1. The compaction factor could then be subsequently converted to a full core length. All stratigraphic data was reported as compaction-corrected depths in millimetres.

$$\textbf{Compaction factor} = \frac{\boldsymbol{L_p - l_{outside}}}{\boldsymbol{L_p - l_{inside}}} \qquad \text{Eq. 4.1}$$

To remove the core from the ground, the pipe was filled with water and sealed at the top using a suction cap, which created suction in the pipe and prevented loss of sediments during extraction of the pipe from the ground (Fig. 4.3a). Two rods were attached to the braces that were used to pull the core out of the ground. The bottom of the core was capped once out of the ground. The top empty aluminium pipe was cut off and then capped. The wetland surface elevation relative to AHD was measured using an RTK-GPS at the time of coring. Cores were labelled and stored in a cold store at 4 °C until processing time.

In total, twelve sediment cores extracted for ^{210}Pb dating: four cores from Minnamurra River (Min_Mg1, Min Mg2, Min_Spo1 and Min_Mix), three from Comerong Island (Cm_Mg2, Cm_Spo, Cm_Dm), two cores from Cararma Inlet (Ca_Mg1 and Ca_Sar1), and three from Currambene Creek (Cb_Mg, Cb_Sar1, Cb_Sar2). Nine of these cores were adjacent to the (r) SETs to allow direct comparison between rates of vertical adjustment derived from the two methods. The logistic relationship between inundation frequency and wetland elevation (Eq. 3.2) was used to establish the position of the sediment cores in the tidal frame. They were either categorised as low, mid, intermediate or high position in the tidal frame. Table 4.1 provides details about the cores, including wetland surface elevation relative to the localised tidal datum, vegetation type and tidal position.

Table 4.1: Sediment cores extracted for ^{210}Pb dated.

Study area	Core ID	Core location		Surface elevation (m AHD)	Position in the tidal frame			
		Latitude	Longitude		Low	Mid	Intermediate	High
Minnamurra River	Min_Mg1	-34° 37' 25.88879''	150° 50' 43.53906''	0.059	*Avicennia marina* (tall)			
	*Min_Mg2	-34° 37' 29.64826''	150° 50' 35.60811''	0.255		*Avicennia marina* (tall)		
	*Min_Mix	-34° 37' 35.19150''	150° 50' 39.40756''	0.526			*Juncus kraussii Sporobolus virginicus Avicennia marina* (shrub)	
	Min_Spo1	-34° 37' 40.85581''	150° 50' 47.84445''	0.710				*Sporobolus virginicus*
Comerong Island	*Cm_Mg2	-34° 53' 56.29259''	150° 45' 8.85190''	0.390		*Avicennia marina* (tall)		
	*Cm_Spo	-34° 52' 55.59729''	150° 44' 23.33260''	0.388			*Sporobolus virginicus*	
	*Cm_Dm	-34° 52' 18.98794''	150° 44' 35.10658''	0.463				*Avicennia marina* (shrub)
Cararma Inlet	*Ca_Mg1	-34° 59' 14.52839''	150° 46' 15.37759''	0.475		*Avicennia marina* (tall)		
	*Ca_Sar1	-34° 59' 6.88908''	150° 46' 30.24039''	0.794				*Sarcocornia quinqueflora*
Currambene Creek	*Cb_Mg	-35° 1' 9.43912''	150° 40' 1.61461''	0.319		*Avicennia marina* (tall)		
	Cb_Sar1	-35° 1' 4.38387''	150° 39' 57.76752''	0.422			*Sarcocornia quinqueflora*	
	*Cb_Sar2	-35° 0' 53.37548''	150° 40' 1.61942''	0.707				Mainly unvegetated

*cores adjacent to SETs at Minnamurra River, Cararma Inlet and Currambene Creek, and next to rSET at Comerong Island

Stratigraphical description was recorded for each core. One half of the core was sub-sampled at every 1-cm up to 20-30 cm for ^{210}Pb dating (Fig. 4.3b). Dry bulk density if the difference between dry weight and wet volume of sample. To determine dry bulk density a small fraction of subsample of known wet volume (cm^3) was dried in an oven at 60 °C a constant mass and presented as g/cm^3. The dry bulk density was used to calculate mass accumulations rates in the sediment samples. The remaining sample was processed for ^{210}Pb dating at ANSTO.

Sample preparation for ^{210}Pb dating

The absorption of unsupported ^{210}Pb is dependent on grain size distribution of the sediment samples being dated (Hollins et al., 2011). As the sediment cores were very sandy, unsupported ^{210}Pb activity was determined in sediment fractions that was < 63 μm to eliminate ^{210}Pb dilution effect produced by sand. Subsamples were wet sieved through a 63 μm sieve to concentrate the ^{210}Pb isotopic element in finer grained particles (mud), oven dried at 60 °C, crushed into powder using mortar and pestle, placed into labelled sample bags and delivered to ANSTO for ^{210}Pb dating.

The crushed samples were chemically processed using methods employed by ANSTO (ANSTO, 2018). Each subsample was spiked with Polonium-209 (^{209}Po) and Barium-133 (^{133}Ba) tracers, and subsequently leached with acids to release ^{209}Po and ^{226}Ra isotopes. ^{209}Po was autoplated onto silver disks and analysed by high resolution alpha spectrometry. ^{226}Ra was co-precipitated with $BaSO_4$ where the ^{226}Ra/^{133}Ba source was also analysed by high resolution alpha spectrometry. The membrane filter was also counted by gamma spectrometry to measure the ^{133}Ba tracer activity before determining the ^{226}Ra recoveries. Preliminary analysis was based on sequential dating of the samples (sample depths of 0-1 cm, 5-6 cm, 10-11 cm and 15-16 cm) from each core to establish the concentration of the isotopes in the samples and establish whether unsupported ^{210}Pb activity exhibited decay down the core profile. If the ^{210}Pb activities were detectable, then additional samples were analysed, thereby improving the ^{210}Pb chronology.

Sediment age determination using ^{210}Pb dating

This study and others indicate that sedimentation rates within coastal wetlands are not stable but vary according to inundation frequency and sea level variability, hence it is reasonable to presume that the CRS model would provide a better sediment chronology than the CIC model as the CRS model accounts for any

irregularities in the unsupported ^{210}Pb activity in the sediment profile. In some cores, a CRS chronology could not be achieved, therefore the CIC age/depth curve was only used to compare sedimentation rates between zones.

4.3.2. Sedimentation rates

Mean sedimentation rates were determined based on the depth of sediment accumulated (mm) between to sediment dates (year). All core depths and dates were adjusted to m AHD based on the wetland surface elevation, or top of the core, at the time of core extraction. Wetland surface elevations were determined using an RTK-GPS. All rates of change are presented to two significant figures and as mm/y. Sedimentation rate uncertainty calculations were based on error propagation calculation (Harvard University, 2007). Sedimentation rates of each core were compared with catchment area of each study site (Table 1.1).

To validate ^{210}Pb chronologies comparisons were made either between sediment dates derived from ^{137}Cs analysed by gamma spectrometry or rates of surface elevation adjustment from SET-MH. As the half-life is small for ^{137}Cs, the recovery of ^{137}Cs was low in many samples, and when this occurred the adjacent SET-MH record was used for validation.

4.3.3. Temporal change in sediment accumulation

Temporal change in annual mean water level was determined from the Fort Denison tide gauge record using partitioning in the statistical software JMP to establish variations in MSL over the tide gauge record. The mean annual water level for each time-step was modelled using a linear regression model. Incremental sedimentation over each ^{210}Pb date time-step for each core was plotted against the temporal MSL data to identify relationships between sedimentation and temporal change in MSL.

4.3.4. Relationship between wetland elevation gain and sea-level rise

Water level data from Fort Denison tide gauge station was used to determine the annual mean maximum sea level (max. SL) and annual mean sea level (MSL). The maximum SL and MSL was compared with wetland surface elevation change in the different tidal positions over the ^{210}Pb dating period. Rate of MSL change was determined between 1914 and 2017.

4.4. Results

4.4.1. Sediment age determination

The unsupported ^{210}Pb concentrations in sediment cores from Minnamurra River (Fig. 4.4), Comerong Island (Fig. 4.5), Cararma Inlet (Fig. 4.6) and Currambene Creek (Fig. 4.7) based mainly on the CRS and in some cases on CIC chronology was used to determine sediment ages. Generally, unsupported ^{210}Pb activity decreased down the sediment profile, but irregular ^{210}Pb activity and varying concentrations of unsupported ^{210}Pb were identified in Minnamurra core profiles of low and high tidal position (Fig. 4.4a and d), Comerong high tidal position core (Fig. 4.5c), Cararma mid tidal position core (Fig. 4.6a), and Currambene intermediate tidal position core (Fig. 4.7b).

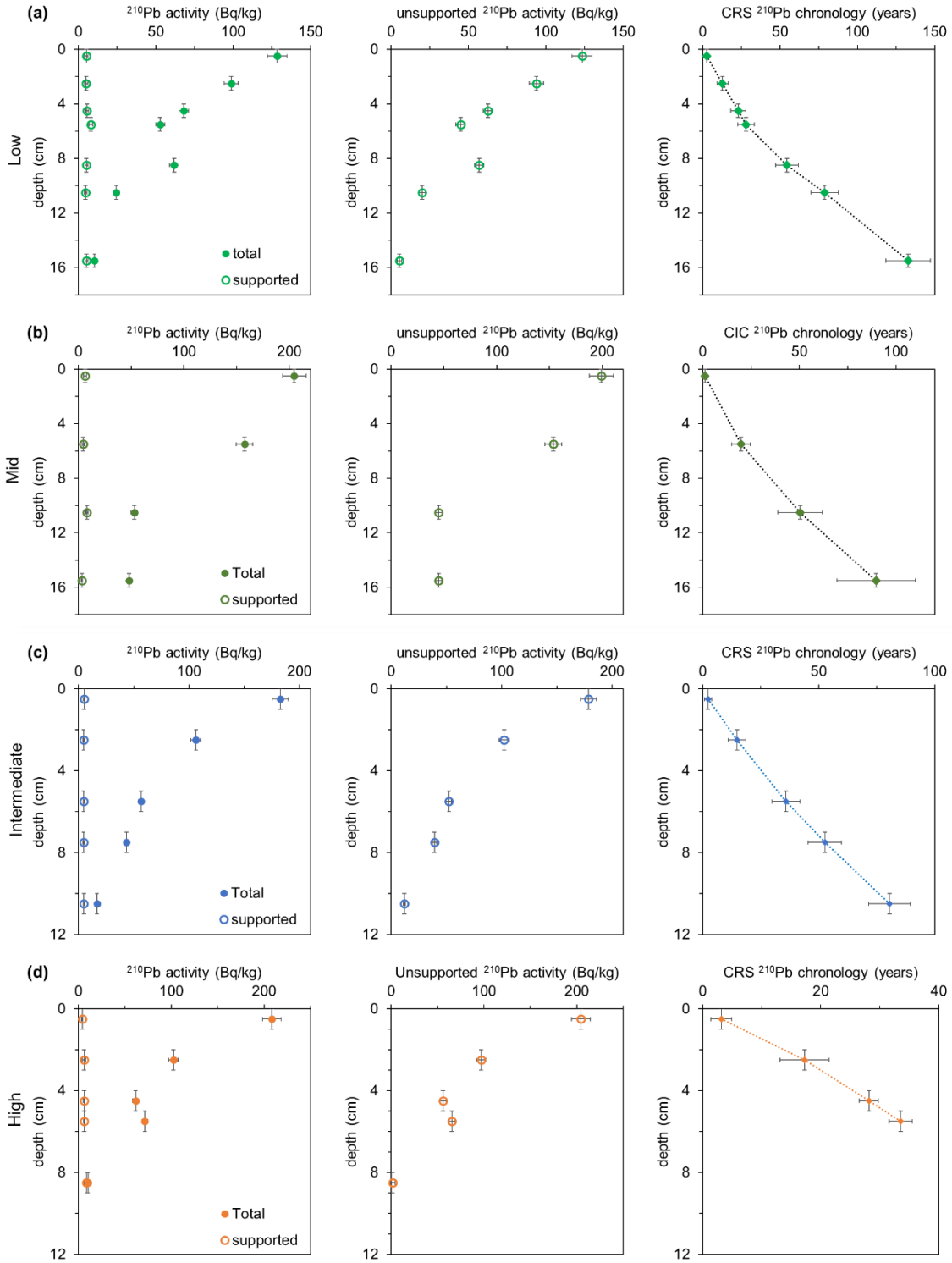

Figure 4.4: Graphs showing the total, supported and unsupported ^{210}Pb activity in sediment cores dated from Minnamurra River, and the corresponding ^{210}Pb chronology in (a) low, (b) mid, (c) intermediate, and (d) high tidal positions.

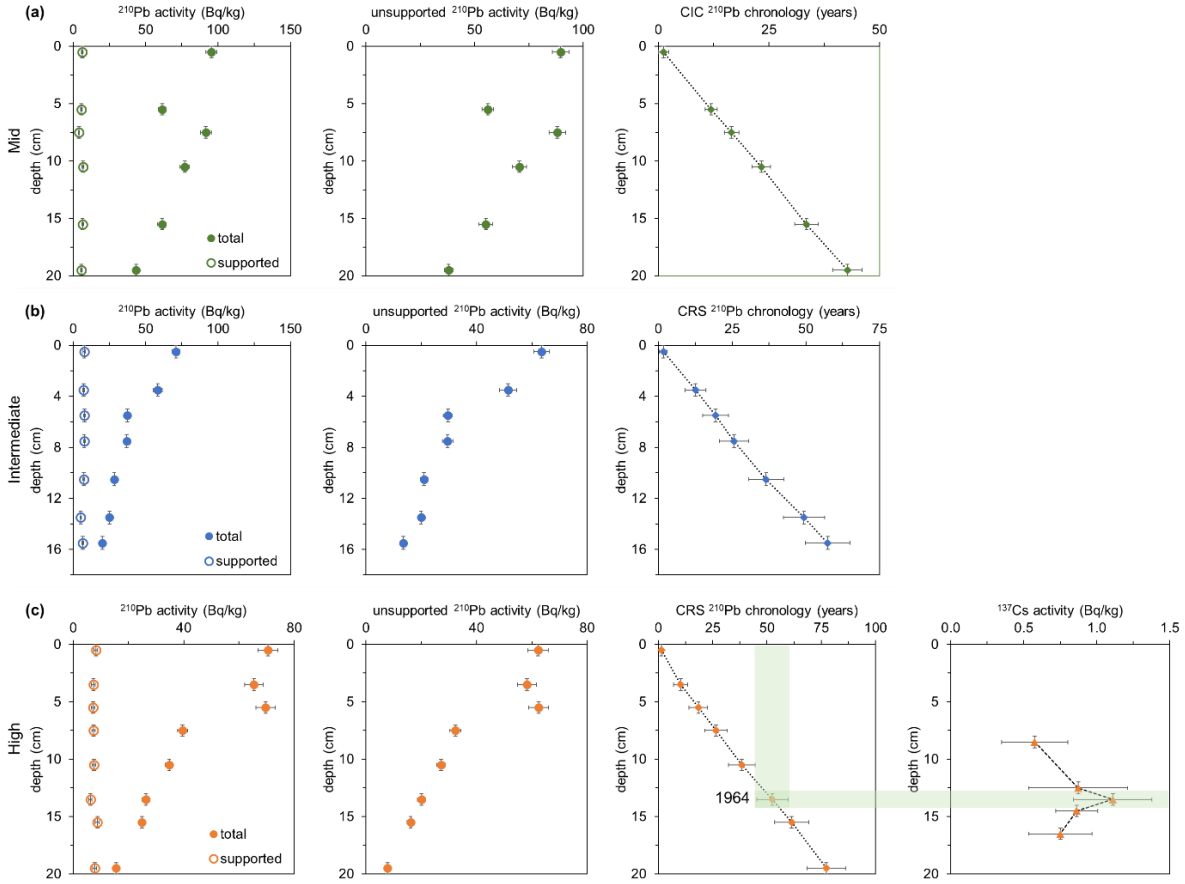

Figure 4.5: Graphs showing the total, supported and unsupported ^{210}Pb activity in sediment cores dated from Comerong Island, and the corresponding ^{210}Pb chronology in (a) mid, (b) intermediate, and (c) high tidal positions. ^{137}Cs activity established for the high tidal position core corresponds to the year 1964, validating the CRS ^{210}Pb chronology for this core.

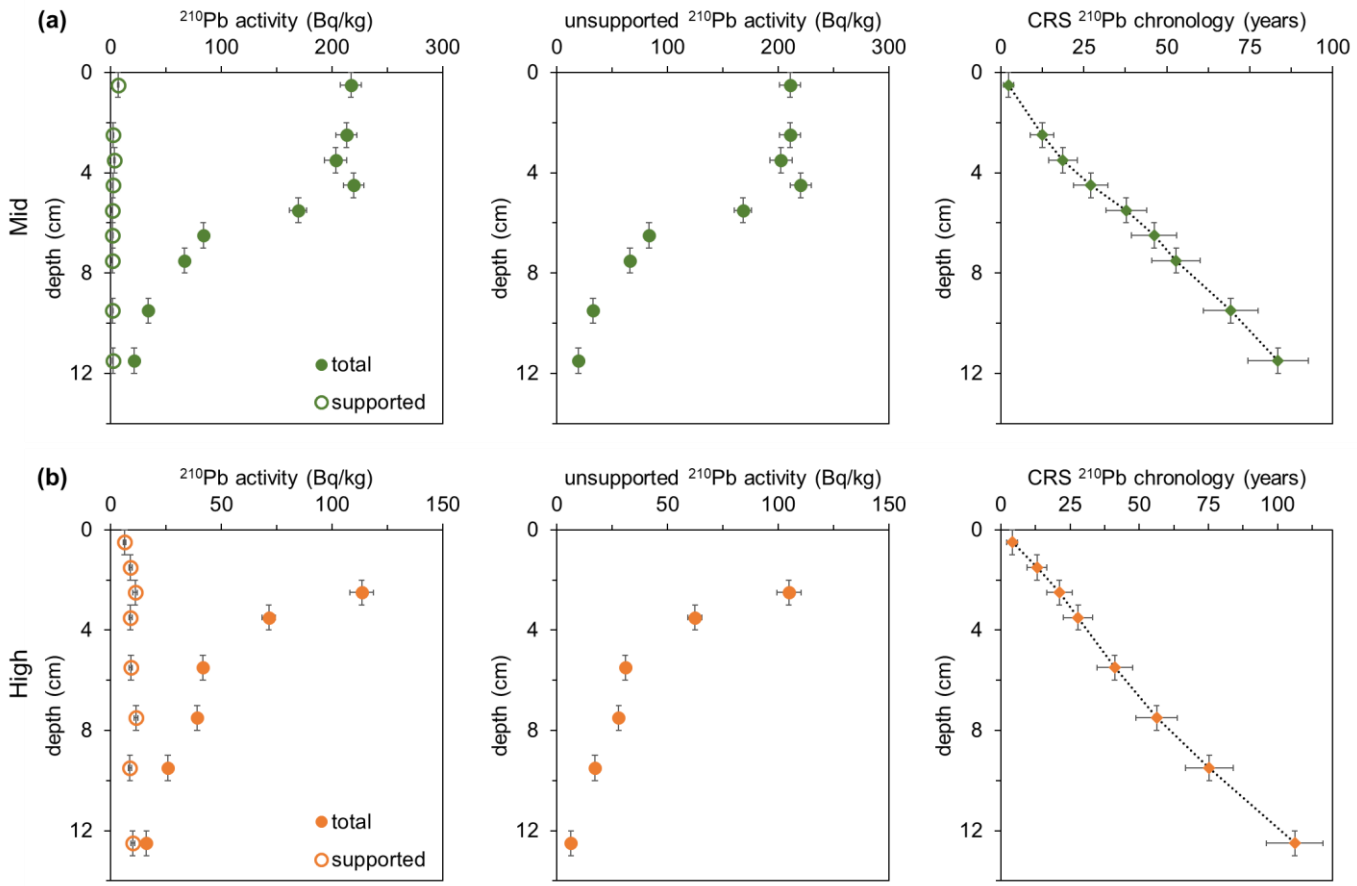

Figure 4.6: Graphs showing the total, supported and unsupported ^{210}Pb activity in sediment cores dated from Cararma Inlet, and the corresponding ^{210}Pb chronology in (a) mid and (b) high tidal positions.

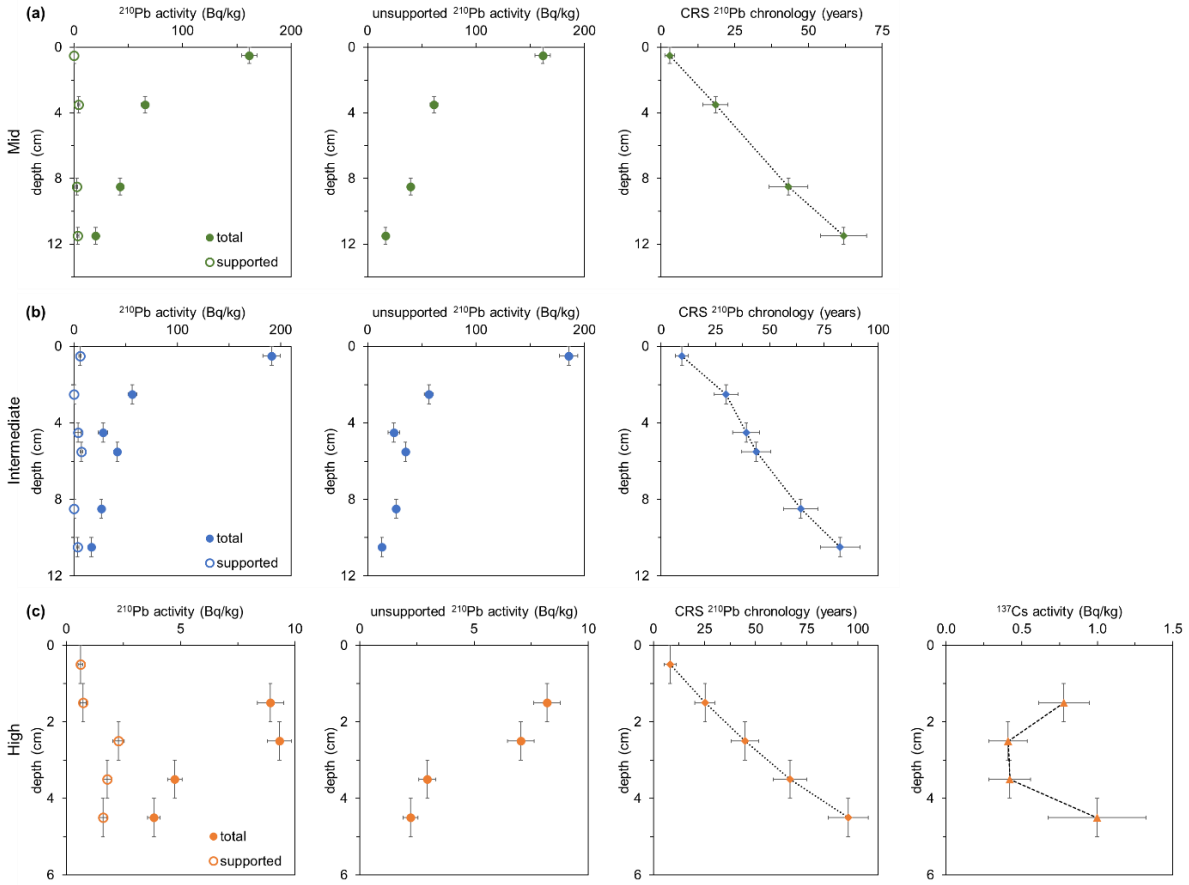

Figure 4.7: Graphs showing the total, supported and unsupported ^{210}Pb activity in sediment cores dated from Currambene Creek, and the corresponding ^{210}Pb chronology in (a) low, (b) mid, (c) intermediate, and (d) high tidal positions. Low ^{137}Cs activity in the high tidal position core did not show a significant peak hence could not be used to validate the ^{210}Pb chronology for this core.

Validation of ^{210}Pb sedimentation

^{137}Cs concentrations were generally low in the high tidal position sediments from Comerong Island (Fig. 4.5c) and Currambene Creek (Fig. 4.7c). However, the peak of ^{137}Cs concentration corresponded to the year 1964 as established from the CRS age/depth curve in the high tidal position Comerong Island core, validating the ^{210}Pb CRS chronology for this core. The ^{137}Cs profile in the Currambene Creek intermediate and high tidal position core did not show a clear ^{137}Cs activity peak and could not be used to validate the CRS chronology. ^{137}Cs was not detected in the other cores but sedimentation rates over the SET data period corresponded to the rate of surface elevation change from the nearest SET in Minnamurra, Cararma and Currambene cores (Table 4.2). The above results provide enough confidence in ^{210}Pb chronologies for these study sites.

Table 4.2: ^{210}Pb sedimentation rates and rate of surface elevation change from SETs at Minnamurra River, Cararma Inlet and Currambene Creek.

Study area	Tidal position	Core ID	^{210}Pb Sedimentation (mm/y)	^{137}Cs detectable	Surface elevation change (mm/y)
Minnamurra River	Low	^Min_Mg1	1.9 ± 0.8 (2004-2017)	Not detected	1.5 ± 0.32 (2001-2017)
	Mid	*^Min_Mg2	4.4 ± 1.2 (1997-2017)	Not detected	1.5 ± 0.32 (2001-2017)
	Intermediate	^Min_Mix	2.2 ± 0.8 (2002-2017)	Not detected	1.3 ± 0.11 (2001-2017)
	High	^Min_Spo1	1.5 ± 0.54 (1999-2016)	Not detected	1.3 ± 0.11 (2001-2017)
Comerong Island	Mid	*Cm_Mg	5.0 ± 0.064 (1974-2017)	Not detected	
	Intermediate	Cm_Sm	3.8 ± 0.054 (1959-2016)	Not detected	
	High	Cm_Mg2	3.4 ± 0.073 (1939-2016)	Detected	
Cararma Inlet	Mid	^Ca_Mg	2.1 ± 0.9 (2001-2013)	Not detected	1.6 ± 0.47 (2001-2013)
	High	^Ca_Sm	1.2 ± 0.6 (2001-2013)	Not detected	1.2 ± 0.58 (2001-2013)
Currambene Creek	Mid	Cb_Mg	2.6 ± 0.8 (1999-2017)		0.35 ± 0.12 (2001-2017)
	Intermediate	^Cb_Sm1	0.65 ± 0.94 (2006-2016)	Low activity	0.23 ± 0.10 (2001-2017)
	High	^Cb_Sm2	0.78 ± 0.68 (2000-2015)	Low activity	0.23 ± 0.10 (2001-2017)

* Sedimentation rate based on CIC chronology
^ ^{210}Pb chronology validated based of nearest SET data

4.4.2. Century-scale sedimentation in mangrove and saltmarsh

Minnamurra River

Radiometric detain indicated that rates of sediment accumulation were proportional to tidal position. The ^{210}Pb chronology provided a 133-year record of

sediment accumulation in the low tidal position, during which time sediments were accumulating at 1.2 ± 0.086 mm/y between 1884 and 2017 (Fig. 4.8a). The intermediate tidal position mixed vegetation zone was accumulating sediments at a rate of 1.7 ± 0.071 mm/y between 1936 and 2017 (Fig. 4.8b), whilst the high tidal position saltmarsh accumulated sediments at 1.6 ± 0.043 mm/y (Fig. 4.8c) over a relatively short period of time (1982 to 2016) (See Table 4.3 for sedimentation rates for Minnamurra cores). The mid tidal position mangrove zone accumulated sediments at 2.7 ± 0.25 mm/y between 1927 and 2017 and presented in Fig. 4.8d for comparing sedimentation rates between the different tidal positions. Relatively high amounts of sedimentation occurred in all the tidal positions with the highest rate occurring in the mid tidal position dominated by tall *Avicennia marina* mangrove.

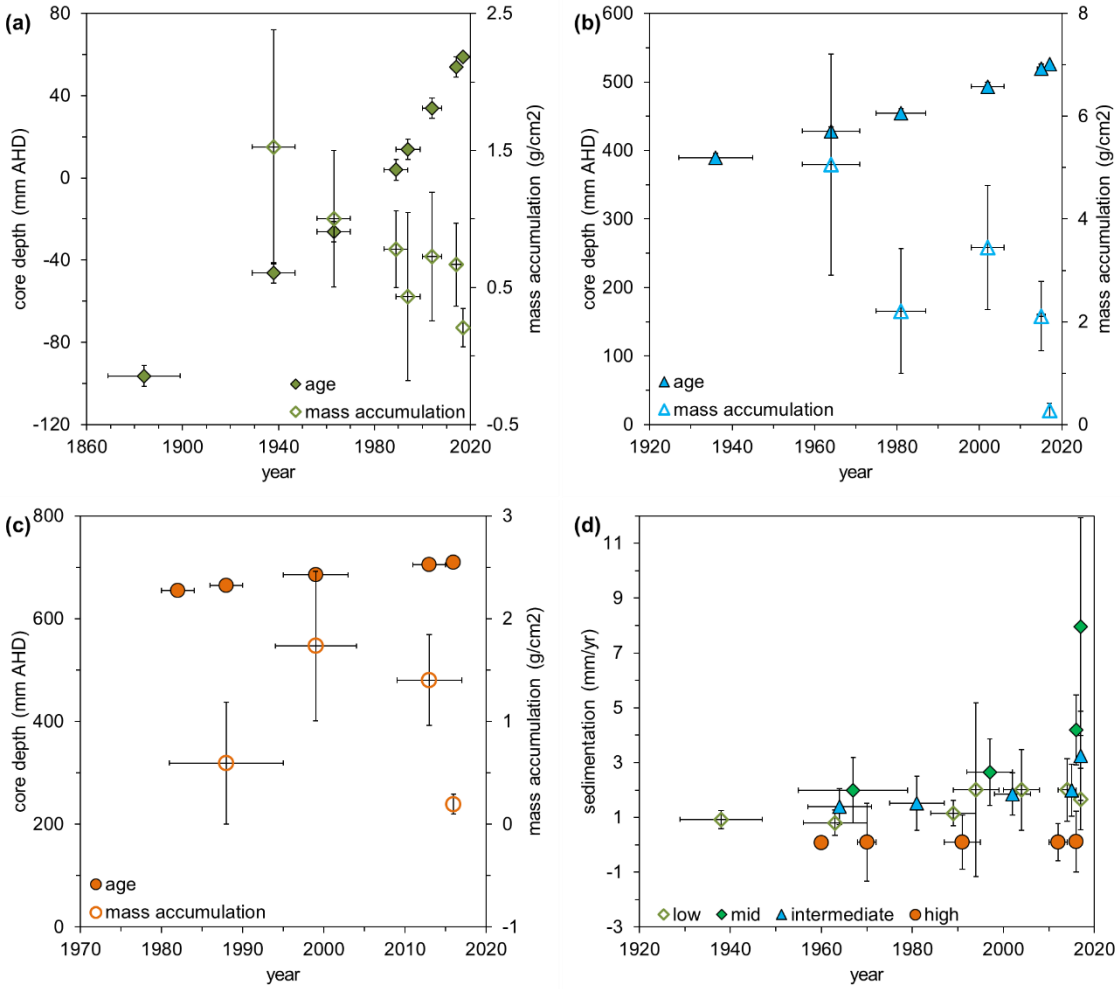

Figure 4.8: CRS age vs depth profile and mass accumulation derived from ^{210}Pb dating (± standard error) in (a) low, (b) intermediate and (c) high tidal position Minnamurra cores. (d) Sedimentation (± standard error) over the ^{210}Pb time interval (the mid tidal position sedimentation rate is included for comparison) in each tidal position.

Table 4.3: The table below summarises the rate of sediment accumulation in the different tidal positions of the study areas determined from ^{210}Pb dating. Mean rates of accumulation for each core is in bold.

Study area	vegetation category	Tidal position	Model used		Sedimentation (mm/y)	Period	CRS mass accumulation ($g/cm^2/y$)
Minnamurra River	Mangrove (Min_Mg1)	Low	CRS	mean	1.2 ± 0.086	1884-2017	0.056±0.0087
				min	0.80 ± 0.46	1938-1963	
				max	2.0 ± 1.5	1989-2014	
	Mangrove (Min_Mg2)	Mid	CIC	mean	2.7 ± 0.25	1927-2017	0.088± 0.020
				min	2.0 ± 1.2	1927-1967	
				max	8.0 ± 4.0	2016-2017	
	Saltmarsh (Min_Mix)	Intermediate	CRS	mean	1.7 ± 0.071	1936-2017	0.155±0.0093
				min	1.4 ± 0.65	1936-1964	
				max	3.2 ± 1.6	2015-2017	
	Saltmarsh (Min_Spo1)	High	CRS	mean	1.6 ± 0.043	1982-2016	0.064±0.0070
				min	1.4 ± 0.68	2013-2016	
				max	1.8 ± 0.98	1999-2013	
Comerong Island	Mangrove (Cm_Mg1)	Mid	CIC	mean	5.0 ± 0.064	1974-2017	0.488±0.036
				min	4.3 ± 0.45	1974-1984	
				max	5.4 ± 1.4	1984-1994	
	Saltmarsh (Cm_Sm)	Intermediate	CRS	mean	3.8 ± 0.054	1959-2016	0.370±0.024
				min	3.4 ± 2.8	1967-1979	
				max	4.6 ± 4.6	1990-1997	
	Mangrove (Cm_Mg2)	High	CRS	mean	3.4 ± 0.073	1939-2016	0.382±0.026
				min	2.9 ± 2.0	1964-1978	
				max	6.8 ± 3.4	2015-2016	
Cararma Inlet	Mangrove (Ca_Mg)	Mid	CRS	mean	1.3 ± 0.040	1929-2013	0.030±0.0027
				min	0.91 ± 0.93	1986-1994	
				max	2.5 ± 1.9	2011-2013	
	Saltmarsh (Ca_Sm)	High	CRS	mean	1.2 ± 0.036	1907-2013	0.127±0.015
				min	1.0 ± 0.48	1907-1938	
				max	1.5 ± 1.1	1985-1992	
Currambene Creek	Mangrove (Cb_Mg)	Mid	CRS	mean	2.5 ± 0.063	1955-2017	0.146±0.017
				min	2.1 ± 1.3	1955-1974	
				max	2.6 ± 1.0	1974-2017	
	Saltmarsh (Cb_Sm1)	Intermediate	CRS	mean	1.8 ± 0.10	1934-2016	0.102 ± 0.017
				min	0.65 ± 0.19	2006-2016	
				max	2.9 ± 2.7	1986-2006	
	Saltmarsh (Cb_Sm2)	High	CRS	mean	0.62 ± 0.030	1920-2015	0.061±0.0086
				min	0.46 ± 0.39	1948-1970	
				max	0.81 ± 0.30	2007-2015	

An increase in sediment accumulation rates was observed in the low, mid and

intermediate tidal positions over the ^{210}Pb dating period, whilst the sedimentation rate appears to be slowing down in the high tidal position which had a mass accumulation rate of 0.064 g/cm^2/y (Fig. 4.8d). Mass accumulation trends varied between sites with the highest mass accumulation rate occurring in the intermediate tidal position of 0.155 g/cm^2/y, and the lowest rate in the low tidal position of 0.056 g/cm^2/y (Refer to Table 4.3 for mass accumulation rates for Minnamurra River). Sediment mass diminished with increasing substrate elevation as sediments accumulated in the low, intermediate and high cores. This indicates that organic material diminished over time within accumulated sediments as there was a greater proportion of organics in deeper sediments.

Comerong Island

^{210}Pb sedimentation rates was proportional to tidal position at Comerong Island. The intermediate tidal position was accumulating sediments at 3.8 ± 0.054 mm/y between 1959 to 2016, whilst the high tidal position was accumulating sediments at 3.4 ± 0.073 mm/y from 1939 to 2016 (Fig. 4.9a). The ^{137}Cs peak in the high tidal position core coincided with the year 1964 from ^{210}Pb CRS model chronology supporting the sediment accumulation rate at this location (Fig. 4.5b, see Table 4.3 for sedimentation rates of Comerong cores). The mid tidal position accumulated sediments at a relatively high rate of 5.0 ± 0.064 mm/y based on the CIC chronology-based between 1974 and 2017.

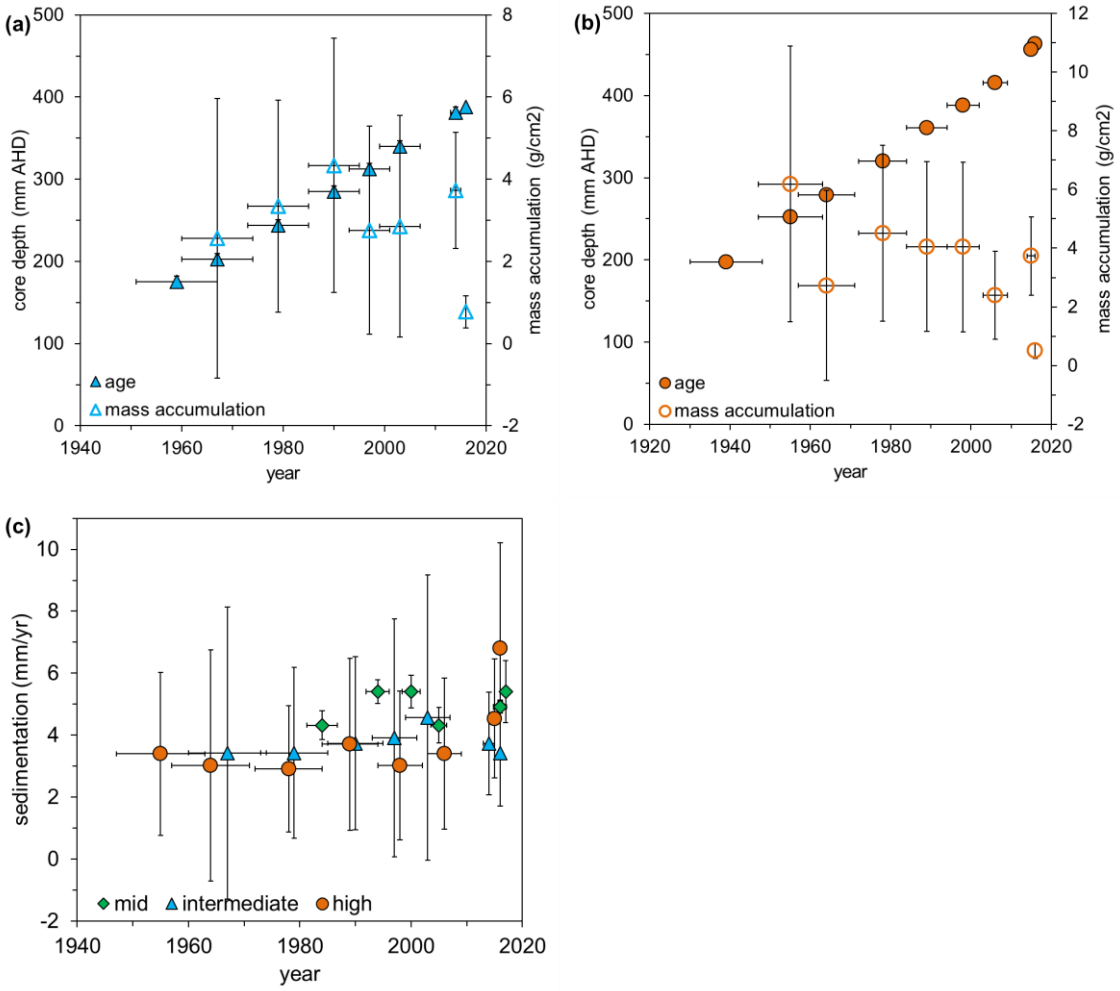

Figure 4.9: CRS age vs depth profile and mass accumulation derived from ^{210}Pb dating (± standard error) in (a) intermediate and (b) high tidal position Comerong cores. (c) Sedimentation (± standard error) over the ^{210}Pb time interval (the mid tidal position sedimentation rate is included for comparison) in each tidal position.

Relatively high sedimentation rates were measured in all tidal positions at Comerong Island, however sedimentation rates decreased across the intertidal zone as wetland elevation above the localised tidal datum (m AHD) increased (Fig. 4.9c). Similarly, mass accumulation rates decreased from 0.49 g/cm^2/y in the mid tidal position to 0.38 g/cm^2/y in the high tidal position (refer to Table 4.3 for mass accumulation rates for Comerong cores). A relationship was established between sedimentation and mass accumulation whereby, sediment mass diminished with increasing sedimentation (Fig. 4.9c).

Cararma Inlet

Sedimentation reflected tidal position at Cararma Inlet, where sedimentation decreased with increasing wetland elevation above the localised tidal datum (m AHD). Sedimentation of 1.3 ± 0.040 mm/y was observed in the mid tidal position mangrove zone from 1929 to 2013, whilst the high tidal position saltmarsh was increasing at a similar rate of 1.2 ± 0.036 mm/y between 1907 and 2013 (Fig. 4.10a and b, see Table 4.3 for sedimentation rates of Cararma cores). Mass accumulation rates were greater at higher elevations in the tidal frame at Cararma Inlet, where mid tidal position was accumulating 0.030 ± 0.0027 g/cm^2/y of sediments, whilst mass accumulation rates of 0.127 ± 0.015 g/cm^2/y was observed at the high tidal position (see Table 4.3 for mass accumulation rates). A decreasing trend in mass accumulation over time was observed in both cores, indicating that the contribution of mineral sediments to substrates is diminishing and/or the organic matter contribution is increasing in the low tidal position core.

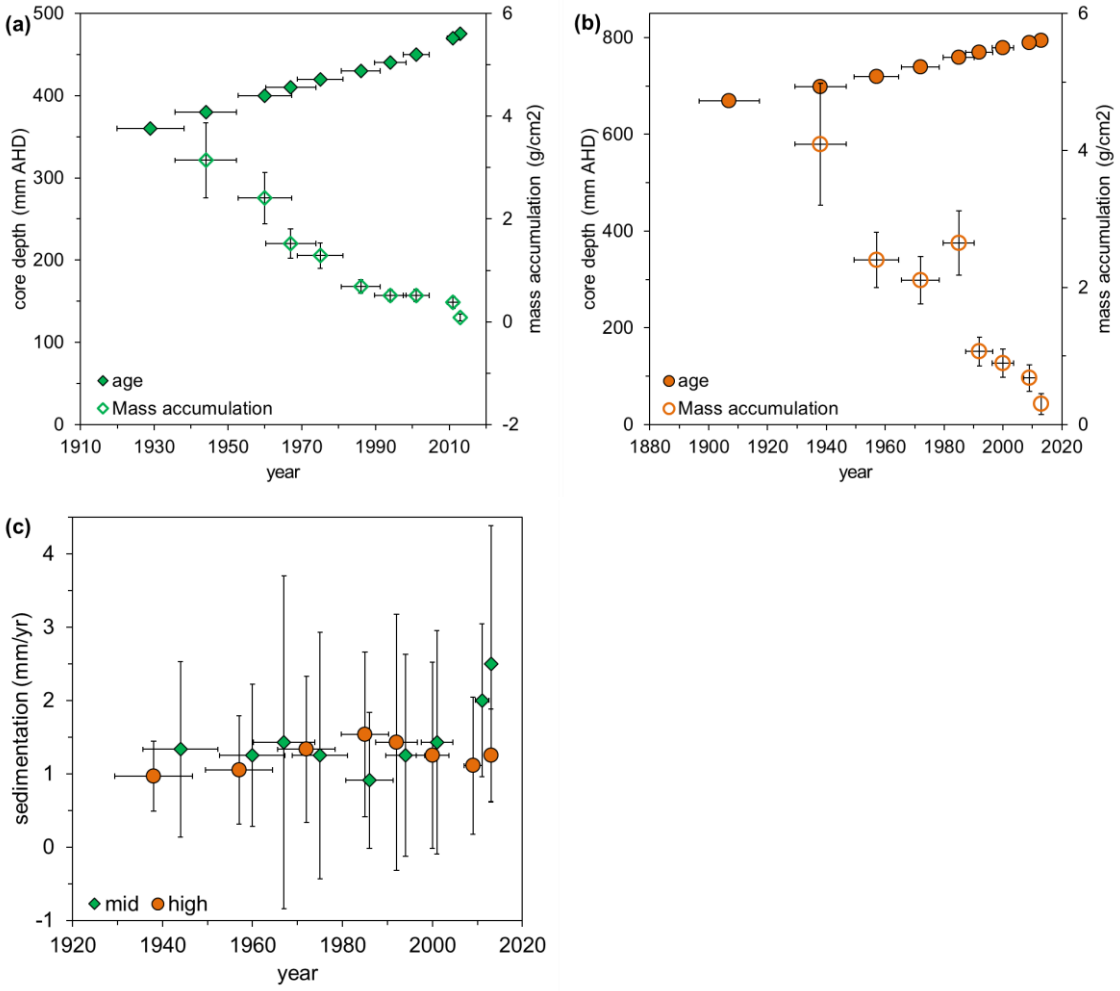

Figure 4.10: CRS age vs depth profile and mass accumulation derived from ^{210}Pb dating (± standard error) in (a) mid and (b) intermediate tidal position Cararma cores. (c) Sedimentation (± standard error) over the ^{210}Pb time interval in each tidal position.

Currambene Creek

Rate of sediment accumulation was proportional to tidal position at Currambene Creek. The mid tidal position mangrove accumulated sediments at the highest rate of 2.5 ± 0.063 mm/y between 1955 and 2017 (Fig. 4.11a), the intermediate tidal position saltmarsh is increasing surface at 1.8 ± 0.10 mm/y between 1934 and 2016 (Fig. 4.11b), whilst sedimentation occurred only at a rate of 0.62 ± 0.030 mm/y in the high tidal position core between 1920 and 2015 (Fig. 4.11c) at Currambene Creek (see Table 4.3 for sedimentation rates for Currambene cores). The high tidal position sedimentation correlated with the SET data validating the

^{210}Pb chronology for this site (Table 3.7).

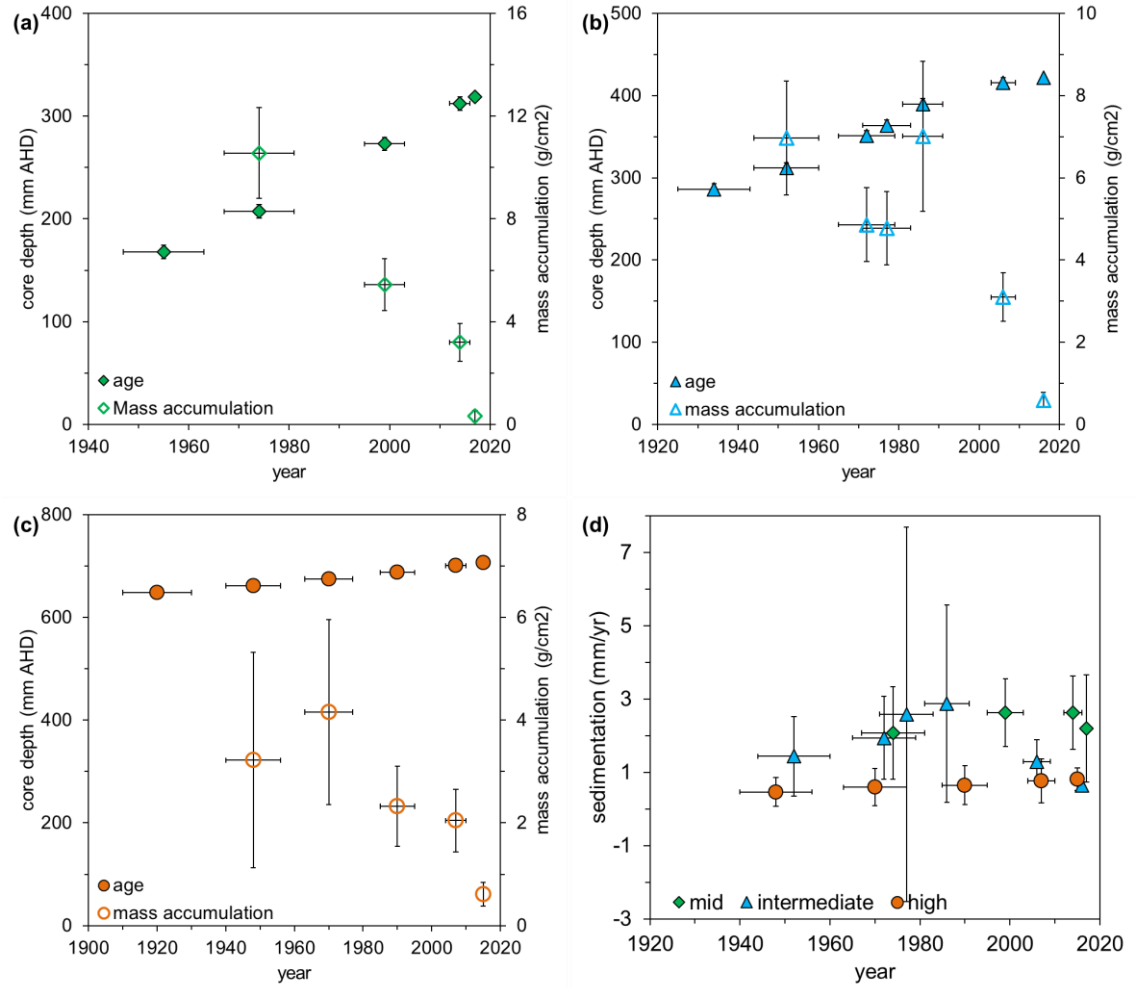

Figure 4.11: CRS age vs depth profile and mass accumulation derived from ^{210}Pb dating (± standard error) in (a) mid, (b) intermediate and (c) high tidal position Currambene cores. (d) Sedimentation (± standard error) over the ^{210}Pb time interval in each tidal position.

Sedimentation pattern at this site reflected tidal position in the landscape (Fig. 4.11d). Like other study sites, mass accumulation diminished over time, whilst sedimentation rate increased. Similarly, mass accumulation and sedimentation decreased from low to high tidal positions. Mass accumulation of 0.146 ± 0.017 g/cm^2/y was observed at mid tidal position, 0.102 ± 0.017 g/cm^2/y at intermediate tidal position and 0.061 ± 0.0086 g/cm^2/y at the high tidal position (see Table 4.3 for mass accumulation rates). An acceleration in sedimentation over the ^{210}Pb dating period was observed at the mid and intermediate tidal positions, whilst no real sedimentation was observed at the high tidal position (Fig. 4.11d).

Regional-scale sedimentation

The catchment size of each study area had a relatively strong influence on the rate of sediment accumulation (Fig. 4.12). Sediments accumulated at a relatively high rate in all tidal positions at Comerong Island which has a catchment area of about 7086 km^2, being part of the Shoalhaven River estuary (Table 1.1). In contrast, Cararma Inlet was smallest catchment area in which relatively lower rates of sedimentation was measured. Minnamurra River and Currambene Creek had a relatively similar catchment area of 117 km^2 and 160 km^2, respectively, in which mangrove accumulated sediments at a higher rate than saltmarsh. This indicates catchment size has a considerable influence on sediment accumulations capabilities of estuarine coastal wetlands.

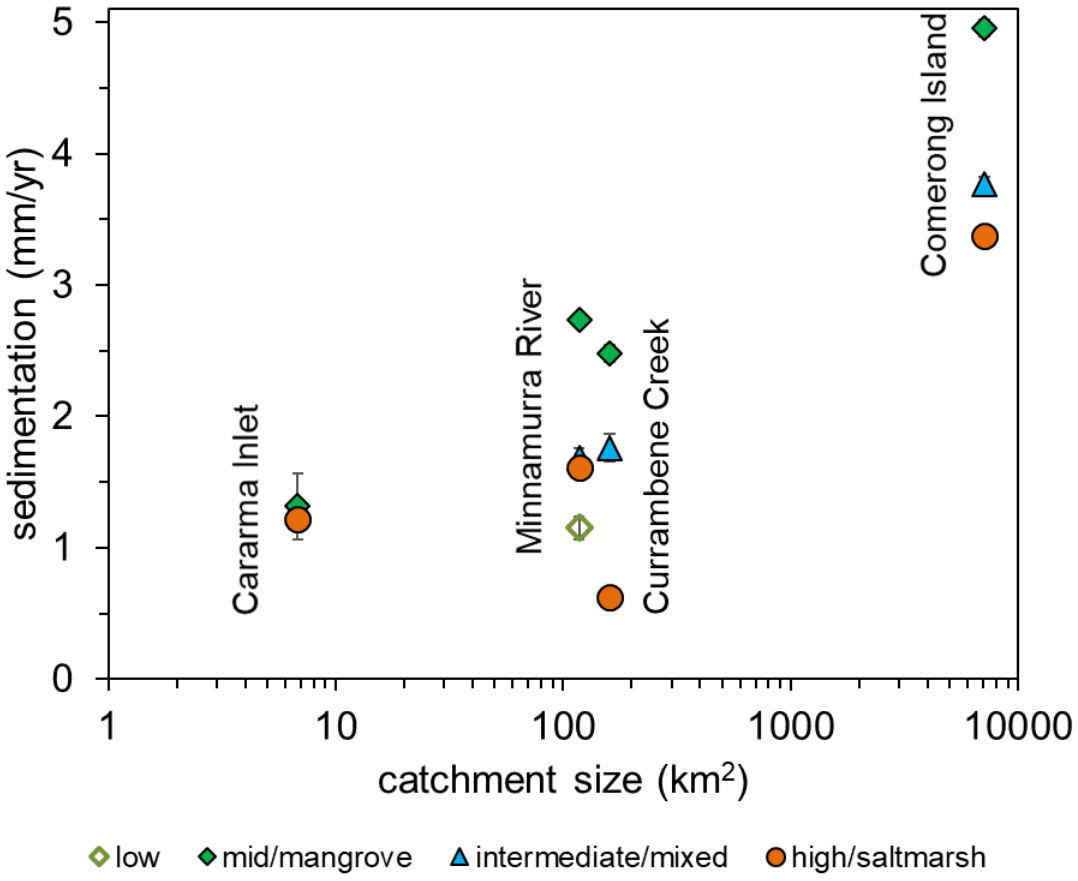

Figure 4.12: Relationship between catchment size and sedimentation rate in each study area.

4.4.3. Temporal change in sedimentation

Partitioning of sea-level measurements from Fort Denison differentiated three periods over which patterns of sea-level change were relatively consistent: (MSL-i) between 1914 and 1949 was a period over which sea level declined at a rate of 0.95 ± 0.35 mm/y (r^2 = 0.1868); (MSL-ii) between 1950 and 2009 when it was starting to increase at 0.61 ± 0.18 mm/y (r^2 = 0.1654); and (MSL-iii) in the last 7 years between 2010 and 2017 sea level increased at a remarkable rate of 8.3 ± 3.1 mm/y (r^2 = 0.5415, Fig. 4.13).

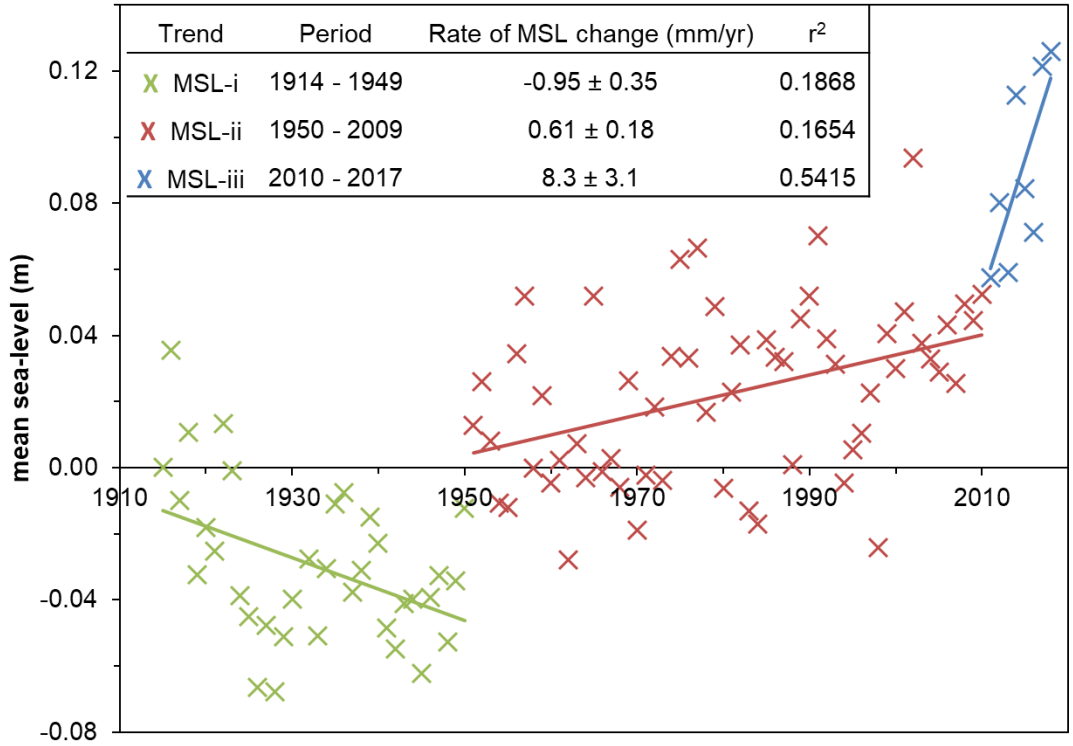

Figure 4.13: Patterns of sea level change between 1914 and 2017 based on the Fort Denison tide gauge record.

Sedimentation rates over the ^{210}Pb dating period correlated with the temporal change in relative MSL, particularly at the mid, intermediate and high tidal positions at Minnamurra River, mid and high tidal positions of Comerong Island, and at mid and high tidal positions at Cararma Inlet (Fig. 4.14). An acceleration in sedimentation corresponded to acceleration in SLR, particularly over the past 15 – 20 years. There was a general pattern of sedimentation in high tidal positions

corresponding to the long-term period of moderate SLR of 0.61 mm/y that occurred between 1950 and 2009, whilst sedimentation in intermediate and mid tidal positions over this period was higher than the observed rate of SLR. In contrast, it was only the lower elevations at Minnamurra River, Comerong Island and Cararma Inlet where sedimentation accelerated as SLR accelerated post 2009.

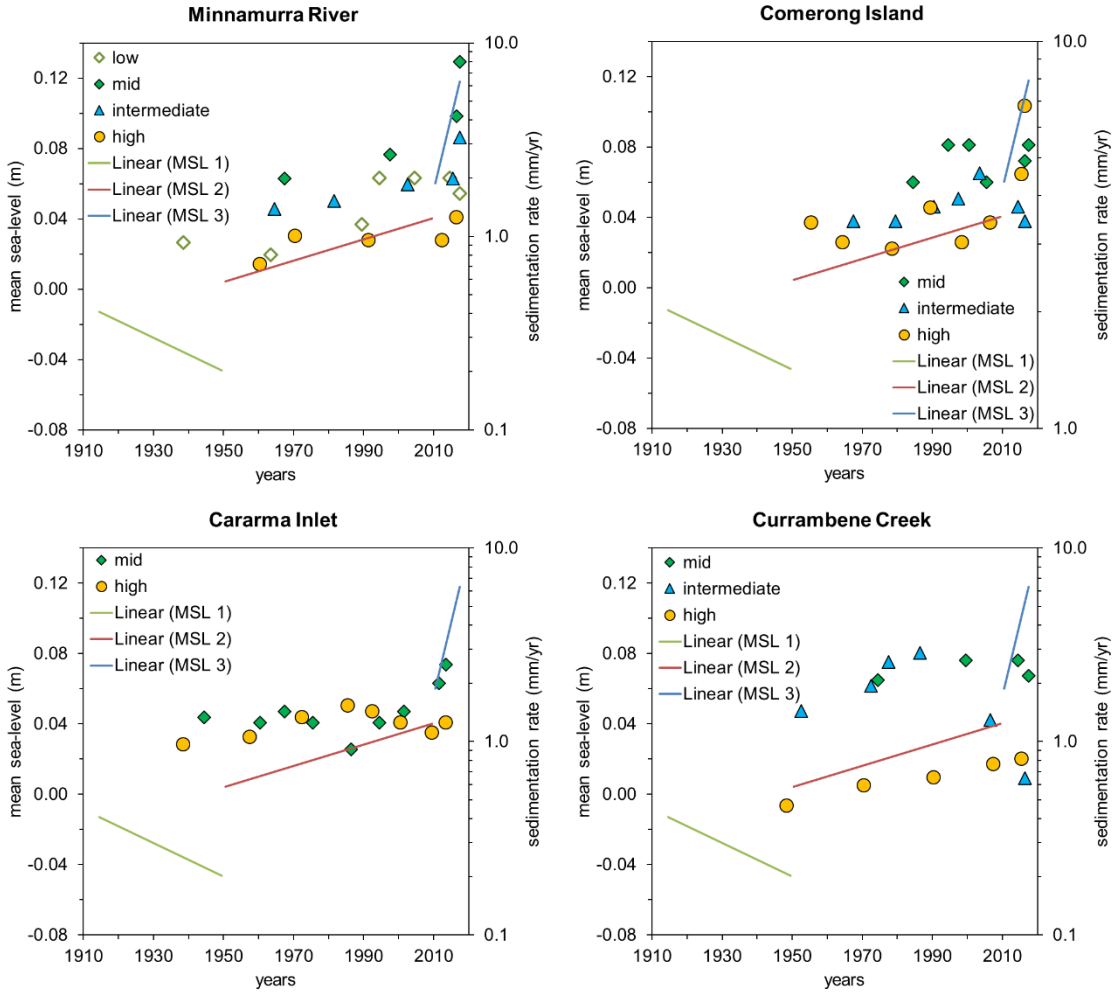

Figure 4.14: Graphs showing correlation between temporal change in relative sea-level and sedimentation in the different tidal positions of individual study sites. Please note the sedimentation rates are represented in logarithmic scale to identify temporal patterns of change over the tide gauge record.

4.4.4. Relationship between wetland elevation and sea-level

MSL over the tide gauge record has been increasing at a rate of 1.0 ± 0.093 mm/y, whilst max. SL has been increasing at 0.77 ± 0.12 mm/y between 1914 and 2017.

Positions higher in the tidal frame, particularly those where saltmarsh occurs, exhibit rates of sediment accumulation that corresponds to rates of SLR, whereas sediment accumulation rates of lower tidal positions is higher than rates of SLR (Fig. 4.15, refer to Table 4.3 for ^{210}Pb sedimentation rates). Comerong Island is accumulating sediments and gaining elevation at much higher rates than mean SLR and maximum SLR at all tidal positions, reinforcing the importance of catchment size on sediment accumulations trends (Fig. 4.12). Cararma Inlet mid and high tidal positions are increasing surface elevation at similar rates to that of mean SLR, maintaining wetland elevation relative to SLR. Currambene Creek high tidal position is the only site that has been increasing wetland elevation at a lower rate than both MSL and max. SL. The mid and intermediate tidal positions sedimentation rates have been higher (Fig. 4.15). The very little change in the sediment accumulation pattern at high saltmarsh-dominated tidal position appears to be losing elevation and creating space for the lateral expansion of mangrove plants.

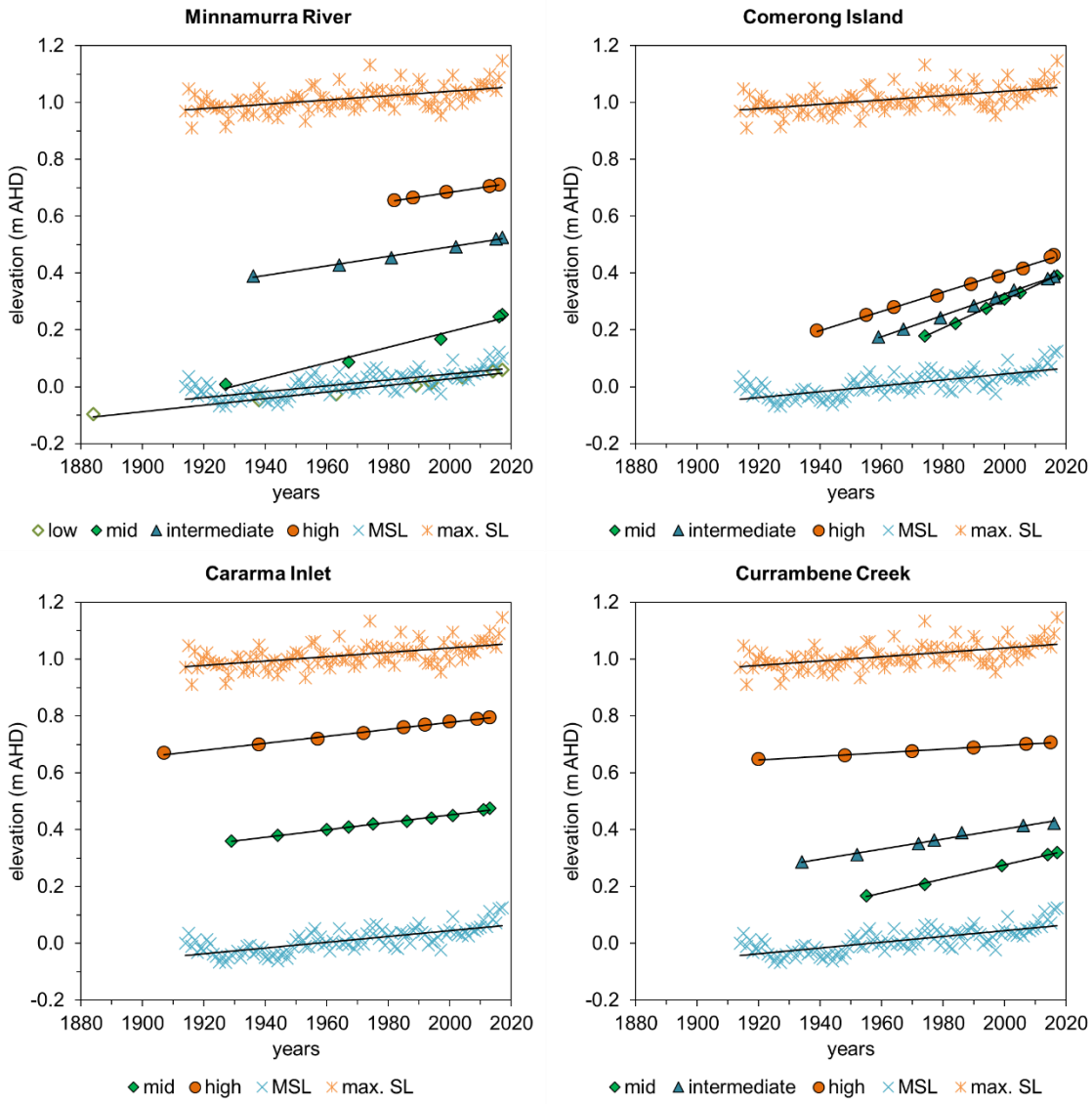

Figure 4.15: Wetland surface elevation over the ^{210}Pb dating period relative to MSL and max. SL over the Fort Denison tide gauge record at Minnamurra River, Comerong Island, Cararma Inlet and Currambene

4.5. Discussion

4.5.1. Spatial patterns of sediment accumulation

Spatial variability in sediment accumulation rates was associated with position in the tidal frame over the ^{210}Pb record. Sedimentation rates were higher in mid tidal position dominated by tall *Avicennia marina*, whereas sedimentation rates were

lower in the high tidal positions typically dominated by saltmarsh. Results from this study demonstrated that over decadal to centurial timescales, sediment accumulation related to accommodation space; where there is more space for sediments to accumulate, sedimentation rates are higher (i.e. in the mangrove). Spatial variability in sediment accumulation rates in intertidal wetlands has been reported in other studies, where accumulation rates decreased with increasing wetland elevations (Allen, 2000; Sanders et al., 2010a, 2010b; Woodroffe, 2018a). The long-term spatial trends in sediment accumulation correlated with spatial patterns in SEC established from SETs at decadal time scales (Chapter 3), whereby sedimentation rates and rate of SEC was higher in mid tidal positions and lower at high tidal positions, which may be associated with relative SLR.

There was geographical difference in sediment accumulation between study sites. For instance, Comerong Island is part of a relatively large Shoalhaven catchment and is accumulating sediments at a higher rate. High amount of sediment accumulation at this study site may be associated with high sediment input from the Shoalhaven catchment in comparison to Cararma Inlet, which has the smallest catchment area and is accumulating sediments at a slower rate (Fig. 4.12). These results demonstrate that catchment size has a considerable influence on the capacity of estuaries to accumulate mineral sediments. This indicates that the sediment delivered by the catchment is particularly important for the development of coastal wetland vegetation, particularly mangroves as demonstrated in other studies (Saintilan et al., 2009; Swales et al., 2015; Woodroffe, 2018b).

4.5.2. Temporal patterns of sediment accumulation

There was relatively little variation in sedimentation rates over time in saltmarsh, whilst an acceleration in sedimentation rates post 2009 was more common in mangrove vegetation over the ^{210}Pb record, which may be associated with the recent acceleration in relative SLR of 8.3 ± 3.1 mm/y post 2009. Even though mangrove plants have the capacity to accumulate sediments *in situ* through

organic matter additions and trapping of mineral sediments can directly contribute to surface elevation gain, these processes alone did not contribute to an acceleration in sedimentation over longer timescales as demonstrated in other studies (Swales et al., 2015). SLR creating more accommodation space for mineral and organic sediment deposition may have resulted in an acceleration in sedimentation rates, a trend also documented in other studies (Kirwan and Megonigal, 2013; Krauss et al., 2014; Rogers et al., 2019a; Schuerch et al., 2018a). The lack of acceleration in saltmarsh may be associated with the settling velocity of suspended sediments that increases exponentially as you move away from the wetland edge (from saltmarsh to mangrove in this study) (Temmerman et al., 2003).

In this study, the saltmarsh surface has increased elevations beyond its capacity to accumulate sediments is maintaining elevations relative to SLR. It is not experiencing any acceleration in sediment accumulation rates because the wetland surface may not be low enough in the tidal frame to trigger an acceleration in sedimentation. A deceleration in sedimentation in the intermediate tidal positions at Comerong Island since 2003 and in Currambene Creek since 1986 indicates that this zone has been losing elevation relative to SLR and appears to be creating space for the lateral expansion of mangrove. Mangrove encroachment into saltmarsh has been documented along the south-eastern coastline, including Currambene Creek and Cararma Inlet (Rogers et al., 2006; Saintilan and Wilton, 2001). Similar trends have been documented in other parts of Australia (Kelleway et al., 2016; Rogers et al., 2005b; Saintilan et al., 2009; Saintilan and Williams, 1999) and elsewhere (Doughty et al., 2016; Saintilan et al., 2013b).

4.5.3. Relationship between wetland elevation and sea level rise

SLR is considered a threat to coastal wetland ecosystems but at centurial timescales it was discovered that they are either exceeding or maintaining elevations relative to SLR by infilling with sediments, whereby the degree of infill

is exponentially proportion to catchment size. An acceleration in sedimentation in mangrove implies that sediment is still being actively delivered to this site and it is only the high tidal positions located higher in the tidal frame are tracking sea level, whereas the lower tidal positions are outpacing SLR.

Saltmarsh sedimentation rate being similar to the rate of SLR indicates that saltmarsh may have reached an equilibrium between sediment accumulation, inundation, and elevation and is maintaining elevation relative to SLR through what has been described as a negative feedback loop (Pethick, 1981; Saintilan et al., 2009). Saltmarsh keeping pace with localised rates of SLR has been documented in other studies, which they do by maintaining a balance between inundation frequency, sediment accumulation and elevation (French et al., 1994; Kirwan and Temmerman, 2009; Saintilan et al., 2009). However, it appears that mangrove will effectively continue accumulating sediments and promote surface elevation gain until their elevation increases significantly within the tidal frame. Mangroves will then reach elevations whereby sediment accumulation rates would equal the rate of SLR as suggested in a recent study by Woodroffe (2018a).

The south-eastern coastline of Australia is tectonically stable and so the availability and size of accommodation space and associated sediment inputs are largely connected to regional-scale SLR (Ruiz-Fernández et al., 2016; Sloss et al., 2007). No evidence was found of any substantial changes in shoreline position or of low elevation mangrove drowning in this study. However, studies have demonstrated that even in the absence of sedimentation there is considerable time before submergence occurs, as they might have elevation capital to spare (Cahoon and Guntenspergen, 2010; Reed, 2002). However, if the wetland surface also starts to lose elevation as sea levels rise then this makes coastal vegetation vulnerable to SLR. This vulnerability of wetland vegetation to SLR was not identified at these study sites over the ^{210}Pb record but demonstrated that sedimentation rates are accelerating in the mangrove, whilst saltmarsh are stable and maintaining elevations relative to SLR over the past few decades.

4.6. Conclusion

Sediment accumulation rates in coastal wetlands is proportional to tidal position, where the mid tidal position mangroves located lower in the tidal frame was accumulating sediments at a higher rate than saltmarshes located higher in the tidal frame. Tidal inundation frequency and accommodation space also had a considerable influence on sedimentation rates in the different tidal position. The mid tidal position mangrove in relation to saltmarsh had a higher inundation frequency and accommodation space and is accumulating sediments at an average rate of 1.3 – 2.5 mm/y, whereas saltmarsh accumulated sediments between 0.62 and 1.6 mm/y over the ^{210}Pb record. At this timescale, coastal wetlands have been infilling and the degree of infill is proportional to catchment size, whereby wetland areas that have a larger catchment area and more sediment supply is accumulating sediments at a higher rate.

In relation to relative SLR, mangrove sedimentation rates exceeded the mean rate of SLR of 1.0 ± 0.093 mm/y over the tide gauge record, whereas saltmarsh zones accumulated sediments at similar rates to that of SLR. Saltmarsh has been maintaining elevation in the tidal frame relative to SLR, whereas mangrove is outpacing the rate of relative SLR. Where accommodation space was high (i.e. in the mangrove) there has been a recent acceleration in sedimentation, which is most likely corresponding to the influence of SLR (post 2009) on accommodation space. A deceleration in sedimentation in the intermediate tidal positions indicated that this zone has been losing elevation relative to SLR and appears to be creating space for the lateral expansion of mangrove. Whilst where accommodation space is low (i.e. saltmarsh), there has been no change in sedimentation rates over this time period. This study demonstrated that at this timescale, wetlands are adjusting to relative SLR that has occurred over the past century and are still infilling implying that there is still some resilience in the coastal wetlands to adjust to higher rates of SLR, but a threshold could not be established from this study. Longer-term sedimentation trends and surface elevation dynamics and modelling could be used

to determine this threshold.

The sediment dynamics in coastal wetland vegetation over the tide gauge record indicate that sea-level variability had a considerable effect on wetland surface elevation and vegetation distribution. The next two chapters explores the long-term surface elevation dynamics in coastal wetlands using benthic foraminiferal assemblages. A regional training set based on the spatial distribution and abundance of benthic foraminiferal assemblages is developed in Chapter 5, which is then used to interpret palaeo-environmental and wetland surface elevation dynamics at millennial conditions in Chapter 6.

Chapter 5

Spatial distribution of benthic foraminiferal assemblages in upper intertidal wetlands

5.1. Introduction

Benthic foraminifera are single-celled microorganisms that live in a range of ecosystems, including freshwater wetlands, and in all marine environments from coastal wetlands to the deep ocean basins. In coastal wetlands, benthic foraminifera occur in either agglutinated or calcareous form, and in intertidal zones in particular, they have been found to exhibit spatial zonation that corresponds to their position in the tidal frame (Edwards and Horton, 2000; Gehrels, 1994; Horton, 1999; Scott and Medioli, 1978). The spatial zonation of foraminiferal assemblages has been attributed to the tidal inundation of the wetland surface, and it has been inferred that sea level variation will have a direct influence on the distribution of assemblages on the wetland surface. Over extended time periods, foraminifera get buried and preserved within the substrate as sediments accumulate reflecting palaeo-depositional environments. Using surface elevation relative to mean sea level as a proxy for tidal inundation, microfossil foraminiferal assemblages within cores can be used to reconstruct former surface elevations and sea levels (Avnaim-Katav et al., 2017; Edwards, 2001; Edwards and Horton, 2000; Gehrels, 1994; Hayward et al., 1999b, 2015; Horton et al., 1999b, 1999a; Kemp et al., 2013; Leorri et al., 2010; Morrison and Ellison, 2017; Woodroffe, 2009a). However, this requires a robust understanding of the vertical distribution of contemporary foraminiferal assemblages within the tidal frame for the interpretation of foraminiferal assemblages within cores.

Benthic foraminifera are climate sensitive and their distribution in coastal environments, and in upper intertidal zones, is highly dependent on site-specific

climatic and sea-level conditions. The strong influence of climatic variables on species distribution indicates that no two locations would have similar assemblage types, it is crucial to establish the occurrence and distribution of assemblages in different geomorphological settings before applying them to palaeo-environmental reconstructions. The aim of this chapter was to characterise the spatial distribution and abundance of benthic foraminiferal assemblages in surficial sample from four upper intertidal wetlands in south-eastern Australia to develop a regional training set. The regional training set was used to interpret past environmental conditions in Chapter 6. The aim of this chapter was achieved by;

i. Determining whether contemporary analysis of foraminiferal assemblages should be undertaken using dead tests or total (dead and live) tests, and to what depth samples should be analysed;
ii. Categorising the dominant taxa and environmental variables to which they respond;
iii. Identifying spatial assemblages in individual study areas;
iv. Characterising principal environmental factor(s) influencing their distribution at each study site and all sites combined;
v. Developing a regional training set based on the spatial associations; and
vi. Exploring the suitability of foraminifera-based transfer function models for past environmental reconstructions.

Preliminary tests were carried out to identify if living, dead or both living plus dead benthic foraminifera should be used in regional training set. Living tests were identified by staining them surficial samples with Rose Bengal. The depth to which surficial samples should be analysed in contemporary assemblages was also investigated by staining core samples. Dominant taxa were identified based on the percent composition of species (relative abundance). Relationships between dominant taxa and environmental variables was established using Pearson's correlation coefficient test. Spatial assemblages in each study site was identified using cluster analysis. Relationships between spatial assemblages and

environmental variables was established using canonical correspondence analysis. A regional training set was developed from dominant taxa data from all study sites. Cluster analysis was used to identify foraminiferal associations in the regional training set. Finally, the suitability of foraminifera-based transfer function for palaeo-environmental reconstructions is explored in this chapter.

5.2. Literature Review

5.2.1. What are foraminifera?

Foraminifera are unicellular microorganisms that belong to the Kingdom Protista. The average foraminifera size ranges from 100 μm to 1000 μm although a few species are larger, such as the genus *Marginopora* commonly found in the Great Barrier Reef, which can be up to 25 mm in diameter (Yassini and Jones, 1995). The nucleus of these single-celled organisms is protected by an outer shell that is referred to as a test. The test wall provides shelter, protection and promotes cell growth (Murray, 2006). The test morphology and orientation of the chambers (uniserial, biserial, or triserial), aperture(s) (shape and position), shape (trochospiral or planispiral), and test composition are important factors to consider when identifying species type (Haynes, 1981; Loeblich and Tappan, 1988; Sen Gupta, 1999; Yassini and Jones, 1995). Refer to Fig. 5.1 for the description of the different test morphologies.

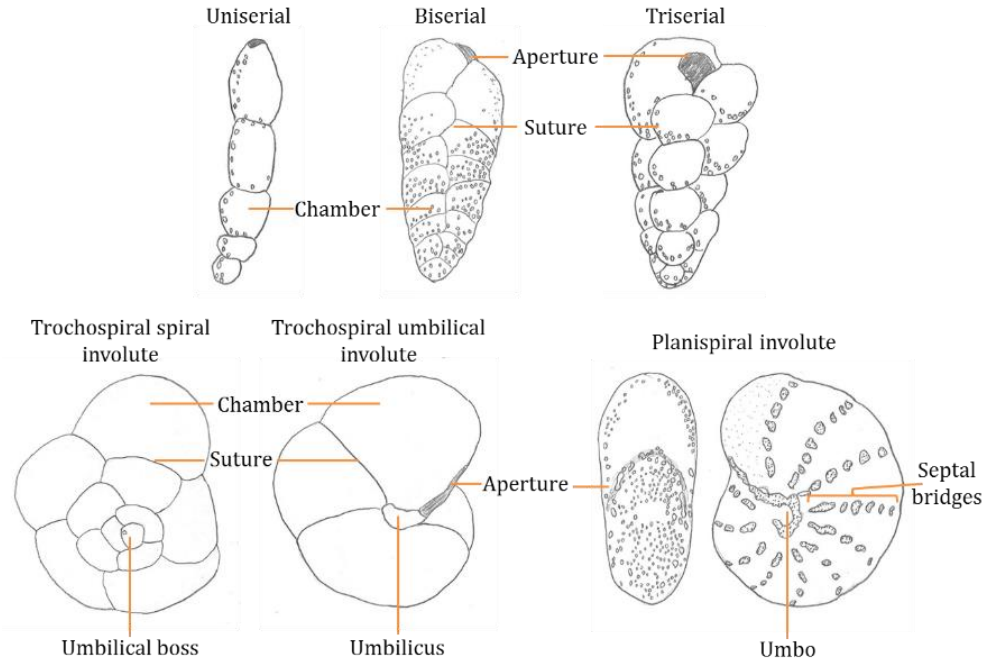

Figure 5.1: Foraminifera classification is based on the characteristics of test morphology and orientation of the test chambers (modified from Culver (1993). Chambers of a test wall are separated by lines of adhesion that are referred to as sutures and can be uniserial, biserial, or triserial. Trochospiral tests, such as *Trochammina inflata* have two different sides, the spiral side that is in a coiled form and umbilical side has the umbilicus, whereas planispiral tests for example, *Cribroelphidium excavatum* have chambers that are identical and symmetrical on both sides.

Test walls are of four main compositions, two of which are found mainly in intertidal zones; agglutinated and calcareous (Sen Gupta, 1999). Agglutinated test walls are made-up of grains, particularly quartz, that are cemented together by either organic, carbonate, or ferric oxide compounds (Debenay, 2012; Lee and Anderson, 1991). Calcareous tests are made-up of secreted calcium carbonate and have three different forms, microgranular, porcelaneous and hyaline (Boltovskoy and Wright, 1976; Hansen, 1999; Loeblich and Tappan, 1988; Sen Gupta, 1999). Microgranular tests are made up of tightly packed equidimensional, rounded grains of calcite, which are now extinct but can still be detected in sedimentary records of the late Palaeozoic. Porcelaneous tests, such as those of genus *Quinqueloculina,* are composed of randomly interlocking microcrystals of magnesium calcite, which gives them a translucent to opaque (milky) look (Debenay, 2012). Hyaline tests, e.g. *Elphidium* and *Ammonia,* are made up of microscopic rod-shaped crystals of calcium carbonate giving the test wall a glassy

appearance. These test walls are sometimes termed perforate as the pores within the hyaline shells penetrate the wall (Haynes, 1981). Refer to Fig. 5.2 for the illustrations of agglutinated, porcelaneous and hyaline foraminifera that commonly occur in intertidal wetlands. Apart from agglutinated and calcareous, there are other two types of tests; proteinaceous (organic) commonly found in low salinity shallow water, and siliceous (silica-walled) tests dwell on the ocean floor, are both outside the scope of this study (Sen Gupta, 1999).

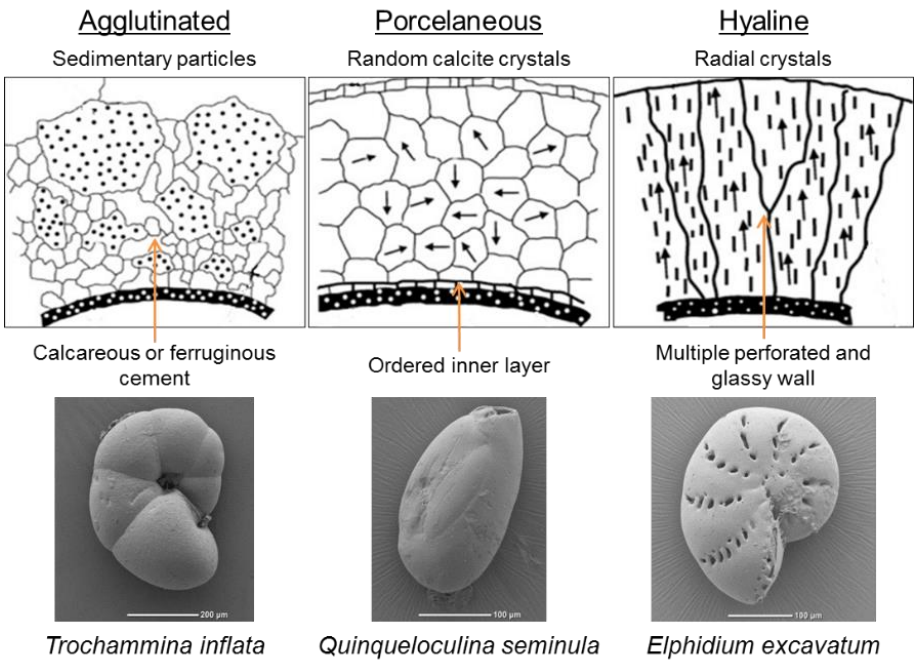

Figure 5.2: The three major test wall types common in intertidal environments. Agglutinated test walls are composed of sediment grains bound with organic, calcareous or ferric oxide cement. Porcelaneous walls are made up of needles of random calcite crystals. Hyaline test walls have crystals oriented radial, oblique, intermediate or compound.

5.2.2. Influence of environmental variables on benthic foraminifera distributions

Characteristically, foraminifera share similar ecological niches, but species composition and abundance (absolute numbers and proportion) depend on substrate characteristics, such as temperature, salinity, pH, oxygen supply and nutrients (de Rijk, 1995; Horton and Murray, 2007; Murray, 2006). For example,

calcareous foraminifera are susceptible to low pH (acidic) conditions that can trigger test wall dissolution, while agglutinated tests can tolerate acidic conditions (Scott and Medioli, 1978). Substrate characteristics are influenced by regional and localised climate, geomorphology, and sea-level variations (Fig. 5.3). Temperature influences the global distribution of foraminifera and controls the reproductive health of individuals (Murray, 1968). Temperature also regulates agglutinated and calcareous test mineralization and/or decomposition rates. High temperatures generally increase diagenetic (chemical) processes and organic cement mineralization of agglutinated taxa but can result in poor test preservation (Murray, 2006). For instance, in intertidal wetlands, air temperature directly affects benthic species during low tides and high rates of evaporation leaving the tests are exposed to the atmosphere can lead to test disintegration.

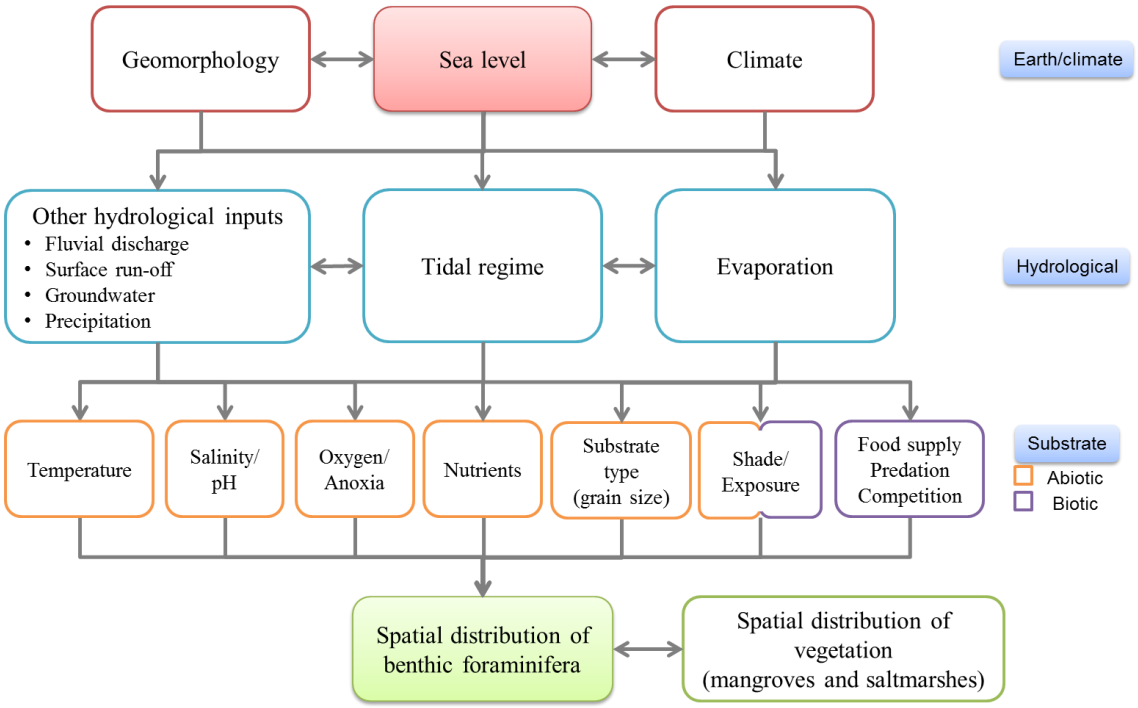

Figure 5.3: Conceptual model of environmental parameters influencing spatial distribution for benthic foraminifera in coastal wetlands.

Sea-level regulates the tidal influence in intertidal wetlands, sediment supply and wetland surface inundation regime. In individual geomorphological settings, the ecological niche of individual species is defined by the localised abiotic and biotic edaphic factors occurring on a site-scale level (Fig. 5.3). In general, marine

foraminifera are euryhaline, although some are more hyaline (e.g. *Haynesina germanica* and *Elphidium* sp.), and agglutinated taxa, such as *Entzia macrescens* (formerly identified as *Jadammina macrescens* and *Trochammina inflata macrescens* (Hayward, 1993)) and *Trochammina inflata* (Dean and De Deckker, 2013; Hayward et al., 2004b; Horton and Murray, 2007). Salinity affects these hyaline organisms through osmosis, where some cells may cease to function at very low salinities (Murray, 2006). Several studies have indicated that pore-water salinity controls foraminiferal composition in intertidal zones (de Rijk, 1995; Fatela et al., 2009; Hayward et al., 2004b; Horton and Murray, 2007; Murray, 2006). On a regional scale, the salinity regime of individual geomorphological settings is a balance between rainfall, seepage of groundwater, freshwater inputs through surface flows, flooding and tidal inundation, which can make it difficult to interpret the spatial distribution of foraminifera with respect to salinity (de Rijk, 1995; de Rijk and Troelstra, 1997; Kemp et al., 2009).

The calcium carbonate nature of calcareous tests makes them susceptible to pH variations. An increase in carbonic acid (H_2CO_3, pH less than 6.0) can trigger test dissolution, whereas an increase in bicarbonate (HCO_3^-, pH between 6.0 and 9.1) can promote test preservation (Berkeley et al., 2007; de Rijk and Troelstra, 1997; Horton et al., 2003, 1999a). In some environments, such as enclosed estuaries and sheltered harbours, low pH is associated with high levels of dissolved organic materials at the sediment–water interface. Aerobic oxidation of organic matter can lower the concentration of oxygen and produce carbon dioxide gas that breaks down to form H_2CO_3 dissolving calcareous tests (Berkeley et al., 2007; Geslin et al., 2011; Goldstein and Watkins, 1999; Hayward et al., 2015, 2004a, 2002). Agglutinated tests are not affected by low pH conditions and are able to tolerate acidic conditions (Scott and Medioli, 1978). Therefore, in intertidal wetland substrate, calcareous taxa mainly occur in the lower position of the upper intertidal and lower intertidal zones, where pH conditions are slightly below the typical seawater pH (approximately 7.2) (Berkeley et al., 2007).

Lateral zonation of species in intertidal zones showed high occurrence of agglutinated foraminifera at higher elevations of the intertidal, where pH was low, sediment grainsize was relatively fine with dense vegetation (Horton et al., 1999a). Calcareous tests are abundant at lower elevations in the tidal frame where pH was higher. Other studies have demonstrated that species distribution patterns are related to salinity gradients in lagoonal and estuarine wetlands. Agglutinated foraminifera generally dominate in the lower salinity zones, while calcareous tests increase in both relative abundance and number of species as salinity reaches to that of seawater (Culver et al., 2012; de Rijk, 1995; Hayward, 1993; Hayward and Hollis, 1994).

In some settings, such as temperate barrier estuaries of NSW (Strotz, 2003, 2012), open embayment (Dean and De Deckker, 2013; Haslett, 2007), intermittently closed lakes and lagoons (Strotz, 2015), and tropical macrotidal estuarine and deltaic sediments of South Alligator River (Wang and Chappell, 2001), salinity was identified as the main environmental factor controlling the distribution of foraminiferal assemblages. In coastal lagoon and estuarine settings, the salinity regime is regulated by entrance conditions, rainfall and rate of evaporation (Yassini and Jones, 1995). In some open estuarine settings, such as Broken Bay , NSW, foraminiferal distribution was not subject to large salinity changes (Albani, 1978).

In some embayment's such as Batemans Bay (Cotter, 1996) as well as in intermittently closed lakes and lagoons (Strotz, 2015) where marine influence is restricted, the overall assemblage composition depict a close relationship to water depth, salinity, substrate type (sediment grainsize) and nutrient supply. Foraminiferal assemblages in channel deposits are largely characterised by allochthonous sedimentation that is transported by tidal currents (Haslett, 2001; Wang and Chappell, 2001). In open coastal subtidal settings, foraminiferal assemblage zonation is related to water depth in tropical waters of north Queensland (Horton et al., 2007), barrier estuarine setting of St Georges Basin,

NSW (Strotz, 2012), and temperate waters in Gulf St. Vincent, South Australia (Cann et al., 1993, 1988).

5.2.3. Distribution of living tests

Oxygen and nutrients availability is vital for cellular metabolism and function in foraminifera (Murray, 2006; Sen Gupta, 1999). Low oxygen levels can slow down the metabolic rate of the organism, however, some calcareous taxa of the genus *Ammonia*, *Quinqueloculina* and *Elphidium* can survive in anoxic conditions for up to 24 hours (Karlsen et al., 2000; Murray, 2006). Phytoplankton (Papaspyrou et al., 2013). Substrate organic matter provides nutrients to the organism, however, processes, such as phytoplankton blooms can deplete oxygen levels and reduce species numbers (Armynot du Chatelet et al., 2009; Hansen, 1999; Hayward et al., 2002; Karlsen et al., 2000; Papaspyrou et al., 2013; Strotz, 2015). Benthic foraminifera not only reproduce and multiply on the surface (epifaunal), tests can live and reproduce in belowground sediments (infaunal) where their distribution is related to oxygen levels in the sediment (Berkeley et al., 2007; Horton, 1999; Horton and Edwards, 2006; Moodley et al., 1997; Papaspyrou et al., 2013). Oxygen is usually transported to belowground sediments and infaunal assemblages through bioturbation.

Infaunal tests have been found living at depths of up to 60 cm deep below the surface in north-eastern saltmarshes of United States (Horton and Edwards, 2006), up to 50 cm deep in saltmarshes of Oregon (Milker et al., 2015a) and in tropical muddy and mangrove-dominated coastlines of Australia (Berkeley et al., 2008), and to a depth of 30 cm below the surface in south-eastern US marshes (Goldstein and Watkins, 1999). In tropical settings the average living depths of foraminifera was between 6 to 10 cm in lower elevation mangrove sediments and intertidal mudflats (Berkeley et al., 2008), about 3 cm below the surface in intertidal muddy sediments of southwest Spain, western Ireland, and Cowpen Marsh in the UK (Horton, 1999; Horton and Edwards, 2006; Papaspyrou et al., 2013), where

approximately 80% of the living population was concentrated in the upper 0 – 0.4 cm (Papaspyrou et al., 2013) and surficial 1 cm (Horton and Edwards, 2006).

It has been suggested that contemporary distribution of species should be described in the top 1 cm sediments only (de Rijk and Troelstra, 1997; Edwards et al., 2004b; Gehrels, 2000; Gehrels et al., 2001; Gehrels, 2002; Horton et al., 1999b; Horton and Edwards, 2003, 2006; Horton and Murray, 2006; Scott and Medioli, 1978; Woodroffe et al., 2005). However, since all alive tests are not just epifaunal as discussed earlier, the top 1-cm foraminifera may not satisfactorily characterise the complete suite of assemblages in the modern analogue. In south-eastern US marshes, subsurface samples from approximately 10 cm below the surface provided an ideal baseline for reconstructions (Goldstein and Watkins, 1999).

Over the past few decades, it has been debated whether dead or total counts of living plus dead foraminifera should be used to categorise modern distributions. In intertidal wetlands, living foraminifera can integrate small seasonal and temporal variations, whilst dead assemblages are not affected by weather and season. Dead assemblages represent a time-averaged accumulation of tests in sub-surface sediments and have been considered to be a better analogue for reconstructing past environments (Callard et al., 2011; Gehrels and Newman, 2004; Horton, 1999; Horton et al., 1999a; Horton and Murray, 2006). Others have suggested that total counts in surficial samples reflect the modern distribution of assemblages in relation to present climatic conditions (de Rijk, 1995; de Rijk and Troelstra, 1997; Gehrels, 2000; Scott and Medioli, 1978), and are indifferent to taphonomic changes that affect live populations after death (Murray and Bowser, 2000). Total assemblages represent all species that eventually become a part of the microfossil cluster as they represent post-depositional events that are more applicable for palaeo-environmental reconstructions.

5.2.4. Benthic foraminifera in intertidal wetlands

In intertidal wetland environments, foraminifera are durable as fossils, easily collected and easily identified between the size range of 63 to 500 μm using a 10-40 X stereomicroscope (Dean and De Deckker, 2013; Edwards et al., 2004a; Horton and Edwards, 2006; Southall et al., 2006). Hence, a comprehensive understanding of the different environmental properties and their influence on species composition and abundance can be established from regional training sets (de Rijk and Troelstra, 1997; Edwards et al., 2004b; Hayward, 1993; Horton, 1999; Horton et al., 1999b; Horton and Edwards, 2003; Leorri et al., 2010; Scott and Medioli, 1978; Woodroffe et al., 2005).

In intertidal wetlands dominated by mangrove and saltmarsh vegetation, surface elevation relative to MSL is used as a proxy for tidal flooding that influences both flora and fauna (Berkeley et al., 2008; Callard et al., 2011; Haslett, 2001; Horton et al., 2003; Horton and Edwards, 2003, 2006; Wang and Chappell, 2001; Woodroffe et al., 2005). Assemblages of benthic foraminifera can be associated with different vegetation communities. For example, in the fringing mangrove environment of the Great Barrier Reef, agglutinated species such as, *Trochammina inflata* were found in relatively high abundance between mean high water (MHW) and highest astronomical tide (HAT) (Berkeley et al., 2008; Horton et al., 2003; Woodroffe et al., 2005). In the same studies, mid-tidal elevations were dominated by *Miliammina fusca* that had a low frequency of *T. inflata*, *Arenoparella mexicana*, *Paratrochammina stoeni*, *Haplophragmoides* spp., and *Miliammina obliqua*. In the mudflat and fringing *Rhizophora* mangrove section at mean tide levels (MTL), the unvegetated areas was dominated by calcareous species of *Ammonia tepida*, *Ammonia aoteana*, *Elphidium* spp., with minor occurrences of *Rosalina* sp., *Triloculina oblonga*, *Ammonia pustulosa* and *Shackoinella globosa* (Berkeley et al., 2008; Horton et al., 2003; Woodroffe et al., 2005). In some studies, a single calcareous-rich assemblage of *Ammonia aoteana*, *Ammonia tepida*, *Pararotalia venusta* and *Parrelina hispidula* was identified in the subtidal zone just below MTL

(Woodroffe et al., 2005). Species composition and zonation in these studies was related to wetland elevation and tidal inundation regime influencing pH, pore-water salinity, sediment grainsize, and vegetation distributions (Fig. 5.3).

In temperate coastal wetlands of south-eastern Australia where mangroves and saltmarshes co-occur, foraminiferal assemblages have been categorised in relation to vegetation type (Haslett et al., 2010). A monospecific assemblage of *T. inflata* was found in the higher elevation saltmarsh zones, whilst in the mangrove, calcareous *Cribrononion* spp. and *Ammonia beccarii* were found in relatively high numbers. Similarly, in extreme high elevation intertidal zones of New Zealand (dominated by saltmarsh), *T. inflata* has been found in association with *Entzia macrescens*. *E. macrescens* has also been identified in intertidal saltmarshes of Tasmania (Callard et al., 2011) and elsewhere (de Rijk and Troelstra, 1997; Edwards et al., 2004b; Horton, 1999; Lewis et al., 2013) where they were laterally constrained to zones between the MHW and HAT. Species such as, *A. beccarii, Elphidium excavatum, M. fusca* and *Haplophragmoides wilberti* were common in the tidal flat and low marshes in New Zealand (Hayward et al., 1999b; Hayward and Hollis, 1994). The above records indicate that spatial distribution patterns of foraminiferal assemblages in intertidal wetlands of Australia is taxonomically similar and depict a comparable distribution pattern to that found in New Zealand (Hayward, 1993; Hayward et al., 1999b; Hayward and Hollis, 1994).

In some regions, spatial distribution of assemblages shows a strong correlation to salinity, a balance between freshwater seepage, rainfall, flooding and tidal inundation (Hayward et al., 2004b). For example, in the Great Marshes, Massachusetts the distribution of foraminiferal assemblages correlated with the salinity regime (de Rijk, 1995; de Rijk and Troelstra, 1997). The marsh fringe experiences freshwater input through groundwater seepage, surface runoff and rainwater, where *Haplophragmoides manilaensis* in association with *Balticammina pseudomacrescens* were common. The middle marsh salinity levels are controlled by infiltration of sea- and/or rainwater and evaporation in which *E. macrescens*

was common. The lower elevation and the marsh edge, that was daily flooded by seawater, support high frequencies of *M. fusca* in association with *Ammotium salsum* and *Trochammina ochracea* (de Rijk and Troelstra, 1997). In tidal flats and intertidal margins of New Zealand, high salinity levels increased species diversity, particularly porcelaneous tests belonging to the order Miliolina and reduced the occurrence of agglutinated taxa (Hayward, 1993).

5.3. Methods

5.3.1. Sample collection and study design

Spatial foraminiferal analysis was carried out in the upper intertidal vegetation zones of Minnamurra River, Comerong Island, Cararma Inlet and Currambene Creek. Surficial samples, 2 cm deep, were collected at every 20 – 40 m intervals along an intertidal transect at each site, from the channel edge to the woodland margin. This was done to capture a range of environmental variables and foraminifera types, while minimising the sampling effort (Fig. 5.4). A few surficial samples were collected strategically to characterise vegetation communities that were not represented by the transect samples. At the time of sample collection, the elevation of each surface sample relative to the local tide datum (meters relative to the Australian Height Datum (m AHD)) was measured using a Trimble Real Time Kinematic-Global Positioning System (RTK- GPS.

The surrounding wetland vegetation type was identified at the location of each surface sample in approximately a 25 m^2 quadrat. Vegetation categories were classified as *high saltmarsh* (elevation > 0.63 m AHD to HAT), *low saltmarsh* (elevation < 0.63 m AHD), *mixed vegetation* (where mangrove and saltmarsh both were present), *shrub/dwarf mangroves* (mangrove tree height < 3 m) and *tree mangroves* (mangrove tree height > 3 m, (Owers et al., 2016)). The distinction between low and high saltmarsh vegetation type was adapted from Sainty et al. (2012). The channel samples were characterised as *channel*.

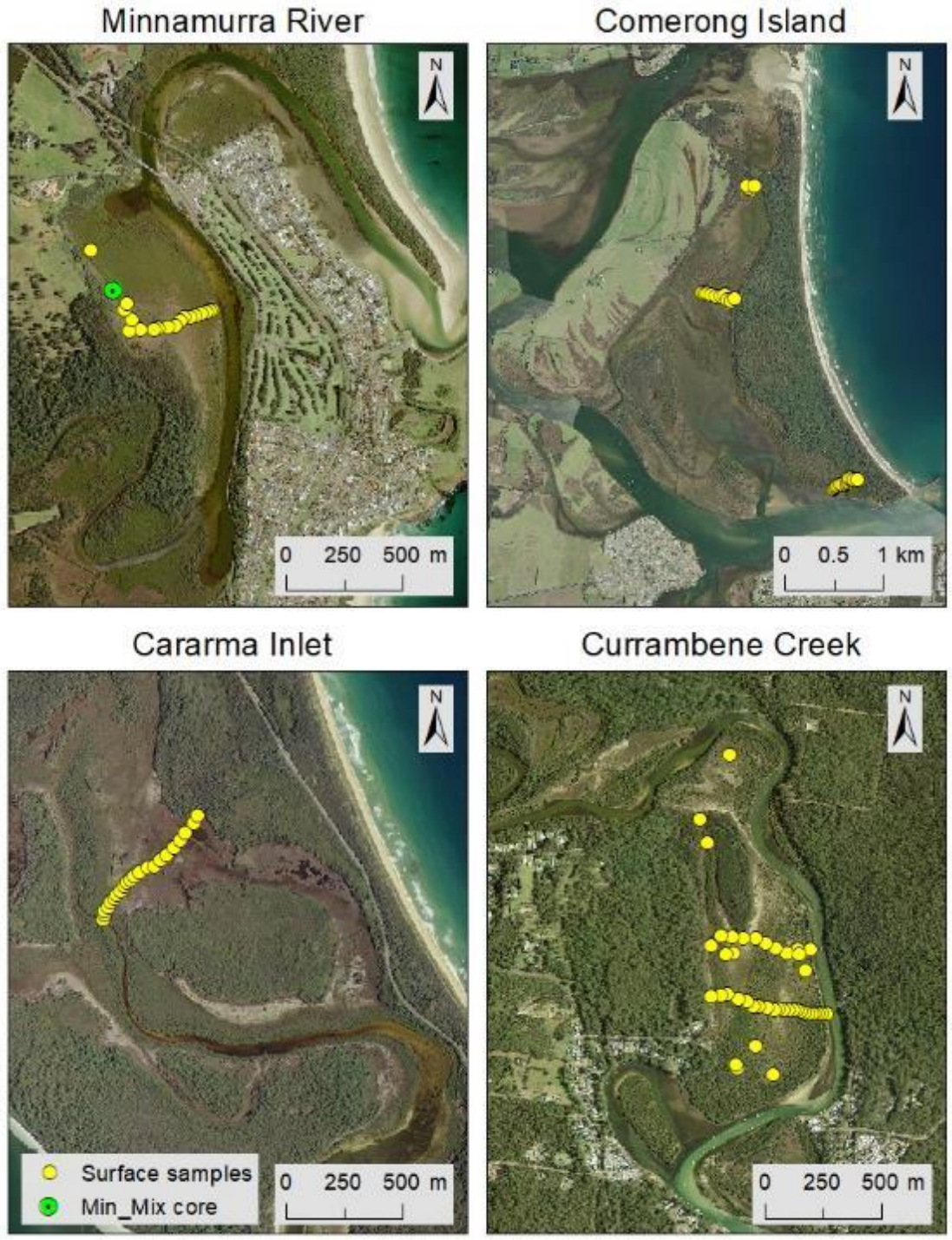

Figure 5.4: Map of study areas showing the location of surface samples and location of Minnamurra River core (Min_Mix).

It was not possible to collect many samples between 0.1 – 0.3 m AHD as there was very little to no mudflat zone between the channel and mangrove vegetation (Fig. 1.3). For example, at Cararma Inlet, the channel was separated from the mangrove

vegetation by a steep bank (approximately 0.7 m high) hence it was not possible to collect samples between -0.2 to 0.3 m AHD. However, samples were collected from a narrow mudflat at Currambene Creek and Comerong Island.

5.3.2. Foraminifera analysis

Contemporary analysis of living and dead foraminifera

Contemporary foraminifera analysis involved identifying living foraminifera from dead tests using the Rose Bengal technique (Murray and Bowser, 2000; Walton, 1952). Rose Bengal is a dye that was made into a staining solution using ethanol at a concentration 60 %, whereby 2 g of Rose Bengal powder was diluted in a litre of ethanol. The solution stains the protoplasm of living tests reddish (or pink) indicating that at the time of sample collection, the stained tests were alive. Surface samples were placed in airtight jars and stained with the dye by the end of the sampling day. Samples were thoroughly mixed with the Rose Bengal solution using a glass rod to maximise the staining of living tests (Fig 5.5a and b). The ethanol in the Rose Bengal solution also acts as a preservative and inhibits test decomposition (Murray, 2006).

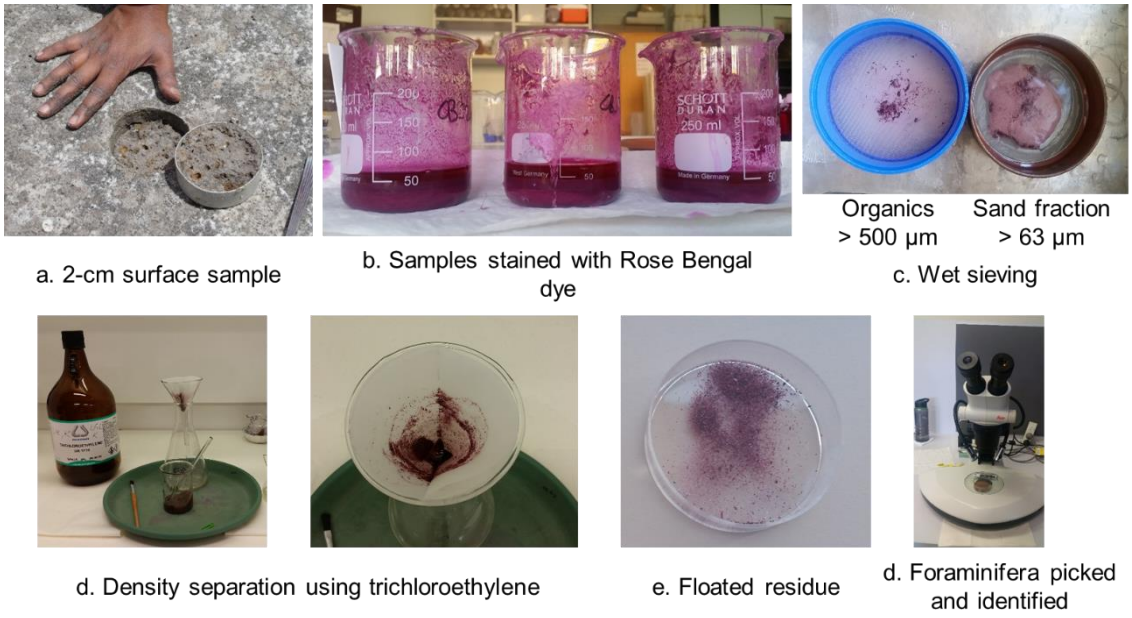

Figure 5.5: Foraminifera analysis where (a) sample collection, (b) samples were stained with the Rose Bengal dye and a known volume measured for analysis, (c) wet sieving through a 500 µm and 63 µm sieve, (d) density separation using trichloroethylene, (e) floated residue containing foraminifera was air dried and stored in petri dish, and (f) foraminifera picked and identified using a stereomicroscope.

Vertical distribution of living tests

Vertical distribution of living foraminifera was determined down a sediment core from Minnamurra River (Min_Mix, Fig. 5.4) as foraminifera live at various depths in sediments (Berkeley et al., 2008; Goldstein and Watkins, 1999; Horton and Edwards, 2006; Milker et al., 2015a). It was important to characterise the depth to which living foraminifera can survive as it was used to determine the sediment depth of the infaunal benthic foraminifera when characterising their contemporary distribution in intertidal wetland environments. The distribution of assemblage was also useful for inferring the vertical distribution of microfossil tests in the next chapter. The core was taken from a mixed mangrove and saltmarsh vegetation community located at an elevation of 0.526 m AHD. Subsamples were taken at 1-cm intervals to a depth of 10-cm, placed in jars and thoroughly mixed with the Rose Bengal solution to stain any living tests in the subsamples. All stratigraphic data from core Min_Mix was represented as compaction corrected depths and reported in centimetres (Section 4.2.1).

Until processing time, all the samples (surface and subsurface) were kept in a cold store at 4 °C to prevent bacterial oxidation of the tests (Horton and Edwards, 2006).

Sample processing and identification

Extraction of foraminiferal tests was conducted using known volume of sample (10 - 50 cm^3, Fig. 5.5b). The sample was wet sieved through a 500 μm sieve to remove large organics and debris. The residue was then sieved through a 63 μm sieve to remove the mud fraction (Fig. 5.5c) and oven-dried at 40 °C overnight. Foraminifera were density separated using trichloroethylene as per Murray (2006, p. 14). Foraminifera and organic debris have a relative low density and weigh very little per unit of volume compared to sand particles making them float in the trichloroethylene solution (Fig. 5.5d). The materials floating in the solution were decanted through a filter paper, air-dried and stored in labelled petri dishes (Fig. 5.5e). When ready for identification, the residue in the petri dishes were mixed with a soft-bristled paintbrush to homogenise any foraminifera and organic constituents and ensure tests were evenly distributed in the sample. The residue was split into small portions and transferred to another dish from which any foraminifera present was picked under a stereomicroscope and placed on a microfossil slide for identification (Fig. 5.5f). The sample size from which foraminifera were identified was reduced to minimise effort in identification and counting and was repeated until about 100 tests were counted from each sample. Samples that had low species density, all the foraminifera present were counted and identified.

Generally, tests were identified to the species level; however, some were grouped under a single genus as they could not be identified properly because the tests were broken but the umbilicus still intact, deformed probably due to growth abnormalities or test dissolution. Some tests were juvenile and exhibited underdeveloped chambers and could not be identified using the 40x magnification

of a stereomicroscope. Tests were considered 'alive' even if only the outer chambers were stained with the dye (Fig. 5.6, showing images of stained tests considered alive at the time of sample collection).

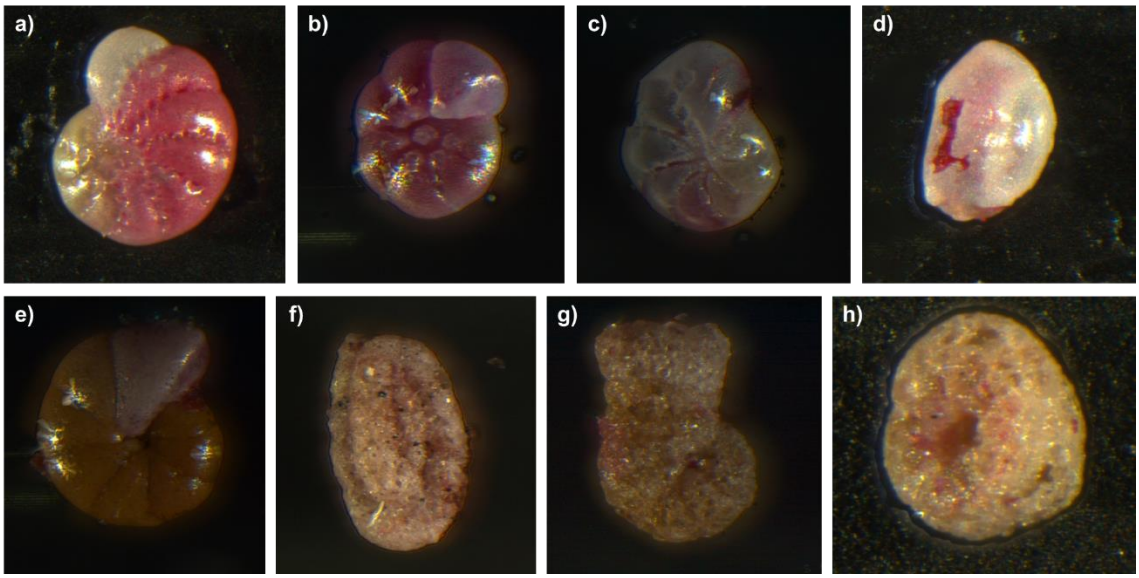

Figure 5.6: A few examples of tests stained by the Rose Bengal dye considered alive at the time of sample collection. (a) *Cribroelphidium excavatum*, (b) *Ammonia beccarii*, (c) *Haynesina depressula*, (d) *Quinqueloculina* spp., (e) *Haplophragmoides wilberti*, (f) *Miliammina fusca*, (g) *Ammobaculites* spp., and (h) *Tritaxis conica*.

5.3.3. Characterising dominant taxa

Relative abundance of species was established based on the percent composition of individual taxa relative to the total number of foraminifera counted. Samples with test density less than 1 test per cm^3 were treated as an anomaly due to low foraminiferal counts and excluded from the data matrix. Species with relative abundance exceeding 10 % in at least one sample were categorised as dominant taxa and included in the data matrix. This threshold was preferred as it established a degree of confidence that the foraminifera most certainly occur in the upper intertidal wetland zones analysed in the region. The relative abundance of dominant taxa ranged in several orders of magnitude from 0 % to 100 %, hence to reduce overemphasis of non-dominant taxa or most abundant taxa, species abundance data was transformed using square root (x + 1) (Gehrels et al., 2001).

Data transformation also homogenised the variance in the values and increased the importance of non-dominant species.

5.3.4. Environmental variables

Environmental variables likely influencing the distribution and abundance of benthic foraminifera in the study areas were measured for each surface sample. These included inundation indicators, such as wetland elevation relative to MSL and hydrological distance of the samples from the channel, and substrate properties, such as pore-water salinity, sediment organic matter and sediment grainsize (described in detail below).

Inundation indicators

Inundation of intertidal wetland surfaces can be characterised in different ways through tidal analysis. For steep slopes, elevation provides an ideal indicator of the frequency of inundation however, as tides propagate along estuaries, tidal creeks and across intertidal surfaces they may amplify or attenuate due to drag force. Although all the study areas are microtidal there is a slight variance in the tidal range that is influencing tidal attenuation in the different intertidal zones. The variation in wetland elevation was standardised using the standardised tidal position index (STPI, Eq. 5.1) to facilitate comparisons between study sites;

$$\boldsymbol{STPI = \frac{e_n - MTL}{TP_{upp} - MTL}} \qquad \text{Eq. 5.1}$$

where e_n is the surface elevation of sample *n* (m above local geodetic datum); MTL is the mean tide level (m AHD) which is equivalent to mean sea level (MSL) in this region, and TP_{upp} is the upper tidal position. TP_{upp} for the region was expressed as High high-water solstices springs (HHWSS). MTL and HHWSS were derived from the automatic water level monitoring stations (tide gauge) harmonic analysis for a period of 20 individual years (1 July 1990 to 30 June 2010) by the NSW Public

Works' Manly Hydraulics Laboratory (Couriel et al., 2013). Similar wetland elevation standardisation methods have been applied in other studies (Hamilton and Shennan, 2005; Horton et al., 1999a; Wright et al., 2011).

Data normalisation between the four sites was carried out using the nearest tide gauge data; Minnamurra tide gauge (Station 214442 for Minnamurra River) recording from 2002 to 2010, Greenwell Point tide gauge (Station 215417 for Comerong Island samples) data over a period of 1990 – 2010, and the Jervis Bay tide gauge data between 1990 to 2010 (HMAS Creswell, Station number 216470 for Cararma Inlet and Currambene Creek).

As tides propagate along the surface the drag force modulates the tidal height and duration in coastal wetland environments (Mazda et al., 1997). The effect of this modulation corresponds to the distance at which tides travel across a surface from the edge of the channel, which can be simulated using DEMs to determine the hydrological distance of a point of interest from the channel. The wetland surface elevation data derived from DEMs was referenced to the Australian Height Datum (m AHD). The LiDAR DEMs was used in the ArcGIS hydrology toolset to establish the distance tidal water flowed from 0 m DEM elevation (MSL), which occurs at the margins of the vegetated portion of the intertidal zone, to higher elevation points during the high tide cycle. To determine the hydrological distance using this toolset, a few preliminary steps were required. Initially the 'Fill' geoprocessing tool was used to fill any DEMs cells that would be terminal and would not allow water flow across the DEM to be simulated. This occurs largely due to depressions in the cells having lower elevation than neighbouring cells. The filled DEM layer was used as an input in the 'Flow Direction' toolset to create a new layer indicating the direction of flow out from each cell to the adjacent lowest lying cell. The flow direction layer was the input layer in the 'Flow Length' toolset to determine the length of the flow path distance tidal water took to reach a point of interest. Hydrological distance was stored as a raster layer in ArcMap and expressed in metres. Hydrological distance of each r-SET and water level logger was extracted

from the Hydrological distance raster layer in ArcMap.

Substrate properties

Additional surficial samples were analysed for pore-water salinity, organic matter content, and sediment grainsize. Salinity aids the growth of the test wall through osmosis (Murray, 2006) and so pore-water salinity of individual surface samples was measured to identify the influence salinity has on the distribution and diversity of benthic foraminiferal assemblages. The electrical conductivity ($EC_{1:5}$) method was used to measure pore-water salinity (Rayment and Lyons 2011, p. 20).

Sediment samples were air-dried in the laboratory for a few days. Once the samples were dry, they were loosely disaggregated in a mortar using a pestle. About 10 g air-dried sediments was weighed in a beaker to which 50 ml of deionised water was added and stirred vigorously with a glass rod to dissolve any soluble salts in the sediments. The mixture was left undisturbed for 30 minutes, re-stirred, and salinity was measured directly in parts per thousand (ppt, ‰) using a conductivity metre that had been calibrated with a standard solution prior to taking measurements.

High amounts of organic materials in sediments can result in low oxygen levels affecting the diversity of benthic foraminifera (Carson et al., 2008; Hayward et al., 2004a; Leckie and Olson, 2003; Scott et al., 2001), hence organic matter content was determined using the Loss-on-Ignition (LOI) technique (Ball, 1964). About 3 g of air-dried sediment was finely ground using a mortar and pestle was placed in a pre-weighed crucible and oven-dried at 105 °C overnight. The crucible was weighed again and placed into a furnace at 375 °C for 16 hours to oxidise any organics present in the sediments. After 16 hours, the crucibles were cooled in a desiccator and re-weighed. The difference in mass of sample before and after combustion represents the amount of organic material lost from the sample and represented as % organic matter content.

Sediment particles are particularly important detritus for building foraminifera test wall; hence sediment grainsize was analysed by laser diffraction using a Malvern Mastersizer-X. A small amount (1 – 5 g) of wet sediment sample was added to the dispersant (water). The particles were agitated in the dispersant using the built-in sonicator in the instrument for a few minutes before the grainsize of each sample was measured. Grainsize was represented as percent sand and mud (silt plus clay) particles and mean grainsize as micron (one millionth of a metre, 1×10^{-6} m).

5.3.5. Relationship between dominant taxa and environmental variables

Environmental variable data ranged in several orders of magnitude across the five measured variables, for instance metres for distance, ppt for salinity, percent for LOI and grainsize, and was transformed using log10 (x + 1) (Patterson et al., 2014) to reduce overemphasis of any of the variables on foraminiferal distribution. The linear (R-value) Pearson correlation coefficient test was performed on the transformed dominant taxa and transformed environmental data using the palaeontological statistical software PAST, version 318 (Hammer et al., 2001). The R-value indicated the direction of the relationship (negative or positive correlation) between dominant taxon and the environmental variables. STPI was used as an independent variable as wetland elevation is not determined by any of the other measured variables. This was done to delineate the key environmental variable(s) influencing the distribution of benthic assemblages in the study areas.

5.3.6. Spatial assemblages

Foraminiferal spatial assemblages were categorised using hierarchical cluster analysis because variation in species diversity was identified between study areas. Cluster analysis was performed on the square root transformed abundance data based on the unweighted pair-group average (UPGMA) algorithm and the

unconstrained Bray-Curtis similarity index (Bray and Curtis, 1957). The Bray-Curtis similarity has been successfully used as the distance measure to classify spatial ecological patterns in coastal and marine environments (Hayward et al., 2004b, 2002; Milker et al., 2015b; Papaspyrou et al., 2013; Strotz, 2015). It defined assemblages based on the mean distance between the foraminiferal assemblages. Spatial clusters were categorised at a similarity index threshold of 70%, but clusters were further sub-divided at a higher threshold if variations in species distribution were apparent from the order of samples in the dendrogram. Sample clusters were classified from foraminiferal assemblages that were categorised into different vegetation communities or upper intertidal zones.

5.3.7. Principal environmental variables influencing assemblages

The variability in environmental data from each study site and all sites combined was presented as a probability distribution with 80% confidence of the mean (± standard deviation). Environmental variables were presented as box and whisker plots for individual study areas and all sites combined. The linear (R-value) Pearson correlation coefficient matrix was used to identify the direction of the relationship in relation to STPI. STPI was used as the independent variable as wetland elevation is not affected by hydrological distance and substrate properties. Environmental variables with p-value less than equal to 0.05 were considered significantly important and were classified as principal environmental factor(s) influencing the distribution of foraminiferal assemblages in the upper intertidal wetland areas.

Canonical correspondence analysis (CCA) was performed on transformed species and environmental data (data transformation described in Section 5.2.6) using the software PAST. CCA is a multivariate technique that related species composition to the principal environmental factors in each study area and for the region (ter Braak, 1986). CCA arranged surficial samples and dominant taxa in a multidimensional space, whereby the ordination axes were constrained to be

linear combinations of the principal environmental variable(s) allowing maximum distribution of taxon scores (Birks, 1995). The CCA ordination diagram displayed the patterns in biological variation of different taxa, represented by its weighted average maximum abundance, in relation to their preferred environmental variable(s).

Wetland elevation and hydrological distance were the consistent environmental variables between study areas and were co-correlated to understand the relationship between them. As wetland elevation data was used to obtain hydrological distance of the surficial samples from the channel, it was treated as the independent variable and analysed using non-linear logistic (3P) curves in statistical software JMP Pro 13. The elevation range of the spatial clusters was presented as box and whiskers with respect to STPI for individual study areas and all sites combined.

5.3.8. Regional training set

Due to the variability in dominant taxa type between sites, data from all study areas were pooled together into a regional training set. Bray-Curtis cluster and the UPGMA algorithm analysis was performed on the square root transformed abundance data. CCA analysis was carried out on the transformed species and principal environmental variables. The STPI range of the vegetation categories (Section 5.2.1) was presented as box and whiskers. Values expressed as 80% confidence of the mean (± standard deviation).

5.3.9. Foraminifera-based transfer function

Numerous foraminifera-based transfer function methods have been developed to quantitatively reconstruct palaeo-environmental variables. Some have a stronger ecological focus, while others have a more statistical basis, but all are fundamentally taxon-environment response models (Birks, 1995). Detrended

canonical analysis (DCA) was used to determine if a linear model or a unimodal (Gaussian) response model of species to their environment was more appropriate. DCA was developed using the statistical software R-studio, available in its "vegan" package. The DCA ordination represented samples as points in multi-dimensional space, plotting similar samples close together and dissimilar samples apart providing an estimate of the gradient length in relation to the environmental variable of interest (x) in standard deviation (SD) units. If the gradient length is short, less than 2 SD, taxa are generally behaving monotonically along the gradient and linear regression and calibration methods are appropriate. If the gradient length is longer than 2 SD units, then unimodal-based methods of regression and calibration is more suitable (Birks, 1995).

Several foraminiferal-based transfer function models developed based on 16 species from 111 samples in program C2 software package, version 1.7.7 (Juggins, 2016). Unimodal weighted averaging (WA) is based upon a theory that at a site, species that have their optima for environmental variable of interest (x) close to the site will be the most abundant species present at that site (Birks, 1995).

The transfer function models produced squared correlation (coefficient of determination, r^2) and root mean square of error (RMSE) between observed and predicted values. The r^2 value measured the strength of the relationship, whist RMSE indicated the systematic differences in observed versus predicted values. In order to access the effectiveness of the predictive abilities of the transfer function, jack-knife (also known as 'leave-one-out' measures) cross-validation was performed (ter Braak and Juggins, 1993). The jack-knife cross validation technique provides a method of evaluating the error involved in making predictions, the Root mean square error of prediction ($RMSEP_{jack}$), which provided a measure of the overall predictive abilities of the modern training set (Birks, 1995). This information was then be used to infer the elevation (former wetland-surface elevations) at which sub-surface sediments that have microfossil assemblages were deposited. Bootstrapping cross-validation is a computer-intensive

resampling procedure that can be used to derive standard error of prediction for individual species in the training set, for individual surficial samples (modern), and RMSEP estimate for the training set. It provides an estimate of the presence or absence of taxa with a particularly strong signal for the environmental variable of interest (Birks, 1995).

5.4. Results

5.4.1. Living vs dead foraminifera

At the time of sample collection about 35 % of the tests counted from all study areas were alive, of which 65 % of the total calcareous taxa counted were living, whilst only 23 % of agglutinated taxa were stained with the Rose Bengal dye. In individual study areas, the highest number of living tests was recorded in surficial samples of Comerong Island of which 83 % of calcareous tests counted were living at the time of sample collection (Fig. 5.7a). About 72 % of calcareous taxa were alive at the time of sample collection at Minnamurra River and around 67 % calcareous were living at Currambene Creek. Overall, both Currambene Creek and Cararma Inlet recorded low counts of living tests, but high counts of agglutinated taxa (Fig. 5.7b). Refer to Appendix 4 for tables containing a full list of living and dead foraminifera in surficial samples for all study sites.

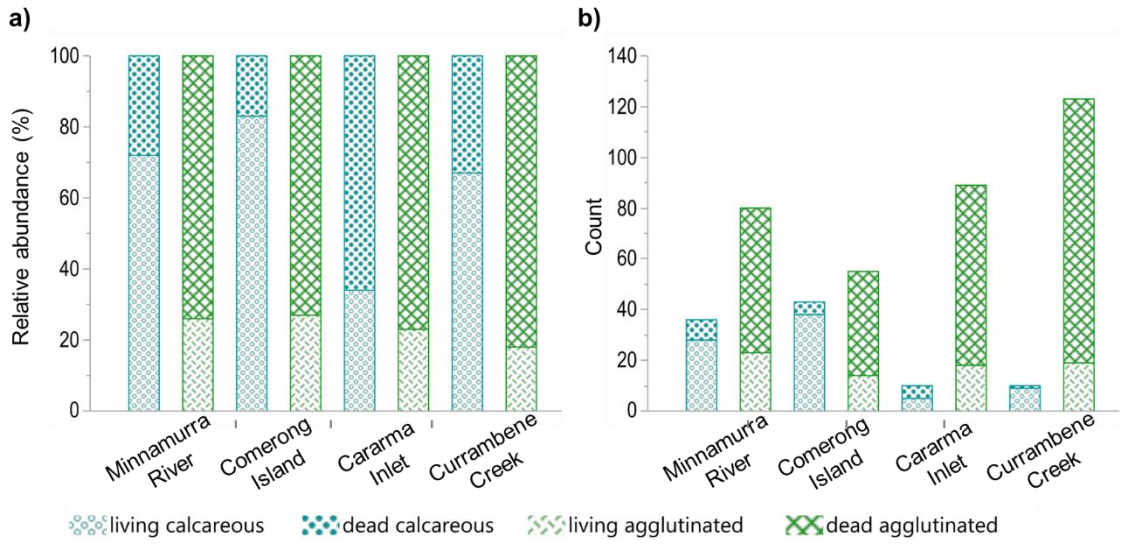

Figure 5.7: Living vs dead foraminiferal assemblage relative abundance (a) and test counts (b) in all study areas.

The relatively high abundance of living calcareous taxa in surficial samples of Comerong Island, Minnamurra River and all sites combined indicate that total counts should be used to establish a complete modern analogue of assemblages. As there was a high number of living tests, the use of only dead assemblages would overemphasise agglutinated taxa populations and some calcareous taxa, such as *Cribroelphidium excavatum* (former *Elphidium excavatum*), *Haynesina depressula*, *Quinqueloculina seminula* and species of the genera *Ammonia* will not be captured in the contemporary distribution. Hence, both living and dead tests were used for all subsequent statistical analyses.

In the sediment core (Min_Mix), infaunal foraminifera were found living to a depth of about 6 cm (compaction corrected depth) below the surface. The single alive *Trochammina inflata* at the depth of 8.5 cm was regarded as an anomaly. In the top 1-cm of sample, 60 % of specimens counted were stained, including all the calcareous taxa and only about 10 % of the agglutinated taxa (Fig. 5.8). Calcareous tests from other depths of 3.2 cm and 5.8 cm were stained by the dye and classified as living at the time of sampling. In 1 – 2 cm subsample, no calcareous taxa were encountered and 8 % of the agglutinated taxa counted were alive. These results indicate that surficial 2-cm samples would allow a more comprehensive

distribution of modern assemblages, capturing both calcareous and agglutinated taxa in surficial samples. This will eliminate bias against agglutinated foraminifera as they occurred predominantly in samples below 1-cm.

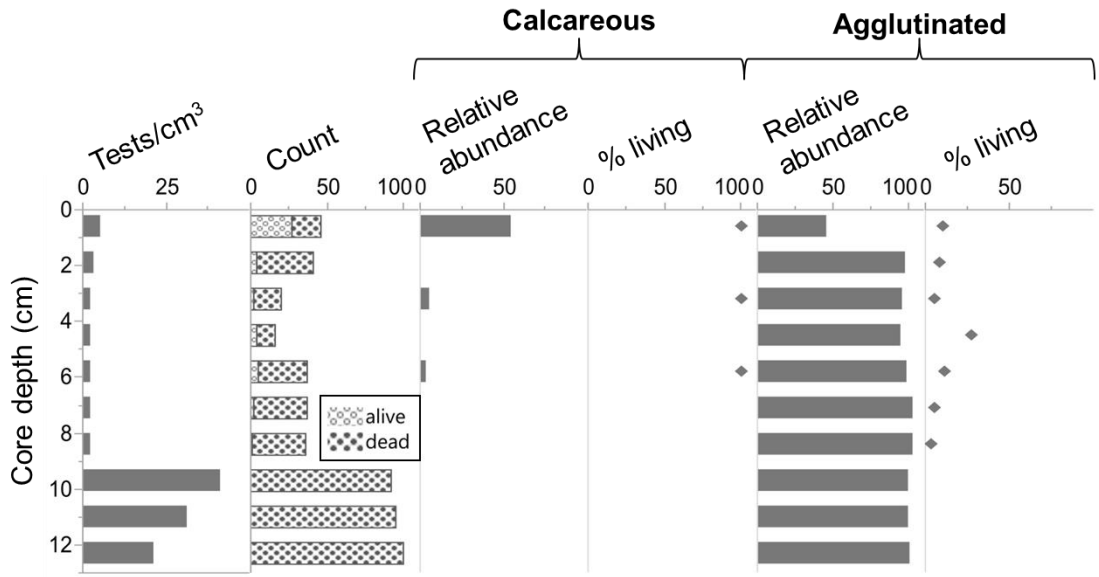

Figure 5.8: Vertical distribution of infaunal foraminifera in Min_Mix and substrate properties of belowground sediments.

5.4.2. Dominant taxa

A total of sixteen dominant benthic taxa were established for the region (see Table 5.1). Calcareous species of *Ammonia* spp. (including *Ammonia beccarii*, *Ammonia tepida* and *Ammonia* spp.), *C. excavatum*, *Haynesina depressula*, *Helenina anderseni* and *Q. seminula* were present in all sites. Agglutinated taxa of *Ammobaculites* spp., *Ammotium directum*, *Entzia macrescens* (former *Jadammina macrescens*), *Miliammina fusca*, *Siphotrochammina lobata* and *T. inflata* occurred in all study areas, with *Ammotium morenoi* (former *Ammotium salsum*), *Arenoparrella mexicana, Haplophragmoides wilberti*, *Miliammina obliqua* and *Tritaxis conica* were restricted to only certain study areas. Dominant taxa are illustrated in Plates 1 and 2 of Appendix 3.

At Minnamurra River, eight dominant taxa were identified, twelve were recognised at Comerong Island and Currambene Creek, and seven at Cararma Inlet, five of

which were dominantly present in all sites (Table 5.1). The correspondence of assemblages between study sites indicate that foraminifera share similar ecological niches; however, species composition depends on environmental conditions of individual geomorphologic settings.

Table 5.1: Presence/absence of benthic foraminiferal taxa at study sites (x – sites in which taxa was present). Out of the 41 taxa of foraminifera, 30 were identified to species level, whilst other 11 could only be identified to the genus level (dominant taxa are in bold are illustrated in Plates 1 and 2 of Appendix 3).

	Benthic foraminifera	**Minnamurra River**	**Comerong Island**	**Cararma Inlet**	**Currambene Creek**
Calcareous	*Ammonia beccarii* (Linnaeus, 1758)	x	x	x	x
	Ammonia spp.	x	x	x	
	Ammonia tepida (Cushman, 1926)	x	x	x	x
	Bolivina pseudoplicata (Heron-Allen & Earland, 1930)		x		
	Bolivina robusta (Brady, 1881)			x	
	Bolivina spp.		x		
	Bolivina striatula (Cushman, 1922)		x		
	Elphidium advenum (Cushman, 1922)			x	
	Cribroelphidium excavatum#** (Terquem, 1875)	x	x	x	x
	Elphidium spp.	x	x	x	x
	Haynesina depressula (Walker & Jacob, 1798)	x	x	x	x
	Helenina anderseni (Warren, 1957)	x	x	x	x
	Miliolinella spp.			x	
	Quinqueloculina seminula# (Linnaeus, 1758)	x	x	x	x
	Quinqueloculina spp.	x	x	x	x
	Rosalina spp.	x		x	
	Spirillina vivipara (Ehrenberg, 1843)		x		x
	Triloculina oblonga (Montagu, 1803)		x		
Agglutinated	*Ammobaculites agglutinans* (d'Orbigny, 1846)		x		
	Ammobaculites exiguus (Cushman & Brönnimann, 1948)	x			x
	*Eratidus foliaceus*** (Brady, 1881)				x
	Ammobaculites spp.	x	x	x	x
	Ammobaculites subcatenulatus (Warren, 1957)	x	x	x	x
	Ammodiscus spp.		x		
	Ammotium directum (Cushman & Brönnimann, 1948)	x	x		
	*Ammotium morenoi**** (Acosta, 1940)		x		x
	Ammotium spp.	x	x		x

	Benthic foraminifera	Minnamurra River	Comerong Island	Cararma Inlet	Currambene Creek
Agglutinated	*Arenoparrella mexicana* (Kornfeld, 1931)	x			x
	Eggerella australis (Collins, 1958)		x		
	Glomospira spp.	x	x	x	
	Haplophragmoides wilberti (Andersen, 1953)	x	x		x
	Entzia macrescens#**** (Brady, 1870)	x	x	x	x
	Miliammina fusca# (Brady, 1870)	x	x	x	x
	Miliammina obliqua (Heron-Allen & Earland, 1930)		x	x	x
	Paratrochammina stoeni (Brönnimann & Zaninetti, 1979)				x
	Polysaccammina ipohalina (Scott, 1976)				x
	Siphotrochammina lobata (Saunders, 1957)	x	x	x	x
	Textularia earlandi (Parker, 1952)	x	x		x
	Tritaxis conica (Parker & Jones, 1865)	x	x		x
	Trochammina inflata# (Montagu, 1808)	x	x	x	x
	Trochammina spp.	x	x	x	x
	Taxon count	25	32	22	27
	Dominant taxa	8	12	7	12

#dominantly present in all study areas. Synonymised names – **Elphidium excavatum*, ***Ammobaculites foliaceus*, ****Ammotium salsum*, *****Jadammina macrescens* (Hayward et al., 2018).

Rare species (average relative abundance < 2 %), which were excluded from the data matrix but have been reported in intertidal and estuarine environments in Australia and the Pacific (Albani, 1978; Haslett, 2001; Hayward, 1993; Hayward et al., 1999b; Horton et al., 2003; Strotz, 2003; Yassini and Jones, 1995); included foraminifera of the genera *Ammodiscus* sp., *Glomospira* sp. and *Miliolinella* sp., and species, such as *Bolivina pseudoplicata*, *Bolivina striatula*, *Eggerella australis*, *Polysaccammina ipohalina*, *Textularia earlandi*, *Triloculina oblonga*, and *Eratidus foliaceus* (former *Ammobaculites foliaceus*) and *A. agglutinans*. The species were found in lower elevation mangrove sediments of Comerong Island and Currambene Creek. *Paratrochammina stoeni* was unique to Currambene Creek and was found in mid-elevation position of the upper intertidal. It has also been reported in upper to low-mangrove environments of Cleveland Bay (Berkeley et al., 2009; Horton et al., 2003; Woodroffe et al., 2005).

Relationship between dominant taxa and environmental variables

The relationship between foraminiferal frequencies of dominant taxa and environmental variables characterised by the correlation matrix showed that more than 50 % of taxa (9 of 16) have a relatively strong relationship with STPI ($r > 0.290$ and $p < 0.05$) (Table 5.2). A total of eight taxa showed a relatively strong relationship to hydrological distance, whilst seven species namely, *Ammonia* spp., *H. anderseni*, *E. macrescens*, *M. fusca*, *S. lobata*, *T. conica* and *T. inflata*, correlated to both inundation indicators (STPI and hydrological distance). Overall, calcareous taxa showed a negative correlation to elevation and hydrological distance, as did some of the agglutinated taxa, such as *M. fusca* and *T. conica*, indicating they occurred in higher abundance at lower elevations. *T. inflata*, *E. macrescens* and *S. lobata* had a relatively high positive correlation to the STPI and hydrological distance.

Table 5.2: Relationship between foraminiferal frequencies of dominant taxa and environmental variables represented as linear r correlation. Values in bold indicate relationship is significantly different to 0 (p-value < 0.05).

Dominant taxa	STPI	Hydrological distance	pore-water salinity	Organic content	Sand	Mud	Mean grainsize
Ammonia	**-0.456**	**-0.402**	0.037	-0.161	0.028	**-0.206**	0.049
C. excavatum	**-0.322**	-0.040	**-0.224**	**-0.363**	**0.207**	-0.131	0.169
H. depressula	-0.143	-0.039	-0.088	-0.039	-0.028	**-0.190**	-0.040
H. anderseni	**-0.486**	**-0.438**	0.037	-0.034	-0.008	-0.028	-0.054
Q. seminula	**-0.329**	-0.168	**-0.222**	-0.096	**-0.243**	**0.210**	**-0.300**
Ammobaculites spp.	-0.162	**-0.253**	**0.213**	**0.237**	-0.164	0.117	-0.128
A. directum	-0.155	0.016	-0.119	0.035	0.032	0.010	-0.006
A. morenoi	-0.056	-0.051	-0.087	-0.110	0.070	-0.015	0.040
A. mexicana	-0.111	-0.109	**-0.204**	-0.149	0.039	0.011	0.010
H. wilberti	0.183	0.135	**-0.190**	-0.015	-0.172	0.082	-0.107
E. macrescens	**0.368**	**0.252**	**0.278**	0.062	0.102	-0.022	0.113
M. fusca	**-0.296**	**-0.199**	-0.177	-0.063	**-0.252**	**0.217**	**-0.308**
M. obliqua	0.154	0.033	-0.069	0.006	-0.103	0.053	-0.103
S. lobata	**0.291**	**0.321**	-0.138	0.058	-0.128	0.076	-0.076
T. conica	**-0.389**	**-0.377**	-0.057	-0.088	0.096	-0.032	0.040
T. inflata	**0.467**	**0.329**	0.041	**0.198**	0.056	-0.104	0.116
Species density	0.077	0.013	0.053	0.164	**-0.259**	**0.319**	**-0.278**

Pore-water salinity had a significant influence on the distribution of *C. excavatum*, *Q. seminula*, *Ammobaculites* spp., *A. mexicana*, *H. wilberti*, and *E. macrescens*. Two taxa, *A. mexicana* and *H. wilberti* did not have a strong correlation to any of the environmental parameters except salinity. Grainsize had a considerable influence on species density, where numbers of tests per cm^3 of sample increased in muddy substrate. *Q. seminula* and *M. fusca* preferred finer grained sediments, while *C. excavatum* showed preference for sandy substrate. Generally, calcareous taxa showed a negative correlation to organic matter content, most particularly *C. excavatum*. A*. directum* and *A. morenoi* did not display a meaningful relationship to any of the environmental variables measured.

5.4.3. Spatial assemblages at each study area

The dominant taxa at each study area were classified into different spatial assemblages, three spatial clusters were identified at Minnamurra River (Fig. 5.9), Comerong Island (Fig. 5.10) and Currambene Creek (Fig. 5.12), and two spatial clusters were identified at Cararma Inlet (Fig. 5.11). A few of the major clusters from the different study areas were further sub-divided to identify specific species associations across transects. Refer to Appendix 4 for tables containing a full list of foraminifera encountered in surficial samples of all study sites.

At Minnamurra River, spatial cluster Min-I was dominated by agglutinated *T. inflata*, *E. macrescens*, *S. lobata* and *H. wilberti*, with subsidiary *M. fusca* (Fig. 5.9a and b). *C. excavatum* was present in relatively high abundance in Min-II with minor *Q. seminula*, whilst cluster Min-III was dominated by *C. excavatum, Q. seminula* and *M. fusca* with subsidiary *Ammobaculites* spp.

Cluster Cm-I was dominated by *T. inflata* with subsidiary *H. wilberti*, *E. macrescens* and *S. lobata*, and relatively high abundance of *C. excavatum* at Comerong Island (Fig. 5.10a). The spread of taxa was not uniform in the surficial samples of Cm-I and further sub-division that showed that Cm-Ia had a higher frequency of *C.*

excavatum, whilst cluster Cm-Ib had a higher abundance of *H. wilberti* and *M. obliqua* (Fig. 5.10b). Cluster Cm-II was dominated by calcareous taxa *C. excavatum* and *H. depressula* and subsidiary *M. fusca*. Other taxa in this cluster included *A. directum*, *H. anderseni* and Ammonia spp. Cluster Cm-III association comprised of *M. fusca*, *Q. seminula*, and *Ammonia* spp., with supplementary *T. inflata*.

T. inflata occurred in relatively high numbers in the upper intertidal zones of Cararma Inlet (Fig 5.11a). At 70 % Bray-Curtis similarity distance, two spatial clusters were identified (Fig. 5.11b). Cluster Ca-I had high numbers of *C. excavatum*, *Ammobaculites* spp. and *M. fusca* with minor *Ammonia* spp., whilst cluster Ca-II was dominated by agglutinated *T. inflata* and *E. macrescens*, with a few occurrences of *Ammobaculites* spp. Further sub-division of both these clusters showed variations in the distribution of species in surficial samples, where cluster Ca-Ia was dominated by *M. fusca* and *Ammobaculites* spp., whilst Ca-Ib was dominated by calcareous *C. excavatum* and *Ammonia* spp. with minor *Ammobaculites* spp. Cluster Ca-IIa was dominated by *T. inflata*, while *E. macrescens* was dominantly present in Ca-IIb (like Min-I).

A. mexicana was present in relatively high abundance at Currambene Creek but not in all zones (Fig. 5.12a). It dominated cluster Cb-I with *T. inflata*, *M. fusca*, *H. wilberti*, *Q. seminula* and subsidiary *S. lobata* and *C. excavatum*. Cluster Cb-II had a high occurrence of agglutinated *M. fusca* and *Ammobaculites* spp. and *C. excavatum,* but further subdivision of Cb-II revealed that a small number of samples (Cb-IIa) did not have any *Ammobaculites* spp. but had *T. conica*, *H. wilberti* and *Q. seminula* in them (Fig. 5.12b). *Ammobaculites* spp. however, was dominantly present in Cb-IIb that did not have any *T. conica* and had relatively low counts of calcareous *Q. seminula* and *Ammonia* spp. Cb-III had high counts of *E. macrescens* and *T. inflata* with subsidiary *C. excavatum*, and *S. lobata* but further division indicates higher abundance of *T. inflata* and *S. lobata* in Cb-IIIa and low occurrence of *E. macrescens* (like Cm-I), but *S. lobata* was not present in cluster Cb-IIIb with relatively high counts of *E. macrescens* and low occurrence of *T. inflata* (like Ca-IIb).

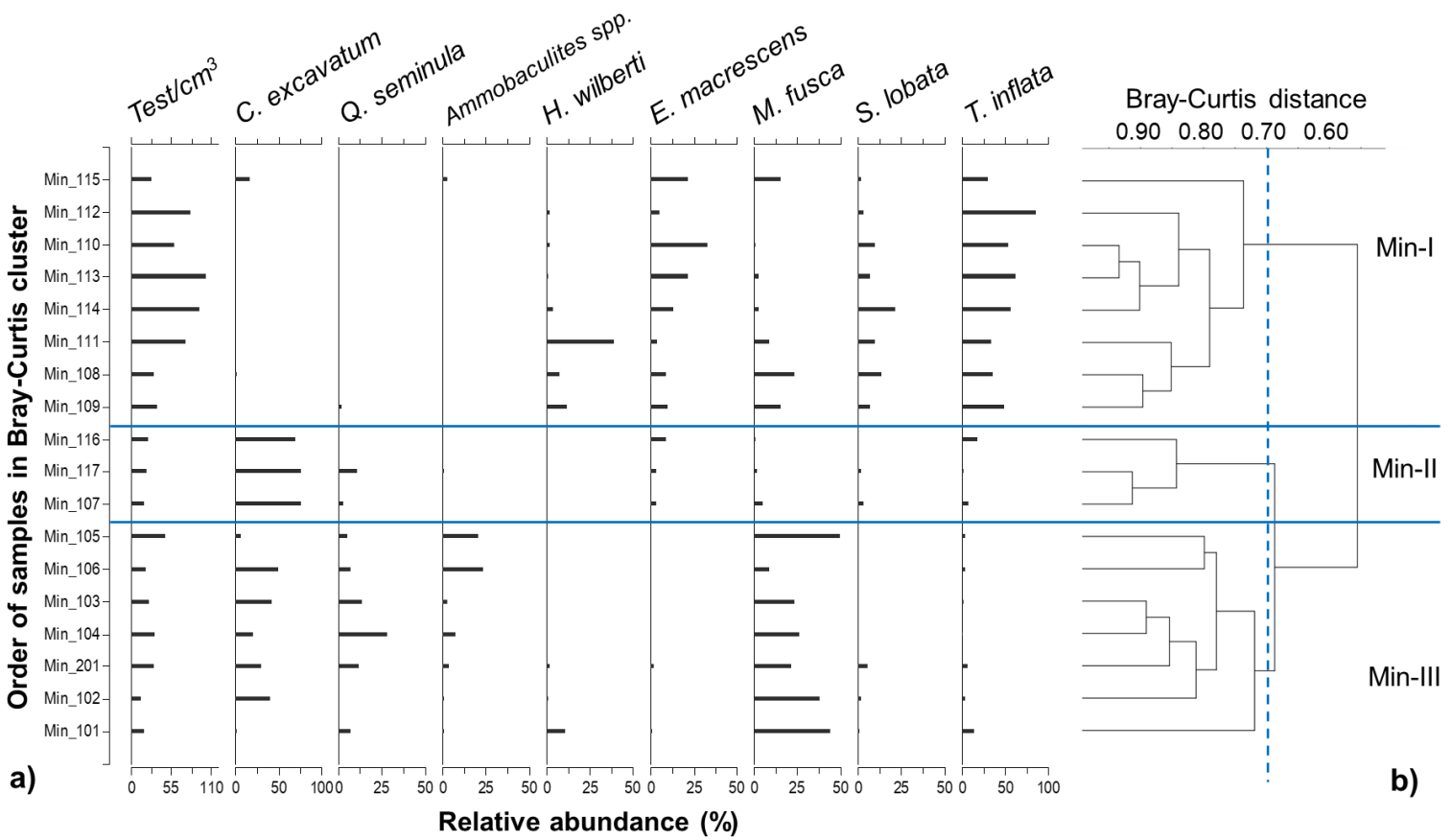

Figure 5.9: (a) Spatial distribution of benthic foraminifera in upper intertidal wetlands of Minnamurra River and (b) Spatial assemblages based on Bray-Curtis cluster analysis.

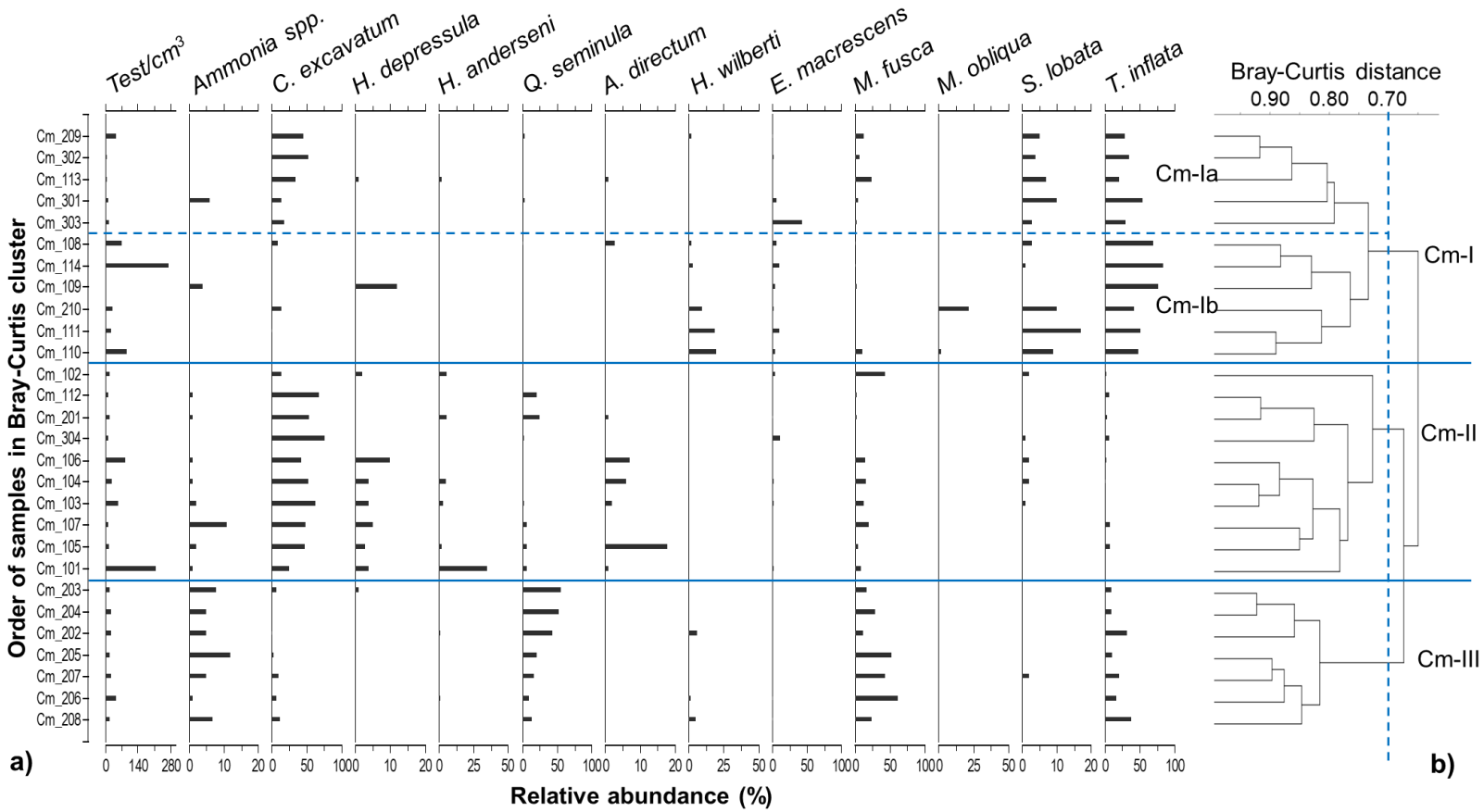

Figure 5.10: (a) Spatial distribution of benthic foraminifera in upper intertidal wetlands of Comerong Island and (b) Spatial assemblage based on Bray-Curtis cluster analysis.

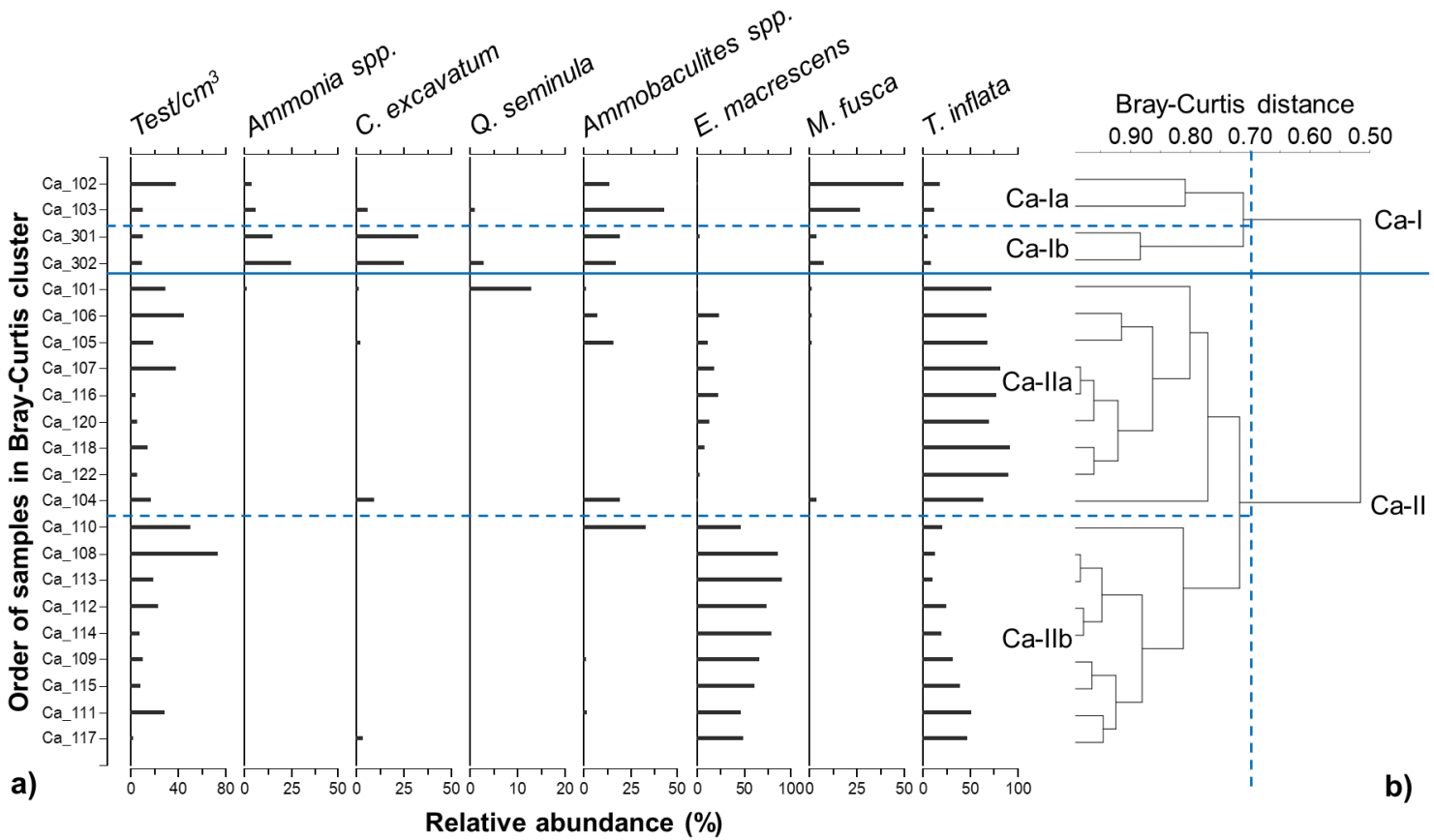

Figure 5.11: (a) Spatial distribution of benthic foraminifera in upper intertidal wetlands of Cararma Inlet and (b) Spatial assemblage based on Bray-Curtis cluster analysis.

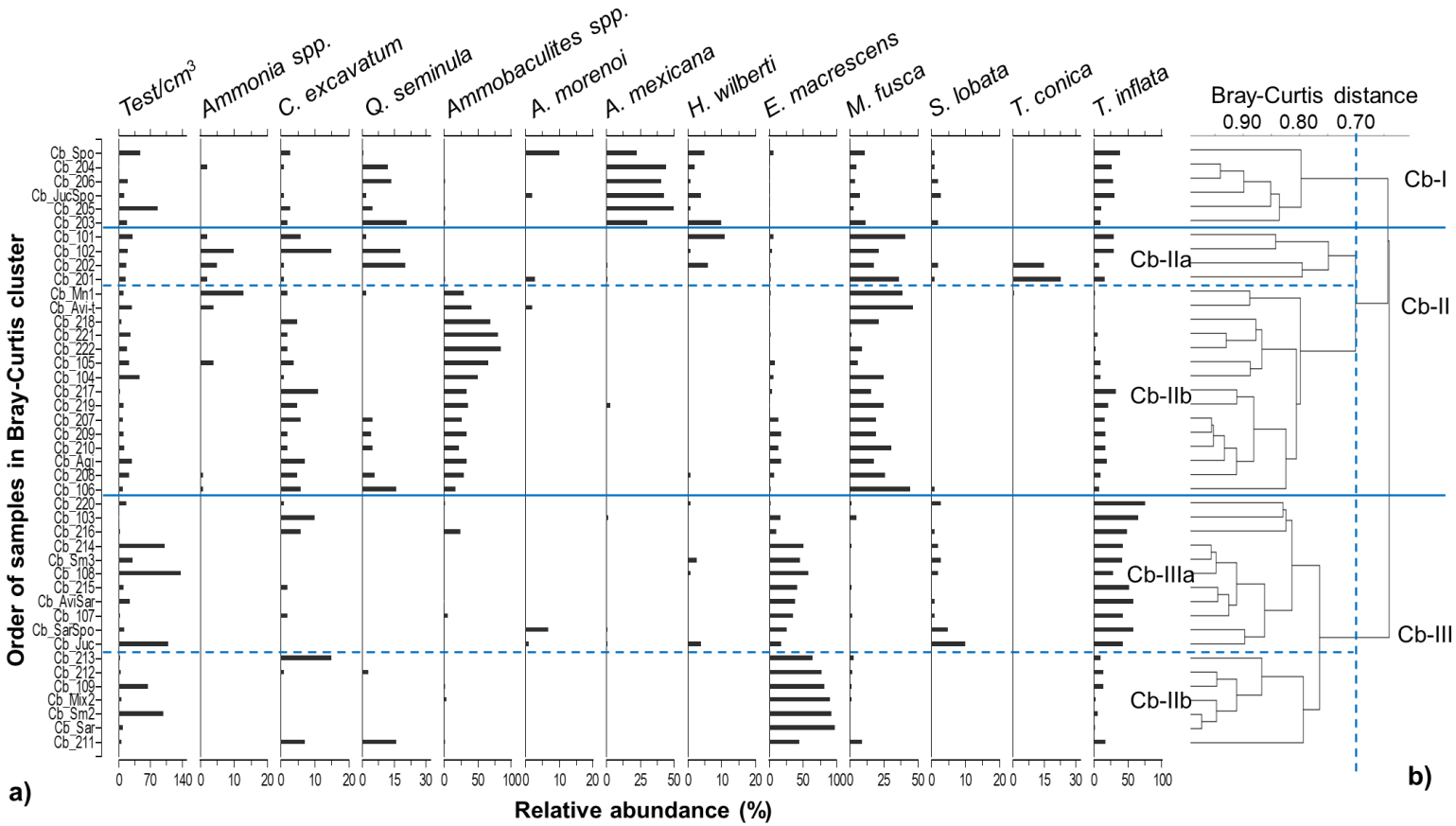

Figure 5.12: (a) Spatial distribution of benthic foraminifera in upper intertidal wetlands of Currambene Creek and (b) Spatial assemblage based on Bray-Curtis cluster analysis.

Dominant taxa varied between study areas, for example, *A. mexicana* was present in relatively high numbers only at Currambene Creek and calcareous *H. depressula* and *H. anderseni* were found in relatively high abundance at Comerong Island. Foraminifera, such as *S. lobata* and *H. wilberti* were found in relatively low abundance in surficial samples of Cararma Inlet. However, some of the foraminiferal associations corresponded between study areas. For instance, assemblage *M. fusca – Ammobaculites* spp. – *C. excavatum* with subsidiary *Q. seminula* was observed in three study areas, clusters Min-III, Ca-I and Cb-IIb. *T. inflata* with subsidiary *E. macrescens* and *S. lobata* was observed in spatial clusters Min-I, Cm-1 and Cb-IIIa. Remarkably, in spatial clusters Ca-II and Cb-III, *T. inflata* and *E. macrescens* dominated conversely, for example, in samples that had a higher frequency of *T. inflata* had lower incidence of *E. macrescens*.

The discrepancy in species assemblages between sites is likely caused by a range of hydrological and geomorphological conditions in the region. Although the study areas share similar geomorphic properties, for example, they all are part of wave-dominated barrier estuaries, they have different inundation characteristics. The impact hydro-geomorphological conditions have on the environmental variables is explored further in the next section.

5.4.4. Principal environmental factor(s)

The environmental variables showed inconstancies between study areas (Fig. 5.13), for example, surface sediment pore-water salinity of 7.7 (± 3.6) ppt at Cararma Inlet was higher than all the other sites. In relation to tidal position in the upper intertidal zones, salinity increased with wetland elevation at Minnamurra River and Currambene Creek, while it decreased at higher elevation at Comerong Island and Cararma Inlet. Pore-water salinity was categorised as key environmental variable for Minnamurra River ($r = 0.634$) and Comerong Island ($r = -0.482$). High substrate organic matter content was also recorded at Cararma Inlet, which showed a positive correlation with wetland elevation and the only site

at which a significant correlation was identified with wetland elevation (r = 0.619) (Fig. 5.13). Sediment particles were mainly muddy (high silt and clay content) from Minnamurra River, whilst samples from Cararma Inlet were largely sandy with relatively larger particle grainsize of 101 (± 66) microns. Sediment grainsize showed a relatively strong relationship to wetland elevation at Comerong Island and Cararma Inlet.

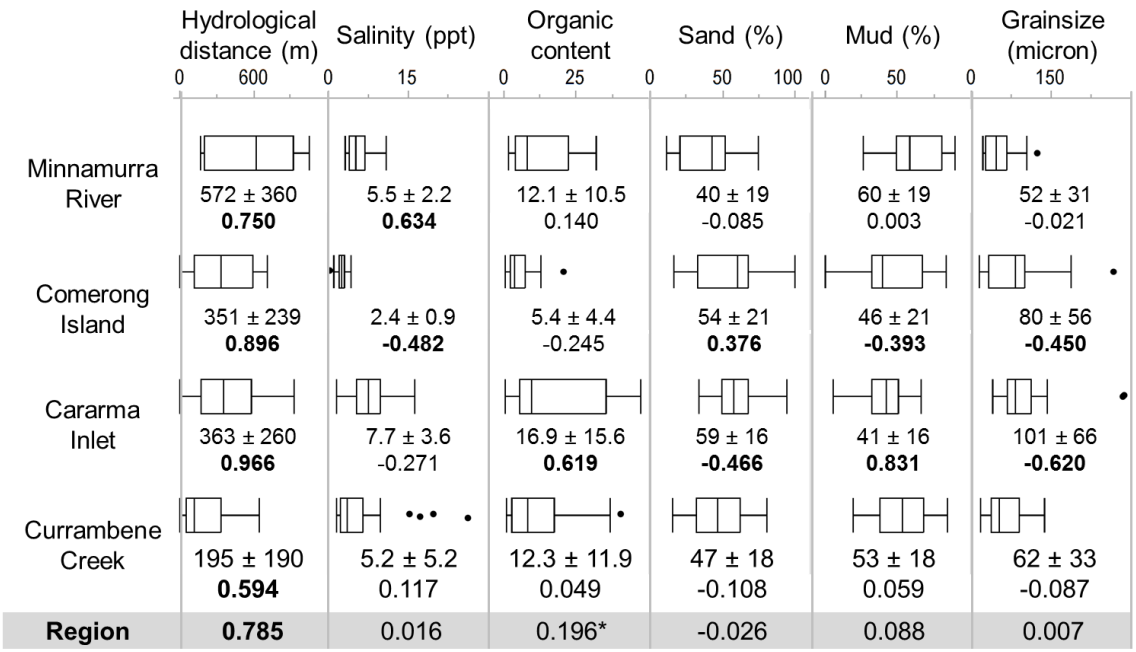

Figure 5.13: Box and whiskers indicating the range in the environmental variables in each site. The boxes show the median and the 25th and 75th percentile, upper and lower whiskers represent range and dots are outliers. Environmental variables are expressed as mean ± standard deviation followed by R-values (indicating the direction of relationship) for each study area. The values in Region are the correlation coefficient values (r). Numbers in bold indicate relationships significantly different to 0 (p-value < 0.05).

Spatial assemblages in relation to the key environmental indicate that cluster Min-I was in the higher position of the upper intertidal at STPI of 0.74 ± 0.05 and located furthest from the channel and was influenced by pore-water salinity (Fig. 5.14a). Min-II occurred at mid-elevations, while Min-III assemblage dominated in the lower position of the upper intertidal (typically below the MHW of 0.5). Like Min-I, Cm-I assemblage occurred in the higher position of the tidal frame at elevations greater than MHW (above 0.5). Cm-Ia occurred in a narrow elevation gradient (STPI 0.63 ± 0.06) with abundant *C. excavatum*, whilst samples of Cm-Ib containing

H. wilberti and *M. obliqua* was influenced by relatively high substrate grainsize (~ 68%) (Fig. 5.14b). Cluster Cm-II represents samples from the lower position of the upper intertidal and Cm-III was constrained to a narrow elevation range (STPI 0.36 ± 0.09) preferring fine-grained sediments (~ 71%) and higher salinity conditions (approximately 3 ppt).

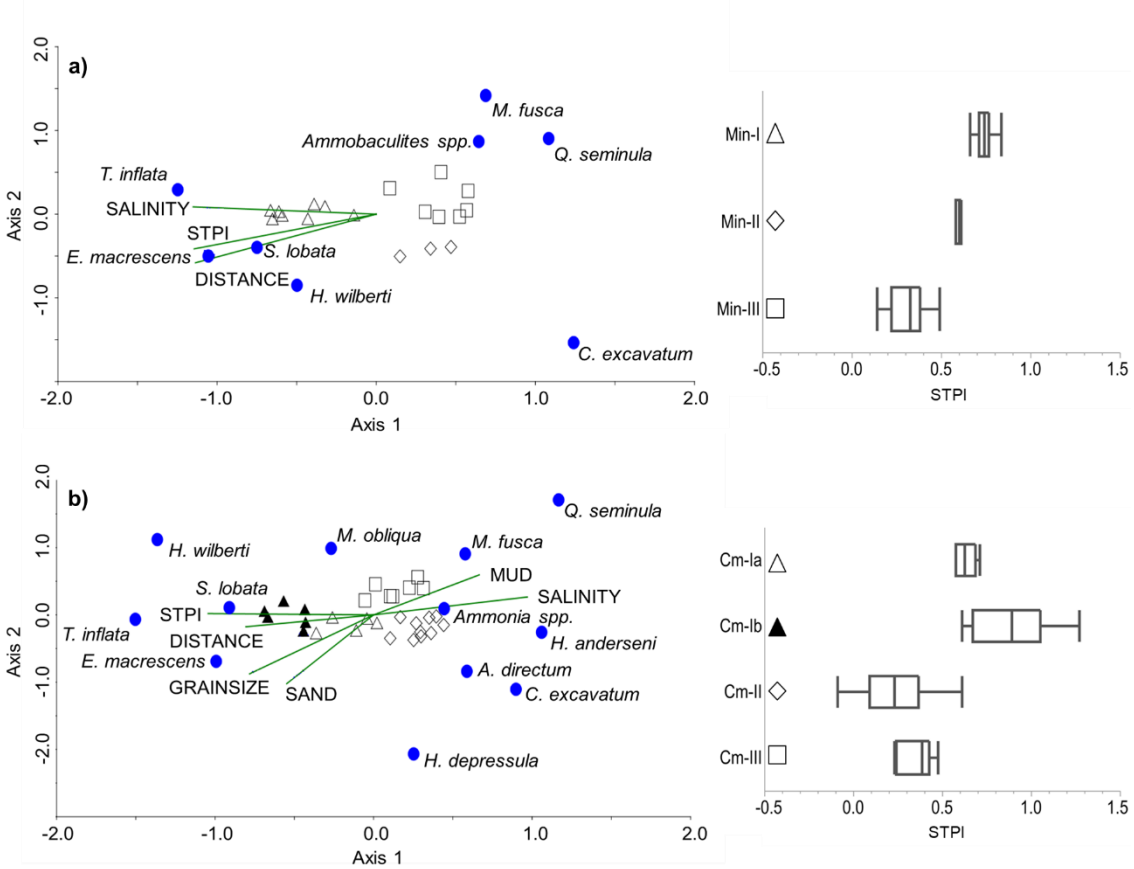

Figure 5.14: Dominant taxa and important environmental variables ordination based upon CCA for; (a) Minnamurra River and (b) Comerong Island. Assemblages are indicated by the different shapes. Graphs on the right represent elevation range of the spatial clusters using box and whiskers, where the boxes are showing the median and the 25th and 75th percentile, upper and lower whiskers represent range.

Results indicate that the variation in spatial cluster Ca-I was likely caused by sediment grainsize (Fig. 5.15c). Samples in cluster Ca-Ia correlated with finer-grained substrate (~ 66%) that had a relatively high organic matter content (~ 43%). Samples in cluster Ca-Ib from the channel were mainly sandy (~ 94%) and were low in organics (~ 0.6%). Samples in cluster Ca-II were located between STPI 0.35 – 0.77, in which *E. macrescens* dominated in a narrow range of samples of

STPI 0.62 (± 0.04). At Currambene Creek, *A. mexicana* was found in relatively high abundance in a narrow wetland elevation range of STPI 0.16 – 0.49 (cluster Cb-I) (Fig. 5.15d). Cb-IIb was constrained to a narrow elevation range of 0.40 (± 0.08) in which *Ammobaculites* spp. dominated. Cb-IIa was constrained to STPI of 0.27 – 0.43 in which *T. conica* was present. Foraminiferal assemblage of cluster Cb-III had similar elevation distribution to cluster Ca-II. At this site, *E. macrescens* dominated in sample at an elevation range of STPI 0.43 – 0.69.

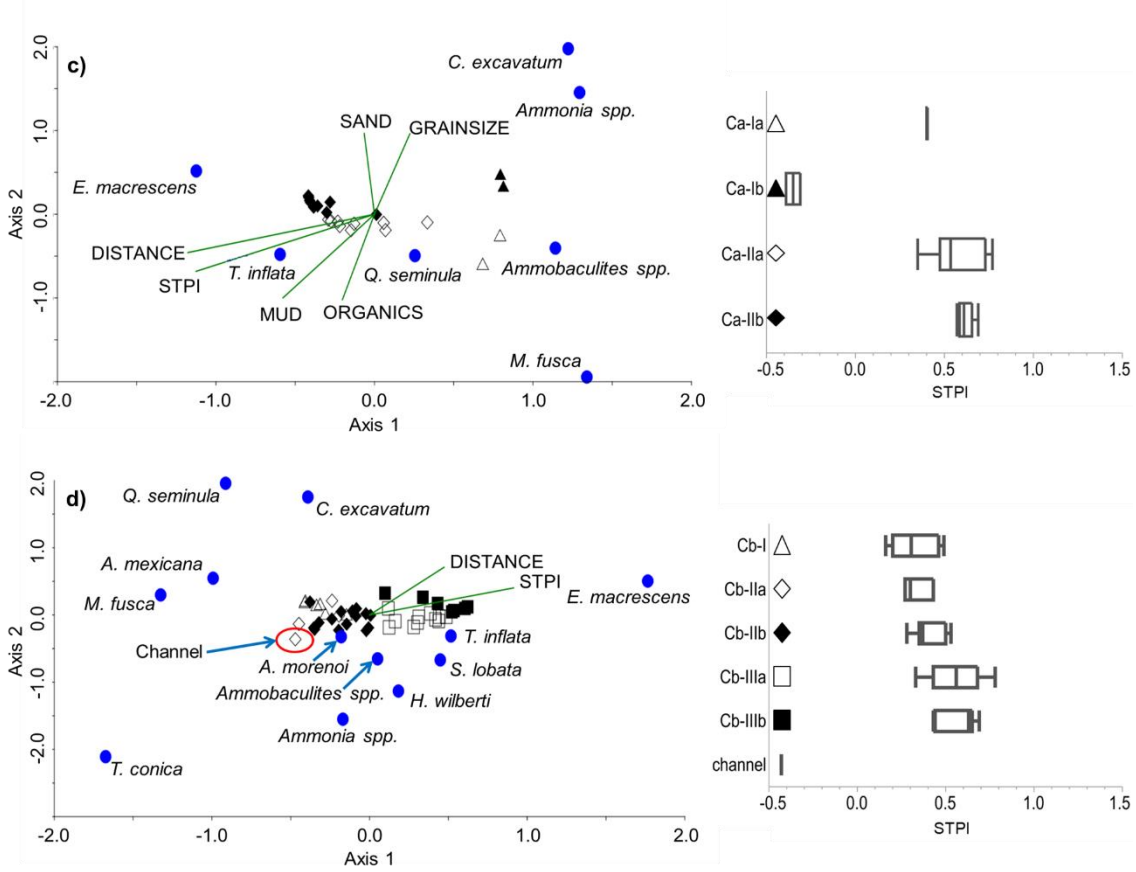

Figure 5.15: Dominant taxa and important environmental variables ordination based upon CCA for; (c) Cararma Inlet and (d) Currambene Creek. Assemblages are indicated by the different shapes. Graphs on the right represent elevation range of the spatial clusters using box and whiskers, where the boxes are showing the median and the 25th and 75th percentile, upper and lower whiskers represent range.

The variation in environmental data between study areas make them distinct from each other, however, inundation indicators (STPI and hydrological distance from the channel) were the consistent controls all the study areas, particularly at

Currambene Creek where none of the other environmental variables showed a meaningful relationship to the distribution of assemblages (Fig. 5.13). Logistic correlation between STPI and hydrological distance gave an r^2 value of 0.5166 (Fig. 5.16). Since hydrological distance is regulated by wetland elevation above MSL, at and below MSL the distance water takes to inundate the surface will be 0 since the lower intertidal is mostly inundated. Additionally, since hydrological distance cannot be projected down sediment cores for palaeo-environmental reconstructions, distribution of foraminiferal assemblages was characterised just with respect to STPI for the region.

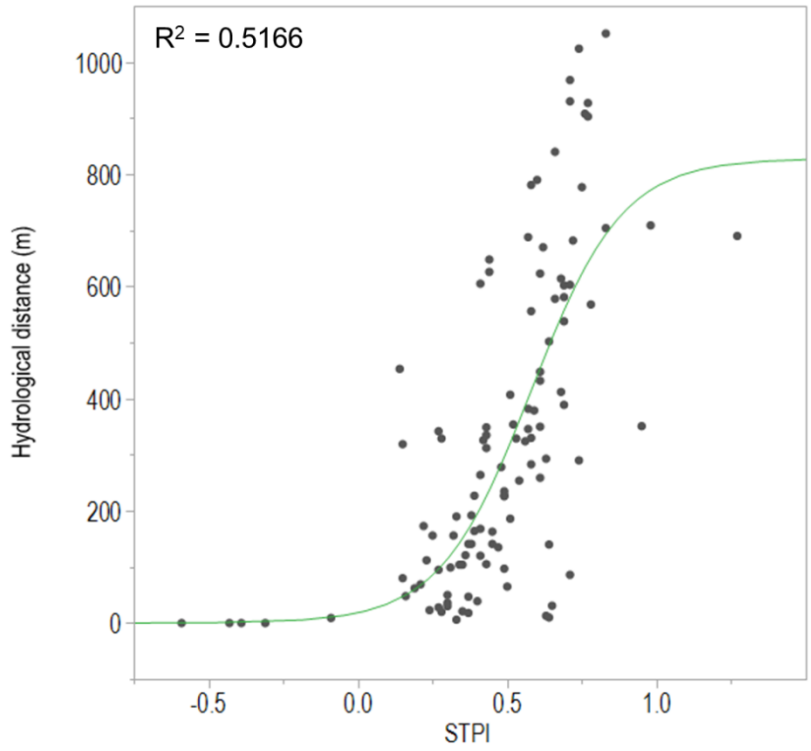

Figure 5.16: Correlation between STPI and hydrological distance.

5.4.5. Regional training set

Benthic foraminifera exhibited a vertical zonation with respect to the tidal frame in the upper intertidal wetland areas (Fig. 5.17a). Calcareous taxa dominated in the lower position of the upper intertidal (below MHW), whilst agglutinated taxa were largely concentrated between mid-tidal to higher position of the upper intertidal.

T. inflata occurred in relatively high abundance across the all intertidal zones with their frequency increasing with wetland elevation. A few agglutinated foraminifera occurred in relatively high abundance below MHW, such as *T. conica* and *A. mexicana*, and *M. fusca*. Species distribution corresponded to vegetation communities (Fig. 5.17b), for instance *S. lobata*, *H. wilberti* and *M. obliqua* occurred in higher frequency above the MHW in areas dominated by saltmarsh, whereas *Q. seminula*, *Ammonia* spp. and *H. anderseni* were present in higher numbers in zones dominated by mangrove plants.

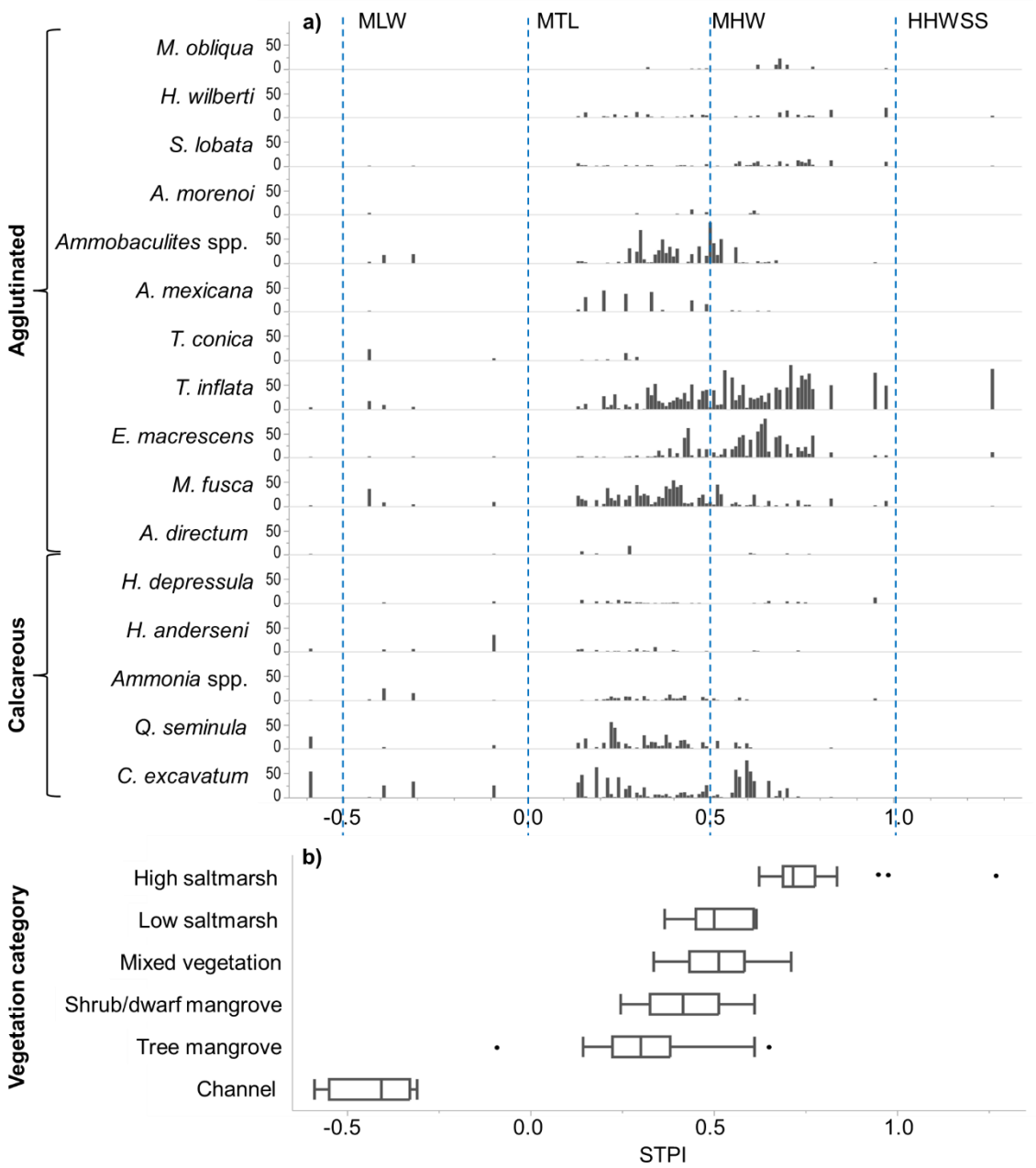

Figure 5.17: (a) Spatial distribution of dominant taxa and (b) vegetation in upper intertidal wetland areas of the study sites. Vegetation categories are expressed using box and whiskers, where the boxes are showing the median and the 25th and 75th percentile, upper and lower whiskers represent range and dots are outliers.

Three major spatial assemblages were classified from the sixteen dominant taxa for the region (Fig. 5.18a). Cluster A dominated by *E. macrescens, T. inflata*, *H. wilberti*, *S. lobata* and *M. obliqua* when and further sub-divided showed that *T. inflata* and *E. macrescens* dominated conversely (Fig. 5.18b) as was observed Cararma Inlet and Currambene Creek (Fig. 5.11 and 5.12). *T. inflata* dominated in

cluster A-I, while A-II was dominated by *E. macrescens* in which *H. wilberti* and *S. lobata* were absent. Species *A. mexicana* occurred in cluster B, with subsidiary *T. inflata* and *Q. seminula* (Fig. 5.18). Assemblage C was dominated by *E. excavatum*, *Q. seminula*, *Ammobaculites* spp. and *M. fusca* (Fig. 5.18a) and further sub-division showed that cluster C-I was dominated by *M. fusca*, *Q. seminula* with subsidiary *Ammonia* spp. *Ammobaculites* spp. dominated cluster C-II with *M. fusca* and *E. macrescens*, and *C. excavatum* was dominantly present in cluster C-III with minor taxa *M. fusca*, *Q. seminula*, *Ammonia* spp. and *Ammobaculites* spp. (Fig. 5.18b).

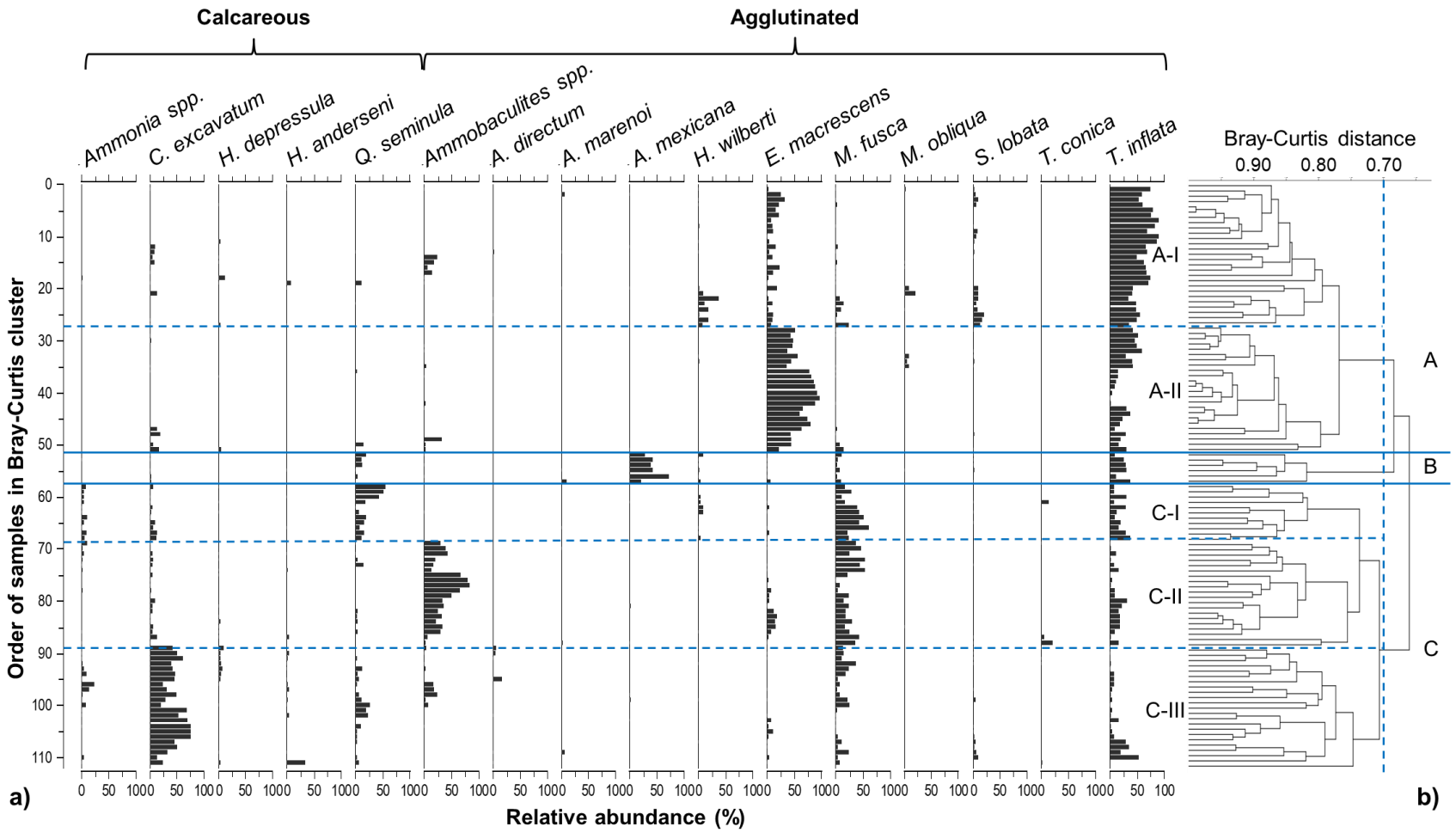

Figure 5.18: (a) Spatial distribution of benthic foraminifera in upper intertidal wetlands of the region. (b) Regional training set spatial assemblages.

CCA revealed a close correlation between sub-clusters and vegetation zones (Fig. 5.19a), where the *Trochammina* – *Entzia* association (A-I) was common in high saltmarsh vegetation typically above MHW (STPI > 0.5) (Fig. 5.19b and c). The *Entzia* – *Trochammina* association (A-II) occurred in a relatively narrow mid-tidal STPI range of 0.43 – 0.71 (0.38 – 0.60 m AHD) in saltmarsh vegetation. Cluster B *Arenoparrella* – *Trochammina* association was constrained to STPI of 0.16 ± 0.49 (0.17 – 0.43 m AHD) in mangrove to mixed substrate. Assemblage C samples occurred at wetland elevation that had an STPI below 0.62. The *Cribroelphidium* – *Miliammina* group (cluster C-III) dispersed over a large elevation range between STPI 0.14 and 0.62 (0.15 – 0.53 m AHD). Within that the *Miliammina* – *Quinqueloculina* association (C-I) occurred in mangrove substrate at STPI of 0.23 – 0.47 (0.22 – 0.41 m AHD), whilst the *Ammobaculites* – *Miliammina* association (C-II) was present at STPI between 0.30 and 0.52 (0.28 – 0.45 m AHD) in mixed vegetation sediments. The channel assemblage occurs below MTL between STPI -0.59 and -0.31 (-0.42 – -0.20 m AHD) (Fig. 5.19c).

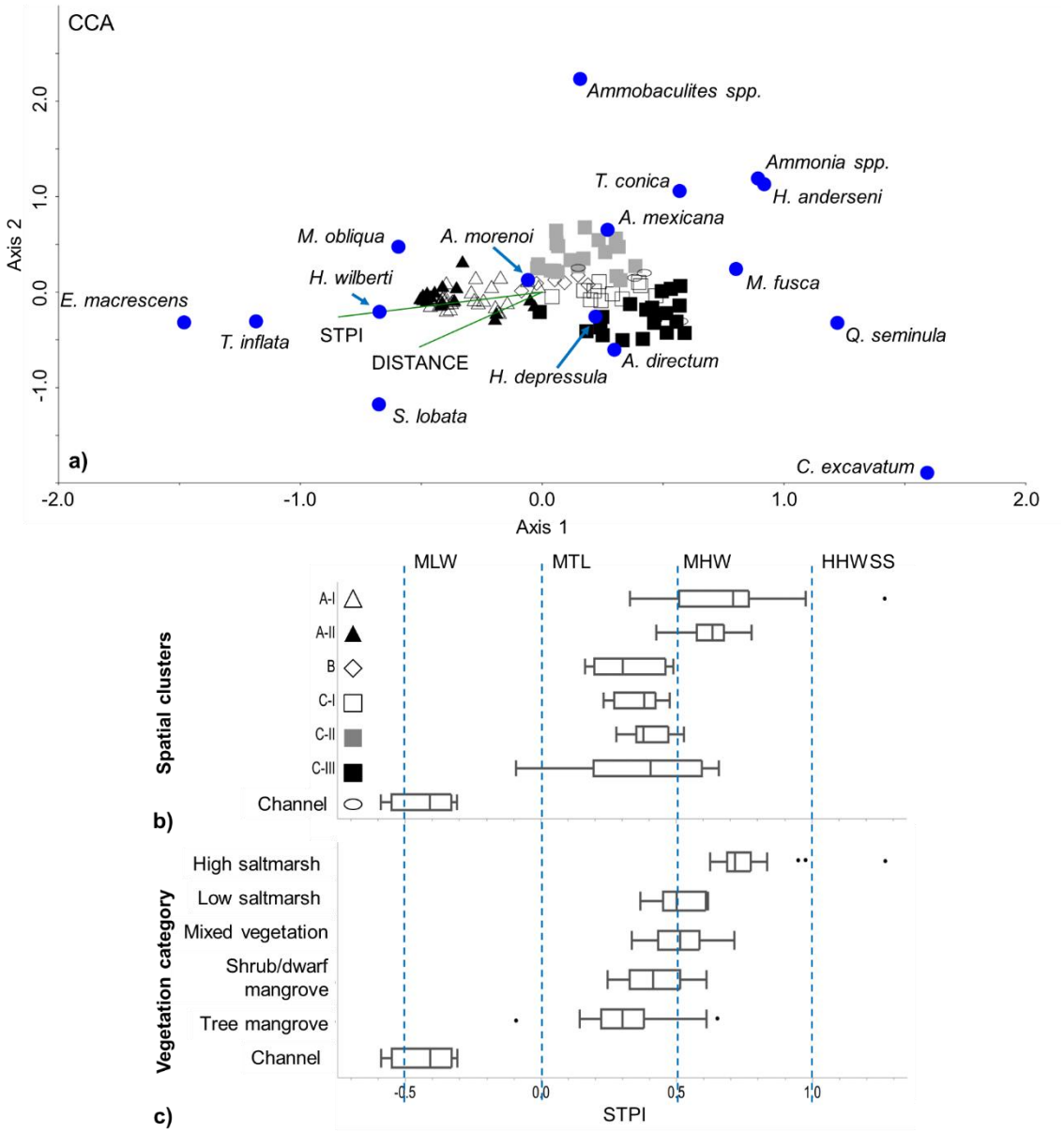

Figure 5.19: (a) CCA ordination of the regional training set. (b) Elevation range of the spatial clusters and (c) vegetation categories represented using box and whiskers, where the boxes are showing the median and the 25th and 75th percentile, upper and lower whiskers represent range and the dot is treated as an outlier.

The above results show that a regional training set provides a comprehensive spatial distribution of benthic foraminifera in the upper intertidal wetland zones dominated by mangrove and saltmarsh. Their distribution is influenced by wetland elevation relative to MSL, which also regulates tidal inundation frequency in the upper intertidal wetlands as was discussed in the previous Chapters (2 and 3). Assemblages lower tidal position prefer higher inundation conditions, while the

upper tidal position assemblages' favour lower inundation environment like saltmarsh vegetation in the region, whilst there are some assemblages that prefer mid-elevation tidal conditions, such as the *Ammobaculites* spp. – *M. fusca* assemblage. The close correlation between assemblages across the intertidal zone and the surrounding vegetation can be used to reconstruct past environments from microfossil assemblages.

5.4.6. Foraminifera-based transfer function models

Unimodal weighted averaging (WA) and weighted averaging partial least squares (WA-PLS) foraminifera-based transfer functions were created based on the DCA ordination gradient length of 3.46 (Fig. 5.20). The gradient length indicated that foraminifera in the regional training set exist in a unimodal nature with respect to STPI, the principal environmental factor influencing the spatial distribution of foraminifera in the region. The weighted averaging tolerance downweighted (WA-TOL) regression (RMSEP = 0.193) performed marginally better than classic WA when jack-knifed errors are considered (RMSEP = 0.263) (Table 5.3). However, the classic WA produces species optima (species ideal elevation) and tolerance (range of elevations a species was encountered in). Species optima are calculated from the abundance weighted average of the STPI values of all samples in which each species occurs, whilst the tolerance is the abundance weighted standard deviation.

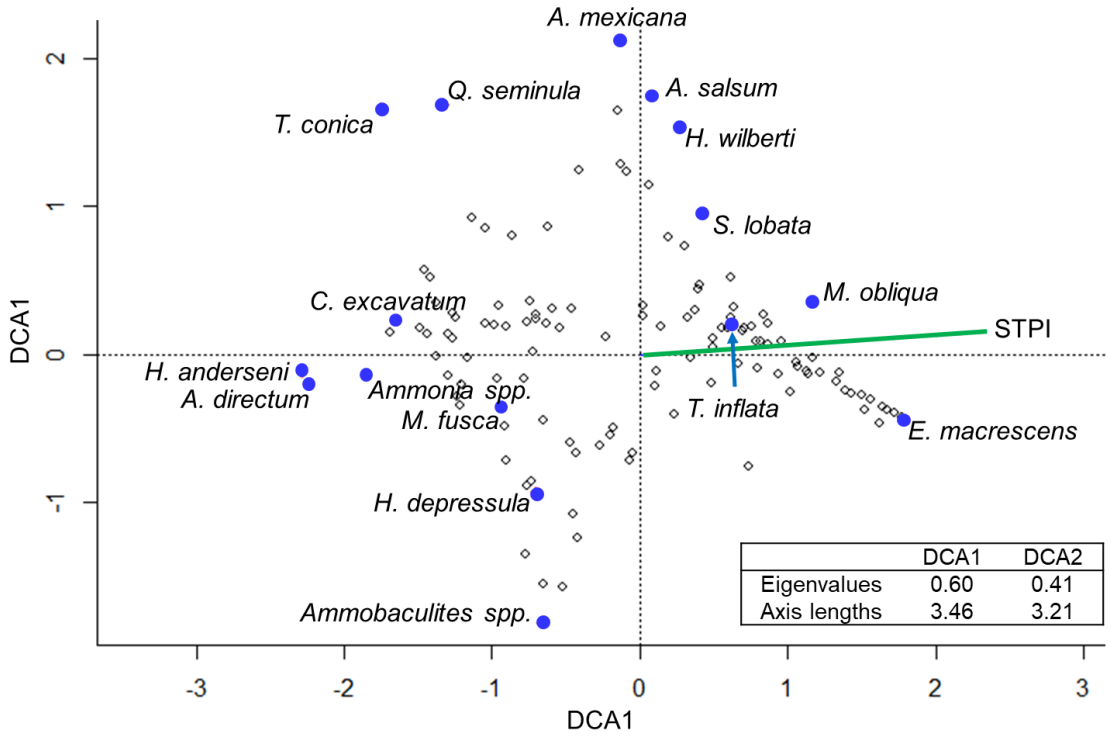

Figure 5.20: DCA showing the ordination between species and STPI, the principal environmental gradient.

Table 5.3: Statistics summary of the transfer function performed on the modern training set.

		Cross-validation			
		None		Jack-knifed	
Model	**Component**	**RMSE**	**r^2**	**RMSEP**	**r^2**
WA	WA_Cla	0.263	0.509	0.278	0.435
	WA-TOL_Inv	0.193	0.481	0.202	0.429
WA-PLS	Component 1	0.187	0.509	0.202	0.429
	Component 2	**0.170**	**0.595**	**0.201**	**0.443**
	Component 3	0.165	0.618	0.225	0.376
	Component 4	0.163	0.627	0.244	0.335
	Component 5	0.162	0.631	0.258	0.317

Figure 5.21 represents the species optima (and tolerances) derived from classical WA of all the dominant taxa data from the region. This can be used to characterise species assemblages, for example cluster A of the regional training set (*T. inflata*, *E. macrescens*, *H. wilberti*, *S. lobata* and *M. obliqua*) have a high STPI and located in

the higher position of the upper intertidal mixed vegetation to saltmarsh vegetation type. Calcareous taxa, on the other hand, are dominantly present at wetland elevations below MHW at mean elevation between 0.09 and 0.35 m AHD in mangrove sediments (Table 5.4).

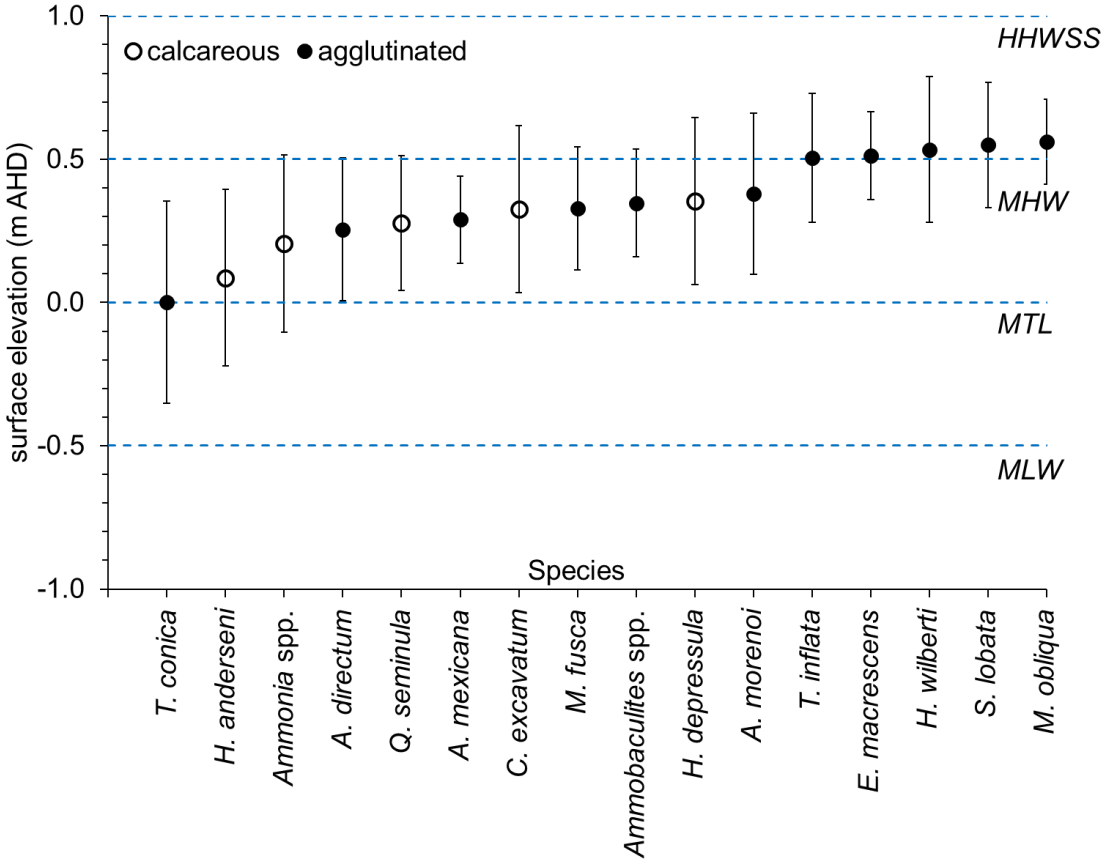

Figure 5.21: Dominant taxa in the modern training set, where species coefficients optima (weighted average) represent the modelled elevation in which the species is most abundant and tolerances (weighted standard deviation) representing the upper and lower limits of their modelled distribution (elevation gradient they were sampled).

Table 5.4: Foraminiferal species optima (weighted average) and tolerances (weighted standard deviation) for surface elevation (m AHD) showing all dominant taxa present in the foraminiferal dataset.

Species	Surface elevation (m AHD)	Error (tolerance ± m)	Elevation range
T. conica	0.001	0.354	-0.353 – 0.355
H. anderseni	0.087	0.308	-0.221 – 0.395
Ammonia spp.	0.205	0.309	-0.105 – 0.514
A. directum	0.255	0.250	0.005 – 0.505
Q. seminula	0.278	0.236	0.042 – 0.513
A. mexicana	0.290	0.152	0.138 – 0.442
C. excavatum	0.326	0.292	0.034 – 0.618
M. fusca	0.328	0.215	0.113 – 0.544
Ammobaculites spp.	0.347	0.188	0.159 – 0.535
H. depressula	0.354	0.291	0.063 – 0.645
A. morenoi	0.380	0.281	0.099 – 0.662
T. inflata	0.505	0.226	0.279 – 0.730
E. macrescens	0.512	0.154	0.358 – 0.665
H. wilberti	0.534	0.255	0.279 – 0.789
S. lobata	0.551	0.219	0.332 – 0.769
M. obliqua	0.561	0.149	0.412 – 0.709

A few agglutinated taxa, such as *A. directum*, *A. mexicana*, *M. fusca*, *Ammobaculites* spp. and *A. morenoi* had their optima below MHW (0.26 to 0.38 m AHD) and occurred in mixed vegetation and mangrove substrate. *T. conica* was an exception and had its optima at MTL (0.001 m AHD) preferring low elevation mangrove and lower intertidal conditions. These results suggest that optima and tolerance to STPI of WA transfer functions have a direct ecological interpretation and can be used to infer wetland elevation from microfossil assemblages.

The WA-PLS performed slightly better than WA (see Table 5.3) as it performs well with noisy, species-rich data, such as for this region that cover a long ecological gradient (>3 SD units from DCA) (ter Braak and Juggins, 1993). Normally, the WA-PLS transfer function produces results for five components. The choice of component depends upon the prediction statistics, which is RMSEP and r^2, and according to the principle of parsimony (choosing the simplest scientific explanation that fits the evidence) can be based on low RMSEP and high r^2. Studies have demonstrated that choosing low prediction errors (RMSEP) and high squared

correlations (r^2) gives an acceptable model that can be used for palaeo-environmental reconstructions (Horton et al., 2007, 1999a; Horton and Edwards, 2006; Leorri et al., 2008b; Mills et al., 2013; Wright et al., 2011). Therefore, component 2 of WA-PLS demonstrated a relatively strong relationship between observed and predicted values (r^2_{jack} = 0.443) and reconstructions of palaeo-upper intertidal wetland surface is possible up to a vertical error of 0.20 m or less ($RMSEP_{jack}$ = 0.201).

5.5. Discussion

5.5.1. Application of living and dead taxa in training sets

Contemporary distribution of benthic foraminiferal assemblages was created using populations of both living and dead foraminifera. Total counts were also used in other studies (de Rijk, 1995; de Rijk and Troelstra, 1997; Gehrels, 2000; Scott and Medioli, 1978) as living and dead assemblages better represent the complete modern analogue of assemblages in surficial samples. The findings of this study demonstrated that training sets developed only with the dead assemblages would overemphasise agglutinated taxa and calcareous species, such as *C. excavatum*, *H. depressula*, *Q. seminula* and species of the genus *Ammonia* would get dismissed as they were found living in relatively high abundance in surficial samples of Comerong Island and Minnamurra River. Regions that have low species abundance, training sets were developed with total counts as suggested in the previous study by Haslett et al. (2010) at Minnamurra River.

Alive tests were found up to the depth of 6 cm below the surface in this study, which is relatively consistent with analyses elsewhere. For example, in intertidal muddy sediments of southwest Spain (Papaspyrou et al., 2013), western Ireland (Horton and Edwards, 2006) and Cowpen Marsh in the UK (Horton, 1999), the average living depth of benthic foraminifera has been recorded to a depth of about 3 cm below the surface. Infaunal tests have been found living at depths of up to 60

cm deep below the surface in north-eastern saltmarshes of United States (Horton and Edwards, 2006). Alive tests have also been found at depths of 50 cm in saltmarshes of Oregon (Milker et al., 2015a) and in tropical mangroves of Australia (Berkeley et al., 2008). In south-eastern US marshes, they have been found living 30 cm below the surface (Goldstein and Watkins, 1999). The temporal distribution of living tests most likely correlates with oxygen availability in belowground sediments (Berkeley et al., 2007; Horton and Edwards, 2006; Moodley et al., 1997; Papaspyrou et al., 2013), demonstrating that infaunal living assemblages in the substrate can represent present-day environmental conditions.

Some studies have demonstrated that contemporary foraminiferal assemblages should be classified from the top 1 cm sediments only (de Rijk and Troelstra, 1997; Edwards et al., 2004b; Gehrels, 2000; Gehrels et al., 2001; Gehrels, 2002; Horton et al., 1999b; Horton and Edwards, 2003, 2006; Horton and Murray, 2006; Scott and Medioli, 1978; Woodroffe et al., 2005). However, in this study we demonstrate that surficial top 2-cm of samples capture a comprehensive distribution of assemblages in the upper intertidal wetland areas. High numbers of calcareous foraminifera were found in the top 1-cm, whilst relatively high abundance of living agglutinated tests occurred in sediments from 1 to 2 cm, hence the top 2-cm of surficial sediments avoids partiality towards calcareous taxa and against agglutinated taxa in the modern analogue of training sets.

5.5.2. Implication of environmental variables on dominant taxa

Calcareous taxa exhibited a negative correlation to substrate organic matter content, which can be associated with low pH conditions as organic materials decompose. Aerobic oxidation of organic matter decreases pore-water oxygen concentrations, but produces carbon dioxide gas that further breaks down to carbonic acid (H_2CO_3) that can dissolve calcareous tests (Berkeley et al., 2007; Geslin et al., 2011; Goldstein and Watkins, 1999; Hayward et al., 2002, 2004a, 2015; Woodroffe et al., 2005). Taxa, such as *Q. seminula* and *M. fusca* favoured

muddy substrate, whilst *C. excavatum* preferred sand grained sediments.

A few studies have demonstrated that the lower positions of the upper intertidal zones have salinity regimes like that of seawater (as they are inundated for longer periods of time), while salinity at higher elevations can be variable (de Rijk and Troelstra, 1997; Hayward et al., 1999b; Horton and Murray, 2007). For instance, if there is greater infiltration of seawater and/or evaporation higher in the tidal frame then pore-water salinity would increase. Salinity decreases or is close to that of freshwater with increased amounts of freshwater inputs, such as rainwater, surface runoff and groundwater intrusion. This might explain why pore-water salinity shows a positive correlation to wetland elevation along the tidal frame at Minnamurra River, while at Comerong Island groundwater intrusion at higher elevations has resulted in an overall decrease in pore-water salinity as wetland elevation increased. Species, such as *A. mexicana* and *H. wilberti* did not show a meaning relationship to any of the environmental parameters except pore-water salinity.

A. directum and *A. morenoi* were found in very low numbers in the region and did not correlate with any of the environmental variables. Studies have shown that *A. morenoi* generally do not preserve well and are easily fragmented because their test walls are loosely cemented with poorly sorted grains (Berkeley et al., 2007; Goldstein and Watkins, 1999), and so oxidation and bacterial activities can easily disintegrate their test wall (de Rijk and Troelstra, 1999). *A. directum* has been reported in low salinity estuarine environments in Malaysia (Culver et al., 2012). In this study *A. directum* were found in high numbers in mangrove sediments of Comerong Island, and correspondingly have been reported in muddy mangrove substrate in Brazil (Semensatto-Jr. et al., 2009) and mid-mangrove zones (0.64 – 0.73 m above MTL) of Northern Queensland (Berkeley et al., 2009).

5.5.3. Spatial distribution of foraminiferal assemblages

In this region, foraminiferal assemblages exhibited a strong lateral zonation along the elevation gradient of the upper intertidal zones as demonstrated by numerous other Australian studies (Albani, 1978; Berkeley et al., 2008; Callard et al., 2011; Cann et al., 1993; Dean and De Deckker, 2013; Haslett, 2001; Horton et al., 2003; Strotz, 2015; Wang and Chappell, 2001; Woodroffe et al., 2005). Foraminiferal distribution is largely influenced by position in the tidal frame. Inundation indicators, STPI and hydrological distance were the consistent controls on foraminiferal distribution, but since hydrological distance cannot be projected down cores when reconstructing palaeo-environmental conditions, wetland elevation was used as the principal control on foraminiferal assemblages in the upper intertidal of the region.

The variation in dominant taxa type and environmental variables between study areas indicated that although all the study areas are part of wave-dominated barrier estuaries, they have different inundation characteristics making them distinct from each other. For instance, *H. depressula* and *H. anderseni* were found in relatively high abundance at Comerong Island, but they occurred in very low numbers in all the other study areas. This has been the first report of *A. mexicana* in intertidal wetlands of NSW and was constrained in a narrow of elevation range of 0.138 – 0.442 m in mangrove to mixed vegetation sediments of Currambene Creek and in low abundance at Minnamurra River. It was not found in the other two study areas having similar elevation and substrate properties. *A. mexicana*, however, has been reported in intertidal zones of Cleveland Bay, north Queensland (Berkeley et al., 2008; Horton et al., 2003), in channel deposits of South Alligator River (Wang and Chappell, 2001) in Australia. *A. Mexicana*, however has been well documented in saltmarsh sediments of the Great Marshes, Massachusetts (de Rijk, 1995; de Rijk and Troelstra, 1997), and mangrove sediments of Trapandé Bay, Brazil (Semensatto-Jr. et al., 2009) and Fiji (Bronnimann et al., 1992).

A few anomalous species, such as *E. australis* were found only in channel

sediments and mangrove sediments (STPI < 0.3) of Comerong Island. *E. australis* has been previously reported in subtidal zones of Broken Bay (Albani, 1978). *T. oblonga* has been documented in modern and core samples of Minnamurra River (Haslett et al., 2010) but was unique to mid-tidal elevations of Comerong Island. *E. advenum* was unique to the subtidal channel samples at Cararma Inlet, and have been reported in other subtidal environments (Albani, 1978; Hayward et al., 2004b; Strotz, 2003), and in mudflat and lower elevation mangrove areas (Horton et al., 2005). These discrepancies in species assemblages identified between sites are a result of hydrological and geomorphological conditions in the region, thus pooling of data provides a more comprehensive distribution of foraminifera in relation to STPI.

5.5.4. Relationship between spatial assemblages and wetland elevation

Calcareous taxa were found in greater diversity in the lower position of the upper intertidal (MTL – MHW), whilst agglutinated taxa were more diverse in the higher position of the upper intertidal (MHW – HHWSS). Similar distribution patterns of calcareous and agglutinated tests were discovered in temperate marshes of United Kingdom (Edwards and Horton, 2000; Horton, 1999; Horton et al., 1999b), New Zealand (Hayward, 1993; Hayward et al., 1999b), and temperate intertidal wetlands (Callard et al., 2011; Haslett et al., 2010) and tropical mangrove mudflats (Haslett, 2001; Horton et al., 2003; Wang and Chappell, 2001; Woodroffe et al., 2005) of Australia.

Intertidal zones lower in the tidal frame have a higher inundation frequency and seawater creates alkaline conditions (substrate pH > 8) creating suitable conditions for calcareous foraminifera to inhabit (Berkeley et al., 2007; Horton et al., 1999a) as they are susceptible to acidic conditions that trigger test wall dissolution. Agglutinated tests on the other hand, can tolerate acidic conditions (Scott and Medioli, 1978). Some studies showed that species distribution patterns

corresponds to salinity gradients in lagoonal and estuarine settings, where agglutinated foraminifera dominated in the lower salinity zones, while calcareous tests increased in both relative abundance and diversity in salinity regimes similar to that of seawater (Culver et al., 2012; de Rijk, 1995; Hayward, 1993; Hayward and Hollis, 1994).

T. inflata was present in relatively high abundance in all study areas and zones occurred in 97 % of the samples between wetland elevations of 0.279 and 0.730 m, particularly in the saltmarsh sediments with minor *E. macrescens*. In a previous study at Minnamurra River foraminiferal assemblages were categorised in relation to elevation-related depositional environments, including saltmarsh, mangrove, the mangrove pneumatophore zone, and unvegetated tidal flat (Haslett et al., 2010). Higher in the tidal frame and in the saltmarsh, a monospecific assemblage of *T. inflata* was documented, while abundant calcareous taxa were reported in the mangrove and the pneumatophore zone. The findings from the above study coincide with the findings of this study, however, Haslett and others (2010) found a high abundance of *Cribrononion* spp. in mangrove sediments of Minnamurra River, but no foraminifera were encountered in our surficial samples from Minnamurra River or any of the other sites that were identified as *Cribrononion* spp. In contrast, we found a relatively high abundance of *C. excavatum* in mangrove sediments.

E. macrescens occurred in relatively high abundance in all study areas, but dominated at between wetland elevations of 0.358 – 0.665 m. It has been reported in upper intertidal elevations between MWH and HAT in temperate environments (de Rijk and Troelstra, 1997; Edwards et al., 2004b; Hayward, 1993; Horton, 1999; Lewis et al., 2013), including the saltmarsh of Tasmania (Callard et al., 2011). The *T. inflata – E. macrescens* assemblage dominated conversely in the regional training set (cluster A), including the spatial clusters at Cararma Inlet and Currambene Creek. The *T. inflata – E. macrescens* assemblages has also been documented in saltmarsh sediments located higher tidal frame of New Zealand (Hayward, 1993).

Agglutinated taxa *M. fusca* and *T. conica* showed a negative correlation with elevation and dominated lower in the tidal frame. Some studies have also reported high occurrence of *M. fusca* at lower elevation zones, such as the tidal flat and low marsh areas (Avnaim-Katav et al., 2017; Horton and Edwards, 2006; Milker et al., 2015a). Other studies have shown that *M. fusca* dominated in high- and middle marsh zone with species, such as *E. macrescens* and *T. inflata* (Horton et al., 1999b; Woodroffe et al., 2005). However, in this research, *M. fusca* was present in relatively high abundance in mid- to low elevations (Figure 5.17 and cluster C in 5.18) in association with *Ammobaculites* spp. and *Q. seminula*.

5.5.5. Regional training set and it's suitability for palaeo-environmental reconstructions

The close correlation between the modern assemblages and vegetation communities in the upper intertidal wetland areas in the region can be used to infer past environmental conditions, provided microfossil assemblages correspond to the modern analogue presented in this study. Presuming the pattern of species distribution with respect to vegetation zones has been consistent with sediment accumulation rate, geomorphological evolution of Minnamurra River was reconstructed in the context of Holocene sea-level rise (Haslett et al., 2010). The five stage evolutionary model was based on benthic foraminiferal evidence (Haslett et al., 2010), lithological evidence (Panayotou et al., 2007) and barrier-estuary evolution model (Roy et al., 2001).

Spatial assemblages dominated by calcareous taxa, particularly *C. excavatum* which is a common shallow-water species (Cann et al., 1988, 1993; Hayward et al., 1999b) and *Ammonia* spp., indicate subtidal and lower intertidal conditions, transitioning into mudflat if *T. conica* is present. Occurrence of other calcareous taxa, such as *H. depressula* and *H. anderseni* and *Q. seminula* together with agglutinated *M. fusca* indicated upper intertidal mangrove zone. High abundance of *Ammobaculites* spp. indicate a transition of wetland vegetation to mixed mangrove

and saltmarsh vegetation at mid-tidal positions. Presence of *A. mexicana* suggests mangrove vegetation below MHW. Assemblages dominated by *E. macrescens* with subsidiary *T. inflata* suggest a transition from mixed vegetation to saltmarsh higher in the tidal frame.

The modelled wetland elevation range of the dominant taxa represented their upper and lower limits. The WA-PLS transfer function model as it is a simple and robust reconstruction method (Horton and Edwards, 2006; Leorri et al., 2008b; ter Braak and Juggins, 1993) that is not affected by autocorrelation (Mills et al., 2013). Component 2 of WA-PLS transfer function further demonstrated that palaeo-wetland surface can be reconstructed up to a vertical error of about 0.20 m.

5.6. Conclusion

Benthic foraminiferal assemblages displayed a vertical zonation along the tidal frame of upper intertidal wetlands of wave-dominated barrier estuaries, which is related to wetland elevation relative to MSL. There was still a lot of overlap between species and a clear zonation between them could not be established for the region. Species distribution is affected by the inundation frequency of the wetland surface, which also regulates mangrove and saltmarsh vegetation distribution in the region, where mangroves dominate in the lower elevations in the tidal frame and saltmarsh dominate at higher elevations. Majority of the calcareous species were found in the lower elevation mangrove substrate, and whilst some agglutinated species were present in relatively large numbers in saltmarsh vegetation, most were spread out across the whole tidal frame.

Common groups or associations of foraminiferal species linked to different vegetation communities and wetland elevations. The *Trochammina – Entzia* association (A-I) was found in high saltmarsh vegetation typically above MHW; the *Entzia – Trochammina* group (A-II) was common in mixed vegetation to low saltmarsh at mid-tidal elevations. The *Miliammina – Quinqueloculina* association

(C-I) was common mangrove substrate, whilst the *Ammobaculites – Miliammina* association (C-II) was found in mangrove to mixed vegetation. The *Cribroelphidium – Miliammina* group (C-III) was distributed across a relatively large tidal range, from the channel to low saltmarsh, whilst the *Arenoparrella – Trochammina* association (cluster B) was unique to Currambene Creek in mangrove and mixed vegetation below MHW.

The close correlation between the modern assemblages and vegetation communities was used to create a modern benthic foraminiferal analogue for the region. Similarly, the transfer function models created spatial relationships between species type and wetland surface elevation based on empirically derived equations. Collectively, they can be applied in palaeo-environmental reconstruction studies. This relationship is further explored in Chapter 6 where the modern assemblage is used to interpret past vegetation change, whilst the transfer function model is used to reconstruct palaeo-wetland surface elevation.

Chapter 6

Palaeo-environmental reconstruction of coastal wetlands using benthic foraminiferal assemblages

6.1. Introduction

The present form and vegetation characteristics of coastal wetlands in individual geomorphological settings is a result of processes operating currently in a landscape, which was inherited from processes occurring over longer timescales. Past sea level is a particularly important control on the processes and environmental conditions in the past. Benthic foraminiferal assemblages have been widely used as a proxy for past environmental, and to some extent palaeo-sea-level reconstructions, as they can be preserved under certain conditions for long periods of time, acting as an archive reflecting former depositional environments (Edwards et al., 2004a; Edwards and Horton, 2000; Gehrels, 2000, 2002; Horton et al., 1999a; Horton and Edwards, 2003, 2006; Leorri et al., 2008a, 2010; Wright et al., 2011). Microfossil assemblages in cores can be correlated with modern foraminiferal assemblages to establish environmental conditions at the time of deposition. The application of spatial assemblages to microfossil assemblages provides an opportunity to explore environmental conditions of the past in relation to former sea levels, which can provide crucial information for understanding how coastal wetlands may respond to future sea-level rise (SLR).

The use of benthic foraminiferal assemblages for palaeo-environmental reconstructions is based on the understanding that foraminifera that were once living, died and were buried *in situ* as sediments accumulated (Gehrels et al., 2008; Gehrels and Newman, 2004; Haslett et al., 2010; Hayward et al., 1999b; Horton and Edwards, 2006). The distribution of foraminiferal microfossil assemblages in sediment cores can be used as a proxy for palaeo-wetland surface elevation. The

aim of this chapter was to reconstruct the environmental conditions and palaeo-wetland surface elevations over the past few millennia using a foraminifera-based regional training set. This was achieved by;

i. Identifying the stratigraphical distribution of foraminifera microfossils in sediment cores;
ii. Evaluating stratigraphical patterns of change and chronology of the cores;
iii. Correlating foraminifera microfossil assemblages with the regional training set using the modern training set;
iv. Reconstructing past environmental conditions using benthic foraminiferal assemblages.

As this chapter will reconstruct past environmental conditions using benthic foraminiferal assemblages, the literature review addresses the capability of foraminiferal assemblages in palaeo-environmental reconstructions. Stratigraphical distribution of benthic assemblages was identified in each core. Substrate properties, such as organic matter and grain size, and radiocarbon ages of the organic materials dated from the cores are discussed next. The microfossil assemblages were correlated with the regional training set using cluster analysis and transfer function models before reconstructing the past environmental conditions in coastal wetlands of the region.

6.2. Literature Review

6.2.1. Benthic foraminiferal assemblages: a proxy for palaeo-reconstructions

Preliminary studies have been undertaken in different environments around the Australian coast, such as estuaries (Albani, 1978; Dean and De Deckker, 2013; Strotz, 2003, 2015, 2012; Wang and Chappell, 2001; Yassini and Jones, 1995), tropical subtidal and intertidal zones (Haslett, 2001; Horton et al., 2003, 2007;

Woodroffe et al., 2005; Woodroffe, 2009b), temperate coastal wetlands (Haslett et al., 2010), and temperate saltmarshes (Callard et al., 2011; Gehrels et al., 2012) that have shown that benthic foraminiferal assemblages are representative of the environmental conditions they occur in. In coastal margins, foraminifera exhibit a lateral zonation with respect to the tidal frame in coastal wetlands as established in Chapter 5, subsurface foraminifera are representative of modern assemblages.

However, palaeo-environmental reconstructions using benthic foraminifera are based on a few assumptions. One is that foraminifera lived and died *in situ* and formed part of the sedimentary sequence in which they were found represents the elevation gradient in the modern intertidal environment (Gehrels et al., 2008; Gehrels and Newman, 2004; Haslett et al., 2010; Hayward et al., 1999b). A second assumption is that elevation remains the dominant control on species distribution. In this case other environmental variables, such as salinity, pH, temperature and substrate properties do not exert any strong influence on their distribution through time (Barlow et al., 2013; Birks, 1995; Horton and Edwards, 2006). The relationship between surficial foraminiferal assemblages and elevation above mean sea level demonstrates that they are viable palaeo-ecological indicators in this region. Sheltered coastlines, such as wave-dominated barrier estuaries provide protection from species redistribution by tidal waves. However, multiple unknown factors post-deposition taphonomic processes can misrepresent depositional environments affecting the interpretation of past environmental conditions.

6.2.2. Taphonomy of foraminifera microfossils in coastal wetlands

Post-deposition, foraminiferal distribution in coastal wetland sediments can be modified by bioturbation (de Rijk and Troelstra, 1999) and predation (Murray, 2006). Belowground substrate processes, such as fragmentation and abrasion, corrosion due to dissolution, bioerosion (removal of calcium carbonate from calcareous test walls due to biological processes or by other organisms living in the

same area), and encrustation (deposition of a crust or hard coating on the surface) of tests usually occur in the taphonomically active zone, an interval in the sediment profile where post-mortem alteration of organisms takes place (Berkeley et al., 2007; Gordillo et al., 2014; Hayward et al., 2015). High concentration of carbonic acid in sediment pore-water can make ground water acidic (pH less than 7.5 (Hayward et al., 2004a; Woodroffe et al., 2005) and trigger dissolution of calcareous tests (Berkeley et al., 2007; Geslin et al., 2011; Goldstein and Watkins, 1999; Hayward et al., 2015, 2004a, 2002). Under stable sea-level conditions, humic acids derived from decomposing organic materials can also create acidic conditions in belowground sediments (Berkeley et al., 2007; de Rijk and Troelstra, 1997; Horton et al., 2003, 1999a).

Agglutinated taxa are not particularly affected by organic matter concentrations; however, high oxidation rates promoted by aerobic mineralization of sediments particularly during the dry season can lead to poor preservation of agglutinated species in sediment cores (Berkeley et al., 2009, 2007; Woodroffe, 2009b). Some agglutinated species, such as *Pseudothurammina limnetis* and *Ammotium salsum* do not preserve well because the test walls of these organisms are loosely cemented with poorly sorted grains (Berkeley et al., 2007; Goldstein and Watkins, 1999) and so oxidation and bacterial activities can easily disintegrate their test wall (de Rijk and Troelstra, 1999). A few agglutinated foraminifera have been found to sustain to sustain extreme climatic conditions and preserve well in the sediments include *Entzia macrescens* (former *Jadammina macrescens* and *Trochammina inflata macrescens* (Hayward, 1993)), *Trochammina inflata*, *Haplophragmoides manilaensis*, *Balticammina pseudomacrescens*, *Tiphotrocha comprimata* and *Arenoparella mexicana* (de Rijk and Troelstra, 1999).

Poor preservation of tests can lead to inaccurate species identification and result in incorrect interpretations of past environmental conditions. As processes occurring in the sediment-water interface zone can cause tests to disintegrate, only the most resilient tests are preserved and identifiable. In intertidal wetlands, calcareous

taxa may be removed by dissolution, while agglutinated species may be destroyed through bacterial degradation of their test walls (Goldstein and Watkins, 1999). In tropical regions of Australia, only calcareous microfossil assemblages have been used in sea-level reconstructions because of the lack of agglutinated tests in sediment cores (Woodroffe, 2009b). Woodroffe (2009b) demonstrated that calcareous foraminiferal assemblages were able to tolerate a wide range of environmental conditions at lower intertidal and subtidal tropical climate. In temperate intertidal coastlines of other regions, agglutinated saltmarsh foraminifera proved better sea-level indicators (Horton and Edwards, 2006; Scott and Medioli, 1978).

6.2.3. Holocene reconstructions using foraminifera

Approaches

Several techniques have been used to reconstruct palaeo-environments using foraminiferal assemblages. Cluster analysis is one of the most commonly used multivariate analysis technique that is used to categorise species associations into groups/clusters along an environmental gradient (Dean and De Deckker, 2013; Gehrels, 1999; Haslett et al., 2010). Alternatively, transfer function models use empirically derived equations that characterise spatial relationships with respect to a specified variable, such as surface elevation, pH, temperature and/or salinity (Birks, 1995). A few studies around the NE coastline of Australia (Horton et al., 2007, 2003; Woodroffe, 2009a, 2009b) and Tasmania (Callard et al., 2011; Gehrels et al., 2012) have used foraminifera-based transfer functions to reconstruct palaeo-sea-levels.

Foraminifera-based transfer function models have been widely used as a proxy for past environmental reconstructions in coastal wetlands of UK, US and Europe (Edwards et al., 2004a; Edwards and Horton, 2000; Gehrels, 2000, 2002; Horton et al., 1999a; Horton and Edwards, 2003, 2006; Leorri et al., 2008a, 2010; Wright et

al., 2011), but they have not been extensively applied in Australia. Foraminifera-based transfer functions became popular in relative sea-level reconstructions (Edwards, 2001; Edwards et al., 2004a; Gehrels, 2000, 1999; Horton et al., 1999a; Horton and Edwards, 2006) following their adoption to evaluate the magnitude of earthquake-induced coseismic subsidence and tsunami waves (Guilbault et al., 1995; Shennan et al., 1998, 1996). Transfer functions models works best in regions that has evidence of relative sea-level change. It uses empirically derived equations from palaeontological data to quantitatively estimate past environmental parameters such as pH, temperature and salinity in a range of palaeoecological studies (Birks, 1995). Transfer functions are most reliable when they are based on contemporary empirical data collected from a known vertical range within a region. Samples beyond the sampling range cannot be extrapolated in transfer functions and prove problematic interpreting the model.

The elevation gradients of assemblages relative to the localised tidal datum has been the most commonly used environmental variable, which is a proxy for tidal inundation frequency (Horton and Edwards, 2006; Scott and Medioli, 1978), from which palaeo sea-levels can be reconstructed (Gehrels, 2000; Horton et al., 1999a; Horton and Edwards, 2003, 2006; Woodroffe, 2009b). However, as tides propagate across a wetland surface, the vegetation (Mazda et al., 1997; Zhang et al., 2012) and/or substrate type exerts a drag force counter to the direction of flow reducing the tidal prism. Tides can cause composition of species to become increasingly disconnected from elevation.

Over the past decade, there has been some discussion whether datasets standardised at a regional scale or local modern datasets are more appropriate for developing the transfer function for more robust palaeo-sea-level reconstructions (Allen and Haslett, 2002; Horton et al., 1999b; Horton and Edwards, 2006; Leorri et al., 2010). It should be noted that surficial sample elevation is not an ecological parameter that defines the spatial distribution of foraminifera, but it is a proxy for the inundation frequency in intertidal wetlands that has been largely recognised to

have an influence on species distribution (Horton et al., 1999a; Horton and Edwards, 2006; Scott and Medioli, 1978). Other variables such as salinity, pH or oxygen availability (de Rijk, 1995; de Rijk and Troelstra, 1997; Hayward et al., 2004b; Kemp et al., 2009) should also be considered in the transfer function to make the model robust as edaphic factors are delimited by the inundation regime of intertidal wetlands.

From an ecological perspective, transfer functions cannot be interchanged between two different regions (Allen and Haslett, 2002; Gehrels, 2000; Horton et al., 1999a) as faunal composition varies in different geomorphological settings particularly due to site-specific environmental variations. For example, tidal attenuation in different geomorphologic settings varies between macrotidal to microtidal intertidal environments of estuaries and coastal margins. Variation in the size of the intertidal zone will alter the tidal range in which foraminiferal distribution would occur with a greater tidal range for the tropical macrotidal deltas and estuaries (Horton and Edwards, 2006; Wang and Chappell, 2001; Woodroffe et al., 2005), and lesser for the microtidal settings (Callard et al., 2011; Haslett et al., 2010; Southall et al., 2006). The transfer function model assumes that the relationship between different environmental variables remains constant through time (Horton et al., 2003, 1999a).

Stratigraphical and chronostratigraphic data could complement benthic foraminiferal assemblages increase the resolution palaeo-sea-level reconstructions (Horton and Edwards, 2006; Shennan and Horton, 2002). Chrono-stratigraphical ages could be established through radiometric dating techniques, such as radiocarbon (^{14}C) and 210-lead dating (^{210}Pb), and caesium (^{137}Cs) concentrations, trace metals, pollen and charcoal analyses of datable materials (Gehrels et al., 2012, 2008; Gehrels and Woodworth, 2013). Sea-level reconstructions, particularly over the Holocene, can also be improved by using multiple indicators, such as diatoms, pollen, testate amoebae (Gehrels et al., 2001).

Case studies

Benthic foraminiferal assemblages have been used to reconstruct past environmental conditions at Minnamurra River, in SE Australia (Haslett et al., 2010). Modern assemblages were defined into four elevation-related depositional environments; saltmarsh, mangrove, mangrove pneumatophore zone, and unvegetated tidal flat. Agglutinated *Trochammina inflata* was most abundant in saltmarsh vegetation, whereas calcareous taxa of *Ammonia* and *Cribrononion* spp. were more dominant in mangrove and mangrove pneumatophore zone. In the study, species distribution pattern with respect to wetland elevation and vegetation zones was presumed to be consistent with sediment accumulation rates. Integrating this information with radiocarbon ages (marine shells), geomorphological evolution of Minnamurra River was reconstructed in the context of Holocene SLR. Foraminiferal assemblages down core showed that between 7365 – 6889 cal BP was a marine transgressive phase that drowned the upper floodplains of the River into a subtidal setting, which later converted into a drowned river valley during the mid-Holocene high-stand. The transition was evident from the high population of calcareous *Elphidium* spp. in the cores (a common shallow-water species (Cann et al., 1988, 1993; Hayward et al., 1999b)). The increasing diversity of other calcareous species such as *Ammonia beccarii* and *Cribrononion* spp. suggested progradation of the barrier at the entrance that progressively restricted marine influence and tidal access into the basin and the drowned river valley switched back to unvegetated tidal flat. Palaeo-environmental reconstructions by Haslett et al. (2010) using foraminifera was consistent with the five stage evolutionary model reconstructed by Panayotou et al. (2007) and the Roy et al. (2001) model of barrier-estuary evolution.

The distribution of benthic foraminiferal assemblages (and molluscs) in intertidal wetlands of Waitemata Harbour in New Zealand coincided with two major human colonisation events in New Zealand (Hayward et al., 2004a). The first occurred approximately AD 1300 with the arrival of humans, and the second major change

occurred during the early European settlement, *circa* 1840 to 1900. The change in foraminiferal species in sediment cores was attributed to decreasing salinity and low pH conditions, where calcareous-rich *Ammonia* spp. was replaced by agglutinated *Textularia–Schlerochorella* and *Miliammina–Haplophragmoides* associations. This occurred as a result of increased freshwater runoff associated with forest clearance by the early settlers and post European settlement.

Foraminifera-based transfer function models created from saltmarsh foraminifera could predict palaeo-sea-levels within an elevation range of ± 0.10 m in Tasmania (Callard et al., 2011), and ± 0.05 m in New Zealand (Southall et al., 2006). Relative sea-level records established from foraminifera-based transfer functions can be potentially compared with the short-term tidal gauge, and long-term geological records of past sea level (Gehrels et al., 2012, 2008; Gehrels and Woodworth, 2013; Horton and Edwards, 2006; Woodroffe, 2009b). Foraminifera-based testing models and transfer functions were used to reconstruct the Holocene sea-level curve for Queensland in two separate studies based on subtidal (Horton et al., 2007), and intertidal (Woodroffe, 2009a) foraminiferal assemblages. The earlier study showed that sea levels increased over the Holocene and were at about 8.86 ± 4.5 m below AHD between 9300–8600 cal BP, when increased to 1.72 ± 3.9 m above AHD around mid-Holocene high-stand (6900 – 6400 cal BP). The later study showed an approximate sea-level high stand of about 2.8 m above present levels occurred 5000 cal BP after which it remained relatively stable until 2300 cal BP before falling to present levels.

Sedimentary records from saltmarsh cores, comprising foraminiferal analysis, radiometric dating techniques, pollen analyses, and charcoal concentrations were used to reconstruct sea-level records for the Southwest Pacific region, including Tasmania and New Zealand. Gehrels et al. (2008) showed that between AD 1500 and AD 1900 sea level was increasing only at about 0.3 ± 0.3 mm/y but has been increasing at relatively high rates of 2.8 ± 0.5 mm/y over the 20th century. Another study showed that the rate of SLR was highest in the first-half of the century 4.2 ±

0.1 mm/y between 1900 and 1950 but slowed down to 0.7 ± 0.6mm/y for the second half of the century (Gehrels et al., 2012).

6.3. Methods

6.3.1. Sample collection and study design

Core locations were selected within a range of vegetation communities, which were representative of different tidal positions across the upper intertidal frame. Foraminiferal analysis was carried out on a total of 11 cores from the four study areas, three each from Comerong Island, Cararma Inlet and Currambene Creek, and two from Minnamurra River (Fig. 6.1). These study areas exhibit distinct zonation between different vegetation communities, where mangrove dominate at lower elevations in the tidal frame and saltmarsh dominate at higher elevations (Fig. 1.1). Table 6.1 provides a list of the cores analysed, the vegetation communities and position in the upper intertidal.

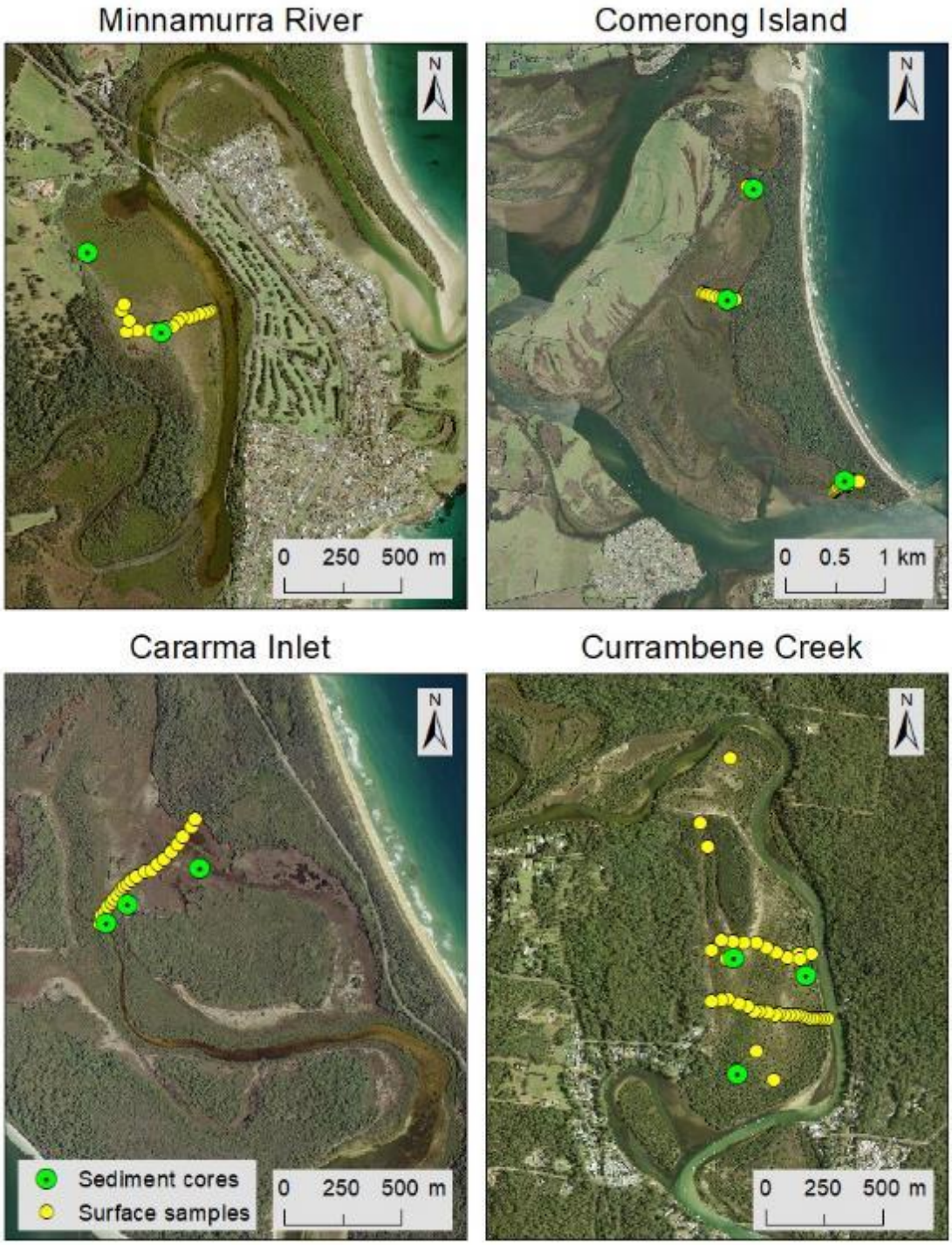

Figure 6.1: Location of sediment cores in relation to surficial samples from Minnamurra River, Comerong Island, Cararma Inlet and Currambene Creek.

Table 6.1: List of sediment cores from the four study areas that were analysed for palaeo-environmental reconstruction.

Site	Core ID	Core location		Elevation (m AHD)	Tidal position		
		Latitude	Longitude		Mid	Intermediate	High
Minnamurra River	*Min_Mg2	-34° 37' 29.64823"	150° 50' 35.60827"	0.255	*Avicennia marina* (tall)		
	Min_Spo2	-34° 37' 41.01710"	150° 50' 47.71864"	0.719			*Sporobolus virginicus*
Comerong Island	Cm_Mg1	-34° 53' 56.26328"	150° 45' 8.57648"	0.373	*Avicennia marina* (tall)		
	*Cm_Spo	-34° 52' 55.59732"	150° 44' 23.33251"	0.388		*Sporobolus virginicus*	
	*Cm_Dm	-34° 52' 18.98791"	150° 44' 35.10647"	0.463			*Avicennia marina* (shrub)
Cararma Inlet	Ca_Mg2	-34° 59' 14.44435"	150° 46' 15.42640"	0.475	*Avicennia marina* (tall)		
	Ca_Tect	-34° 59' 11.90732"	150° 46' 19.02223"	0.692			*Tecticornia arbuscula*
	Ca_Sar2	-34° 59' 7.09394"	150° 46' 31.36660"	0.794			*Sarcocornia quinqueflora*
Currambene Creek	*Cb_Mg	-35° 1' 9.43899"	150° 40' 1.61457"	0.319	*Avicennia marina* (tall)		
	Cb_Spo	-35° 0' 56.16607"	150° 40' 13.64072"	0.470		*Sporobolus virginicus*	
	*Cb_Sar2	-35° 0' 53.37560"	150° 40' 1.61934"	0.707			*Sarcocornia quinqueflora*

* ^{210}Pb dated cores

Cores were collected using the procedure described in Section 4.3.1. From each core, 2-cm subsamples were collected at approximately 10-cm intervals for foraminiferal analysis. The subsample depth size of 2-cm was based on the results from Chapter 5 (Section 5.3.1), which showed that samples of up to 2-cm depth provided an inclusive distribution of infaunal taxa for the regional training set. Based on the sediment characteristics of individual cores, additional samples were analysed at or near depths where a transition in sediment type was evident. Subsamples were placed into labelled bags and stored in the cold store at 4 °C until processing time.

Sample processing and identification

A known volume of subsample (approximately 20 – 30 cm^3) was processed and foraminifera were identified following the 'sample processing and identification' procedure in Section 5.3.2. Foraminifera count of 5 or less per subsample was treated as an anomaly and excluded from the data matrix. Stratigraphical data was represented in compaction-corrected depths (Section 4.3.1).

6.3.2. Sediment analysis and ^{14}C dating

Sediment analysis

Each subsample was analysed for organic matter content using the loss-on-ignition method, and sediment grain size using the Mastersizer-X following the method outlined in Section 5.3.4.

Radiocarbon dating

There were relatively few carbon materials available within cores for radiocarbon dating but, in some cores, materials such as marine shells, mangrove roots, and foraminifera were sent to radiocarbon dating facilities for dating. These materials were embedded in the sediment profile and considered *in situ* because they are found in a buried vertically in the sediment profile. From Cararma Inlet, shell and shell fragments from cores Ca_Mg2 and Ca_Sar2, and mangrove roots from Currambene Creek cores Cb_Mg and Cb_Sar2 were sent to the Australia National University (ANU) Radiocarbon Dating Centre, Canberra for dating (ANU Radiocarbon Dating Centre, 2010). Foraminifera test density was generally very low in all the cores but core Cm_Mg1 from Comerong Island had enough calcareous tests, and these were sent to the Beta Analytic Radiocarbon Dating Laboratory in Florida, USA for radiocarbon dating. The maps in Fig. 6.1 provide the location of cores from which materials were submitted for ^{14}C dating. A list of materials

submitted for ^{14}C dating is provided in Table 6.2.

Table 6.2: List of cores and materials submitted for radiocarbon dating. Location of the cores provided in Table 6.1.

Core	Surface vegetation	material dated	sample depth range (cm)	sample mid-depth (cm)
Cm_Mg1	Mangrove	Calcareous foraminifera	140-142	141
Ca_Mg2	Mangrove	marine shell fragment (*Katelysia rhytiphora*)	78-80	79
Ca_Sar2	Saltmarsh	marine shell (*Cacozeliana granarium*)	111	111
Cb_Sar2	Saltmarsh	Mangrove root	83-90	86.5
Cb_Mg	Mangrove	Mangrove root	126-131	128.5

The shell and root materials were collected, labelled and submitted for radiocarbon dating (Fig. 6.2). At the ANU Radiocarbon Dating laboratory these samples were dated using the Accelerator Mass Spectrometry (AMS) method following the procedure outlined on the ANU radiocarbon laboratory website (2018). AMS dating is an advanced method of radiocarbon dating samples in comparison to the conventional radiometric dating method. The conventional method detects beta particles from the decay of carbon 14 atoms, while AMS count the number of carbon 14 atoms present in the sample. The AMS technique requires small sample size, takes less time and has a higher precision than radiometric techniques.

Calcareous foraminifera were picked from the processed (floated) samples and submitted for AMS dating using the method outlined on the Beta Analytic Inc. website (2018).

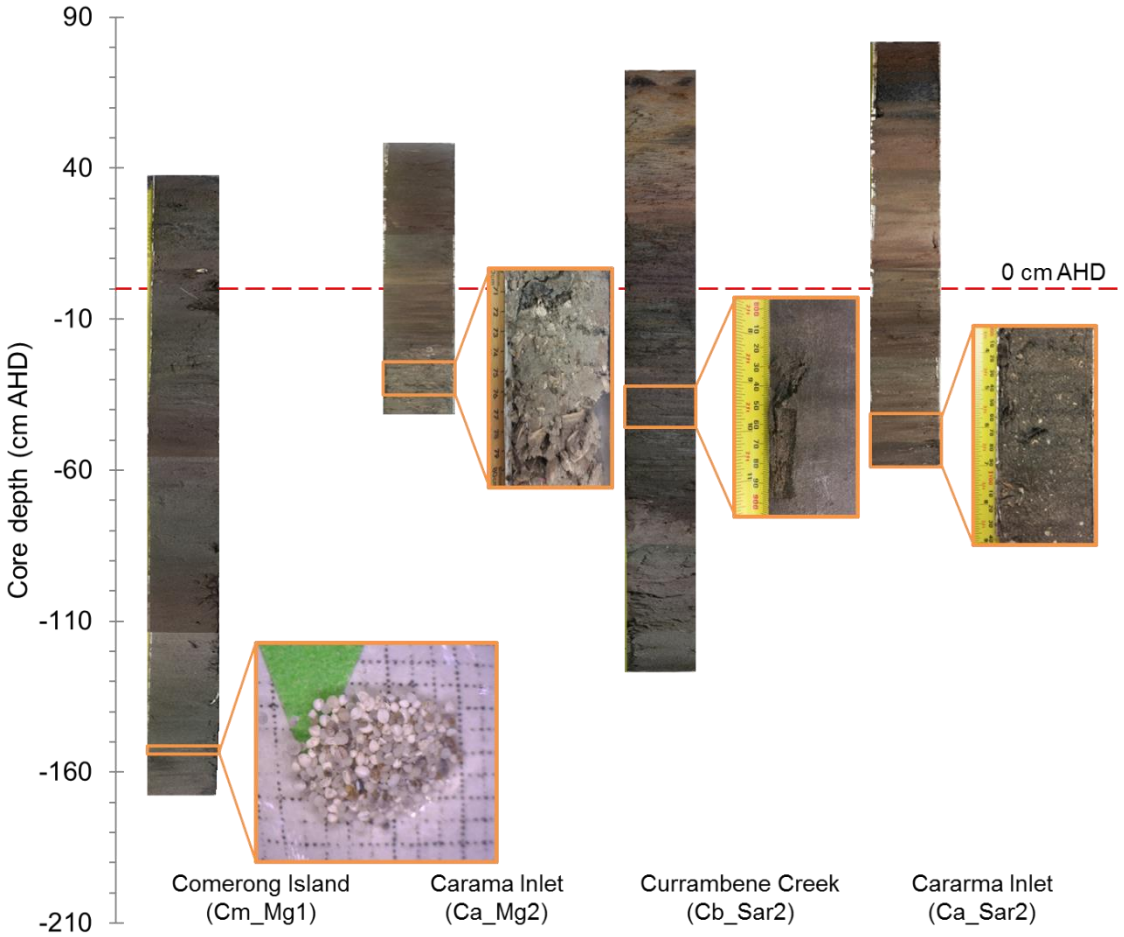

Figure 6.2: Cores from which materials (inset) that were radiocarbon dated.

All ^{14}C ages were calibrated using the southern hemisphere calibration SHCal13 curve (Hogg et al., 2013) using the program CALIB 7.10 (Stuiver et al., 2018). Radiocarbon age was based on 95.4 % confidence limits and presented as cal BP (calendar or calibrated years before present (present being 1950)). It is assumed that the materials that were ^{14}C dated were part of the stratigraphic sequence that they lived and died *in situ* and were subsequently buried with continued sediment accumulation. Hence, ^{14}C age of the materials provided an estimate time of death of the organism, which was used to infer the period over which sediment accumulated.

6.3.3. Stratigraphic microfossil assemblages

Stratigraphic microfossil associations or clusters were classified using the

constrained incremental sums of squares (CONISS) cluster analysis using the software Tilia, version 2.1.1 (Grimm, 1991), which stratigraphically-ordered foraminiferal microfossil assemblages in each core.

6.3.4. Palaeo-environmental reconstruction

Palaeo-environmental reconstruction using benthic foraminiferal assemblages in this study was done in two stages: (i) regional training set compilation from Chapter 5; and (ii) palaeo-environmental analysis based on two approaches that are independent approaches used by others; foraminifera-based cluster analysis (de Rijk and Troelstra, 1999; Gehrels, 1994; Haslett et al., 2010; Hayward et al., 1999a, 1999b), and foraminifera-based transfer function (Edwards et al., 2004a; Edwards and Horton, 2000; Gehrels, 2000; Horton et al., 1999a; Horton and Edwards, 2006; Scott and Medioli, 1978). Both these methods will be used to elucidate the palaeo-environmental story from foraminiferal microfossil assemblages.

Foraminifera-based cluster analysis

The stratigraphically-ordered microfossil associations in each core was averaged and transformed using square root (x + 1), which reduced overemphasis of non-dominant taxa or most the abundant taxa and homogenised the variance in the values and increased the importance of non-dominant species (Gehrels et al., 2001). Palaeo-environmental reconstruction was done by correlating the microfossil associations with the modern association using unconstrained cluster analysis based on unweighted Euclidean distance (UPGMA algorithm) in the palaeontological statistical software PAST, version 318 (Hammer et al., 2001).

Palaeo-wetland vegetation reconstruction was carried out through foraminifera-based cluster analysis. This was done by correlating the microfossil assemblages with regional training set foraminifera spatial clusters associations identified in

Section 5.3.6. The relative abundance of species from each microfossil cluster was averaged and transformed. Unconstrained cluster analysis based on unweighted Euclidean distance (UPGMA algorithm) was performed in the palaeontological statistical software PAST, version 318 (Hammer et al., 2001).

Transfer function

Foraminifera-based transfer function was used to determine palaeo-wetland surface elevation as surface elevation above the localised tidal datum, which is the Australian height datum (AHD) adjusted to mean sea level (MSL), in the form of STPI (Section 5.3.5). Elevation above MSL, a proxy for tidal inundation was categorised as the primary factor influencing the distribution and abundance of modern assemblages in the upper intertidal wetland environments. The axis gradient length of 3.46 determined from detrended canonical analysis (DCA in Fig. 5.17) indicated that a unimodal response model best describes the species distribution for the region (Section 5.3.6). Hence the WA-PLS regression was the preferred transfer function model for palaeo-wetland surface reconstruction. WA-PLS is one of the most preferred transfer functions as it effectively considers the influence of additional environmental variables and performs well with noisy, species-rich data that cover a long ecological gradient (>3 SD units) (ter Braak and Juggins, 1993). It utilises any structure present in the weighted averaging (WA) residuals, which would otherwise be discarded by the other models and least affected by autocorrelation (Mills et al., 2013).

Normally, the WA-PLS transfer function produces results for five components. The choice of component depended upon the prediction statistics that is root mean square error of prediction (RMSEP) and r^2. According to the principle of parsimony (choosing the simplest scientific explanation that fits the evidence) can be based on low prediction errors (RMSEP) and high r^2 which will provide an acceptable model that can be used for palaeo-environmental reconstruction (Horton et al., 2007, 1999a; Horton and Edwards, 2006; Leorri et al., 2008b; Mills et al., 2013;

Wright et al., 2011).

Component 2 of WA-PLS was selected as it demonstrated a relatively strong relationship between observed and foraminiferal-predicted upper intertidal wetland elevation, which demonstrated a relatively strong relationship between observed and predicted foraminifera in the upper intertidal surface elevation (r^2_{jack} = 0.443) and wetland surface elevation with a vertical error of typically 0.201 m or less based on $RMSEP_{jack}$ of 0.201 (Section 5.3.6). Depending on the composition of the fossil assemblages, RMSEP for an environmental variable in the past can vary from sample to sample.

WA-PLS model used the average distribution of taxa along the standardised tidal position index (STPI, the environmental gradient of choice), weighted by their abundance, to estimate the microfossil surface elevations. For this reason WA-PLS is generally considered 'simple, robust and widely used' transfer function approach (Horton and Edwards, 2006; Leorri et al., 2008b; ter Braak and Juggins, 1993). The WA-PLS technique was performed in the palaeo-environmental program, C2 version 1.7.7 (Juggins, 2016). The standard error of prediction (SEP) and an estimate of STPI range of individual subsamples was determined using bootstrapping cross-validation in C2 program, which provided. Palaeo-wetland surface elevation relative to AHD was back calculated from STPI in Eq. 5.1 as palaeo-environmental reconstruction was all about wetland elevation in the tidal frame.

6.4. Results

6.4.1. Stratigraphical distribution of foraminifera microfossils

Ten new genera of foraminifera were identified in core sediments that were not encountered in the modern training set in Chapter 5 (Table 6.3). These foraminifera were mainly calcareous (except for *Textularia* spp.) and are typically

found in shallow intertidal to subtidal settings (Yassini and Jones, 1995). Nine of the ten genera were found only in core Cm_Mg1 from Comerong Island, in which one type of planktonic foraminifer belonging to the genus *Globigerina* was also encountered in three sub-surface samples ranging between 126 and 167 cm below AHD.

Table 6.3: Additional genera (numbered in the table below) of foraminifera identified in the core sediments.

Type		Genus and/or species
Benthic	1	*Cibicidoides* spp. (Thalmann, 1939)
	2	*Conorbella pulvinata* (Brady, 1884)
	3	*Cribrononion simplex* (Cushman, 1933)
	4	*Favulina hexagona* (Williamson, 1848)
	5	*Guttulina* spp. (d'Orbigny, 1839) *Guttulina subelliptica* (Galloway and Wissler, 1927)
	6	*Parrelina* spp. (Carter, 1958) *Parrelina imperatrix* (Brady, 1881) *Parrelina verriculata* (Brady, 1881) *Parrelina hispidula* (Cushman, 1936) accepted as *Elphidium hispidulum* (Cushman, 1936)
	7	*Sigmoidella* sp. (Cushman & Ozawa, 1928)
	8	*Spiroloculina* spp. (d'Orbigny, 1826)
	9	*Triloculina* spp. (d'Orbigny, 1826) *Triloculina oblonga* (Montagu, 1803) *Triloculina trigonula* (Lamarck, 1804)
	10	*Trochulina dimidiata* accepted as *Lamellodiscorbis dimidiatus* (Jones & Parker, 1862)
		Elphidium crispum (Linnaeus, 1758) *Elphidium macellum* (Fichtel & Moll, 1798) *Elphidium jenseni* accepted as *Elphidium fichtelianum* (d'Orbigny, 1846)
		Quinqueloculina incisa (Vella, 1957)
		Textularia candeiana (d'Orbigny, 1839) *Textularia pseudogramen* (Chapman & Parr, 1937)
Planktonic	1	*Globigerina* spp. (d'Orbigny, 1826) *Globigerina bulloides* (d'Orbigny, 1826)

All the sediment cores show a pattern in the distribution and abundance of species in the core profiles, where the upper-most foraminiferal assemblages (top 10 to 20 cm sediments) correspond to current upper intertidal vegetation. *Trochammina inflata* was found in all the cores, whilst *Entzia macrescens*, *Tritaxis conica*, *Ammobaculites* spp. and *Miliammina fusca* were also encountered at a high

frequency in the sediment cores. *T. conica* was present in relatively high abundance in most of the cores except for Ca_Mg2 and Ca_Sar2 from Cararma Inlet but was found in the saltmarsh *Tecticornia arbuscula* (Ca_Tect) core, even though *T. conica* was not encountered in any of the surficial samples from Cararma Inlet. A few other species such as *Arenoparella mexicana* and *Haplophragmoides wilberti* were not found in the modern samples at Cararma Inlet but were found in sediment cores. Likewise, *Miliammina obliqua* was not encountered in any of the modern samples from Minnamurra River but it occurred in relatively high abundance in core Min_Spo2. This shows that species occurrence in modern samples was not consistent between sites and further reinforces the need to pool data from individual study sites into a regional training set. Regional training set also included tests that only occurred in mudflats and/or lower intertidal zones because these settings are no longer part of most mature eateries, such as Cararma Inlet and Minnamurra River.

6.4.2. Stratigraphic patterns of change and chronology

Sediment composition in the cores was mainly sandy, except for the mangrove core from Minnamurra River (Fig. 6.3) and mangrove and saltmarsh (Ca_Sar2) cores from Cararma Inlet (Fig. 6.4). These cores had a high percentage of mud (silt and clay) in the active root zone, top 15 to 30-cm below the surface. Substrate organic matter content varied between 20 and 38 % in the fine-grained muddy sediments of these cores. In the rest of the cores, substrate organic content range between 2 to 8 % in sandy sediments. Overall, organic matter content decreased with increasing substrate grainsize, and organic-rich mud was found in mangrove cores and some saltmarsh cores, indicating a time of prolific mangrove growth.

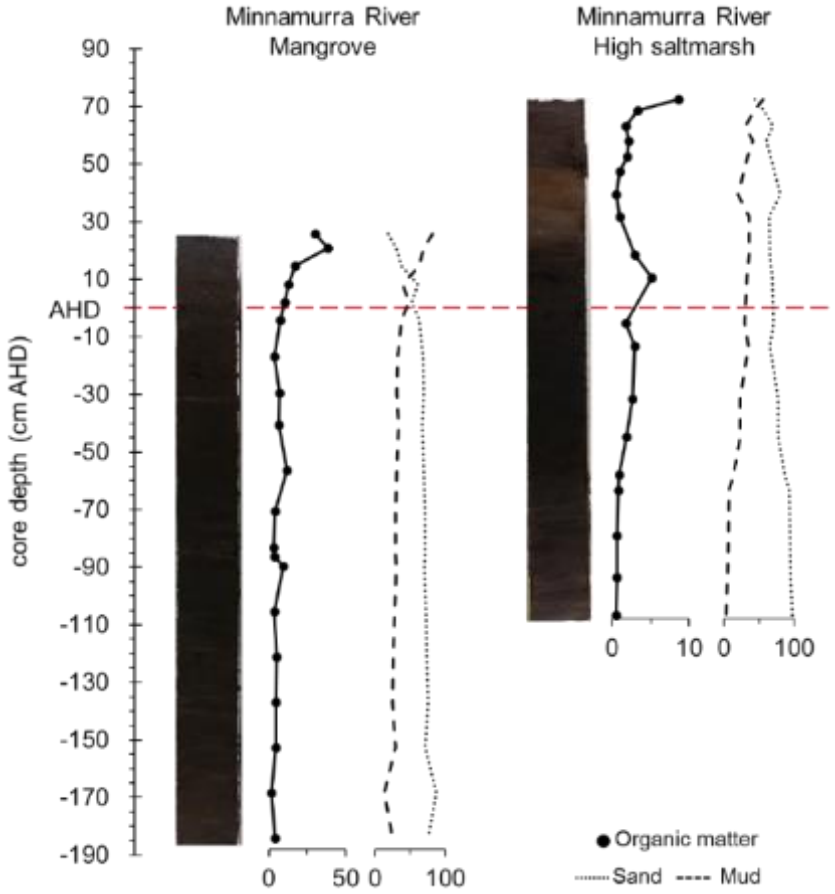

Figure 6.3: Photographs of Minnamurra River mangrove (Min_Mg2) and high saltmarsh (Min_Spo2) cores and their stratigraphic composition. Stratigraphic log of all the cores are provided in Appendix 5.

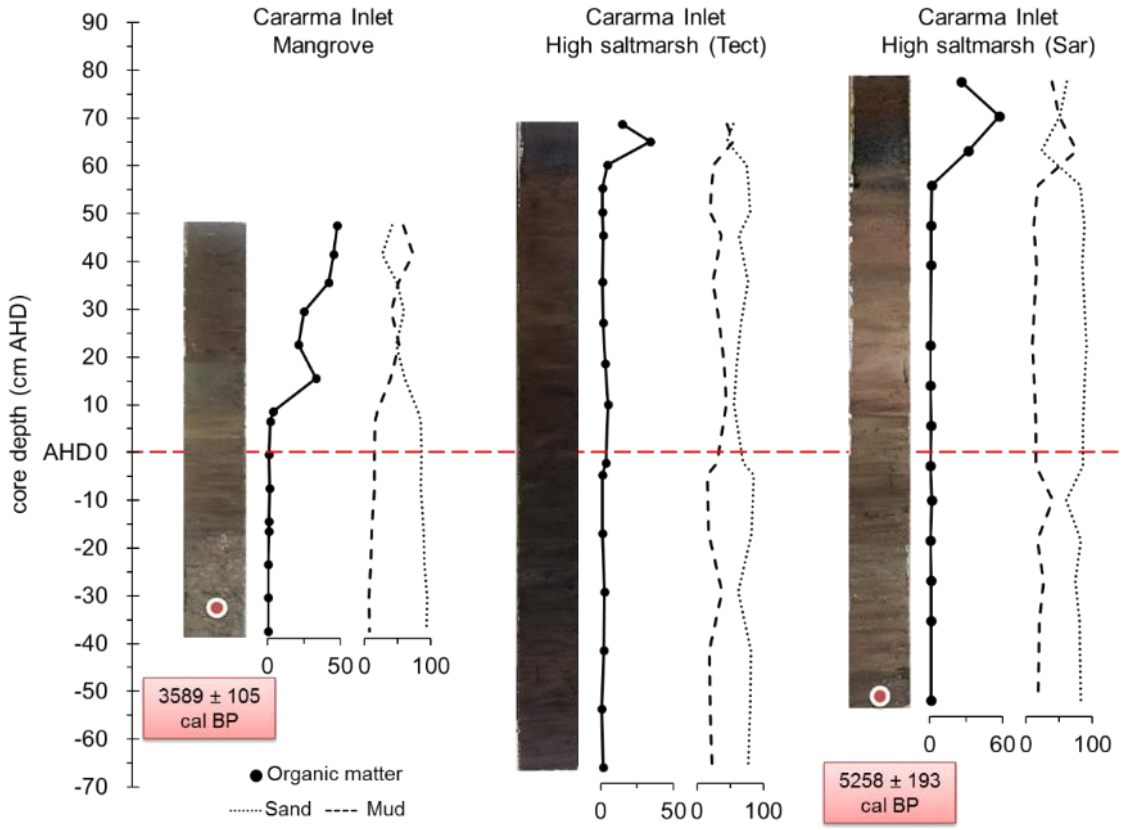

Figure 6.4: Photographs of Cararma Inlet mangrove core (Ca_Mg2), and high saltmarsh cores (Ca_Tect and Ca_Sar2) and their stratigraphic composition. Shells had an age of 3589 ± 105 cal BP 32 cm below AHD in the mangrove core and 5258 ± 193 cal BP 54 cm below AHD in the high saltmarsh core (Sar2). Stratigraphic log of all the cores are provided in Appendix 5.

The variability in organic matter content and sediment grainsize in all the sediment cores including cores from Comerong Island (Fig. 6.5) and Currambene Creek (Fig. 6.6) suggest that these landscapes are dynamic and has experienced constant change. However, there is some variable stratigraphy observable in the cores. All the cores are generally sandy. Muddy substrate corresponded to high organic matter content as observed in the mangrove cores of Comerong Island at about 70 cm below AHD (Fig. 6.5), and about 80 cm below AHD in the saltmarsh cores at Currambene Creek and at 110 cm below AHD in the mangrove core (Fig. 6.6). Organic matter additions were likely from the mangrove plants located lower in the tidal frame.

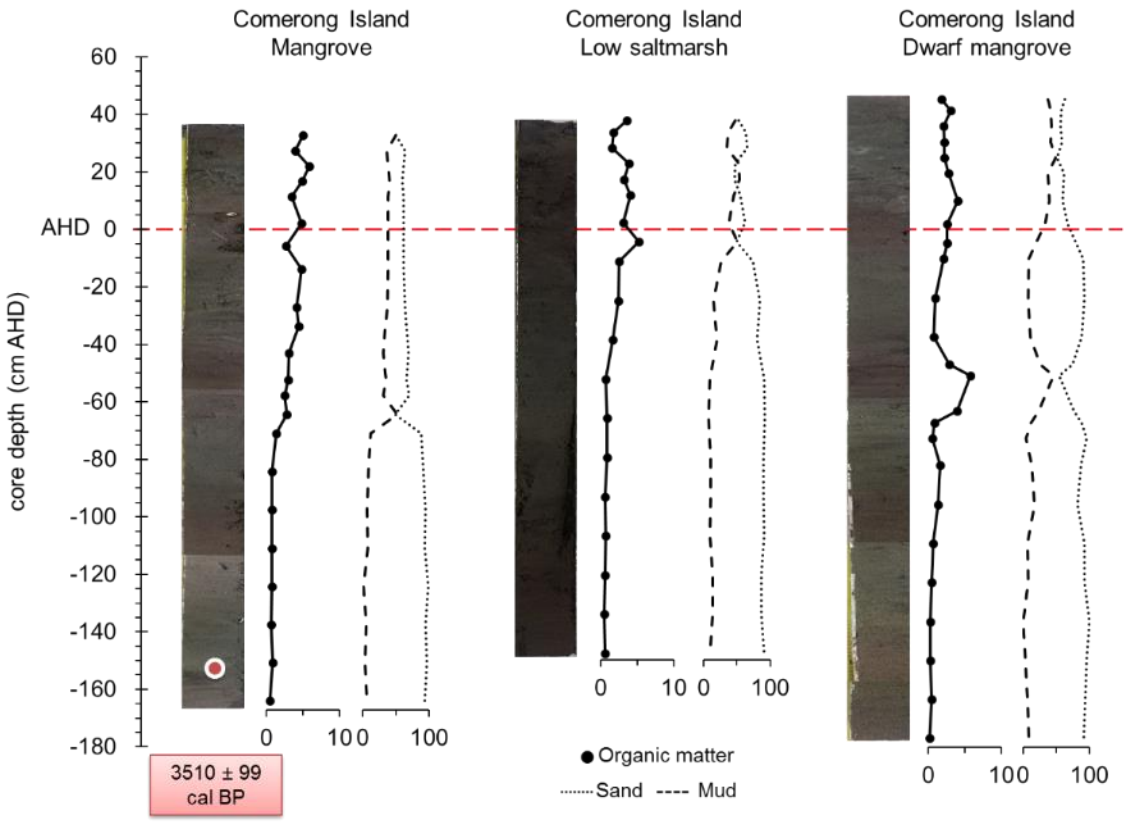

Figure 6.5: Photographs of Comerong Island mangrove (Cm_Mg1), low saltmarsh (Cm_Spo) and shrub mangrove (Cm_Dm) cores and their stratigraphic composition. Calcareous foraminifera 153 cm below AHD had an age of 3510 ± 99 cal BP. Stratigraphic log of all the cores are provided in Appendix 5.

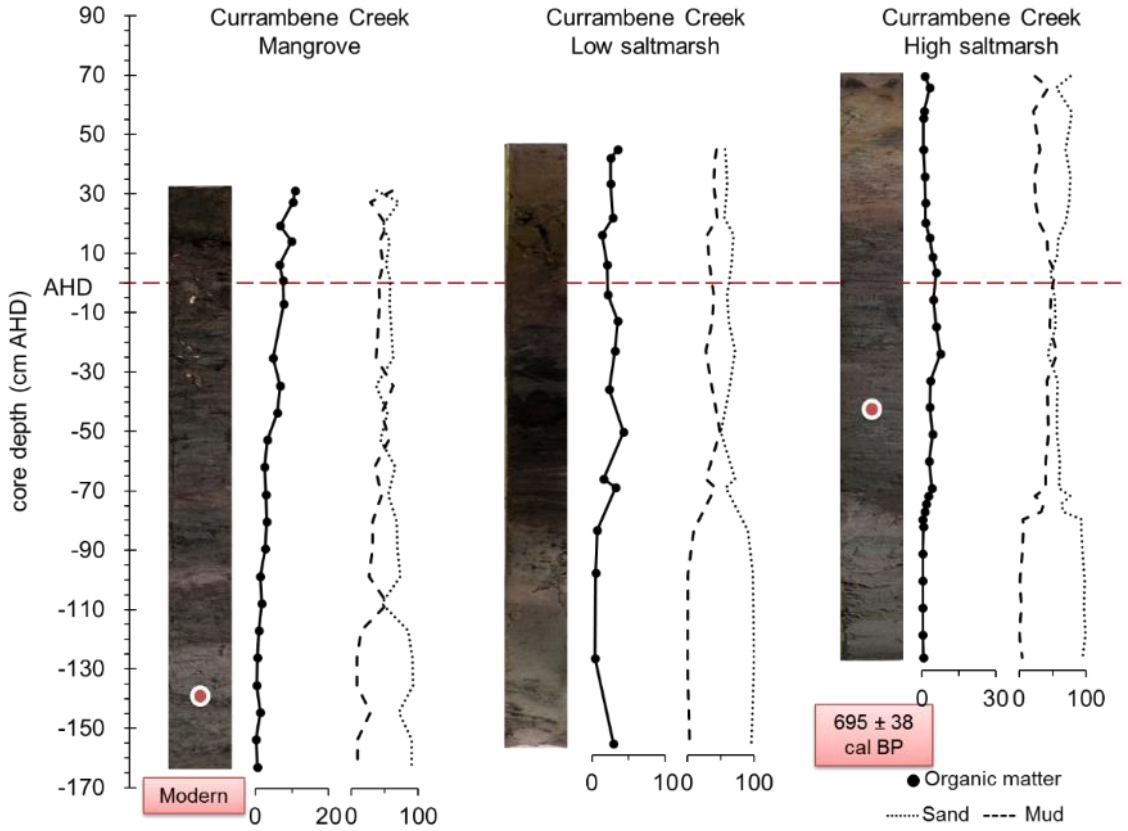

Figure 6.6: Photographs of Currambene Creek mangrove (Cb_Mg), low saltmarsh (Cb_Spo) and high saltmarsh (Cb_Sar2) cores and their stratigraphic composition. Mangrove roots had a modern age 137 cm below AHD in the mangrove core and 695 ± 38 cal BP 42 cm below AHD in the high saltmarsh core. Stratigraphic log of all the cores are provided in Appendix 5.

An age of 5258 ± 193 cal BP was determined on *Cacozeliana granarium*, while the *Katelysia rhytiphora* had an age of 3589 ± 105 cal BP (Table 6.4). The marine shells were found at shallow depths of 54 cm and 32 cm below AHD in mangrove and saltmarsh cores, respectively. *Cacozeliana granarium* is endemic to Australia and typically found in seagrass and sandy substrates in estuaries (Beechey, 2018). They have also been reported in moderately exposed coasts under rocks in silty situations. An age of 3510 ± 99 cal BP was determined on calcareous foraminifera from the Comerong Island 153 cm below AHD. The porcelaneous species, belonging to the genus *Triloculina* and *Quinqueloculina*, and hyaline tests of the genus *Cibicidoides*, *Ammonia* and *Elphidium* largely occur in shallow intertidal to subtidal settings (Debenay, 2012; Yassini and Jones, 1995).

Table 6.4: Radiocarbon age on the materials dated from the cores.

Core ID	Laboratory code	corrected specimen depth		$\delta^{13}C$	^{14}C age (yr BP)	Calibrated ^{14}C age (cal BP)
		cm below surface	cm below AHD			
Ca_Sar2	50026	133	54	6.93	4632 ± 27	5258 ± 193 (5065 – 5451)
Ca_Mg2	50025	79	32	5.13	3402 ± 27	3589 ± 105 (3484 – 3693)
Cm_Mg1	479350	191	153	0.8	3330 ± 30	3510 ± 99 (3411 – 3609)
Cb_Sar2	49416	113	42	-25.97	800 ± 33	695 ± 38 (657 – 733)
Cb_Mg	49418	169	137	-23.00	Modern	

The mangrove root age of 695 ± 38 cal BP from Currambene Creek saltmarsh core (Cb_Sar2) from shallow sediments 42 cm below AHD indicate that roots of older mangrove trees can remain embedded in the soil profile (Fig. 6.7). The modern mangrove root dates from the other two Currambene cores suggest that modern roots can penetrate deep into the substrate, in this case 169 cm to 188 cm below the wetland surface. The modern mangrove dates from the mangrove cores indicate that *Avicennia marina* roots can penetrate deep into the sediment profile, in this case up to 188 cm below the surface and about 166 cm below MSL. These dates thus did not provide a credible chronology for Currambene Creek. Nevertheless, the radiocarbon ages from the marine biogenic materials provide evidence that the sea level has been close to its present level throughout the late Holocene.

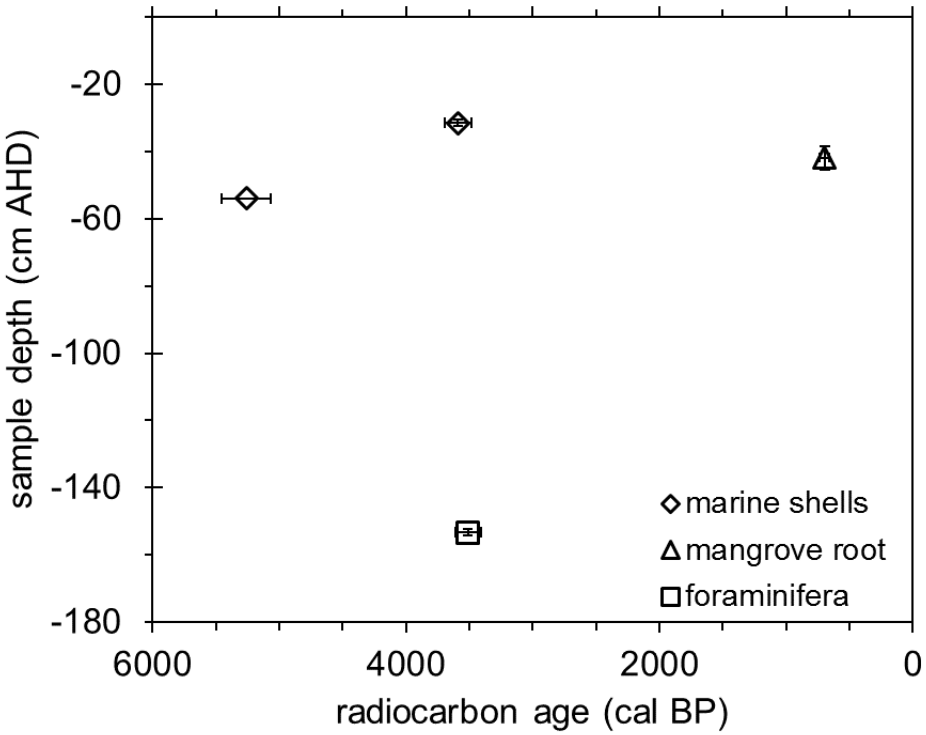

Figure 6.7: Radiocarbon age of the materials dated.

6.4.3. Relationship between microfossil assemblages and the regional training set

Microfossil assemblages from the cores corresponded to the regional training set; for example, the modern *Trochammina – Entzia* (A-I) association commonly found in high saltmarsh vegetation above MHW was encountered in the saltmarsh cores dominated by *Sporobolus virginicus* at Minnamurra River (Fig. 6.9), Comerong Island (Fig. 6.11) and Currambene Creek (Fig. 6.17). A similar association was also found in the shrub Comerong mangrove core (Fig. 6.12), and Cararma mangrove core (Fig. 6.13). Modern *Entzia – Trochammina* (A-II) association dominated in mixed to low saltmarsh vegetation was found in the Currambene saltmarsh core dominated by *Sarcocornia quinqueflora* (Fig. 6.18). The modern *Ammobaculites – Miliammina* (C-II) association mangrove to mixed vegetation was also found in the Comerong mangrove core (Fig. 6.10) and Currambene mangrove core (Fig. 6.16). In the other cores, the microfossil assemblages represented a few common modern species but not any specific association (Fig. 6.8, 6.14 and 6.15).

Tritaxis conica was present in relatively high abundance in the cores from Currambene Creek, Minnamurra River and Comerong Island, indicating an environmental setting not common to the vegetated upper intertidal zones of the region. In the regional training set however, low abundance of *T. conica* was found within an elevation range of -0.4 and 0.3 m AHD (weighted average of 0.001 ± 0.354 m, Fig. 5.18). The living tests (stained with the dye at the time of sample collection) represented the narrow mudflat zone at the channel edge comprising pneumatophores from the adjacent tall *Avicennia marina* and experiencing frequent inundation at Currambene Creek and Comerong Island. *T. conica* has been reported in coastal lagoons and intertidal zones of the inner shelf from coastal areas of south-eastern Australia (Yassini and Jones, 1995). In the previous study of the Minnamurra River Haslett et al (2010) found *T. conica* at elevations around mean tide levels in the mangrove pneumatophore zone. Strotz (2012) identified *T. conica* as *Portatrochammina sorosa* (Strotz, 2012, p. 373 Fig. 4 image 10, 11) in mean water depths of 0.4 m in St Georges Basin, NSW. The above literature from the region suggest that a change from *T. conica* to no *T. conica* suggest a transition from low intertidal and/or mudflat setting to present day mangrove and saltmarsh zones.

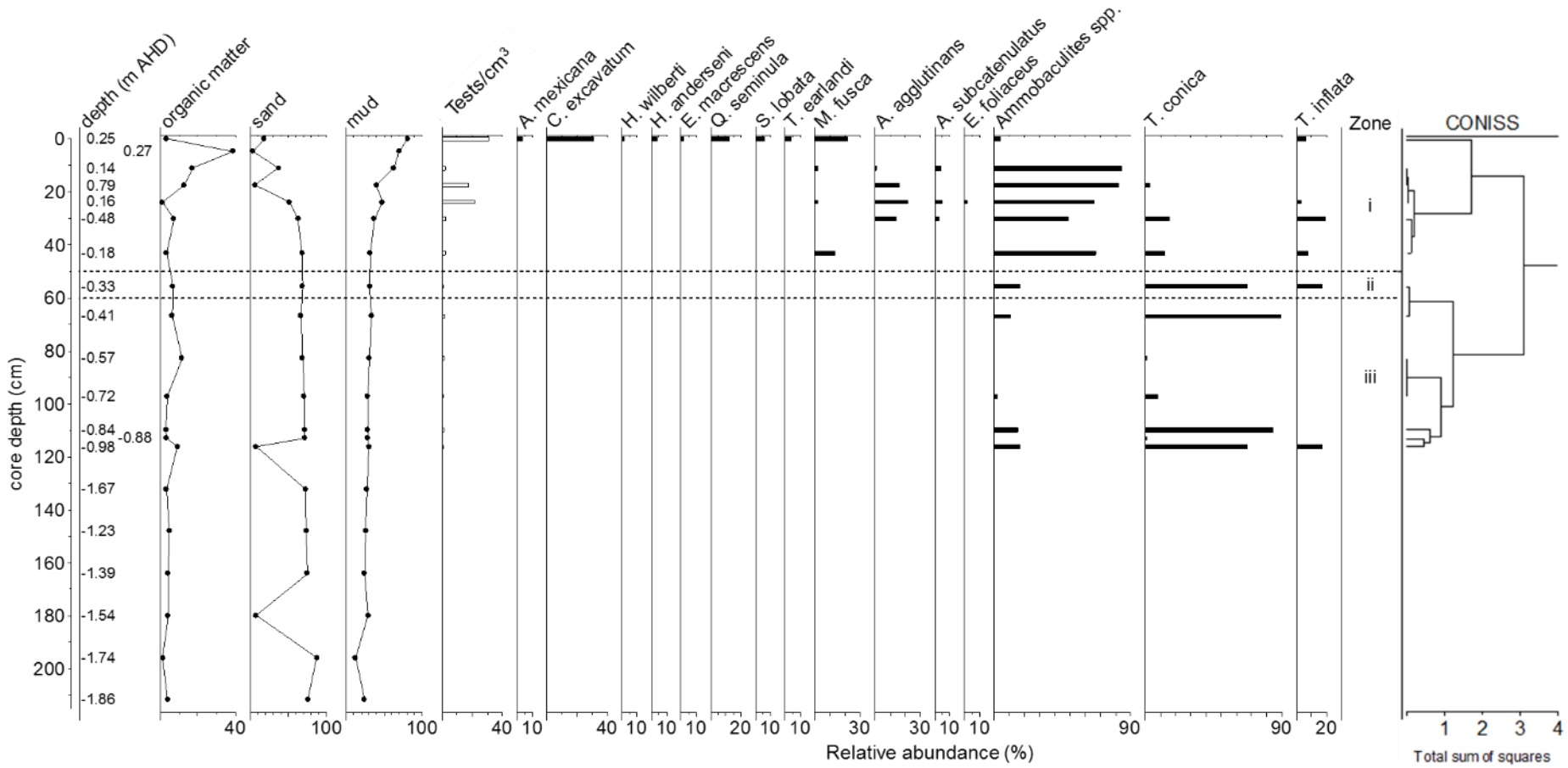

Figure 6.8: Depth constrained cluster analysis based on unweighted Euclidean distance (CONISS) of stratigraphical foraminiferal assemblages in Min_Mg2 dominated by *Avicennia marina*.

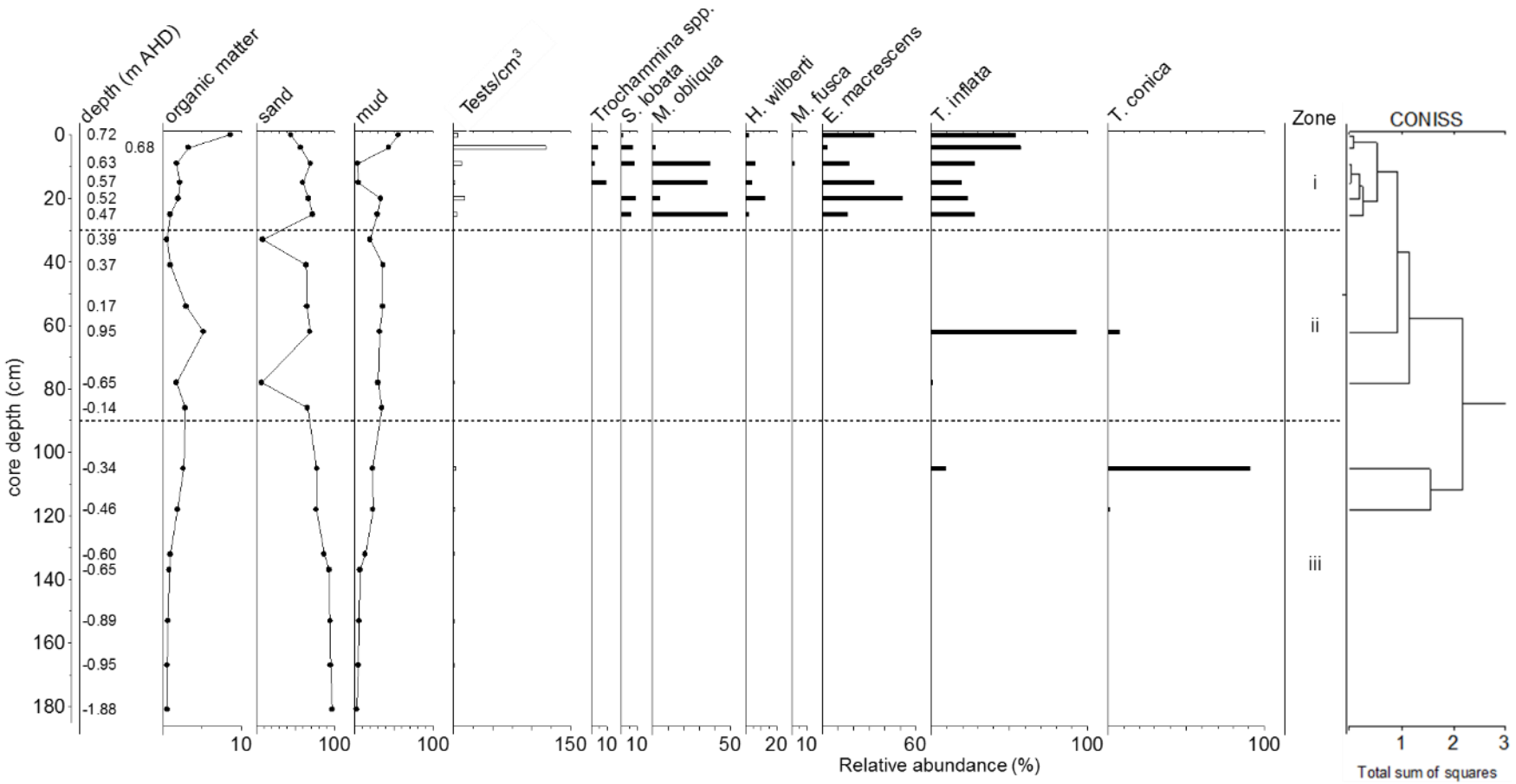

Figure 6.9: Depth constrained cluster analysis based on unweighted Euclidean distance (CONISS) of stratigraphical foraminiferal assemblages in Min_Spo2 dominated by *Sporobolus virginicus*.

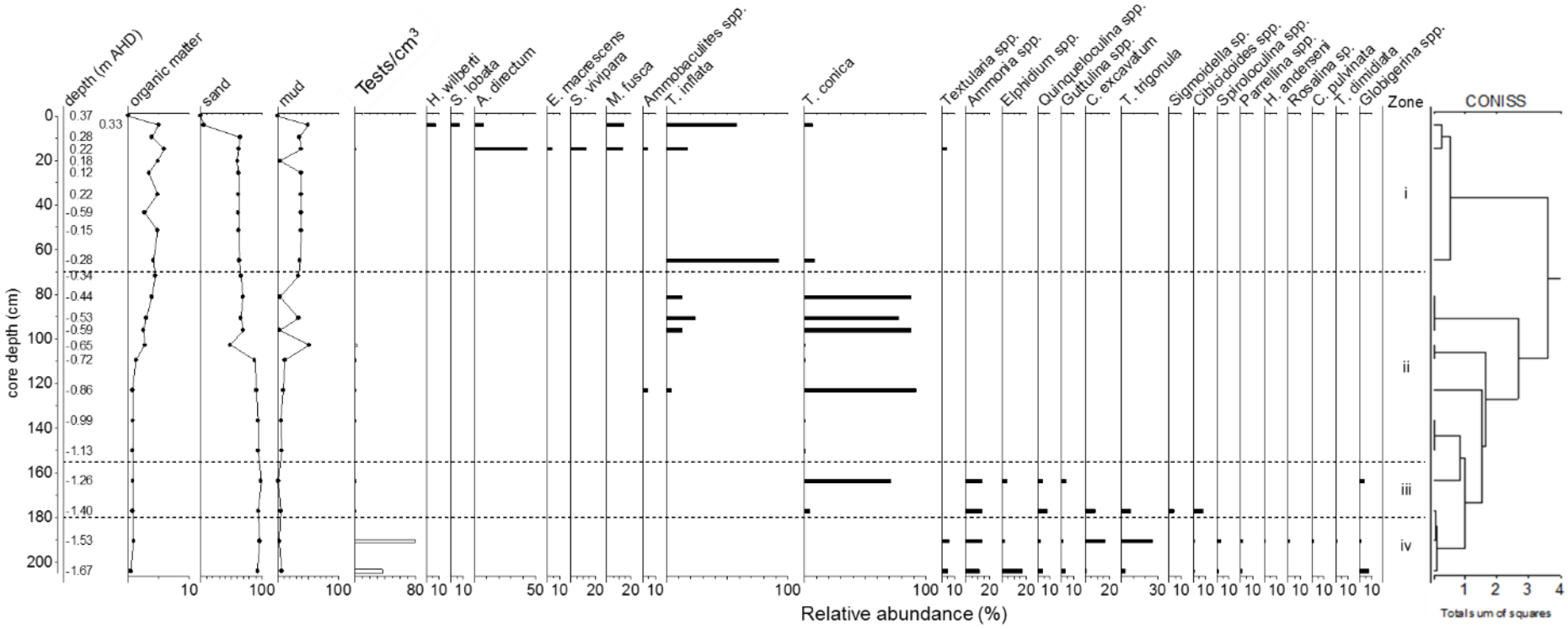

Figure 6.10: Depth constrained cluster analysis based on unweighted Euclidean distance (CONISS) of stratigraphical foraminiferal assemblages in Cm_Mg1 dominated by *Avicennia marina*.

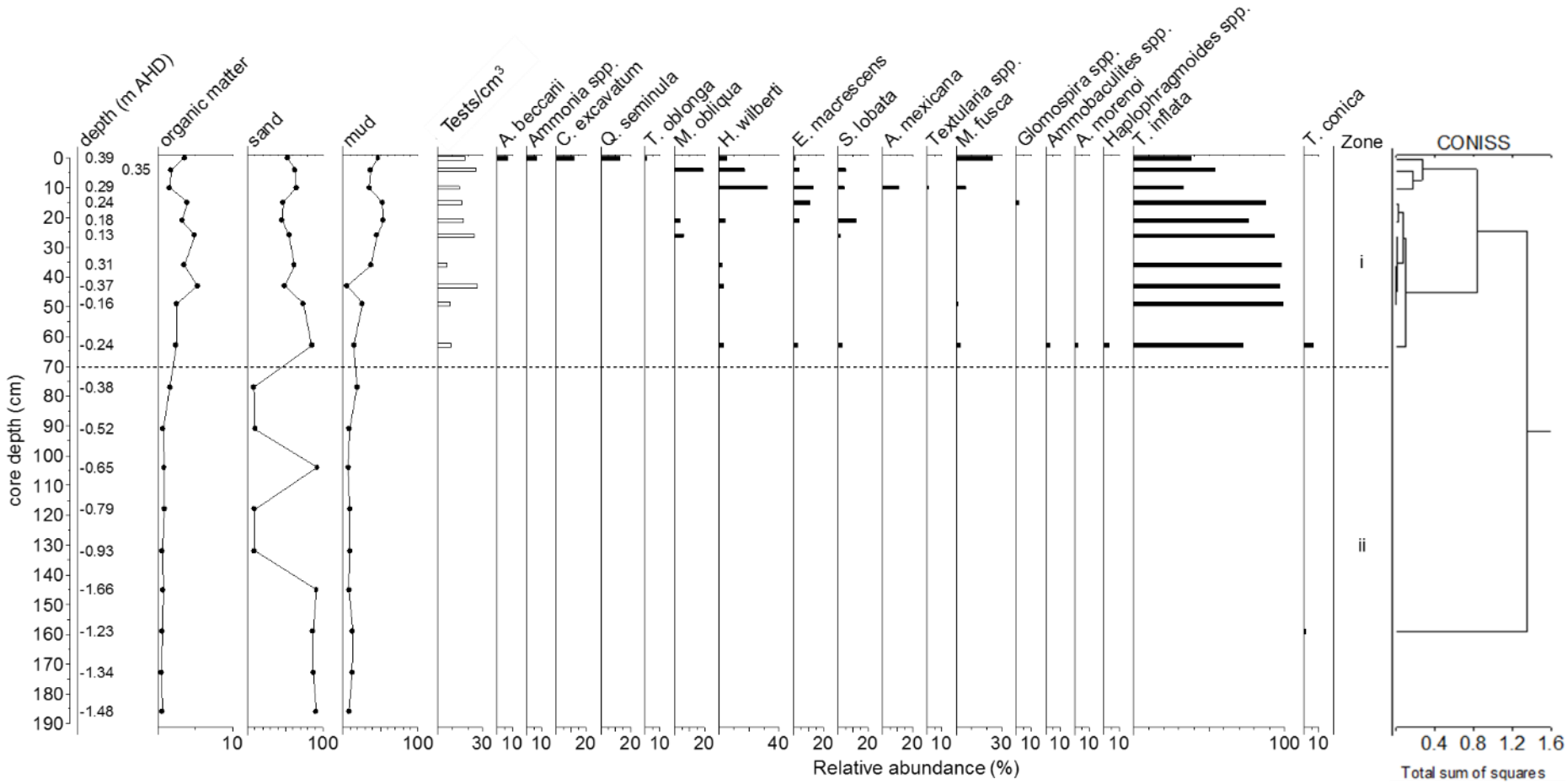

Figure 6.11: Depth constrained cluster analysis based on unweighted Euclidean distance (CONISS) of stratigraphical foraminiferal assemblages in Cm_Spo dominated by *Sporobolus virginicus*.

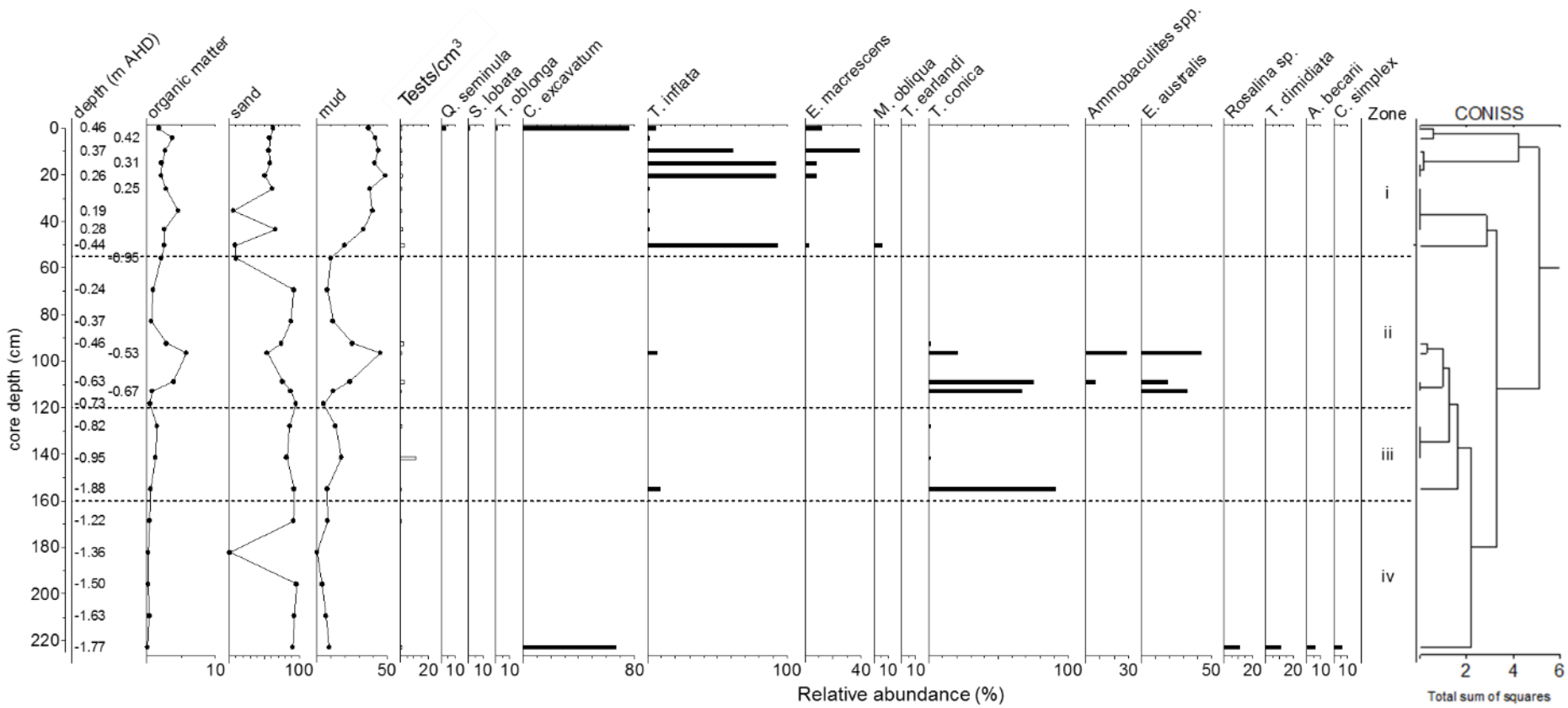

Figure 6.12: Depth constrained cluster analysis based on unweighted Euclidean distance (CONISS) of stratigraphical foraminiferal assemblages in Cm_Dm dominated by shrub *Avicennia marina*.

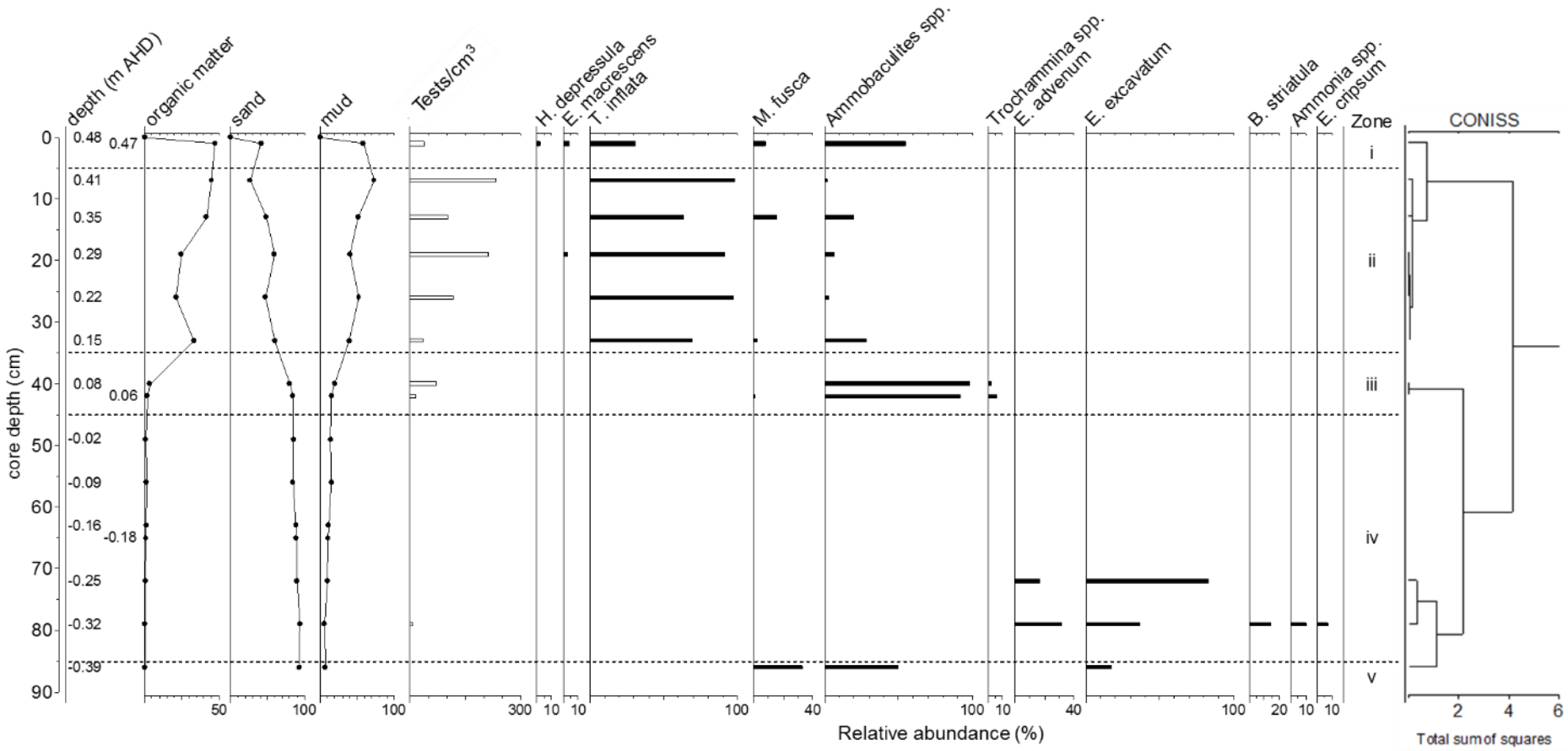

Figure 6.13: Depth constrained cluster analysis based on unweighted Euclidean distance (CONISS) of stratigraphical foraminiferal assemblages in Ca_Mg2 dominated by *Avicennia marina*.

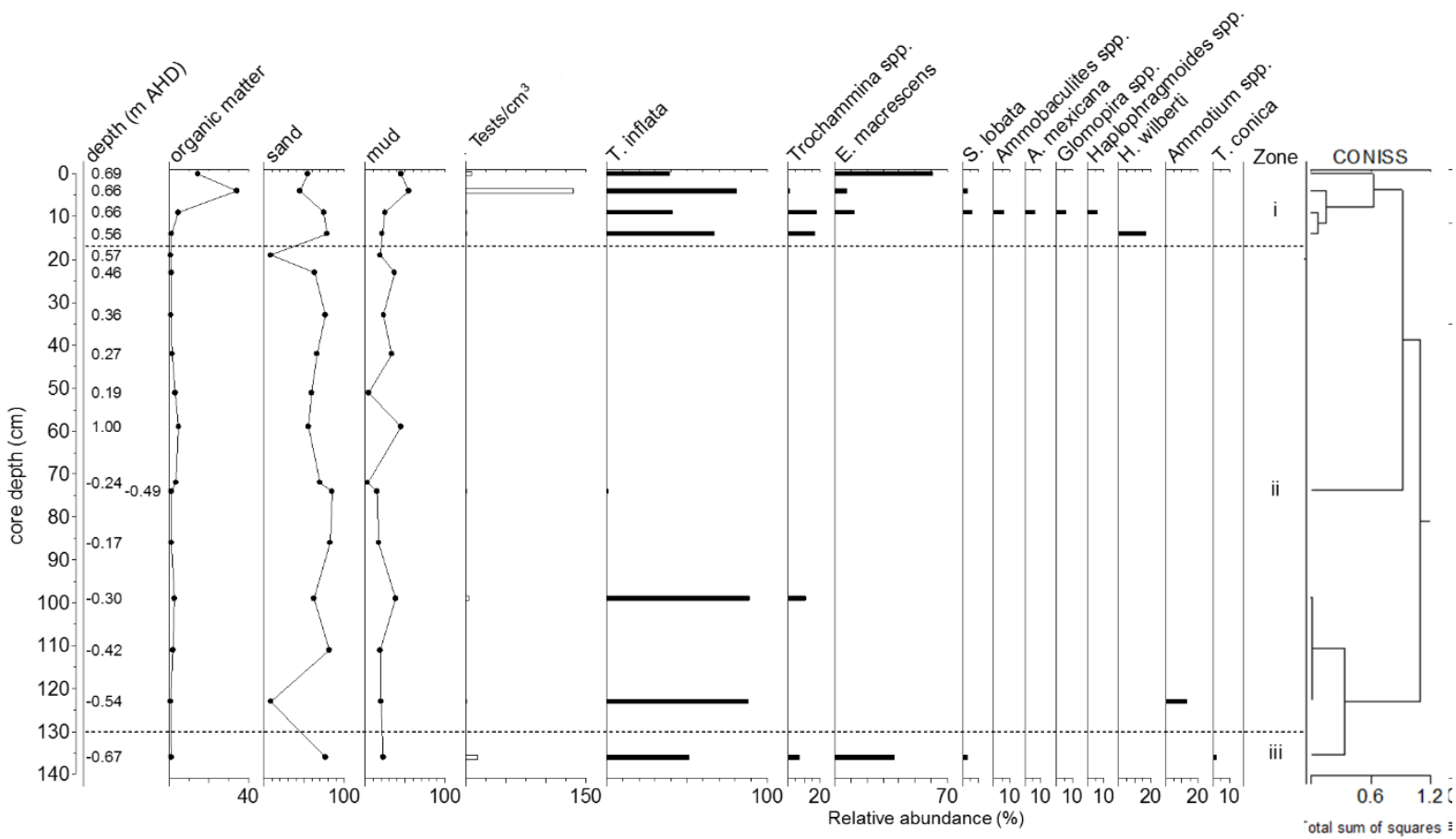

Figure 6.14: Depth constrained cluster analysis based on unweighted Euclidean distance (CONISS) of stratigraphical foraminiferal assemblages in Ca_Tect dominated by *Tecticornia arbuscula*.

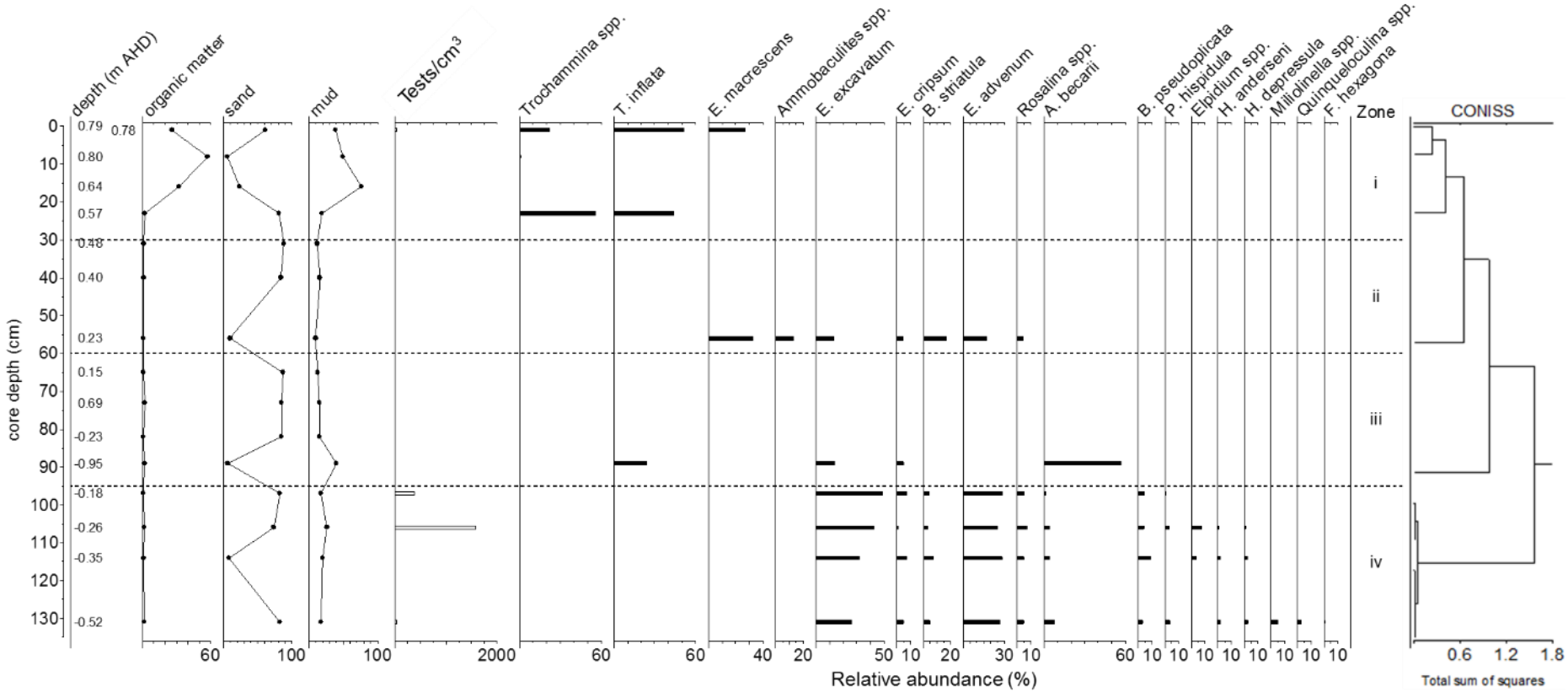

Figure 6.15: Depth constrained cluster analysis based on unweighted Euclidean distance (CONISS) of stratigraphical foraminiferal assemblages in Ca_Sar2 dominated by *Sarcocornia quinqueflora*.

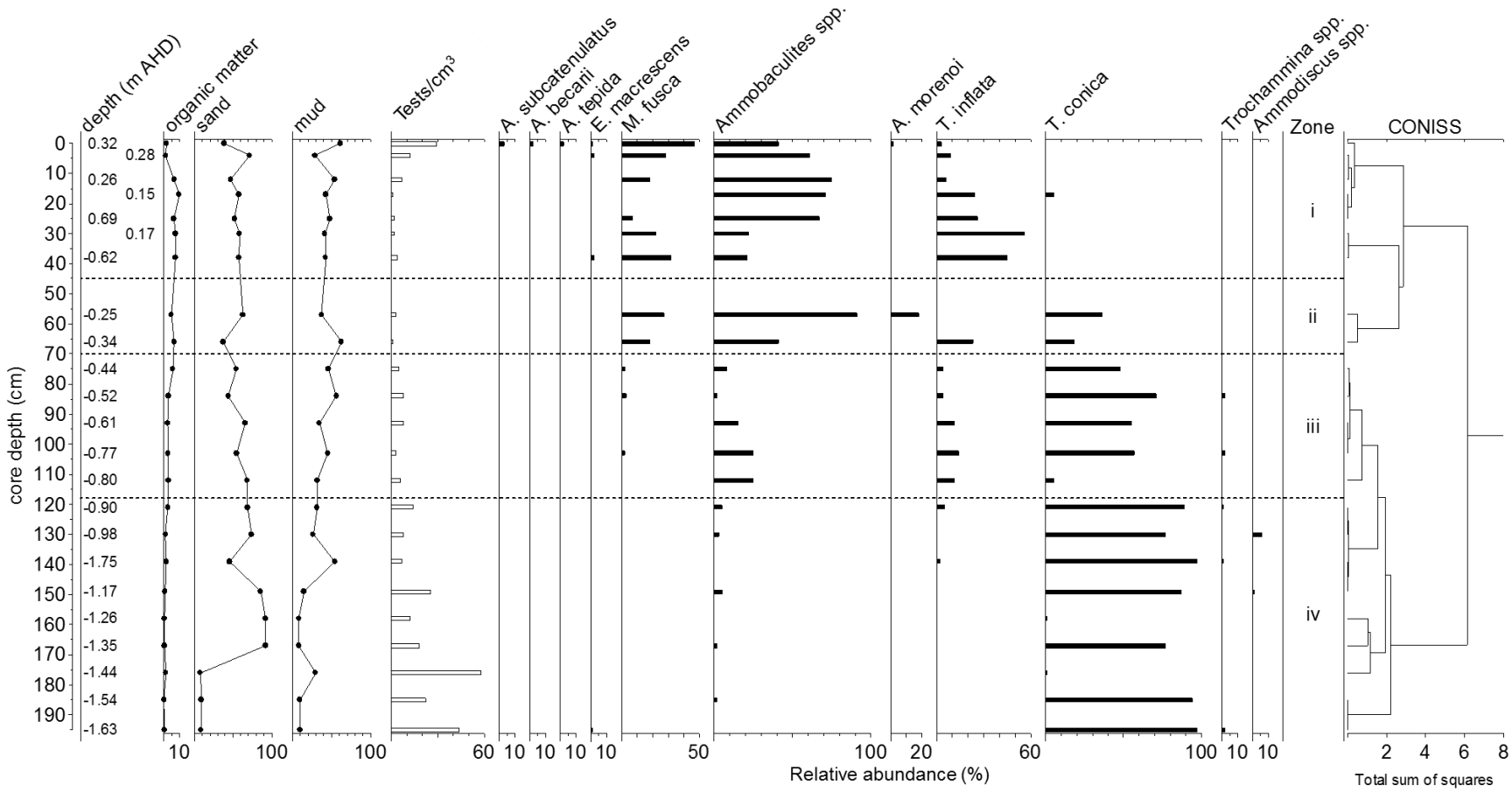

Figure 6.16: Depth constrained cluster analysis based on unweighted Euclidean distance (CONISS) of stratigraphical foraminiferal assemblages in Cb_Mg dominated by *Avicennia marina*.

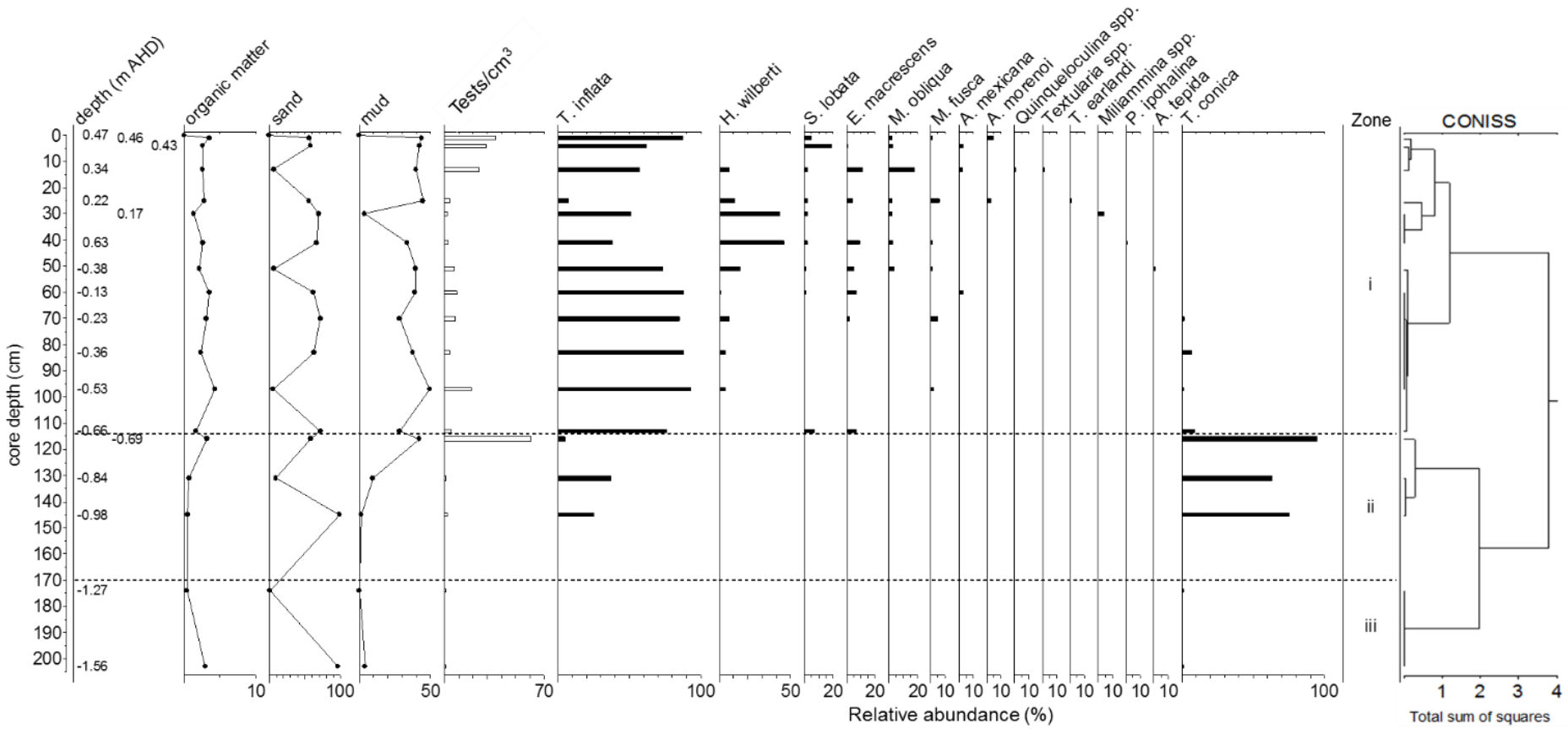

Figure 6.17: Depth constrained cluster analysis based on unweighted Euclidean distance (CONISS) of stratigraphical foraminiferal assemblages in Cb_Spo dominated by *Sporobolus virginicus*.

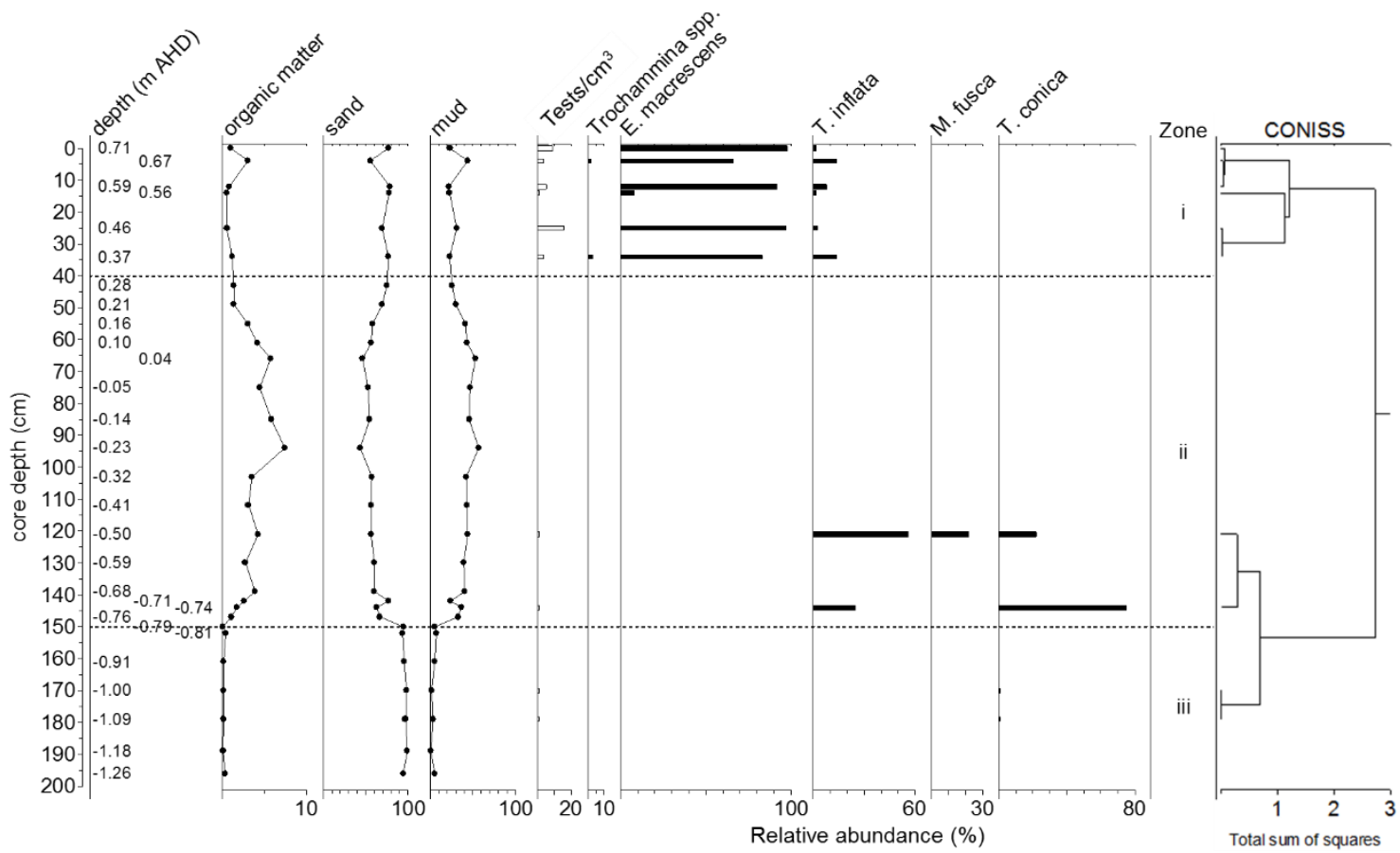

Figure 6.18: Depth constrained cluster analysis based on unweighted Euclidean distance (CONISS) of stratigraphical foraminiferal assemblages in Cb_Sar2 dominated by *Sarcocornia quinqueflora*.

6.4.4. Palaeo-environmental reconstruction

Minnamurra River

The intertidal barrier estuary of Minnamurra River transformed from an unvegetated tidal mudflat to mangrove-dominated intertidal zone (Fig. 6.19). This was indicated by the mudflat foraminifera in the sediment cores (Fig. 6.8 and 6.9) and the reconstructed wetland surface elevation typically below MHW. The organic-rich mud in the cores further supports the foraminiferal evidence. An apparent mangrove zone could not be established in the high Minnamurra core because of gaps in microfossil data, however, the organic-rich substrate 54 to 86 cm below the surface and mangrove foraminifera suggests the occurrence of mangrove vegetation. Stratigraphical data from the high saltmarsh core further indicates that areas located higher in the tidal frame and farthest from the channel later transitioned into saltmarsh. The transition may have been associated with high sediment accumulation between 54 and 86 cm below the surface which increased wetland surface elevation, subsequently lowering the tidal inundation frequency and mangrove was replaced by saltmarsh.

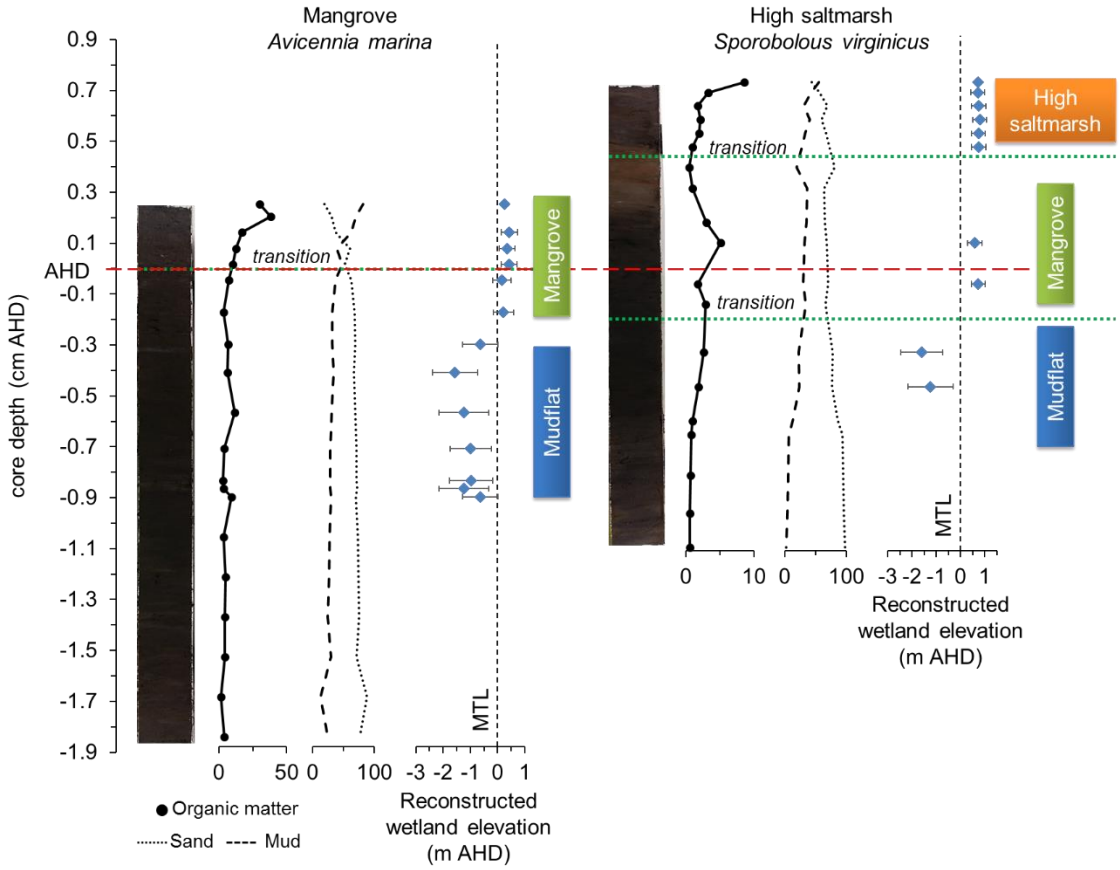

Figure 6.19: Palaeo-environmental reconstruction of Minnamurra River based on microfossil data (Fig. 6.8 and 6.9), core stratigraphy and transfer function based palaeo-wetland surface elevation.

Comerong Island

Near the entrance of Crookhaven River, the southern part of Comerong Island dominated by tall *Avicennia marina* at present was largely an unvegetated sandy subtidal zone 3510 ± 99 cal BP as was indicated by the calcareous foraminiferal assemblage 153 cm below AHD (Fig. 6.10). Palaeo-wetland surface elevation reconstruction revealed that this area infilled with about 130 cm of sandy sediments (elevation < MTL) before converting into present-day mangrove. The calcareous assemblage 177 cm below AHD in the shrub mangrove core (Fig. 6.12) located on the northern side of the island correlates with the palaeo-environment transformation of southern mangrove environment, where conditions transformed from subtidal to mudflat to mangrove, which later transitioned to saltmarsh until

recently converting back into mangrove. The recent establishment of mangrove is likely as Mangrove colonisation in the northernmost site is largely associated with increased inundation frequency with SLR over the past century.

The gaps in microfossil data in the *Sporobolus virginicus* core (Fig. 6.11) and to some extent in the shrub mangrove core made interpretation of past environments difficult (Fig. 6.20). However, the organic-rich mud and microfossil assemblage in the low saltmarsh core indicate that environmental conditions transition from mudflat to mixed vegetation and/or saltmarsh to present-day saltmarsh. The existing mangrove trees at this location (Fig. 2.3) further suggests that this site was likely dominated by mangrove even though microfossil data is not showing this.

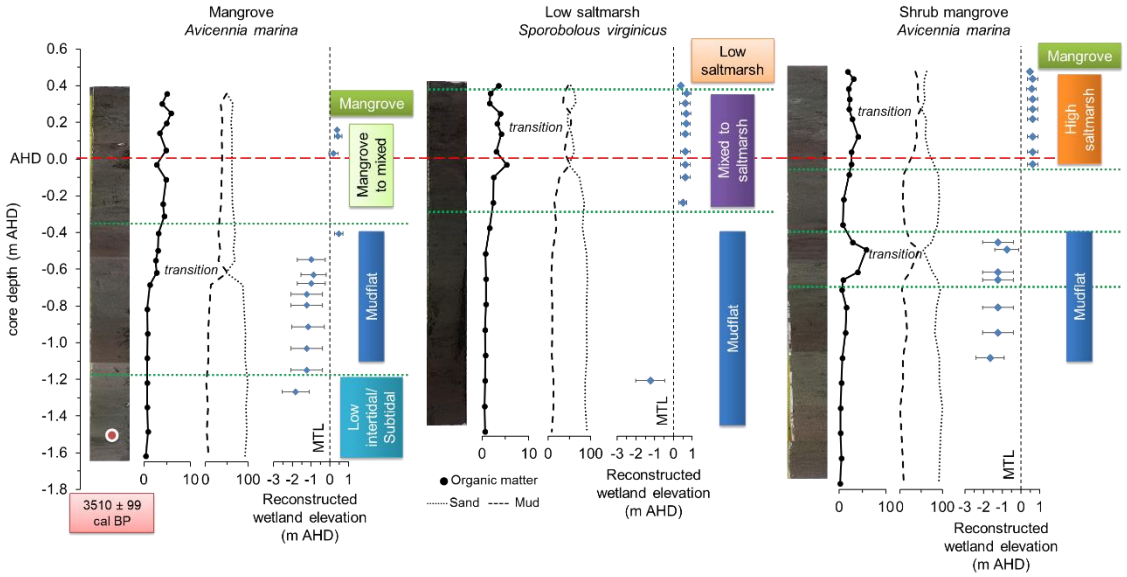

Figure 6.20: Palaeo-environmental reconstruction of Comerong Island based on microfossil data (Fig. 6.10, 6.11 and 6.12), core stratigraphy and transfer function based palaeo-wetland surface elevation.

Jervis bay – Cararma Inlet and Currambene Creek

The foraminifera microfossil data, reconstructed wetland surface elevation, organic matter content and substrate grainsize indicate that the mangrove zone at Cararma Inlet was a marine dominated subtidal and/or lower intertidal zone 3589 ± 105 cal BP (Fig. 6.21). It accumulated about 37 cm of sandy marine sediments

before mangrove plants established. The high rate of organic-rich mud accumulation increased wetland surface elevation and it appears that saltmarsh vegetation occupied the zone for a little while before transforming back into mangrove-dominated zone (Fig. 6.21). The *Sarcocornia quinqueflora* core from Cararma Inlet showed a similar environmental story to the mangrove core, however, the microfossil assemblage (Fig. 6.15) and shell radiocarbon date indicate that Cararma Inlet was a marine dominated subtidal and/or lower intertidal zone for a longer period dating back to 5258 ± 193 cal BP. This zone accumulated about 108 cm of sediments before transforming into mangrove, indicated by the organic-rich mud, before transitioning into present-day saltmarsh dominated by *Sarcocornia quinqueflora* (Fig. 6.21).

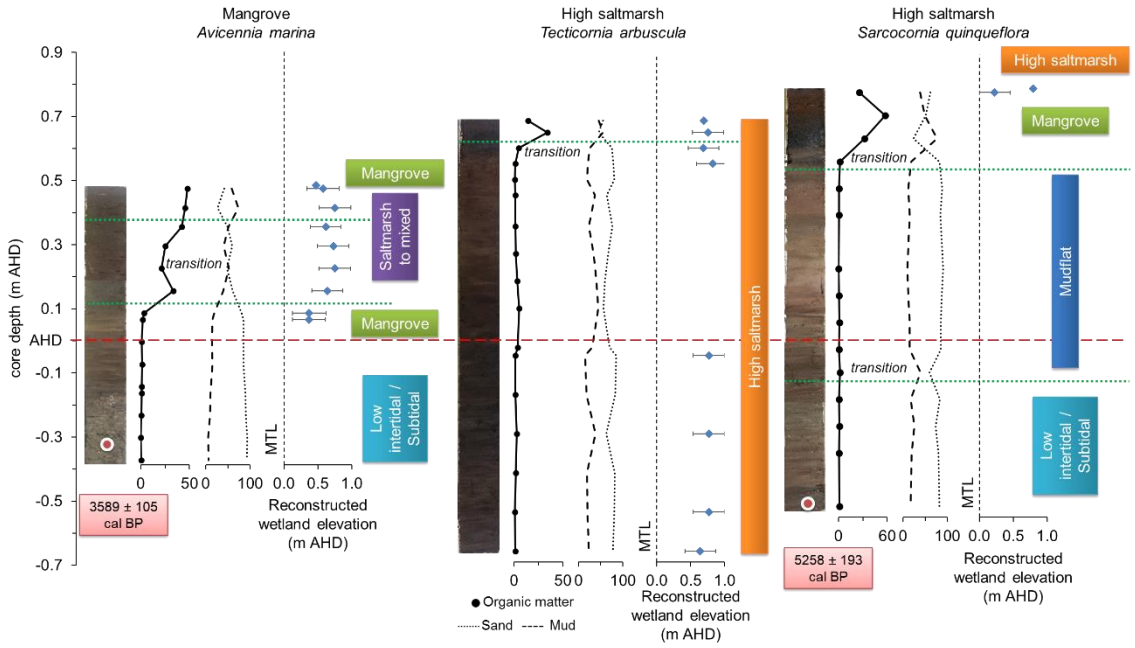

Figure 6.21: Palaeo-environmental reconstruction of Cararma Inlet based on microfossil data (Fig. 6.14, 6.15 and 6.16), core stratigraphy and transfer function based palaeo-wetland surface elevation.

The gaps in microfossil data in the high saltmarsh cores (Fig. 6.14, 6.15 and 6.18) likely caused by test dissolution and fragmentation, and sparsity due to low preservation of tests, makes the palaeo-environmental is story at Cararma Inlet incomplete. The *Tecticornia arbuscula* core is showing no change in vegetation type and that environmental conditions remained like present-day saltmarsh (Fig.

6.21). This core was exceptional in relation to the mangrove zones and other study areas which transformed from subtidal and/or mudflat zone into mangrove before transitioning to saltmarsh as a rule.

The relatively high abundance of *T. conica* in the sediment cores from Currambene Creek (Fig. 6.16, 6.17 and 6.18) suggest that this area was an unvegetated mudflat before turning into present-day intertidal wetland environment. The mangrove and high saltmarsh cores indicate the change from mudflat to mangrove indicated by the organic-rich mud (Fig. 6.22). The modern age of the mangrove root at 137 cm below AHD in the mangrove core suggest that roots can go this deep and into belowground mudflat substrate. The root can decompose and contribute to ^{14}C age that is younger than the general time of deposition of the sediments within which they occur.

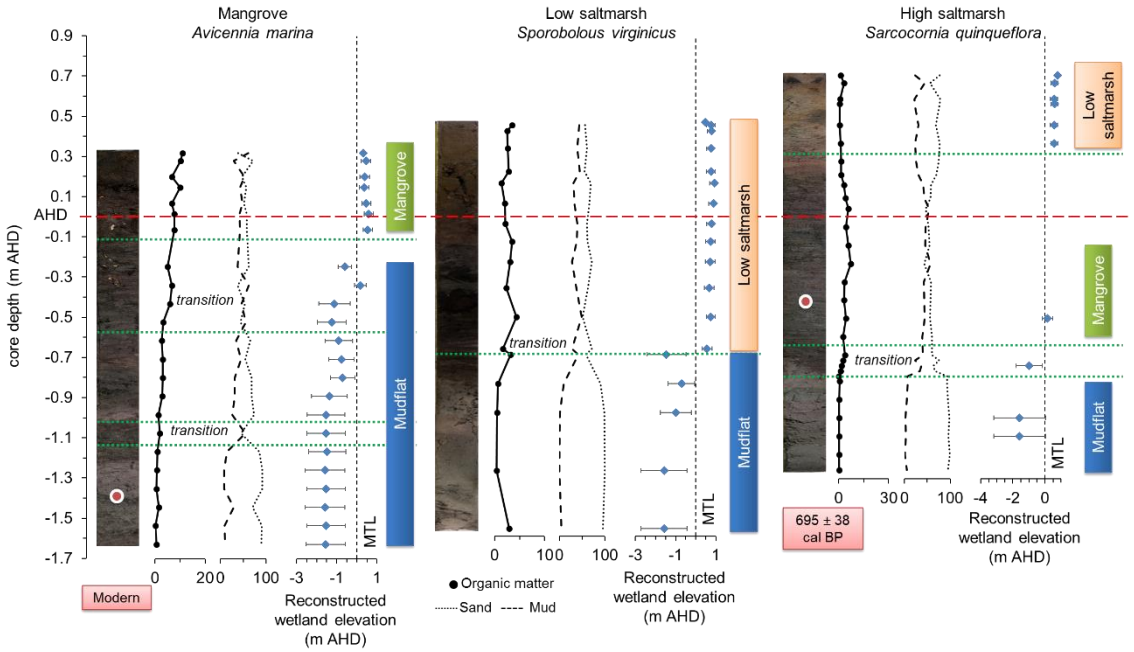

Figure 6.22: Palaeo-environmental reconstruction of Currambene Creek based on microfossil data (Fig. 6.17, 6.18 and 6.19), core stratigraphy and transfer function based palaeo-wetland surface elevation.

A clear mangrove signal could not be obtained in the high saltmarsh core because of gaps in microfossil data but the relatively young age of 695 ± 38 cal BP of the mangrove root 112 cm below the surface, suggests the existence of mangrove

vegetation. The age of mangrove root does not necessarily indicate the time of sediment deposition because mangrove roots can penetrate deep into the substrate as established from the mangrove root age in the mangrove core. The evidence of mangrove in this zone, however, is further supported by organic-rich sediments 55 to 147 cm below the surface. The lower elevation mangrove zone closer to the channel remained mangrove-dominated, however areas located higher in the tidal frame and farthest from the channel later transitioned into saltmarsh. This transition occurred after about 90 cm of mangrove sediment accumulated that likely increased wetland surface elevation in relation to MTL before mangrove was replaced by saltmarsh dominated by *Sarcocornia quinqueflora* (Fig. 6.22).

Gaps in foraminifera data in the saltmarsh cores at Currambene Creek proved interpreting past environmental conditions like those in Cararma Inlet, however, organic-rich mud in the cores suggested occurrence of mangrove vegetation. The organic-rich mud low 50 to 75 cm below AHD in the saltmarsh Currambene core implies mangrove may have existed in this narrow transition zone before converting to present day saltmarsh dominated by *Sporobolus virginicus* (Fig. 6.22). Prior to that, the occurrence of the *T. conica* and *T. inflata* assemblage implies that wetland elevation was near MTL.

6.5. Discussion

6.5.1. Longer-term behaviour of coastal wetlands

The longer-term behaviour of coastal wetlands was to accumulate sediments over the mid to late Holocene. The gradual transition from sediments deposited in lower intertidal/subtidal positions to mangrove and saltmarsh over the past few millennia. The calcareous foraminifera and marine shell radiocarbon ages from Comerong Island and Cararma Inlet demonstrated that present mangrove-dominated zones within these mature wave-dominated estuaries were primarily

marine in character and the surface was possibly exposed to air when the tide was lowest. There is some evidence that sea level may have been 1 to 1.5 m higher than present level until about 2000 years ago before falling to present levels (Lambeck, 2002; Lewis et al., 2013; Long, 2001; Sloss et al., 2007). The carbonate-rich substrate and marine shells deposited may have deposited during this mid-Holocene high-stand. The marine sandy substrate accumulated at different rates between 5200 and 3500 years ago at Cararma Inlet and Comerong Island before transforming into upper intertidal wetlands that has persisted over the past 3000 years. Minnamurra River and Currambene Creek show similar environmental change whereby mudflat substrate in the lower sections of the cores also suggests a time when lower intertidal conditions prevailed before it transitioned into upper intertidal wetlands.

The findings of this study demonstrated that benthic foraminifera in upper intertidal wetlands can give a good indication of previous estuarine environments. However, this study did not resolve the debate about whether there was a mid-Holocene sea level high-stand and subsequent sea-level fall to present levels. The slight falling trend of sea-level from a high stand is not easily distinguishable from the present sea level along the south-eastern coastline of Australia (Thom and Roy, 1985). The Holocene sea-level history has been linked to the patterns of sedimentation on the inner shelf, in bay barriers and in estuaries based on the depositional environments and sequences within bed-rock embayments. Foraminiferal microfossil assemblages did not enable the discrimination of a fall in sea level from sediment accumulations as has been demonstrated in other studies in Australia (Horton et al., 2007; Woodroffe, 2009a) and other far-field regions (Callard et al., 2011; Gehrels et al., 2012; Southall et al., 2006).

The study sites are classified as wave dominated barrier estuaries that are in a mature stage of sediment infilling (Roy et al., 2001), in which wetland vegetation is confined to the estuary and not exposed to the open coast. In the early stages of evolution, these estuaries were characterised by a central mud basin that

accumulated sediments supplied to the system from the catchment. The low energy sheltered, and less exposed intertidal shorelines of these barrier estuaries provided an ideal platform for mangrove propagules to establish as the central mud basin infilled with sediments. The organic-rich muddy substrate suggests a time when accumulation of fine-grained sediments may have been facilitated by mangrove plants. Relatively stable sea-level conditions over an extended period may have provided considerable time for the dissolution of foraminifera within substrates. Tests dissolution and gaps in microfossil assemblages down core limited the ability to effectively apply transfer function models and accurately delineate palaeo-wetland surface elevations. This was particularly evident in the case of saltmarsh substrates that persisted for the longest time periods, and where zones with few preserved foraminifera were identified. Species density in belowground sediments did not show any significant relationship to sediment grainsize or organic matter in the cores suggesting that taphonomic processes, such as post-mortem transportation of tests by tidal action and preservation may be affecting species abundance (Berkeley et al., 2007; Gordillo et al., 2014; Hayward et al., 2015; Wang and Chappell, 2001).

The transformation of wetland vegetation from mangrove to saltmarsh was based on the relationship between inundation frequency and mineral and organic sediment additions. As the basin infilled with sediments, accommodation space decreased as proposed in the Roy model of estuary infill (Roy et al., 2001). As the estuary infilled it decreased sediment trapping efficiency of the basin as surface elevations reached at and/or near mean sea level (Heap et al., 2004; Panayotou et al., 2007; Roy et al., 2001), consequently reducing inundation frequency creating suitable conditions for mangrove propagules to establish in the soft substrate (Saintilan et al., 2009). Sea-level fall over the late Holocene (past 2000 years) reduced accommodation space and mangroves were later replaced by saltmarshes higher in the tidal frame as indicated by the foraminiferal microfossil assemblages.

6.5.2. Limitations of palaeo-environmental reconstruction

Discrepancies between modern and microfossil assemblages made it difficult to interpret past environmental conditions as only agglutinated foraminifera were encountered in several of the cores ranging across each of the study sites. Some microfossil assemblages were not encountered in the modern training set as it typically comprised to species that are upper intertidal dwellers are based on current climatic/environmental conditions, making it difficult to interpret past environmental conditions. Microfossil foraminifera may have been deposited in an environment that is no longer represented in the present coastal wetland setting. This was mainly an issue for tests that occurred in mudflats and/or lower intertidal zones, particularly at Cararma Inlet. Some microfossil assemblages showed inconsistencies within study sites, for instance, species such, as *A. mexicana*, *H. wilberti* and *M. obliqua* were found in subsurface sediments of study sites where they were not encountered in the surficial samples. However, 94 % of dominant taxa encountered in belowground sediments were part of the modern assemblage, consequently, pooling foraminiferal data from the region was adopted for palaeo-environmental reconstruction.

Gaps in microfossil data could also be associated with belowground processes, such as erosion and transportation of tests, destruction through abrasion and test dissolution. It is likely calcareous tests have been dissolved from some of the cores, as discussed in section 6.2.2. Agglutinated taxa are not particularly affected by low pH conditions and in at least half of the cores, only agglutinated tests were present. Poor preservation of agglutinated species in mangrove sediments can occur as a result of oxidation promoted by aerobic mineralization in the dry season (Berkeley et al., 2009, 2007; Woodroffe, 2009b). Where microfossil assemblages did not correspond to surficial associations, existing literature was used to determine their depositional environments, which further aided the interpretation of past environmental conditions.

6.5.3. Efficacy of transfer function models

The transfer function models work well in areas where there has been evidence of relative SLR as a result of either eustatic sea-level rise or coseismic land subsidence (Guilbault et al., 1996, 1995; Horton et al., 2017; Shennan et al., 1996; Shennan and Horton, 2002). The southeast Australian coastline, however, has remained largely tectonically stable over the late Holocene (Thom and Roy, 1985). The transfer function model also did not work well in this study, which it demonstrated by giving a relatively low coefficient of determination (r^2) indicating low confidence in predicting palaeo-wetland elevation from the modern assemblages. It may be possible to resolve this by analysing the complete intertidal gradient ranging from the lowest limit to the highest limit of the tides. However, this was one of the limitations of this study because mudflat and low intertidal zones were either very narrow or absent from the study areas. The cluster analysis provided a more effective means of interpreting palaeo-wetland environments as modern foraminiferal associations exhibited strong spatial patterns with vegetation and inundation frequency.

Discrepancies in modern distributions can also disrupt transfer function models when some species can occur across the tidal frame (Table 5.18), illustrating that they have a high tolerance to the environmental variables. One such species in this study was *Trochammina inflata* that was encountered across the tidal frame in almost all study sites. However, it was common in association with *Entzia macrescens* in high saltmarshes above MHW. Other problems may arise where only one species of foraminifera dominates in part of the intertidal zone; for example, high abundance of agglutinated tests can lead to application of the transfer functions to reconstruct past environments using only intertidal agglutinated assemblages as demonstrated by others (Woodroffe, 2009b).

6.6. Conclusion

The interpretation of palaeo-environments was based on two lines of evidence; foraminifera-based assemblages from the regional training set and palaeo-wetland surface elevation from foraminifera-based transfer functions. Existing literature from the region proved valuable when interpreting species assemblages that are no longer part of the modern upper intertidal wetland assemblage. The foraminifera-based transfer function model did not work well because of absence of foraminifera from some sections of cores and was unreliable in interpreting palaeo-wetland surface elevation. It did, however, indicate the transition in wetland elevation from subtidal and/or lower intertidal to upper intertidal setting supporting the barrier estuary evolution model for the region. Correlation between these interpretations provided enough confidence in reconstructing past environmental conditions within the wave-dominated barrier estuaries of the region but could not be used to reconstruct past sea level. Over the late Holocene, the lower intertidal and/or subtidal settings transformed into present-day upper intertidal zones occurred as a result of the relationship between sediment infilling, accommodation space and surface elevation. As the central mud basin infilled with organic and mineral sediments, indicated by mangrove microfossil assemblages and organic-rich mud in belowground substrates, accommodation space diminished as wetland elevations increased and mangrove was replaced by saltmarsh higher in the tidal frame.

Chapter 7

Synthesis and Conclusions

7.1. Introduction

Coastal wetlands dominated by mangrove and saltmarsh are highly effective in minimising shoreline erosion, protecting from big waves and storm surges, and enhancing water quality. Wetland vegetation are biologically diverse, and in recent years their carbon sequestration capabilities has added value to the ecosystem services they provide (Barbier et al., 2011; Chmura et al., 2003; Friess et al., 2016; Guo et al., 2009; Howe et al., 2009; Marchio et al., 2016; Rogers et al., 2019a; Saintilan et al., 2013a; Sanders et al., 2010b). Coastal vegetation losses, due climate change, sea-level rise (SLR) and the continued coastal development pressures, affect the ability of coastal wetlands to provide these ecosystems services. It is therefore, important to assess the value of coastal wetlands and apply them appropriately in coastal management and planning as SLR accelerates this century.

This thesis quantified surface elevation dynamics within coastal wetlands of south-eastern Australia in response to sea-level changes across a range of timescales. The techniques used focused on specific timescales over which changes occur: the rod-surface elevation table and marker horizon (rSET-MH) technique over 2 years, and original-SET-MH over up to 20 years were used to characterise surface elevation, vertical accretion and belowground dynamics; radiometric sediment dating techniques using the radio isotopes of ^{210}Pb and ^{137}Cs were used to quantify sedimentation occurring at decadal to centurial timescales; and foraminiferal analyses were used to quantify palaeo-wetland elevation and vegetation changes occurring at millennial timescales. Results from this thesis represents the first attempt to integrate SET data with information across a range of timescales at the same study sites. By considering changes across a range of timescales, it was

anticipated that this information would improve our capacity to connect processes influencing wetland elevation changes with the response of coastal wetlands to SLR (Rogers et al., 2016). Understanding the response of coastal wetland to SLR is crucial for projecting the response of coastal wetlands to the anticipated SLR associated with anthropogenic global warming and will improve capacity to accommodate wetlands and the ecosystem services they provide within plans, policy and management.

7.2. Surface elevation dynamics over annual to decadal timescales

At annual to decadal timescales, surface elevation (SE) change was found to be related to tidal inundation frequency, with SE gain always higher when inundation frequency was higher (i.e. in the mangrove zone) and either had a very little change or declining elevation where inundation frequency was lower. This pattern was relatively consistent within the 2-year rSET study at Comerong Island and the decadal SET study sites at Cararma Inlet and Minnamurra River, where the mangrove substrate was increasing surface elevation at rates of 4.3 ± 2.0 mm/y, 1.9 ± 0.25 mm/y and 1.3 ± 0.31 mm/y, respectively. Very little change in SE was observed in the saltmarsh zones of Comerong Island and Minnamurra River, 0.0087 ± 1.5 mm/y and 0.52 ± 0.51 mm/y, respectively, whilst Cararma Inlet saltmarsh was increasing SE at 1.2 ± 0.28 mm/y. Mangrove and saltmarsh zones represent areas where accommodation space is high and low, respectively, and it was therefore anticipated that SE gain would be higher where accommodation space is high. SE gain trends is relatively common and has been reported for mangrove and saltmarsh in this region (Rogers et al., 2006). In some areas where rates of mangrove SE gain has not been higher than rates of saltmarsh SE gain typically occurs where the niche for both vegetation types overlap, as observed along the Atlantic and Gulf of Mexico coastlines (McKee, 2011; McKee et al., 2007).

Currambene Creek exhibited a different spatial pattern in SE change whereby the

mangrove zone, where accommodation space was high, very little change over almost two decades was observed (0.089 ± 0.076 mm/y). The mixed vegetation zone was increasing surface elevation at 1.4 ± 0.10 mm/y, whilst the saltmarsh zone was losing SE at 0.22 ± 0.048 mm/y. Loss of SE at high tidal position may be due to decomposition of below-ground organic matter exceeding rates of organic matter and mineral sediment addition. There was, however, substantial SE gain at intermediate elevations, perhaps indicating a transition towards mangrove occupying higher elevations. Monitoring of mangrove SE changes at Currambene Creek should remain a priority to determine the longer-term resilience of low elevation mangrove at this site.

Vertical accretion (VA), however, did not exhibit a strong relationship with patterns of inundation at annual timescales, with accretion only starting to correspond to patterns of inundation at decadal timescales. This was specifically established in Chapter 2 where VA at Comerong Island did not correspond to tidal position over the 2-year study period, where mangrove was accreting sediments at 2.1 ± 1.7 mm/y whilst higher in the tidal frame the mixed vegetation zone was 3.6 ± 0.45 mm/y. Over decadal timescales however, VA measured from MH and using ^{210}Pb chronologies in chapters 2 and 3 did correspond to tidal position, except for Currambene Creek. Rogers et al. (2006) found, using the same network of SET-MH used in this study site, that VA did not correspond to tidal position at Currambene Creek over their three-year study period, where VA occurred at approximately 0.65 mm/y in mangrove, 1.37 mm/y in mixed and 0.33 mm/y in saltmarsh. This pattern in VA has been maintained at this study site to decadal timescales. This study proposes that the decoupling of VA from tidal position at Currambene Creek may relate to the proximity of SETs to a smaller tidal creek that funnels water to higher elevations within the wetland. Over the two-year study period that MH were used to monitor VA at Comerong Island, a similar pattern of decoupling was identified, which may also relate to the proximity of higher elevation MHs to the tidal creek funnelling water along Comerong Bay. VA corresponding to tidal position at decadal timescales has been established for some time for saltmarshes

(Allen, 2000; Pethick, 1981), whilst modulation of pattern of VA on the basis of distance to tidal creeks has been incorporated into various models developed from empirical data (Temmerman et al., 2003).

SE and VA did not correspond to each other at most study sites, except for Cararma Inlet. This further substantiates the observations of Kaye and Barghoorn (1964) that VA does not always result in SE gain, which accentuated the need to measure and report belowground processes that influenced substrate volumes. SE gain being less than the degree of VA could be explained by decomposition of organic matter and compaction and/or consolidation of belowground substrate (Cahoon et al., 2004; McKee, 2011; McKee et al., 2007). However, this study found that at some tidal positions, SE gain exceeded the degree of VA. Coupling of deep and shallow-rSETs at Comerong Island enabled the processes of organic matter decomposition and addition at different depths within substrates to be distinguished from processes of VA operating at the surface (Fig. 7.1). Organic matter addition to the mangrove root zone at mid elevations made a significant contribution to SE gain at Comerong Island, whilst decomposition of organic matter in the shallow zone at intermediate elevations and decomposition of organic matter in deep and shallow zones at higher elevations was the primary process contributing to a deceleration in SE gain at intermediate averaged 0.0087 mm/y, whereas a decline of about 2.5 mm/y in SE higher in the tidal frame. The pattern of SE gain exceeding VA was also identified at intermediate elevation at Currambene Creek where invasion of mangrove into saltmarsh has occurred over the past few decades (Saintilan and Williams, 1999; Saintilan and Wilton, 2001).

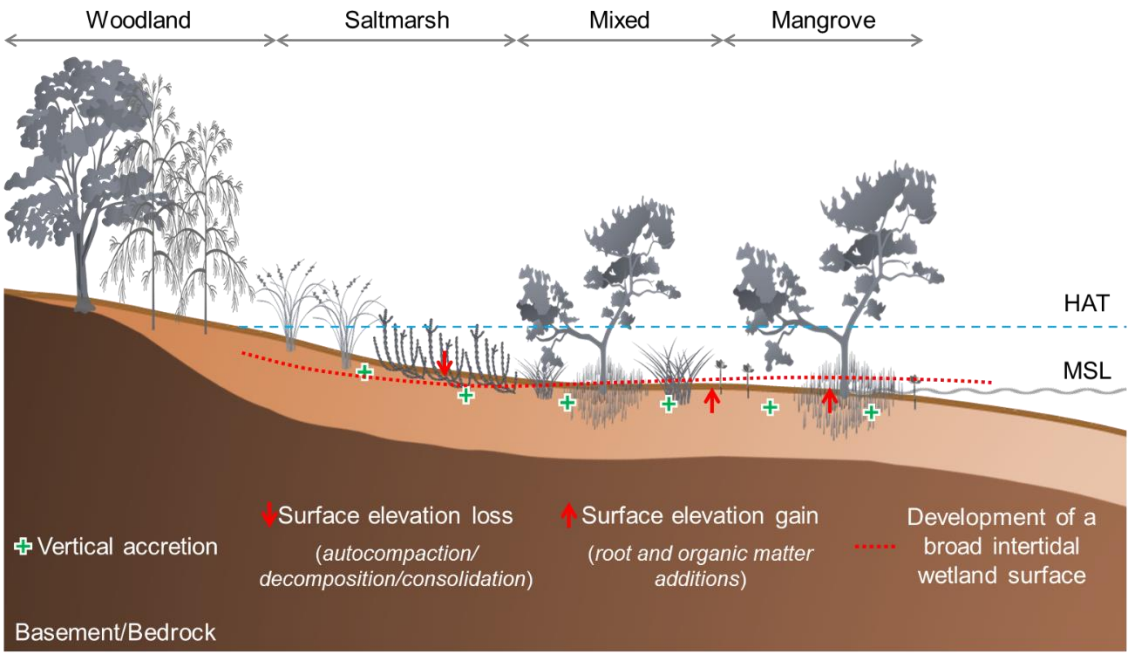

Figure 7.1: Vertical accretion was observed at all tidal positions, but surface elevation change was predominantly regulated by belowground processes. Organic matter additions by mangrove vegetation contribute to surface elevation gain in the mangrove and intermediate mixed vegetation, whilst shallow autocompaction, and decomposition and/or consolidation of belowground substrate result in surface elevation loss higher in the tidal frame (i.e. in saltmarsh vegetation) despite high rates of vertical accretion.

Organic matter addition to substrates was found to be an important process contributing to elevation gain, and plays a significant role in offsetting lower rates of VA. SE gain exceeding VA was identified by Rogers et al. (2005a) at Homebush Bay, and much like this study, was associated with substantial additions of organic matter to substrates as mangroves that had undergone senescence recovered. Organic matter addition to substrates has been established as an important mechanism for mangroves in Australia (Lovelock et al., 2011), the Caribbean (McKee, 2011), and Gulf of Mexico (Cahoon et al., 2004). The capacity for saltmarsh to add substantial organic matter to substrates has largely been established along Atlantic coastlines where mid-elevation *Spartina alterniflora* dominates (Morris et al., 2002). The ability of high elevation saltmarsh to add substantial volumes of organic matter to substrates has not been established in Australia where saltmarsh is limited to wetland elevations where there is relatively little accommodation space, supporting the hypothesis of Rogers et al. (2019a) that accommodation space has a significant influence on organic matter addition and carbon storage.

The overall pattern of SE change being related to inundation frequency contributes to the development of broad intertidal wetland surfaces, and modelling in chapter 2 indicated that all tidal positions may transition towards the same elevation over time (Fig. 2.23) as proposed in Woodroffe (2018a). The influence of SLR on this pattern of elevation change over time was not detected in patterns of SE gain measured at decadal timescales. This is not surprising as the observed degree of SLR over this study period, reported to be 4.1 (± 1.1) mm/y at Fort Denison between 2000 and 2017, is smaller than the degree of variability in sea level associated with climatic perturbations and storms that have occurred over this time period. Lags between the elevation response of wetland surfaces to SLR have been suggested in modelling studies (Fagherazzi et al., 2012; Kirwan and Temmerman, 2009) and could explain why surface elevation gain is not yet coupled with SLR in this study.

7.3. Sediment accumulation over decadal to centurial timescales

Analyses of excess ^{210}Pb confirmed that where accommodation space was higher (i.e. the mangrove zone) sediment accumulation over the past few decades to century was higher than accumulation where there has been less accommodation space (i.e. in the saltmarsh zone). This corresponds to patterns of SE gain found with SETs whereby greater inundation provides more opportunities for sediment deposition and accumulation. There is a paucity of studies that have analysed sediment accumulation across the intertidal zone or based on varying accommodation space, as was undertaken in this study. The approach used in this study provides the opportunity for regional comparison of sediment accumulation across the intertidal zone (Fig. 7.2). Comparison of rates of sediment accumulation amongst study sites over the full study period of ^{210}Pb analysis found that where accommodation space was low in the saltmarsh, the rate of sediment accumulation corresponded to the long-term rate of SLR at Fort Denison for the period 1914 –

2017 of 1.0 ± 0.0093 mm/y, as indicated by the slope of the best fit line in Figure 7.2. Where accommodation space was higher in the mangrove zone, rates of sediment accumulation at decadal to centurial timescales exceeded the long-term rate of SLR, indicating that infilling of accommodation space was occurring at this timescale. Mangrove sediment accumulation rates has exceeded SLR indicates that these wetlands are not tracking SLR but were still undergoing infill even at the observed relatively low rates of SLR over the past century. These trends in sediment accumulation contrast with studies elsewhere, particularly along the Atlantic coastline of the US, where SLR has been more pronounced, and sediment accumulation has more closely corresponded to patterns of SLR (Kolker et al., 2010).

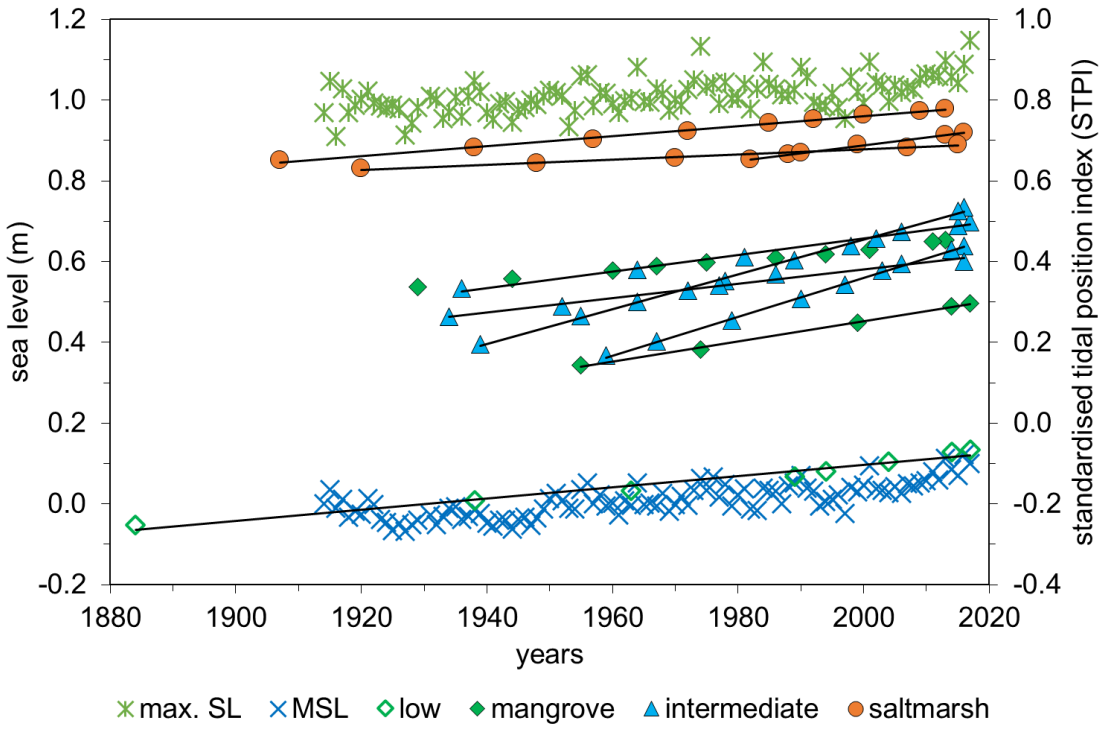

Figure 7.2: Sedimentation trend in low tidal position mangrove, mid tidal position mangrove, intermediate tidal position mangrove and saltmarsh vegetation, and high tidal position saltmarsh over the ^{210}Pb record in relation to maximum sea level (max. SL) and mean sea level. Wetland elevation of all tidal positions are represented as standardised tidal position index (STPI).

The decadal scale pattern of sediment accumulation indicates that sedimentation exceeded SLR where there is more accommodation space, high rates of

sedimentation was identified in tidal positions that had more accommodation space (i.e. in the mangrove cores). High rates of sediment accumulations were not identified in saltmarsh cores where accommodation space was more limited, but sedimentation rates coincided with the rate of SLR over the past century. The findings from this study demonstrated sedimentation coupled with SLR and its influence on available accommodation space. Relatively high rates of sediment accumulation was also identified at Lake Macquarie where accommodation space was substantially increased following mine subsidence beneath the Chain Valley Bay wetlands in the mid-1980s (Rogers et al., 2019a).

Sediment supply is crucial for maintaining a coupled relationship between accommodation space and sedimentation, as has been widely reported (Cahoon et al., 1999; McKee et al., 2007; Rogers et al., 2013b; Saintilan et al., 2009). Sediment supply plays a crucial role in increasing the resilience of coastal wetlands to SLR by demonstrating that rates of sediment accumulation were positively related to catchment size (Fig. 4.12). In particularly, rates of sedimentation were substantially higher at Comerong Island, with sediments being sourced from the large Shoalhaven River catchment (7086 km^2) and contrasted with the more conservative rates of sedimentation at Cararma Inlet where the catchment area was 7 km^2.

7.4. Palaeo-wetland surface elevations over millennial timescales

On the basis of developing a regional foraminiferal training set, this study demonstrated that the longer-term behaviour of coastal wetlands in south-eastern Australia was to accumulate sediments, infill accommodation space and for estuaries to transition from an immature to mature geomorphological stage, as described by Roy et al. (2001) over the past few millennia. Subtidal and/or lower intertidal habitats to mangrove subsequently transitioned to saltmarsh vegetation at higher elevations as accommodation spaced decreased with falling sea-levels.

Palaeo-wetland surface elevation gain over the past few millennia coincided with a period when sea level was relatively stable, or may have been up to 2 m higher than present (Sloss et al., 2007). Debate about the pattern of sea-level change in south-eastern Australia over the past few millennia continues (Murray-Wallace and Woodroffe, 2014). Palaeo-reconstructions using benthic foraminifera in this study does not provide any information that can resolve this debate about whether there was a high-stand and subsequent fall in sea level to current levels over the past millennia, as foraminiferal analysis does not provide the opportunity to differentiate sediment accumulation from sea-level fall. This has been emphasised using foraminiferal studies at locations where there has been similar patterns of sea-level change (Callard et al., 2011; Gehrels et al., 2012; Horton et al., 2007; Southall et al., 2006; Woodroffe, 2009b).

The inability to differentiate sea-level conditions over the past few millennia is partly limited because relatively stable sea-level conditions for this extended period may have provided considerable time for the dissolution of foraminifera within substrates. This was particularly evident in saltmarsh substrates where zones with no or very few preserved foraminifera were identified. Inconsistency in foraminiferal assemblages down cores limited the ability to effectively apply transfer function approaches to cores and accurately delineate palaeo-wetland surface elevations as has been effectively applied in other studies (Edwards et al., 2004a; Edwards and Horton, 2000; Gehrels, 2000, 2002; Horton et al., 1999a; Horton and Edwards, 2003, 2006; Leorri et al., 2008a, 2010; Woodroffe, 2009a). Consequently, vegetation reconstruction based on foraminiferal assemblages within cores provided a more effective means of interpreting palaeo-wetland environments at millennial timescales.

Modern foraminiferal assemblages correspond to vegetation composition and patterns of inundation across the tidal frame, where the *Trochammina – Entzia* association (A-I) was found in high saltmarsh vegetation typically above MHW; the *Entzia – Trochammina* group (A-II) was common in mixed vegetation to low

saltmarsh at mid-tidal elevations. The *Miliammina – Quinqueloculina* association (C-I) was common mangrove substrate, whilst the *Ammobaculites – Miliammina* association (C-II) was found in mangrove to mixed vegetation. Foraminiferal associations provided a strong foundation for a regional training set in palaeo-wetland surface elevations and vegetation composition reconstructions. To increase the power of the analysis, and partly due to the dissolution of foraminifera within sedimentary cores, this study utilised both living and dead foraminifera to develop the regional training set as it significantly increased the power of this approach. There has been some debate about the appropriateness of this approach (de Rijk and Troelstra, 1999, 1997; Gehrels, 2000; Horton, 1999; Horton et al., 1999a; Horton and Murray, 2006; Scott and Mediolo, 1980), but inclusion of both living and dead was essential in this study for palaeo-wetland reconstruction, as use of only living foraminifera reduced the number of dominant taxa that could be included in the training set.

Use of a regional training set, rather than site-specific training sets, was also crucial for palaeo-wetland reconstructions as it increased the probability that all zones within wetlands and associated foraminiferal assemblages were characterised within the training set. Use of regional training sets is being used more widely (de Rijk and Troelstra, 1997; Edwards et al., 2004b; Hayward, 1993; Horton, 1999; Horton et al., 1999b; Horton and Edwards, 2003; Leorri et al., 2010; Scott and Medioli, 1978; Woodroffe et al., 2005) and this study emphasises the utility of this approach. Despite using a regional training set, there were some foraminiferal assemblages within cores that were not present within the training set, which was not surprising. Given the degree of infill of the wetlands that had occurred over this timescale and was continuing to occur even at decadal timescales. More specifically, the maturity of the wetlands analysed meant that assemblages associated with palaeo mudflat environments where there would have been substantial accommodation space was not characterised well within the regional training set as these environments are no longer prevalent at study sites. In this case existing literature describing mudflat assemblages elsewhere in SE

Australia (Yassini and Jones, 1995), and elsewhere(Berkeley et al., 2009; Woodroffe et al., 2005) were used.

7.5. Integrating wetland substrate changes across timescales

Surface elevation dynamics within coastal wetlands of south-eastern Australia was quantified to examine their response to sea-level changes across a range of timescales. It intentionally relied upon techniques that measured processes contributing to elevation change at annual to decadal timescales, and the response of coastal wetlands to these processes at decadal to millennial timescales.

Much of the record contained within the cores was deposited during a time when the sea was relatively stable as is characteristic of far-field regions like Australia, which is remote from former icesheets. The infilling of estuaries with sediment dominated patterns of wetland surface elevation change, whereby the gradual transition of vegetation communities was consistent with accommodation space. Where there was more available accommodation space, such as mudflats and mangroves, transitioned to vegetation communities that occur at high elevations within the tidal frame and have little accommodation space, such as saltmarshes. This pattern of infilling has continued over the past century and where accommodation space is high (i.e. in the mangrove) is increasing sediments at relatively high rates over recent decades (Fig. 7.2). Importantly, sedimentation exceeding rates of SLR within mangrove zones at all study sites confirms that infilling is still occurring despite SLR of up to 1.0 mm/y over the past century. In addition, high rates of sediment accumulation in mangrove implies that the capacity of mangrove forests to adapt to the anticipated SLR has not yet been exhausted. Where accommodation space is more limited (i.e. saltmarsh), the rate of sediment accumulation was not significantly different from relative SLR indicating a balanced negative feedback relationship between SLR and sedimentation (Pethick, 1981; Saintilan et al., 2009).

The capacity of mangrove forests to adjust to SLR was found to not only be controlled by mineral sediment addition but was augmented by organic matter addition, particularly within the root zone of mangrove, provides an important mechanism for increasing wetland elevations as the sea rises. Organic matter addition therefore provides an important subsidy to mineral sedimentation, and mangroves appear to be effectively adding organic matter to substrates than saltmarsh at over short timescales, supported by others (Allen, 2000; Cahoon et al., 2004; McKee, 2011; Rogers et al., 2019a). The limited ability of saltmarsh to subsidise mineral sediment addition with organic matter in substrates over shorter time scales may explain why saltmarsh has been increasingly encroached upon by mangrove in south-eastern Australia.

7.6. Implications

There has been some debate about the relevant timescale at which empirical data should be used within models to project the response of coastal wetlands to SLR (Breithaupt et al., 2018; Kirwan et al., 2016). This study demonstrated that rates of sedimentation and surface elevation vary over time. The variation of sedimentation within and between study sites was high at decadal timescales yet started to correspond at available accommodation space at centurial timescales (Table 7.1). The findings from this study also demonstrates that surface elevation change is related to tidal inundation at the shortest timescales and accommodation space at decadal to millennial timescales. Therefore, models of the response of coastal wetlands based upon a relationship between; (i) sedimentation or surface elevation change, and (ii) inundation or accommodation space are more likely to account for the interacting effect of sedimentation and SLR over time and will result in more accurate projections of the response of wetlands to future SLR. Integrating information across timescales on the basis of changes to accommodation space has been advocated in studies of the response of open coasts to SLR (Cowell and Thom, 1994; Woodroffe et al., 2016), but has yet to be widely undertaken when projecting the response of coastal wetlands to SLR.

Table 7.1: Rates of surface elevation change from rod- and original-SETs (mean rates of changes based on the results from Chapters 2 and 3), and sedimentation over the ^{210}Pb record (mean rates of change based on the results from Chapter 4).

Study area	Vegetation type	Tidal position	Decadal (mm/y)	Centurial (mm/y)
Minnamurra	Mangrove	Mid	1.3 ± 0.31	2.7 ± 0.25
	Saltmarsh	Intermediate	0.13 ± 0.10	1.7 ± 0.071
Comerong Island	Mangrove	Mid	4.3 ± 2.0	5.0 ± 0.064
	Saltmarsh	Intermediate	0.0087 ± 1.5	3.8 ± 0.054
	Dwarf mangrove	High	-1.2 ± 1.4	3.4 ± 0.073
Cararma Inlet	Mangrove	Mid	1.9 ± 0.25	1.3 ± 0.040
	Saltmarsh	High	1.2 ± 0.28	1.2 ± 0.036
Currambene Creek	Mangrove	Mid	0.089 ± 0.076	2.5 ± 0.063
	Saltmarsh	High	-0.51 ± 0.13	0.62 ± 0.030

This study also emphasised the crucial role of sediment supply and subsequent sedimentation for wetland surface elevation change, and the importance of maintaining sediment availability when seas are rising, and accommodation space is increasing. In Australia where water availability is becoming increasingly limited due to climate change, dams for water supply may limit sediment supply over time and maintenance of sediment supply should be prioritised. Policies that support removal of mangrove as they encroach upon saltmarshes with the intention of maintaining saltmarsh extents and the ecosystem services they provide may be limiting the overall capacity of wetlands to adapt to SLR through organic matter addition to substrates, which is largely achieved by mangrove vegetation (Rogers et al., 2016). As saltmarshes have limited capacity to adjust to SLR through organic matter addition, landward retreat zones will become increasingly important, and removal of barriers to landward retreat should be prioritised in coastal zone management plans.

List of References

Adam, P., 2009. Australian saltmarshes in a global context, in: Saintilan, N., Adam, P. (Eds.), Australian Saltmarsh Ecology. CSIRO Publishing, Collingwood, pp. 1–22.

Adame, M.F., Neil, D., Wright, S.F., Lovelock, C.E., 2010. Sedimentation within and among mangrove forests along a gradient of geomorphological settings. Estuarine, Coastal and Shelf Science 86, 21–30. doi:10.1016/j.ecss.2009.10.013

Albani, A.D., 1978. Recent foraminifera of an estuarine environment in Broken Bay, New South Wales. Australian Journal of Marine and Freashwater Research 29, 355–398.

Allen, J.R.L., 1999. Geological impacts on coastal wetland landscapes: some general effects of sediment autocompaction in the Holocene of northwest Europe. The Holocene 9, 1–12. doi:10.1191/095968399674929672

Allen, J.R.L., 2000. Morphodynamics of Holocene salt marshes: a review sketch from the Atlantic and Southern North Sea coasts of Europe. Quaternary Science Reviews 19, 1155–1231. doi:10.1016/S0277-3791(99)00034-7

Allen, J.R.L., Haslett, S.K., 2002. Buried salt-marsh edges and tide-level cycles in the mid-Holocene of the Caldicot Level (Gwent), South Wales, UK. The Holocene 12, 303–324. doi:10.1191/0959683602hl537rp

ANSTO, 2018. Dating of sediment cores using Lead-210 [WWW Document]. URL http://webext.ansto.gov.au/ResearchHub/OurInfrastructure/IsotopeTracinginNaturalSystems/Datingofsedimentcores/index.htm (accessed 7.6.16).

ANU Radiocarbon Dating Centre, 2010. The next chapter in radiocarbon dating at the Australian National University: Status report on the single stage AMS. Nuclear Instruments and Methods in Physics Research B 268, 898–901.

ANU Radiocarbon Laboratory, 2018. Laboratory Methods [WWW Document]. URL http://rses.anu.edu.au/services/anu-radiocarbon-laboratory/laboratory-methods (accessed 8.16.18).

Appleby, P.G., 2008. Three decades of dating recent sediments by fallout radionuclides: a review. The Holocene 18, 83–93. doi:10.1177/0959683607085598

Appleby, P.G., Oldfield, F., 1978. The calculation of lead-210 dates assuming a constant rate of supply of unsupported 210Pb to the sediment. Catena 5, 1–8. doi:10.1016/S0341-8162(78)80002-2

Appleby, P.G., Oldfield, F., 1992. Application of Lead-210 to sedimentation studies, in: Ivanovich, M., Harmon, R.S. (Eds.), Uranium-Series Disequlibrium: Applications to Earth, Marine, and Environmental Sciences. Clarendon Press, Oxford, pp. 731–783.

Armynot du Chatelet, E., Bout-Roumazeilles, V., Riboulleau, A., Trentesaux, A., 2009. Sediment (grain size and clay mineralogy) and organic matter quality control on living benthic foraminifera. Revue de Micropaleontologie 52, 75–84. doi:10.1016/j.revmic.2008.10.002

Avnaim-Katav, S., Roland Gehrels, W., Brown, L.N., Fard, E., MacDonald, G.M., 2017. Distributions of salt-marsh foraminifera along the coast of SW California, USA: Implications for sea-level reconstructions. Marine Micropaleontology 131, 25–43. doi:10.1016/j.marmicro.2017.02.001

Ball, D.F., 1964. Loss-on-ignition as an estimate of organic matter and organic carbon in non-calcareous soils. Journal of Soil Science 15, 84–92. doi:10.1111/j.1365-2389.1964.tb00247.x

Ball, M.C., 1988. Salinity tolerance in the mangroves Aegiceras corniculatum and Avicennia marina. I. Water use in relation to growth, carbon partitioning, and salt balance. Australian Journal of Plant Physiology 15, 447–464. doi:10.1071/PP9880447

Barbier, E.B., Hacker, S.D., Kennedy, C., Koch, E.W., Stier, A.C., Silliman, B.R., 2011. The value of estuarine and coastal ecosystem services. Ecological Monographs 81, 169–193. doi:10.1890/10-1510.1

Barlow, N.L.M., Shennan, I., Long, A.J., Gehrels, W.R., Saher, M.H., Woodroffe, S.A., Hillier, C., 2013. Salt marshes as Late Holocene tide gauges. Global and Planetary Change 106, 90–110. doi:10.1016/j.gloplacha.2013.03.003

Beechey, D., 2018. The seashells of New South Wales [WWW Document]. URL https://seashellsofnsw.org.au/index.htm (accessed 7.10.18).

Berkeley, A., Perry, C.T., Smithers, S.G., Horton, B.P., 2008. The spatial and vertical distribution of living (stained) benthic foraminifera from a tropical, intertidal environment, north Queensland, Australia. Marine Micropaleontology 69, 240–261. doi:10.1016/j.marmicro.2008.08.002

Berkeley, A., Perry, C.T., Smithers, S.G., Horton, B.P., Cundy, A.B., 2009. Foraminiferal biofacies across mangrove-mudflat environments at Cocoa Creek, north Queensland, Australia. Marine Geology 263, 64–86. doi:10.1016/j.margeo.2009.03.019

Berkeley, A., Perry, C.T., Smithers, S.G., Horton, B.P., Taylor, K.G., 2007. A review of the ecological and taphonomic controls on foraminiferal assemblage development in intertidal environments. Earth-Science Reviews 83, 205–230. doi:10.1016/j.earscirev.2007.04.003

Beta Analytic Inc., 2018. Introduction to radiocarbon determination by the Accelerator Mass Spectrometry method. Miami.

Birks, H.J.B., 1995. Quantitative palaeoenvironmental reconstructions, in: Maddy, D., Brew, I.S. (Eds.), Statistical Modelling of Quaternary Science Data. Quaternary Research Association, Cambridge, pp. 161–236.

Boltovskoy, E., Wright, R., 1976. Recent Foraminifera. Junk, The Hague.

Boumans, R.M., Day, J.W.J., 1993. High precision measurements of sediment elevation in shallow coastal areas using a sedimentation–erosion table. Estuaries 16, 375–380.

Bray, J.R., Curtis, J.T., 1957. An ordination of the upland forest communities of Southern Wisconsin. Ecological Monographs 27, 325–349.

Breithaupt, J.L., Smoak, J.M., Byrne, R.H., Waters, M.N., Moyer, R.P., Sanders, C.J., 2018. Avoiding timescale bias in assessments of coastal wetland vertical change. Limnology and Oceanography 63, 477–495. doi:10.1002/lno.10783

Brenner, M., Kenney, W.F., 2013. Dating wetland sediment cores, in: DeLaune, R.D., Reddy, K.R., Richardson, C.J., Megonigal, J.P. (Eds.), Methods in Biogeochemistry of Wetlands. Soil Science Society of America, Madison, pp. 879–900.

Bronnimann, P., Whittaker, J.E., Zaninetti, L., 1992. Brackish water foraminifera from mangrove sediments of southwestern Viti Levu, Fiji Islands, southwest Pacific. Revue de Paleobiologie 11, 13–65.

Brown, N., 2010. AUSGeoid09 : Converting GPS heights to AHD heights, AUSGEO news.

Cahoon, D.R., 2006. A review of major storm impacts on coastal wetland elevations. Estuaries and Coasts 29, 889–898.

Cahoon, D.R., 2015. Estimating relative sea-level rise and submergence potential at a coastal wetland. Estuaries and Coasts 38, 1077–1084. doi:10.1007/s12237-014-9872-8

Cahoon, D.R., Day, J.W., Reed, D.J., 1999. The influence of surface and shallow subsurface soil processes on wetland elevation: A synthesis. Current Topics in Wetland Biogeochemistry 3, 72–88.

Cahoon, D.R., Ford, M.A., Hensel, P.F., 2004. Ecogeomorphology of Spartina patens-dominated tidal marshes: Soil organic matter accumulation, marsh elevation dynamics, and disturbance, in: Fagherazzi, S., Marani, M., Blum, L.K. (Eds.), The Ecogeomorphology Oftidal Marshes: Coastal Estuarine Studies. American Geophysical Union, Washington, pp. 247–266. doi:10.1029/ce059p0247

Cahoon, D.R., French, J.R., Spencer, T., Reed, D., Möller, I., 2000a. Vertical accretion versus elevational adjustment in UK saltmarshes: an evaluation of alternative methodologies, in: Pye, K., Allen, J.R.L. (Eds.), Coastal and Estuarine Environments:" Sedimentology, Geomorphology and Geoarchaeology. Geological Society, London, Special Publications, London, pp. 223–238. doi:10.1144/gsl.sp.2000.175.01.17

Cahoon, D.R., Guntenspergen, G.R., 2010. Climate change, sea-level rise, and coastal wetlands. National Wetlands Newsletter 32, 8–12.

Cahoon, D.R., Hensel, P., Rybczyk, J., McKee, K.L., Proffitt, E.D., Perez, B.C., 2003. Mass tree

mortality leads to mangrove peat coppalse at Bay Islands, Honduras after Hurricane Mitch. Journal of Ecology 91, 1093–1105. doi:10.1021/bk-2009-1006.ch004

Cahoon, D.R., Hensel, P.F., Spencer, T., Reed, D.J., McKee, K.L., Saintilan, N., 2006. Coastal wetland vulnerability to relative sea-level rise: Wetland elevation trends and process controls, in: Verhoeven, J.T.A., Beltman, B., Bobbink, R., Whigham, D.F. (Eds.), Wetlands and Natural Resource Management. Springer-Verlag Berlin Heidelberg, pp. 271–292.

Cahoon, D.R., Lynch, J.C., 1997. Vertical accretion and shallow subsidence in a mangrove forest of southwestern Florida, U.S.A. Mangroves and Salt Marshes 1, 173–186. doi:10.1023/A:1009904816246

Cahoon, D.R., Lynch, J.C., Hensel, P.F., Boumans, R., Perez, B.C., Segura, B., Day, J.W., 2002a. High-precision measurements of wetland sediment elevation: I. Recent improvements to the Sedimentation-Erosion Table. Journal of Sedimentary Research 72, 730–733.

Cahoon, D.R., Lynch, J.C., Perez, B.C., Segura, B., Holland, R.D., Stelly, C., Stephenson, G., Hensel, P., 2002b. High-precision measurements of wetland sediment elevation: II. The Rod Surface Elevation Table. Journal of Sedimentary Research 72, 734–739. doi:10.1306/020702720734

Cahoon, D.R., Marin, P.E., Black, B.K., Lynch, J.C., 2000b. A method for measuring vertical accretion, elevation, and compaction of soft, shallow-water sediments. Journal of Sedimentary Research 70, 1250–1253. doi:10.2110/jsr.2005.038

Cahoon, D.R., Perez, B.C., Segura, B.D., Lynch, J.C., 2011. Elevation trends and shrink-swell response of wetland soils to flooding and drying. Estuarine, Coastal and Shelf Science 91, 463–474. doi:10.1016/j.ecss.2010.03.022

Cahoon, D.R., Reed, D.J., Day, J.W., 1995. Estimating shallow subsidence in microtidal salt marshes of the southeastern United States: Kaye and Barghoorn revisited. Marine Geology 128, 1–9. doi:10.1016/0025-3227(95)00087-F

Callard, S.L., Gehrels, W.R., Morrison, B. V., Grenfell, H.R., 2011. Suitability of salt-marsh foraminifera as proxy indicators of sea level in Tasmania. Marine Micropaleontology 79, 121–131. doi:10.1016/j.marmicro.2011.03.001

Callaway, J.C., Cahoon, D.R., Lynch, J.C., 2013. The Surface Elevation Table-Marker Horizon method for measuring wetland accretion and elevation dymanics, in: DeLaune, R.D., Reddy, K.R., Richardson, C.J., Megonigal, J.P. (Eds.), Methods in Biogeochemistry of Wetlands. Soil Science Society of America, Madison, pp. 901–917.

Cann, J.H., Belperio, A.P., Gostin, V.A., Murray-Wallace, C. V., 1988. Sea-level history, 45,000 to 30,000 yr B.P., inferred from Benthic foraminifera, Gulf St. Vincent, South Australia. Quaternary Research 29, 153–175. doi:10.1016/0033-5894(88)90058-0

Cann, J.H., Belperio, A.P., Gostin, V.A., Rice, R.L., 1993. Contemporary benthic foraminifera

in Gulf St Vincent, South Australia, and a refined Late Pleistocene sea-level history. Australian Journal of Earth Sciences 40, 197–211. doi:10.1080/08120099308728074

Carson, B.E., Francis, J.M., Leckie, R.M., Droxler, A.W., Dickens, G.R., Jorry, S.J., Bentley, S.J., Peterson, L.C., Opdyke, B.N., 2008. Benthic Foraminiferal response to sea level change in the mixed siliciclastic-carbonate system of southern Ashmore Trough (Gulf of Papua). Journal of Geophysical Research: Earth Surface 113, 1–18. doi:10.1029/2006JF000629

Chafer, C.J., 1998a. The effect of temporal geomorphological processes in shorebird populations at Shoalhaven Heads , NSW. University of Wollongong.

Chafer, C.J., 1998b. A Spatio-temporal analysis of estuarine vegetation change in the Minnamurra River 1938-1997. University of Wollongong.

Chanton, J.P., Martens, C.S., Kipphut, G.W., 1983. Lead-210 sediment geochronology in a changing coastal environment. Geochimica et Cosmochimica Acta 47, 1791–1804. doi:10.1016/0016-7037(83)90027-3

Chappell, J., Omura, A., Esat, T., McCulloch, M., Pandolfi, J., Ota, Y., Pillans, B., 1996. Reconciliaion of late Quaternary sea levels derived from coral terraces at Huon Peninsula with deep sea oxygen isotope records. Earth and Planetary Science Letters 141, 227–236. doi:10.1016/0012-821X(96)00062-3

Chappell, J., Shackleton, N.J., 1986. Oxygen isotopes and sea level. Nature 324, 137–140. doi:10.1038/324137a0

Chmura, G.L., Anisfeld, S.C., Cahoon, D.R., Lynch, J.C., 2003. Global carbon sequestration in tidal, saline wetland soils. Global Biogeochemical Cycles 17, n/a-n/a. doi:10.1029/2002GB001917

Church, J.A., White, N.J., 2011. Sea-level rise from the Late 19th to the Early 21st Century. Surveys in Geophysics 32, 585–602. doi:10.1007/s10712-011-9119-1

Church, J.A., White, N.J., Coleman, R., Lambeck, K., Mitrovica, J.X., 2004. Estimates of the regional distribution of sea level rise over the 1950–2000 period. Journal of Climate 17, 2609–2625. doi:10.1175/1520-0442(2004)017<2609:EOTRDO>2.0.CO;2

Church, J.A., White, N.J., Hunter, J.R., 2006. Sea-level rise at tropical Pacific and Indian Ocean islands. Global and Planetary Change 53, 155–168. doi:10.1016/j.gloplacha.2006.04.001

Clarke, P.J., Hutchings, P.A., Adam, P., 1995. Mangroves and saltmarshes, in: Cho, G., Georges, A., Stoutjesdijk, R., Longmore, R. (Eds.), Kowari 5: Jervis Bay - A Place of Cultural, Scientific and Educational Value. Australian Nature Conservation Agency, Canberra, pp. 133–136.

Cotter, K.L., 1996. Benthic foraminiferal assemblages in the Clyde River Estuary, Batemans Bay, N.S.W., in: Proceedings of the Linnean Society of New South Wales. pp. 193–208.

Couriel, E., Alley, K., Modra, B., 2013. OEH NSW Tidal Planes Analysis: 1990-2010 Harmonic Analysis (No. MHL2053).

Cowell, P.J., Thom, B.G., 1994. Morphodynamics of coastal evolution, in: Carter, R.W.G., Woodroffe, C.D. (Eds.), Coastal Evolution: Late Quaternary Shoreline Morphodynamics. Cambridge University Press, Cambridge, pp. 33–86.

Cuffey, K.M., Vimeux, F., 2001. Covariation of carbon dioxide and temperature from the Vostok ice core after deuterium-excess correction. Nature 412, 523–527. doi:10.1038/35087544

Culver, S.J., 1993. Foraminifera, in: Lipps, J.H. (Ed.), Fossil Prokaryotes and Protists. Blackwell Scientific Publications, Boston.

Culver, S.J., Mallinson, D.J., Corbett, D.R., Leorri, E., Rouf, A.A., Shazili, N.A.M., Yaacob, R., Whittaker, J.E., Buzas, M.A., Parham, P.R., 2012. Distribution of foraminifera in the Setiu estuary and lagoon, Terengganu, Malaysia. Journal of Foraminiferal Research 42, 109–133.

de Rijk, S., 1995. Salinity control on the distribution of salt marsh foraminifera (Great Marshes, Massachusetts). Journal of Foraminiferal Research 25, 156–166. doi:10.2113/gsjfr.25.2.156

de Rijk, S., Troelstra, S., 1999. The application of a foraminiferal actuo-facies model to salt-marsh cores. Palaeogeography, Palaeoclimatology, Palaeoecology 149, 59–66.

de Rijk, S., Troelstra, S.R., 1997. Salt marsh foraminifera from the Great Marshes, Massachusetts: environmental controls. Palaeogeography, Palaeoclimatology, Palaeoecology 130, 81–112.

Dean, L.F., De Deckker, P., 2013. Recent benthic foraminifera from Twofold Bay, Eden NSW: community structure, biotopes and distribution controls. Australian Journal of Earth Sciences 60, 475–496. doi:10.1080/08120099.2013.792294

Debenay, J.-P., 2012. A Guide to 1,000 Foraminifera from Southwestern Pacific: New Caledonia. Publications Scientifiques du Muséum, Paris.

Doughty, C.L., Langley, J.A., Walker, W.S., Feller, I.C., Schaub, R., Chapman, S.K., 2016. Mangrove Range Expansion Rapidly Increases Coastal Wetland Carbon Storage. Estuaries and Coasts 39, 385–396. doi:10.1007/s12237-015-9993-8

Edwards, R.J., 2001. Mid- to late Holocene relative sea-level change in Poole Harbour, southern England. Journal of Quaternary Science 16, 221–235. doi:10.1002/jqs.585

Edwards, R.J., Horton, B.P., 2000. Reconstructing relative sea-level change using UK salt marsh foraminifera. Marine Geology 169, 41–56.

Edwards, R.J., van de Plassche, O., Gehrels, W.R., Wright, A.J., 2004a. Assessing sea-level data from Connecticut, USA, using a foraminiferal transfer function for tide level.

Marine Micropaleontology 51, 239–255. doi:10.1016/j.marmicro.2003.11.003

Edwards, R.J., Wright, A.J., van de Plassche, O., 2004b. Surface distributions of salt-marsh foraminifera from Connecticut, USA: Modern analogues for high-resolution sea level studies. Marine Micropaleontology 51, 1–21. doi:10.1016/j.marmicro.2003.08.002

Fagherazzi, S., Kirwan, M.L., Mudd, S.M., Guntenspergen, G.R., Temmerman, S., D'Alpaos, A., van de Koppel, J., Rybczyk, J.M., Reyes, E., Craft, C., Clough, J., 2012. Numerical models of salt marsh evolution: ecological, geomorphic, and climatic factors. Reviews of Geophysics 50, 2011RG000359. doi:10.1029/2011RG000359

Fatela, F., Moreno, J., Moreno, F., Araújo, M.F., Valente, T., Antunes, C., Taborda, R., Andrade, C., Drago, T., 2009. Environmental constraints of foraminiferal assemblages distribution across a brackish tidal marsh (Caminha, NW Portugal). Marine Micropaleontology 70, 70–88. doi:10.1016/j.marmicro.2008.11.001

Fleming, K., Johnston, P., Zwartz, D., Yokoyama, Y., Lambeck, K., Chappell, J., 1998. Refining the eustatic sea level curve since the Last Glacial Maximum using far and intermediate field sites. Earth and Planetary Science Letters 163, 327–342.

Ford, M.A., Cahoon, D.R., Lynch, J.C., 1999. Restoring marsh elevation in a rapidly subsiding salt marsh by thin-layer deposition of dredged material. Ecological Engineering 12, 189–205. doi:10.1016/S0925-8574(98)00061-5

French, P.W., Allen, J.R.L., Appleby, P.G., 1994. 210-Lead dating of a modern period saltmarsh deposit from the Severn Estuary (Southwest Britain), and its implications. Marine Geology 118, 327–334. doi:10.1016/0025-3227(94)90092-2

Friess, D.A., Richards, D.R., Phang, V.X.H., 2016. Mangrove forests store high densities of carbon across the tropical urban landscape of Singapore. Urban Ecosystems 19, 795–810. doi:10.1007/s11252-015-0511-3

Gehrels, W.R., 1994. Determining relative sea-Level change from salt-marsh foraminifera and plant zones on the coast of Maine, U.S.A. Journal of Coastal Research 10, 990–1009.

Gehrels, W.R., 1999. Middle and Late Holocene Sea-Level Changes in Eastern Maine Reconstructed from Foraminiferal Saltmarsh Stratigraphy and AMS 14C Dates on Basal Peat. Quaternary Research 52, 350–359. doi:10.1006/qres.1999.2076

Gehrels, W.R., 2000. Using foraminiferal transfer functions to produce high-resolution sea-level records from salt-marsh deposits, Maine, USA. The Holocene 103, 367–376. doi:10.1191/095968300670746884

Gehrels, W.R., 2002. Intertidal foraminifera as plaeoenvironmental indicators, in: Haslett, S.K. (Ed.), Quaternary Environmental Micropalaeontology. Arnold, London, pp. 91–114.

Gehrels, W.R., Callard, S.L., Moss, P.T., Marshall, W.A., Blaauw, M., Hunter, J., Milton, J.A.,

Garnett, M.H., 2012. Nineteenth and twentieth century sea-level changes in Tasmania and New Zealand. Earth and Planetary Science Letters 315–316, 94–102. doi:10.1016/j.epsl.2011.08.046

Gehrels, W.R., Hayward, B.W., Newnham, R.M., Southall, K.E., 2008. A 20th century acceleration of sea-level rise in New Zealand. Geophysical Research Letters 35, 1–5. doi:10.1029/2007GL032632

Gehrels, W.R., Newman, S.W.G., 2004. Salt-marsh foraminifera in Ho Bugt, western Denmark, and their use as sea-level indicators. Geografisk Tidsskrift Danish Journal of Geography 104, 97–106. doi:10.1080/00167223.2004.10649507

Gehrels, W.R., Roe, H.M., Charman, D.J., 2001. Foraminifera, testate amoebae and diatoms as sea-level indicators in UK saltmarshes: A quantitative multiproxy approach. Journal of Quaternary Science 16, 201–220. doi:10.1002/jqs.588

Gehrels, W.R., Woodworth, P.L., 2013. When did modern rates of sea-level rise start? Global and Planetary Change 100, 263–277. doi:10.1016/j.gloplacha.2012.10.020

Geslin, E., Risgaard-Petersen, N., Lombard, F., Metzger, E., Langlet, D., Jorissen, F., 2011. Oxygen respiration rates of benthic foraminifera as measured with oxygen microsensors. Journal of Experimental Marine Biology and Ecology 396, 108–114. doi:10.1016/j.jembe.2010.10.011

Gilman, E.L., Ellison, J., Duke, N.C., Field, C., 2008. Threats to mangroves from climate change and adaptation options: A review. Aquatic Botany 89, 237–250. doi:10.1016/j.aquabot.2007.12.009

Goldstein, S.T., Watkins, G.T., 1999. Taphonomy of salt marsh foraminifera: an example from coastal Georgia. Palaeogeography, Palaeoclimatology, Palaeoecology 149, 103–114.

Gordillo, S., Bayer, M.S., Boretto, G., Charó, M., 2014. Mollusk shells as bio-geo-archives: Evaluating environmental changes during the Quaternary. Springer. doi:10.1007/978-3-319-03476-8

Grimm, E.C., 1991. Tilia. Illinois State Museum, Springfield.

Guilbault, J.-P., Clague, J.J., Lapointe, M., 1995. Amount of subsidence during a late Holocene earthquake-evidence from fossil tidal marsh foraminifera at Vancouver Island, west coast of Canada. Palaeogeography, Palaeoclimatology, Palaeoecology 118, 49–71. doi:10.1016/0031-0182(94)00135-U

Guilbault, J.-P., Clague, J.J., Lapointe, M., 1996. Foraminiferal evidence for the amount of coseismic subsidence during a late holocene earthquake on Vancouver Island, west coast of Canada. Quaternary Science Reviews 15, 913–937.

Guo, H., Noormets, A., Zhao, B., Chen, Jiquan, Sun, G., Gu, Y., Li, B., Chen, Jiakuan, 2009. Tidal effects on net ecosystem exchange of carbon in an estuarine wetland. Agricultural

and Forest Meteorology 149, 1820–1828. doi:10.1016/j.agrformet.2009.06.010

Hamilton, S., Shennan, I., 2005. Late Holocene relative sea-level changes and the earthquake deformation cycle around upper Cook Inlet, Alaska. Quaternary Science Reviews 24, 1479–1498. doi:10.1016/j.quascirev.2004.11.003

Hammer, O., Harper, D.A.T., Ryan, P.D., 2001. PAST: Paleontological Statistics Software Package for Education and Data Analysis. Palaeontologia Electronica 4, 1–9. doi:10.1016/j.bcp.2008.05.025

Hansen, H.J., 1999. Shell construction in modern calcareous Foraminifera, in: Gupta, B.K. Sen (Ed.), Modern Foraminifera1. Kluwer Academic Press, Dordrecht, pp. 57–70.

Harvard University, 2007. A Summary of Error Propagation [WWW Document]. Physical Sciences 2. URL http://ipl.physics.harvard.edu/wp-uploads/2013/03/PS3_Error_Propagation_sp13.pdf

Haslett, S.K., 2001. The palaeoenvironmental implications of the distribution of intertidal foraminifera in a tropical Australian estuary: a reconnaissance study. Australian Geographical Studies 39, 67–74.

Haslett, S.K., 2007. The distribution of foraminifera in the surface sediments of the Clyde River Estuary and Batemans Bay (New South Wales, Australia). Revista española de micropaleontología 39, 63-70.

Haslett, S.K., Davies-Burrows, R., Panayotou, K., Jones, B.G., Woodroffe, C.D., 2010. Holocene evolution of the Minnamurra River estuary, southeast Australia: foraminiferal evidence. Zeitschrift für Geomorphologie, Supplementary Issues 54, 79–98. doi:10.1127/0372-8854/2010/0054S3-0020

Haslett, S.K., Davies, P., Curr, R.H.F., Davies, C.F.C., Kennington, K., King, C.P., Margetts, A.J., 1998. Evaluating late-Holocene relative sea-level change in the Somerset Levels, southwest Britain. Holocene 8, 197–207. doi:10.1191/095968398669499299

Haynes, J.R., 1981. Foraminifera. Macmillan Publishers Ltd, London.

Hayward, B.W., 1993. Estuarine foraminifera, Helena Bay, Northland, New Zealand. Tane 34, 79–88.

Hayward, B.W., Grenfell, H.R., Nicholson, K., Parker, R., Wilmhurst, J., Horrocks, M., Swales, A., Sabaa, A.T., 2004a. Foraminiferal record of human impact on intertidal estuarine environments in New Zealand's largest city. Marine Micropaleontology 53, 37–66. doi:10.1016/j.marmicro.2004.03.001

Hayward, B.W., Grenfell, H.R., Reid, C.M., Hayward, K.A., 1999a. Recent New Zealand shallow-water benthis foraminifera: Taxonomy, ecological distribution, biogeography, and use in paleoenvironmental assessment, in: Institute of Geological and Nuclear Sciences Monograph 21. p. 264.

Hayward, B.W., Grenfell, H.R., Scott, D.B., 1999b. Tidal range of marsh foraminifera for determining former sea level heights in New Zealand. New Zealand Journal of Geology and Geophysics 42, 395–413. doi:10.1080/00288306.1999.9514853

Hayward, B.W., Hollis, C.J., 1994. Brackish foraminifera in New Zealand: A taxonomic and ecological review. Micropaleontology 40, 185–222.

Hayward, B.W., Le Coze, F., Gross, O., 2018. World Foraminifera Database [WWW Document]. URL http://www.marinespecies.org/foraminifera (accessed 7.2.18).

Hayward, B.W., Neil, H., Carter, R., Grenfell, H.R., Hayward, J.J., 2002. Factors influencing the distribution patterns of recent deep-sea benthic foraminifera, east of New Zealand, Southwest Pacific Ocean. Marine Micropaleontology 46, 139–176.

Hayward, B.W., Sabaa, A.T., Grenfell, H.R., Cochran, U.A., Clark, K.J., Litchfield, N.J., Wallace, L., Marden, M., Palmer, A.S., 2015. Foraminiferal record of Holocene paleo-earthquakes on the subsiding south-western Poverty Bay coastline, New Zealand. New Zealand Journal of Geology and Geophysics 58, 104–122. doi:10.1080/00288306.2014.992354

Hayward, B.W., Scott, G.H., Grenfell, H.R., Carter, R., Lipps, J.H., 2004b. Techniques for estimation of tidal elevation and confinement (~salinity) histories of sheltered harbours and estuaries using benthic foraminifera: examples from New Zealand. The Holocene 14, 218–232. doi:10.1191/0959683604hl678rp

Heap, A.D., Bryce, S., Ryan, D.A., 2004. Facies evolution of Holocene estuaries and deltas: A large-sample statistical study from Australia. Sedimentary Geology 168, 1–17. doi:10.1016/j.sedgeo.2004.01.016

Hogg, A.G., Hua, Q., Blackwell, P.G., Niu, M., Buck, C.E., Guilderson, T.P., Heaton, T.J., Palmer, J.G., Reimer, P.J., Reimer, R.W., Turney, C.S.M., Zimmerman, S.R.H., 2013. SHCAL13 Southern Hemisphere Calibration, 0–50,000 Years cal BP. Radiocarbon 55, 1889–1903. doi:doi:10.2458/azu_js_rc.55.16783

Hollins, S.E., Harrison, J.J., Jones, B.G., Zawadzki, A., Heijnis, H., Hankin, S., 2011. Reconstructing recent sedimentation in two urbanised coastal lagoons (NSW, Australia) using radioisotopes and geochemistry. Journal of Paleolimnology 46, 579–596. doi:10.1007/s10933-011-9555-4

Horton, B.P., 1999. The distribution of contemporary intertidal foraminifera at Cowpen Marsh, Tees Estuary, UK: Implications for studies of Holocene sea-level changes. Palaeogeography, Palaeoclimatology, Palaeoecology. doi:10.1016/S0031-0182(98)00197-7

Horton, B.P., Culver, S.J., Hardbattle, M.I.J., Larcombe, P., Milne, G.A., Morigi, C., Whittaker, J.E., Woodroffe, S.A., 2007. Reconstructing Holocene Sea-Level Change for the Central Great Barrier Reef (Australia) Using Subtidal Foraminifera. Journal of Foraminiferal Research 37, 327–343. doi:10.2113/gsjfr.37.4.327

Horton, B.P., Edwards, R.J., 2003. Seasonal distributions of foraminifera and their implications for sea-level studies, Cowpen Marsh, U.K. SEPM (Society for Sedimentary Geology) Special Publication 75, 21–30.

Horton, B.P., Edwards, R.J., 2006. Quantifying Holocene sea-level change using intertidal foraminifera: Lessons from the British Isles. Cushman Foundation Special Publication 40, 1–97.

Horton, B.P., Edwards, R.J., Lloyd, J.M., 1999a. A foraminiferal-based transfer function: Implications for sea-level studies. Journal of Foraminiferal Research 29, 117–129.

Horton, B.P., Edwards, R.J., Lloyd, J.M., 1999b. UK intertidal foraminiferal distributions: Implications for sea-level studies. Marine Micropaleontology 36, 205–223. doi:10.1016/S0377-8398(99)00003-1

Horton, B.P., Larcombe, P., Woodroffe, S.A., Whittaker, J.E., Wright, M.R., Wynn, C., 2003. Contemporary foraminiferal distributions of a mangrove environment, Great Barrier Reef coastline, Australia: Implications for sea-level reconstructions. Marine Geology 198, 225–243. doi:10.1016/S0025-3227(03)00117-8

Horton, B.P., Milker, Y., Dura, T., Wang, K., Bridgeland, W.T., Brophy, L., Ewald, M., Khan, N.S., Engelhart, S.E., Nelson, A.R., Witter, R.C., 2017. Microfossil measures of rapid sea-level rise: Timing of response of two microfossil groups to a sudden tidal-flooding experiment in Cascadia. Geology 45, G38832.1. doi:10.1130/G38832.1

Horton, B.P., Murray, J.W., 2006. Patterns in cumulative increase in live and dead species from foraminiferal time series of Cowpen Marsh, Tees Estuary, UK: Implications for sea-level studies. Marine Micropaleontology 58, 287–315. doi:10.1016/j.marmicro.2005.10.006

Horton, B.P., Murray, J.W., 2007. The roles of elevation and salinity as primary controls on living foraminiferal distributions: Cowpen Marsh, Tees Estuary, UK. Marine Micropaleontology 63, 169–186. doi:10.1016/j.marmicro.2006.11.006

Horton, B.P., Whittaker, J.E., Thomson, K.H., Hardbattle, M.I.J., Kemp, A., Woodroffe, S.A., Wright, M.R., 2005. The development of a modern foraminiferal data Set for sea-level reconstructions, Wakatobi Marine National Park, Southeast Sulawesi, Indonesia. Journal of Foraminiferal Research 35, 1–14. doi:10.2113/35.1.1

Howe, A.J., Rodríguez, J.F., Saco, P.M., 2009. Surface evolution and carbon sequestration in disturbed and undisturbed wetland soils of the Hunter estuary, southeast Australia. Estuarine, Coastal and Shelf Science 84, 75–83. doi:10.1016/j.ecss.2009.06.006

IPCC, 2014. Climate Change 2014: Synthesis Report. Contribution of Working Groups I, II and III to the Fifth Assessment Report of the Intergovernmental Panel on Climate Change. Geneva.

Ivanovich, M., Harmon, R.S., 1982. Uranium Series Disequilibrium: Applications to Environmental Problems. Oxford University, New York.

Jervey, M.T., 1988. Quantitative geological modeling of siliciclastic rock sequences and their seismic expression, in: Wilgus, C., Hastings, B., Posamentier, H., Wagoner, J. Van, Ross, C., Kendall, C. (Eds.), Sea-Level Changes: An Integrated Approach. SEPM Special Publication, Tulsa, OK, pp. 47–69. doi:10.2110/pec.88.01.0047

Juggins, S., 2016. C2, version 1.7.7. [WWW Document]. URL https://www.staff.ncl.ac.uk/stephen.juggins/software/C2Home.htm (accessed 9.19.16).

Karlsen, A.W., Cronin, T.M., Ishman, S.E., Willard, D.A., Kerhin, R., Holmes, C.W., Marot, M., 2000. Historical Trends in Chesapeake Bay Dissolved Oxygen Based on Benthic Foraminifera from Sediment Cores. Estuaries 23, 488. doi:10.2307/1353141

Kaye, C.A., Barghoorn, E.S., 1964. Late Quaternary sea-level change and crustal rise at Boston, Massachusetts, with notes on the autocompaction of peat. Geological Society of America Bulletin 75, 63–80.

Kelleway, J.J., Saintilan, N., Macreadie, P.I., Skilbeck, C.G., Zawadzki, A., Ralph, P.J., 2016. Seventy years of continuous encroachment substantially increases "blue carbon" capacity as mangroves replace intertidal salt marshes. Global Change Biology 22, 1097–1109. doi:10.1111/gcb.13158

Kemp, A.C., Horton, B.P., Culver, S.J., 2009. Distribution of modern salt-marsh foraminifera in the Albemarle–Pamlico estuarine system of North Carolina, USA: Implications for sea-level research. Marine Micropaleontology 72, 222–238. doi:10.1016/j.marmicro.2009.06.002

Kemp, A.C., Horton, B.P., Vane, C.H., Bernhardt, C.E., Corbett, D.R., Engelhart, S.E., Anisfeld, S.C., Parnell, A.C., Cahill, N., 2013. Sea-level change during the last 2500 years in New Jersey, USA. Quaternary Science Reviews 81, 90–104. doi:10.1016/j.quascirev.2013.09.024

Kirwan, M., Temmerman, S., 2009. Coastal marsh response to historical and future sea-level acceleration. Quaternary Science Reviews 28, 1801–1808. doi:10.1016/j.quascirev.2009.02.022

Kirwan, M.L., Guntenspergen, G.R., 2010. Influence of tidal range on the stability of coastal marshland. Journal of Geophysical Research: Earth Surface 115, 1–11. doi:10.1029/2009jf001400

Kirwan, M.L., Guntenspergen, G.R., D'Alpaos, A., Morris, J.T., Mudd, S.M., Temmerman, S., 2010. Limits on the adaptability of coastal marshes to rising sea level. Geophysical Research Letters 37. doi:10.1029/2010GL045489

Kirwan, M.L., Megonigal, J.P., 2013. Tidal wetland stability in the face of human impacts and sea-level rise. Nature 504, 53–60. doi:10.1038/nature12856

Kirwan, M.L., Mudd, S.M., 2012. Response of salt-marsh carbon accumulation to climate change. Nature 489, 550–3. doi:10.1038/nature11440

Kirwan, M.L., Temmerman, S., Skeehan, E.E., Guntenspergen, G.R., Faghe, S., 2016. Overestimation of marsh vulnerability to sea level rise. Nature Climate Change 6, 253–260. doi:10.1038/nclimate2909

Kolker, A.S., Kirwan, M.L., Goodbred, S.L., Cochran, J.K., 2010. Global climate changes recorded in coastal wetland sediments: Empirical observations linked to theoretical predictions. Geophysical Research Letters 37, 1–5. doi:10.1029/2010GL043874

Krauss, K.W., Allen, J.A., Cahoon, D.R., 2003. Differential rates of vertical accretion and elevation change among aerial root types in Micronesian mangrove forests. Estuarine, Coastal and Shelf Science 56, 251–259. doi:10.1016/S0272-7714(02)00184-1

Krauss, K.W., McKee, K.L., Lovelock, C.E., Cahoon, D.R., Saintilan, N., Reef, R., Chen, L., 2014. How mangrove forests adjust to rising sea level. New Phytologist 202, 19–34. doi:10.1111/nph.12605

Laegdsgaard, P., Kelleway, J., Williams, R.J., Harty, C., 2009. Protection and management of coastal saltmarsh, in: Saintilan, N. (Ed.), Australian Saltmarsh Ecology. CSIRO Publishing, Collingwood, pp. 179–210.

Lambeck, K., 2002. Sea level change from mid Holocene to Recent time: An Australian example with global implications. Ice Sheets, Sea Level and the Dynamic Earth. doi:10.1029/GD029p0033

Lambeck, K., Nakada, M., 1990. Late Pleistocene and Holocene sea-level change along the Australian coast. Global and Planetary Change 3, 143–176. doi:10.1016/0921-8181(90)90060-P

Leckie, R.M., Olson, H.C., 2003. Foraminifera as proxies for sea-level change on siliciclastic margins. SEPM (Society for Sedimentary Geology) Special Publication 5–19.

Lee, J.J., Anderson, O.R., 1991. Cytology and fine structure, in: Lee, J.J., Anderson, O.R. (Eds.), Biology of Foraminifera. Academic Press Inc., San Diego, pp. 7–40.

Leorri, E., Cearreta, A., Horton, B.P., 2008a. A foraminifera-based transfer function as a tool for sea-level reconstructions in the southern Bay of Biscay. Geobios 41, 787–797. doi:10.1016/j.geobios.2008.03.003

Leorri, E., Gehrels, W.R., Horton, B.P., Fatela, F., Cearreta, A., 2010. Distribution of foraminifera in salt marshes along the Atlantic coast of SW Europe: Tools to reconstruct past sea-level variations. Quaternary International 221, 104–115. doi:10.1016/j.quaint.2009.10.033

Leorri, E., Horton, B.P., Cearreta, A., 2008b. Development of a foraminifera-based transfer function in the Basque marshes, N. Spain: Implications for sea-level studies in the Bay of Biscay. Marine Geology 251, 60–74. doi:10.1016/j.margeo.2008.02.005

Lewis, S.E., Sloss, C.R., Murray-Wallace, C. V., Woodroffe, C.D., Smithers, S.G., 2013. Post-

glacial sea-level changes around the Australian margin: A review. Quaternary Science Reviews 74, 115–138. doi:10.1016/j.quascirev.2012.09.006

Loeblich, A.R.J., Tappan, H., 1988. Foraminiferal genera and their classification, Vol. 1. ed. Van Nostrand Reinhold Co., New York.

Long, A., 2001. Mid-Holocene sea-level change and coastal evolution. Progress in Physical Geography 25, 399–408. doi:10.1177/030913330102500307

Lovelock, C.E., Adame, M.F., Bennion, V., Hayes, M., Reef, R., Santini, N., Cahoon, D.R., 2015a. Sea level and turbidity controls on mangrove soil surface elevation change. Estuarine, Coastal and Shelf Science 153, 1–9. doi:10.1016/j.ecss.2014.11.026

Lovelock, C.E., Bennion, V., Grinham, A., Cahoon, D.R., 2011. The role of surface and subsurface processes in keeping pace with sea-level rise in intertidal wetlands of Moreton Bay, Queensland, Australia. Ecosystems 14, 745–757. doi:10.1007/s10021-011-9443-9

Lovelock, C.E., Cahoon, D.R., Friess, D.A., Guntenspergen, G.R., Krauss, K.W., Reef, R., Rogers, K., Saunders, M.L., Sidik, F., Swales, A., Saintilan, N., Thuyen, L.X., Triet, T., 2015b. The vulnerability of Indo-Pacific mangrove forests to sea-level rise. Nature 526, 559. doi:10.1038/nature15538

Lynch, J.C., Hensel, P., Cahoon, D.R., 2015. The surface elevation table and marker horizon technique: A protocol for monitoring wetland elevation dynamics, Natural Resource Report NPS/NCBN/NRR. National Park Service, Fort Collins, Colorado.

Marchio, D.A., Savarese, M., Bovard, B., Mitsch, W.J., 2016. Carbon sequestration and sedimentation in mangrove swamps influenced by hydrogeomorphic conditions and urbanization in Southwest Florida. Forests 7. doi:10.3390/f7060116

Mazda, Y., Wolanski, E., King, B., Sase, A., Ohtsuka, D., Magi, M., 1997. Drag force due to vegetation in mangrove swamps. Mangroves and Salt Marshes 1, 193–199. doi:10.1023/A:1009949411068

McFadden, L., Spencer, T., Nicholls, R.J., 2007. Broad-scale modelling of coastal wetlands: what is required? Hydrobiologia 577, 5–15. doi:10.1007/s10750-006-0413-8

McKee, K., Rogers, K., Saintilan, N., 2012. Response of salt marsh and mangrove wetlands to changes in atmospheric CO2, climate, and sea level, in: Middleton, B.A. (Ed.), Global Change and the Function and Distribution of Wetlands. Springer, Dordrecht, pp. 63–96.

McKee, K.L., 2011. Biophysical controls on accretion and elevation change in Caribbean mangrove ecosystems. Estuarine, Coastal and Shelf Science 91, 475–483. doi:10.1016/j.ecss.2010.05.001

McKee, K.L., Cahoon, D.R., Feller, I.C., 2007. Caribbean mangroves adjust to rising sea level through biotic controls on change in soil elevation. Global Ecology and Biogeography

16, 545–556. doi:10.1111/j.1466-8238.2007.00317.x

Mcleod, E., Chmura, G.L., Bouillon, S., Salm, R., Björk, M., Duarte, C.M., Lovelock, C.E., Schlesinger, W.H., Silliman, B.R., 2011. A blueprint for blue carbon: toward an improved understanding of the role of vegetated coastal habitats in sequestering CO2. Frontiers in Ecology and the Environment 9, 552–560. doi:10.1890/110004

Milker, Y., Horton, B.P., Nelson, A.R., Engelhart, S.E., Witter, R.C., 2015a. Variability of intertidal foraminiferal assemblages in a salt marsh, Oregon, USA. Marine Micropaleontology 118, 1–16. doi:10.1016/j.marmicro.2015.04.004

Milker, Y., Horton, B.P., Vane, C.H., Engelhart, S.E., Nelson, A.R., Witter, R.C., Khan, N.S., Bridgeland, W.T., 2015b. Annual and seasonal distribution of intertidal foraminifera and stable carbon isotope geochemistry, Bandon Marsh, Oregon, USA. Journal of Foraminiferal Research 45, 146–166. doi:10.2113/gsjfr.45.2.146

Mills, H., Kirby, J., Holgate, S., Plater, A., 2013. The distribution of contemporary saltmarsh foraminifera in a macrotidal estuary: An assessment of their viability for sea-level studies. Journal of Ecosystem & Ecography 3. doi:10.4172/2157-7625.1000131

Mills, M., Leon, J.X., Saunders, M.I., Bell, J., Liu, Y., O'Mara, J., Lovelock, C.E., Mumby, P.J., Phinn, S., Possingham, H.P., Tulloch, V., Mutafoglu, K., Morrison, T., Callaghan, D., Baldock, T., Klein, C.J., Hoegh-Guldberg, O., 2015. Reconciling development and conservation under coastal squeeze from rising sea-level. Conservation Letters in press, 1–7. doi:10.1111/conl.12213

Milne, G.A., 2014. Sea Level, in: Masselink, G., Gehrels, W.R. (Eds.), Coastal Environments and Global Change. Wiley, Somerset, pp. 28–51.

Moodley, L., van der Zwaan, G.J., Herman, P.M.J., Kempers, L., van Breugel, P., 1997. Differential response of benthic meiofauna to anoxia with special reference to Foraminifera (Protista: Sarcodina). Marine Ecology Progress Series 158, 151–163.

Morris, J.T., Sundareshwar, P.V., Nietch, C.T., Kjerfve, B., Cahoon, D.R., 2002. Responses of coastal wetlands to rising sea level. Ecology 83, 2869–2877.

Morrison, B. V., Ellison, J.C., 2017. Palaeo-environmental approaches to reconstructing sea level changes in estuaries, in: Weckström, K., Saunders, K., Gell, P., Skilbeck, G. (Eds.), Applications of Paleoenvironmental Techniques in Estuarine Studies. Developments in Paleoenvironmental Research, pp. 471–494. doi:10.1007/978-94-024-0990-1

Mudd, S.M., Fagherazzi, Sergio, Morris, J.T., Furbish, D.J., 2004. Flow, sedimentation, and biomass production on a vegetated salt marsh in South Carolina: Toward a predictive model of marsh morphologic and ecologic evolution, in: Fagherazzi, S., Marani, A., Blum, L.K. (Eds.), Coastal and Estuarine Studies. American Geophysical Union, Washington D.C., pp. 165–187. doi:10.1029/ce059p0165

Murray-Wallace, C. V., Ferland, M.A., Roy, P.S., Sollar, A., 1996. Unravelling patterns of reworking in lowstand shelf deposits using amino acid racemisation and radiocarbon

dating. Quaternary Science Reviews 15, 685–697. doi:10.1016/0277-3791(96)00031-5

Murray-Wallace, C. V., Woodroffe, C.D., 2014. Quaternary Sea-Level Changes. Cambridge University Press, Cambridge.

Murray, J.W., 1968. The Living Foraminiferida of Christchurch Harbour, England. Micropaleontology 14, 83–96.

Murray, J.W., 2006. Ecology and Applications of Benthic Foraminifera. Cambridge University Press, Cambridge.

Murray, J.W., Bowser, S.S., 2000. Mortality, protoplasm decay rate, and reliability of staining techniques to recognize "living" Foraminifera: A review. Journal of Foraminiferal Research 30, 66–70. doi:10.2113/0300066

Nolte, S., Koppenaal, E.C., Esselink, P., Dijkema, K.S., Schuerch, M., De Groot, A. V., Bakker, J.P., Temmerman, S., 2013. Measuring sedimentation in tidal marshes: A review on methods and their applicability in biogeomorphological studies. Journal of Coastal Conservation 17, 301–325. doi:10.1007/s11852-013-0238-3

NPWS, 1998. Seven Mile Beach National Park and Comerong Island Nature Reserve.

Nuttle, W.K., Hemond, H.F., Stolzenbach, K.D., 1990. Mechanims of water storage in saltmarsh sediments: The importance of dilation. Hydrological Process 4, 1–13.

Owers, C.J., Rogers, K., Woodroffe, C.D., 2016. Identifying spatial variability and complexity in wetland vegetation using an object-based approach. International Journal of Remote Sensing 37, 4296–4316. doi:10.1080/01431161.2016.1211349

Panayotou, K., Woodroffe, C.D., Jones, B.G., Chenhall, B., Mclean, E., Heijnis, H., 2007. Patterns and Rates of Sedimentary Infill in the Minnamurra River Estuary , South-Eastern Australia. Journal of Coastal Conservation 688–692.

Papaspyrou, S., Diz, P., García-Robledo, E., Corzo, A., Jimenez-Arias, J.-L., 2013. Benthic foraminiferal community changes and their relationship to environmental dynamics in intertidal muddy sediments (Bay of Cádiz, SW Spain). Marine Ecology Progress Series 490, 121–135. doi:10.3354/meps10447

Patterson, R.T., Dalby, A.P., Roe, H.M., Guilbault, J., Hutchinson, I., Clague, J.J., 2014. Relative utility of foraminifera, diatoms and macrophytes as high resolution indicators of paleo-sea level in coastal British Columbia, Canada. Quaternary Science Reviews 24, 2002–2014. doi:10.1016/j.quascirev.2004.11.013

Pethick, J.S., 1981. Long-term Accretion Rates on Tidal Salt Marshes. Journal of Sedimentary Petrology 51, 571–577. doi:10.1306/212f7cde-2b24-11d7-8648000102c1865d

Pirazzoli, P.A., 1991. World Atlas of Holocene Sea-Level Changes, Elsevier Oceanography

Series. Elsevier, Amsterdam.

Pratolongo, P.D., Kirby, J.R., Plater, A., Brinson, M.M., 2009. Temperate Coastal Wetlands: Morphology, sediment processes, and plant communities, in: Perillo, G.M.E., Wolanski, E., Cahoon, D.R., Brinson, M.M. (Eds.), Coastal Wetlands: An Integrated Ecosystem Approach. Elsevier, Amsterdam, pp. 89–118.

Rayment, G.E., Lyons, D.J., 2011. Soil Chemicals Methods - Australasia. CSIRO Publishing, Collingwood.

Reed, D.J., 2002. Sea-level rise and coastal marsh sustainability: Geological and ecological factors in the Mississippi delta plain. Geomorphology 48, 233–243. doi:10.1016/S0169-555X(02)00183-6

Rogers, K., 2004. Mangrove and saltmarsh surface elevation dynamics in relation to environmental variables in southeastern Australia. University of Wollongong.

Rogers, K., Boon, P., Lovelock, C., Saintilan, N., 2017. Coastal Halophytic Vegetation, in: Keith, D.A. (Ed.), Australian Vegetation. Cambridge University Press, Cambridge, pp. 544–569.

Rogers, K., Boon, P.I., Branigan, S., Duke, N.C., Field, C.D., Fitzsimons, J.A., Kirkman, H., Mackenzie, J.R., Saintilan, N., 2016. The state of legislation and policy protecting Australia's mangrove and salt marsh and their ecosystem services. Marine Policy 72, 139–155. doi:10.1016/j.marpol.2016.06.025

Rogers, K., Kelleway, J.J., Saintilan, N., Megonigal, J.P., Adams, J.B., Holmquist, J.R., Lu, M., Schile-Beers, L., Zawadzki, A., Mazumder, D., Woodroffe, C.D., 2019a. Wetland carbon storage controlled by millennial-scale variation in relative sea-level rise. Nature. doi:10.1038/s41586-019-0951-7

Rogers, K., Krauss, K.W., 2018. Moving from generalisations to specificity about mangrove –saltmarsh dynamics. Wetlands 1–24. doi:10.1007/s13157-018-1067-9

Rogers, K., Saintilan, N., 2008. Relationships between Surface Elevation and Groundwater in Mangrove Forests of Southeast Australia. Journal of Coastal Research 24, 63–69. doi:10.2112/05-0519.1

Rogers, K., Saintilan, N., Cahoon, D.R., 2005a. Surface Elevation Dynamics in a Regenerating Mangrove Forest at Homebush Bay, Australia. Wetlands Ecology and Management 13, 587–598. doi:10.1007/s11273-004-0003-3

Rogers, K., Saintilan, N., Copeland, C., 2012. Modelling wetland surface elevation dynamics and its application to forecasting the effects of sea-level rise on estuarine wetlands. Ecological Modelling 244, 148–157. doi:10.1016/j.ecolmodel.2012.06.014

Rogers, K., Saintilan, N., Copeland, C., 2013a. Managed Retreat of Saline Coastal Wetlands: Challenges and Opportunities Identified from the Hunter River Estuary, Australia. Estuaries and Coasts 37, 67–78. doi:10.1007/s12237-013-9664-6

Rogers, K., Saintilan, N., Heijnis, H., 2005b. Mangrove encroachment of saltmarsh in Western Port Bay, Victoria: the role of sedimentation, subsidence, and sea level rise. Estuaries 28, 551–559.

Rogers, K., Saintilan, N., Howe, A.J., Rodríguez, J.F., 2013b. Sedimentation, elevation and marsh evolution in a southeastern Australian estuary during changing climatic conditions. Estuarine, Coastal and Shelf Science 133, 172–181. doi:10.1016/j.ecss.2013.08.025

Rogers, K., Saintilan, N., Mazumder, D., Kelleway, J.J., 2019b. Mangrove dynamics and blue carbon sequestration. Biology Letters 15. doi:10.1098/rsbl.2018.0471

Rogers, K., Wilton, K.M., Saintilan, N., 2006. Vegetation change and surface elevation dynamics in estuarine wetlands of southeast Australia. Estuarine, Coastal and Shelf Science 66, 559–569. doi:10.1016/j.ecss.2005.11.004

Rogers, K., Woodroffe, C.D., 2014. Tidal Flats and Salt Marshes, in: Masselink, G., Gehrels, W.R. (Eds.), Coastal Environments and Global Change. Wiley, Somerset, pp. 227–250.

Roper, T., Creese, B., Scanes, P., Stephens, K., Williams, R., Dela-Cruz, J., Coade, G., Coates, B., Fraser, M., 2011. Assessing the condition of estuaries and coastal lake ecosystems in NSW, Monitoring, evaluation and reporting program, Technical report series. Sydney.

Roy, P.S., 1984. New South Wales estuaries: their origin and evolution, in: Thom, B.G. (Ed.), Coastal Geomorphology in Australia. Academic Press, New York, pp. 99–121.

Roy, P.S., Williams, R.J., Jones, A.R., Yassini, I., Gibbs, P.J., Coates, B., West, R.J., Scanes, P.R., Hudson, J.P., Nichol, S., 2001. Structure and Function of South-east Australian Estuaries. Estuarine, Coastal and Shelf Science 53, 351–384. doi:10.1006/ecss.2001.0796

Ruiz-Fernández, A.C., Sanchez-Cabeza, J.A., Serrato de la Peña, J.L., Perez-Bernal, L.H., Cearreta, A., Flores-Verdugo, F., Machain-Castillo, M.L., Chamizo, E., García-Tenorio, R., Queralt, I., Dunbar, R., Mucciarone, D., Diaz-Asencio, M., 2016. Accretion rates in coastal wetlands of the southeastern Gulf of California and their relationship with sea-level rise. The Holocene 26, 1126–1137. doi:10.1177/0959683616632882

Saintilan, N., Rogers, K., 2013. The significance and vulnerability of Australian saltmarshes: implications for management in a changing climate. Marine and Freshwater Research 64, 66. doi:10.1071/MF12212

Saintilan, N., Rogers, K., Howe, A., 2009. Geomorphology and habitat dynamics, in: Saintilan, N., Rogers, K., Howe, A. (Eds.), Australian Saltmarsh Ecology. CSIRO Publishing, Collingwood.

Saintilan, N., Rogers, K., Mazumder, D., Woodroffe, C.D., 2013a. Allochthonous and autochthonous contributions to carbon accumulation and carbon store in southeastern Australian coastal wetlands. Estuarine, Coastal and Shelf Science 128, 84–92. doi:10.1016/j.ecss.2013.05.010

Saintilan, N., Williams, R.J., 1999. Mangrove transgression into saltmarsh environments in south-east Australia. Global Ecology and Biogeography 8, 117–124. doi:10.1046/j.1365-2699.1999.00133.x

Saintilan, N., Wilson, N.C., Rogers, K., Rajkaran, A., Krauss, K.W., 2013b. Mangrove expansion and salt marsh decline at mangrove poleward limits. Global Change Biology 20, 147–57. doi:10.1111/gcb.12341

Saintilan, N., Wilton, K., 2001. Changes in the distribution of mangroves and saltmarshes in Jervis Bay, Australia. Wetlands Ecology and Management 9, 409–420. doi:10.1023/A:1012073018996

Sainty, G., Hosking, J., Carr, G., Adam, P. (Eds.), 2012. Estuary plants and what's happening to them in south-east Australia. Sainty and Associates, Sydney.

Sanders, C.J., Smoak, J.M., Naidu, A.S., Araripe, D.R., Sanders, L.M., Patchineelam, S.R., 2010a. Mangrove forest sedimentation and its reference to sea level rise, Cananeia, Brazil. Environmental Earth Sciences 60, 1291–1301. doi:10.1007/s12665-009-0269-0

Sanders, C.J., Smoak, J.M., Naidu, A.S., Sanders, L.M., Patchineelam, S.R., 2010b. Organic carbon burial in a mangrove forest, margin and intertidal mud flat. Estuarine, Coastal and Shelf Science 90, 168–172. doi:10.1016/j.ecss.2010.08.013

Schoot, P.M., De Jong, J.E.A., 1982. Sedimentation and erosion measure- ments with the use of the Sed-Eros Table, SET. doi:Notitie DDM1 82.401

Schuerch, M., Spencer, T., Temmerman, S., Kirwan, M.L., Wolff, C., Lincke, D., McOwen, C.J., Pickering, M.D., Reef, R., Vafeidis, A.T., Hinkel, J., Nicholls, R.J., Brown, S., 2018a. Future response of global coastal wetlands to sea-level rise. Nature 561, 231–234. doi:10.1038/s41586-018-0476-5

Schuerch, M., Spencer, T., Temmerman, S., Kirwan, M.L., Wolff, C., Lincke, D., McOwen, C.J., Pickering, M.D., Reef, R., Vafeidis, A.T., Hinkel, J., Nicholls, R.J., Brown, S., 2018b. Future response of global coastal wetlands to sea-level rise. Nature 561, 231–234. doi:10.1038/s41586-018-0476-5

Scott, D.B., Mediolo, F.S., 1980. Living vs. total foraminiferal populations: Their relative usefulness in Paleoecology.pdf. Journal of Paleontology 54, 814–831.

Scott, D.B., Mediolo, F.S., Schafer, C.T., 2001. Monitoring in coastal environments using foraminifera and thecamoebian indicators, 1st ed. Cambridge University Press, Cambridge.

Scott, D.S., Medioli, F.S., 1978. Vertical zonations of marsh foraminifera as accurate indicators of former sea-levels. Nature 272, 528–531. doi:10.1038/272528a0

Semensatto-Jr., D.L., Funo, R.H.F., Dias-Brito, D., Coelho-Jr., C., 2009. Foraminiferal ecological zonation along a Brazilian mangrove transect: Diversity, morphotypes and

the influence of subaerial exposure time. Revue de Micropaleontologie 52, 67–74. doi:10.1016/j.revmic.2008.06.004

Sen Gupta, B.K., 1999. Introduction to modern foraminifera, in: Sen Gupta, B.K. (Ed.), Modern Foraminifera. Springer Netherlands, Dordrecht, pp. 3–6. doi:10.1007/0-306-48104-9_1

Shennan, I., Horton, B., 2002. Holocene land- and sea-level changes in Great Britain. Journal of Quaternary Science 17, 511–526. doi:10.1002/jqs.710

Shennan, I., Long, A.J., Rutherford, M.M., Green, F.M., Innes, J.B., Lloyd, J.M., Zong, Y., Walker, K.J., 1996. Tidal marsh stratigraphy, sea-level change and large earthquakes, I: A 5000 year record in Washington, U.S.A. Quaternary Science Reviews 15, 1023–1059. doi:10.1016/S0277-3791(96)00007-8

Shennan, I., Long, A.J., Rutherford, M.M., Innes, J.B., Green, F.M., Walker, K.J., 1998. Tidal marsh stratigraphy, sea-level change and large earthquakes—II: Submergence events during the last 3500 years at Netarts Bay, Oregon, USA. Quaternary Science Reviews 17, 365–393.

Sloss, C.R., Murray-Wallace, C. V., Jones, B.G., 2007. Holocene sea-level change on the southeast coast of Australia: a review. The Holocene 17, 999–1014. doi:10.1177/0959683607082415

Southall, K.E., Gehrels, W.R., Hayward, B.W., 2006. Foraminifera in a New Zealand salt marsh and their suitability as sea-level indicators. Marine Micropaleontology 60, 167–179. doi:10.1016/j.marmicro.2006.04.005

Strotz, L., 2003. Holocene foraminifera from Tuross Estuary and Coila Lake, South Coast, New South Wales: A preliminary study. Proceedings of the Linnean Society of New South Wales 124, 163–182.

Strotz, L.C., 2012. Foraminiferal Fauna and Biotopes of a Barrier Estuary System: St Georges Basin, New South Wales, Australia. Journal of Foraminiferal Research 42, 369–382. doi:10.2113/gsjfr.42.4.369

Strotz, L.C., 2015. Spatial patterns and diversity of foraminifera from an intermittently closed and open lagoon, Smiths Lake, Australia. Estuarine, Coastal and Shelf Science 164, 340–352. doi:10.1016/j.ecss.2015.07.048

Stuiver, M., Reimer, P.J., Reimer, R.W., 2018. CALIB 7.1 [WWW Document]. URL http://calib.org/calib/calib.html (accessed 10.26.18).

Swales, A., Bentley, S.J., Lovelock, C.E., 2015. Mangrove-forest evolution in a sediment-rich estuarine system: Opportunists or agents of geomorphic change? Earth Surface Processes and Landforms 40, 1672–1687. doi:10.1002/esp.3759

Taylor, G., Abell, R., Paterson, I., 1995. Geology, geomorphology, soils and earth resources, in: Cho, G., Georges, A., Stoutjesdijk, R., Longmore, R. (Eds.), Kowari 5: Jervis Bay - A

Place of Cultural, Scientific and Educational Value. Australian Nature Conservation Agency, Canberra, pp. 41–51.

Temmerman, S., Govers, G., Meire, P., Wartel, S., 2003. Modelling long-term tidal marsh growth under changing tidal conditions and suspended sediment concentrations, Scheldt estuary, Belgium. Marine Geology 193, 151–169.

Temmerman, S., Govers, G., Wartel, S., Meire, P., 2004. Modelling estuarine variations in tidal marsh sedimentation: response to changing sea level and suspended sediment concentrations. Marine Geology 212, 1–19. doi:10.1016/j.margeo.2004.10.021

Temmerman, S., Meire, P., Bouma, T.J., Herman, P.M.J., Ysebaert, T., De Vriend, H.J., 2013. Ecosystem-based coastal defence in the face of global change. Nature 504, 79–83. doi:10.1038/nature12859

ter Braak, C.J.F., 1986. Canonical correspondence analysis: a new eigenvector technique for multivariate direct gradient analysis. Ecology 67, 1167–1179.

ter Braak, C.J.F., Juggins, S., 1993. Weighted averaging partial least squares regression (WA-PLS): an improved method for reconstructing environmental variables from species assemblages. Hydrobiologia 269/270, 485–502. doi:10.1007/BF00028046

Thom, B.G., Roy, P.S., 1985. Relative sea levels and coastal sedimentation in southeast Australia in the Holocene. Journal of Sedimentary Petrology 55, 0257–0264.

Torio, D.D., Chmura, G.L., 2013. Assessing Coastal Squeeze of Tidal Wetlands. Journal of Coastal Research 290, 1049–1061. doi:10.2112/JCOASTRES-D-12-00162.1

Tyler, A.N., Carter, S., Davidson, D.A., Long, D.J., Tipping, R., 2001. The extent and significance of bioturbation on 137 cs distributions in upland soils. Catena 43, 81–99. doi:10.1016/S0341-8162(00)00127-2

Walker, M., 2005. Quaternary Dating Methods. John Wiley & Sons Ltd, Chichester.

Walton, W.R., 1952. Techniques for recognition of living foraminifera. Contribution of Cushman Foundation for Foraminiferal Research 3, 56–60.

Wang, P., Chappell, J., 2001. Foraminifera as Holocene environmental indicators in the South Alligator River, Northern Australia. Quaternary International 83–85, 47–62. doi:10.1016/S1040-6182(01)00030-1

Webb, E.L., Friess, D.A., Krauss, K.W., Cahoon, D.R., Guntenspergen, G.R., Phelps, J., 2013. A global standard for monitoring coastal wetland vulnerability to accelerated sea-level rise. Nature Climate Change 3, 458–465. doi:10.1038/nclimate1756

Whelan, K.R.T., Smith, T.J., Anderson, G.H., Ouellette, M.L., 2009. Hurricane Wilma's impact on overall soil elevation and zones within the soil profile in a mangrove forest. Wetlands 29, 16–23. doi:10.1672/08-125.1

Whelan, K.R.T., Smith, T.J., Cahoon, D.R., Lynch, J.C., Anderson, G.H., 2005. Groundwater control of mangrove surface elevation: Shrink and swell varies with soil depth. Estuaries 28, 833–843. doi:10.1007/BF02696013

White, N.J., Haigh, I.D., Church, J. a., Koen, T., Watson, C.S., Pritchard, T.R., Watson, P.J., Burgette, R.J., McInnes, K.L., You, Z.-J., Zhang, X., Tregoning, P., 2014. Australian sea levels—Trends, regional variability and influencing factors. Earth-Science Reviews 136, 155–174. doi:10.1016/j.earscirev.2014.05.011

Woodroffe, C.D., 2002. Coasts: Form, process and evolution. Cambridge University Press, Cambridge.

Woodroffe, C.D., 2018a. Mangrove response to sea level rise: Palaeoecological insights from macrotidal systems in northern Australia. Marine and Freshwater Research 69, 917–932. doi:10.1071/MF17252

Woodroffe, C.D., 2018b. The morphology and development of coastal wetlands in the Tropics, in: Perillo, G.M.E., Wolanski, E., Cahoon, D.R., Hopkinson, C.S. (Eds.), Coastal Wetlands: An Integrated Ecosystem Approach. Elsevier, Amsterdam, pp. 79–103. doi:10.1016/b978-0-444-63893-9.00002-2

Woodroffe, C.D., Lovelock, C.E., Rogers, K., 2014. Mangrove Shorelines, in: Masselink, G., Gehrels, W.R. (Eds.), Coastal Environments and Global Change. Wiley, Somerset, pp. 251–267.

Woodroffe, C.D., Murray-Wallace, C. V., 2012. Sea-level rise and coastal change: the past as a guide to the future. Quaternary Science Reviews 54, 4–11. doi:10.1016/j.quascirev.2012.05.009

Woodroffe, C.D., Rogers, K., McKee, K.L., Lovelock, C.E., Mendelssohn, I. a., Saintilan, N., 2016. Mangrove sedimentation and response to relative sea-level rise. Annual Review of Marine Science 8, annurev-marine-122414-034025. doi:10.1146/annurev-marine-122414-034025

Woodroffe, S.A., 2009a. Testing models of mid to late Holocene sea-level change, North Queensland, Australia. Quaternary Science Reviews 28, 2474–2488. doi:10.1016/j.quascirev.2009.05.004

Woodroffe, S.A., 2009b. Recognising subtidal foraminiferal assemblages: implications for quantitative sea-level reconstructions using a foraminifera-based transfer function. Journal of Quaternary Science 24, 215–223. doi:10.1002/jqs

Woodroffe, S.A., Horton, B.P., Larcombe, P., Whittaker, J.E., 2005. Intertidal mangrove foraminifera from the central Great Barrier Reef shelf, Australia: implications for sea-level reconstruction. Journal of Foraminiferal Research 35, 259–270.

Wright, A.J., Edwards, R.J., van de Plassche, O., 2011. Reassessing transfer-function performance in sea-level reconstruction based on benthic salt-marsh foraminifera from the Atlantic coast of NE North America. Marine Micropaleontology 81, 43–62.

doi:10.1016/j.marmicro.2011.07.003

Yassini, I., Jones, B.G., 1995. FORAMINIFERIDE and OSTRACODA from estuarine and shelf environments on the southeastern coast of Australia. The University of Wollongong Press, Wollongong.

Zhang, K., Liu, H., Li, Y., Xu, H., Shen, J., Rhome, J., Smith, T.J., 2012. The role of mangroves in attenuating storm surges. Estuarine, Coastal and Shelf Science 102–103, 11–23. doi:10.1016/j.ecss.2012.02.021

Appendices

Appendix 1: Supplementary data for Chapter 2

Appendix 1.1: Supplementary data for Chapter 2. Statistical difference in rSET-MH rates of deep and shallow SEC, VA, and total, shallow and deep autocompaction over time, between tidal position and within the tidal positions over time at Comerong Island. Statistical differences between measures and tidal positions are also provided. Values in bold are significantly different to 0.

Measure	Time	Tidal position	rSETs stations	Time * tidal position	Time * rSET
Deep SEC	<0.0001				
Mid	0.0034	0.0117	0.1208	<0.0001	0.6937
Intermediate	<0.0001		0.8363		0.4660
High	<0.0001		0.0021		0.0006
Shallow SEC	<0.0001				
Mid	0.0008	0.2771	0.5387	0.0025	0.3446
Intermediate	0.1703		0.9459		0.6610
High	0.1287		0.0210		0.1815
VA	<0.0001				
Mid	0.1592	0.0025	0.2428		
Intermediate	0.0302		0.3161		
High	0.0038		0.3589		
Total zone	0.0681				
Mid	0.3095	0.0492	0.0905	<0.0001	0.3520
Intermediate	<0.0001		0.4986		0.2027
High	<0.0001		0.0011		0.0004
Shallow zone	0.0412				
Mid	0.0267	0.2660	0.6207	0.0137	0.2583
Intermediate	0.1567		0.5114		0.4669
High	0.1820		0.0158		0.1694
Deep zone	0.2506				
Mid	0.0109	0.6015	0.1860	0.0026	0.5134
Intermediate	0.3125		0.8660		0.0354
High	0.0014		0.8772		<0.0001

Appendix 1.2: Supplementary data for Chapter 2. Interaction effect between rates of change; deep SEC vs VA, shallow SEC vs VA, total autocompaction vs shallow autocompaction and deep autocompaction vs shallow autocompaction over time, between measures and within measures over time at rSET-MH monitoring stations at Comerong Island. Statistical differences between measures and tidal positions are also provided. Values in bold are significantly different to 0.

Measures	Time	Measure	Measure * time
Deep SEC * VA	<0.0001	0.7035	0.1207
Shallow SEC * VA	<0.0001	0.3354	0.0585
Total AC * shallow AC	0.0004	0.6062	0.6074
Deep AC * shallow AC	<0.0001	0.7218	0.7412

Appendix 2: Supplementary data for Chapter 3

Appendix 2.1: Supplementary data for Chapter 3. Statistical difference in SET-MH rates of SEC, VA, and subsurface autocompaction over time, between tidal positions and within the tidal positions over time at Minnamurra River. Statistical differences between measures and tidal positions are also provided. Values in bold are significantly different to 0.

Measure		Time	Tidal position	rSETs stations	Time * tidal position	Time * rSET
SEC		<0.0001	0.0159		<0.0001	
	Mangrove	0.0004		0.4049		0.3314
	Saltmarsh	0.0094		0.2496		0.7382
VA*		0.3902		0.3010		0.5197
Total AC*		0.0167		0.3594		0.6830

* Only saltmarsh SET-MH

Appendix 2. 2: Supplementary data for Chapter 3. Interaction effect between rates of change SEC vs VA, SEC vs AC and VA vs AC in the saltmarsh SET-MH monitoring stations at Minnamurra River. Statistical differences between measures and tidal positions are also provided. Values in bold are significantly different to 0.

Measures	Time	Measure	Measure * time
SEC * VA	0.0059	0.0099	0.0188
SEC vs AC	0.0054	0.1820	<0.0001
VA * AC	0.0530	0.0647	0.0023

Appendix 2.3: Supplementary data for Chapter 3. Statistical difference in SET-MH rates of SEC, VA, and subsurface autocompaction over time, between tidal positions and within the tidal positions over time at Cararma Inlet. Statistical differences between measures and tidal positions are also provided. Values in bold are significantly different to 0.

Measure		Time	Tidal position	rSETs stations	Time * tidal position	Time * rSET
SEC		<0.0001	0.3698		0.0002	
	Mangrove	0.2186		<0.0001		0.5291
	Saltmarsh	0.0136		0.8790		0.2716
VA*		<0.0001		0.2095		<0.0001
Total AC*		0.0737		0.9649		0.4965

* Only saltmarsh SET-MH

Appendix 2.4: Supplementary data for Chapter 3. Interaction effect between rates of change SEC vs VA, SEC vs AC and VA vs AC saltmarsh SET-MH monitoring stations at Cararma Inlet. Statistical differences between measures and tidal positions are also provided. Values in bold are significantly different to 0.

Measures	Time	Measure	Measure * time
SEC * VA	<0.0001	0.3501	<0.0001
SEC vs AC	<0.0001	0.5285	<0.0001
VA * AC	<0.0001	0.6672	0.0003

Appendix 2.5: Supplementary data for Chapter 3. Statistical difference in SET-MH rates of SEC, VA, and subsurface autocompaction over time, between tidal positions and within the tidal positions over time at Currambene Creek. Statistical differences between measures and tidal positions are also provided. Values in bold are significantly different to 0.

Measure	Time	Tidal position	rSETs stations	Time * tidal position	Time * rSET
SEC	0.0005	0.0102		0.0003	
Mangrove	0.0009		0.0230		0.0004
Mixed	0.0020		0.3536		<0.0001
Saltmarsh	0.0156		0.3058		<0.0001
VA*	0.0145	0.0676		0.0260	
Mixed	0.0152		0.8155		0.5944
Saltmarsh	0.9334		0.9163		0.9864
Total AC*	<0.0001	0.4888		<0.0001	
Mixed	0.1152		0.1801		0.1351
Saltmarsh	0.0320		0.3452		0.0312

* Only mixed and saltmarsh SET-MH

Appendix 2.6: Supplementary data for Chapter 3. Interaction effect between rates of change SEC vs VA, SEC vs AC and VA vs AC mixed and saltmarsh SET-MH monitoring stations at Cararma Inlet. Statistical differences between measures and tidal positions are also provided. Values in bold are significantly different to 0.

Measures	Time	Measure	Measure * time
Mixed			
SEC * VA	0.0662	0.2633	0.0267
SEC vs AC	<0.0001	0.6208	0.0722
VA * AC	0.1955	0.6085	0.0009
Saltmarsh			
SEC * VA	0.0037	0.0517	0.1347
SEC vs AC	<0.0001	0.4117	0.0002
VA * AC	0.0586	0.0043	0.0004

Appendix 3: Benthic foraminifera illustrations

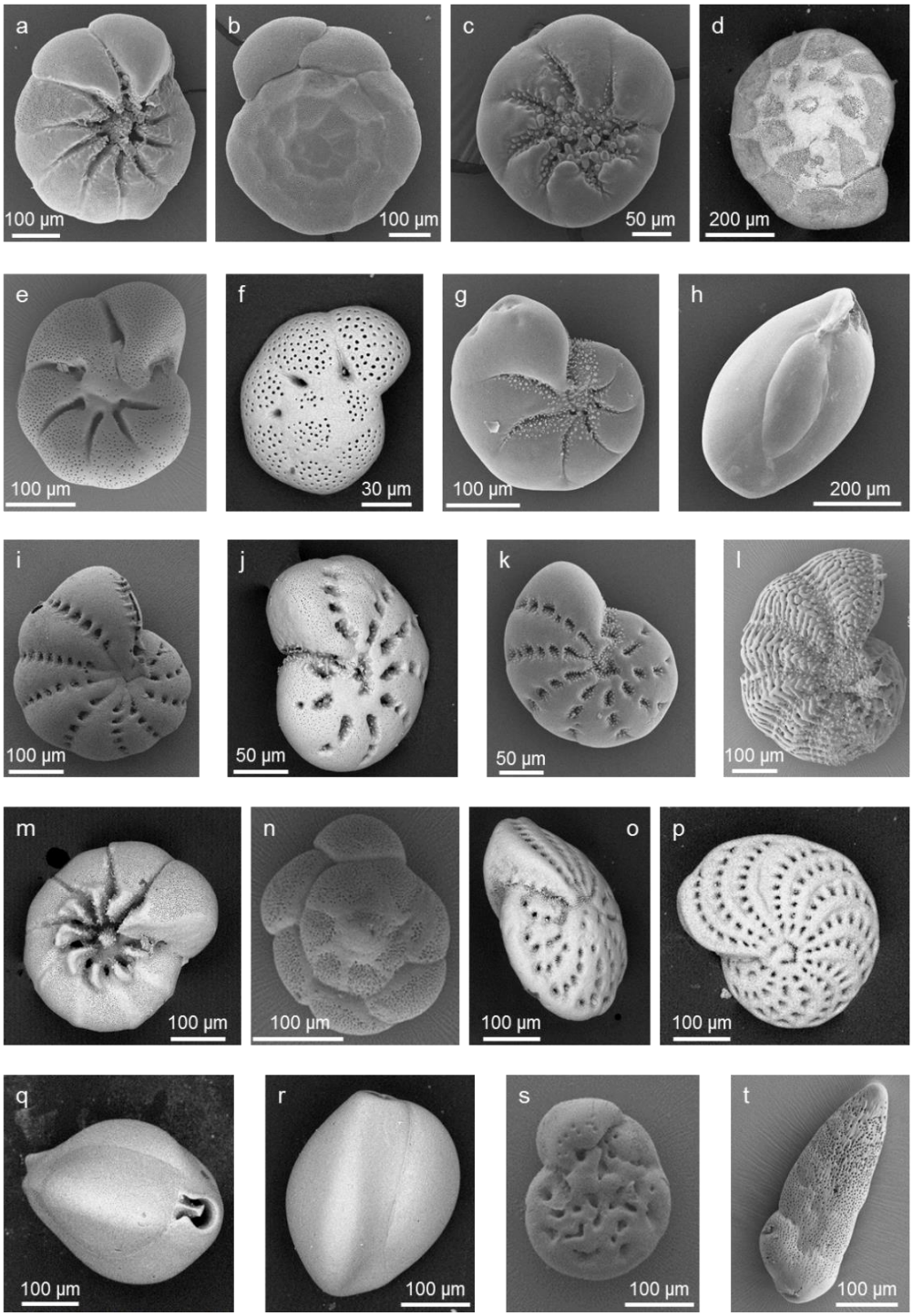

Plate 1

a & b *Ammonia beccarii*; c & d *Ammonia* spp.; e & f *Helenina anderseni*; g *Haynesia depressula*; h *Quinqueloculina seminula*; i & j *Criboelphidium excavatum*; k *Elphidium* spp.; l *Elphidium hispidulum*; m & n *Ammonia tepida*; o & p *Elphidium advenum*; q & r *Triloculina oblonga* ; s *Rosalina* spp.; t *Bolivina striatula*.

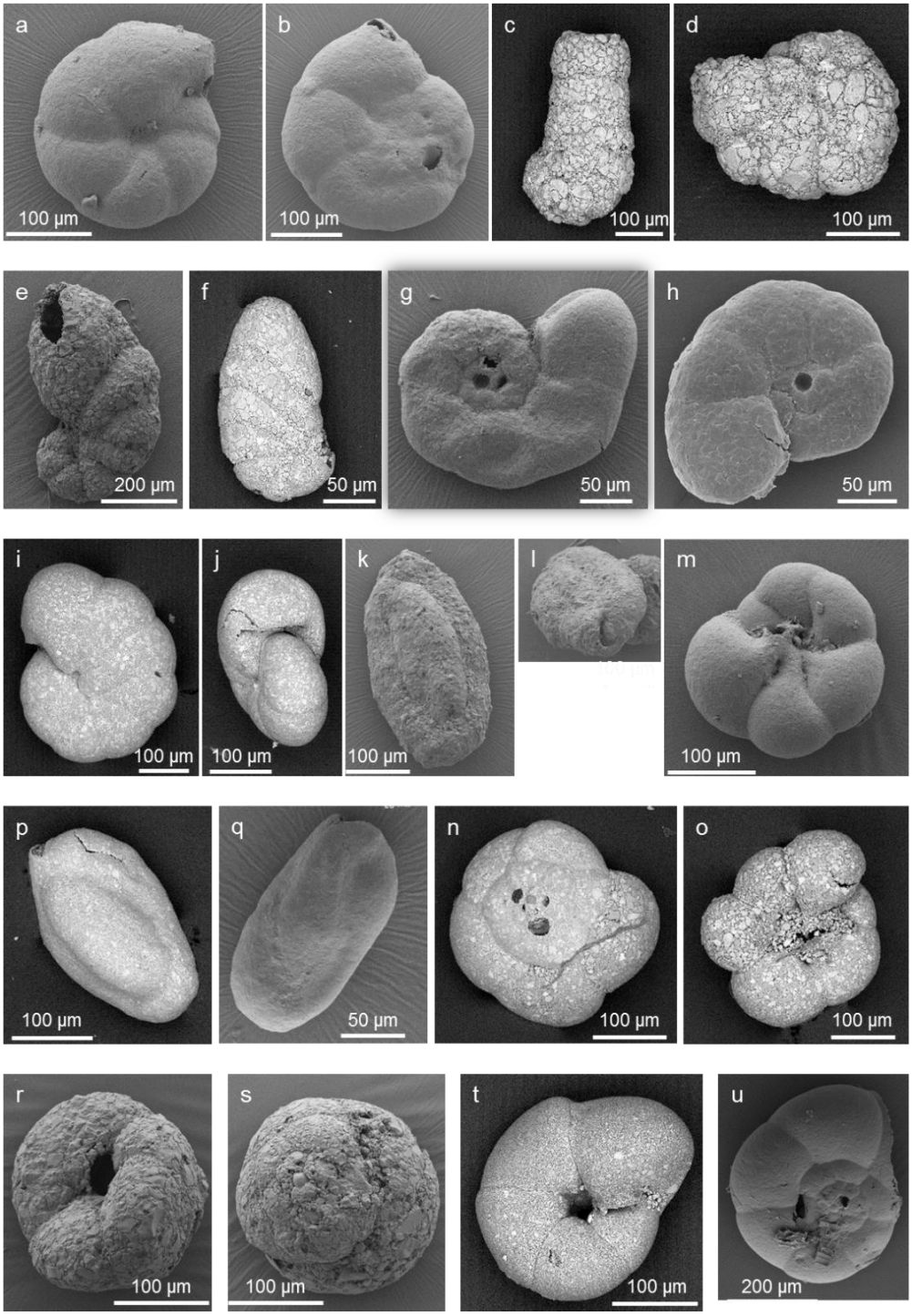

Plate 2

a & b *Arenoparrella mexicana*; c & d *Ammobaculites* spp.; e *Ammotium directum*, f *Ammotium morenoi* (former *Ammotium salsum*); g & h *Entzia macrescens* (former *Jadammina macrescens*); i & j *Haplophragmoides wilberti*; k & l *Miliammina fusca*; m, n & o *Siphotrochammina lobata*; p & q *Miliammina obliqua*; r & s *Tritaxis conica*; t & u *Trochammina inflata*.

Appendix 4: Dataset of surficial samples

Appendix 4.1: Data table of surficial samples from Minnamurra River (species data is represented as relative abundance in each surface sample).

Sample_ID	Spatial Cluster	Elevation (m AHD)	STPI	Salinity (ppt)	LOI (%)	Sand (%)	Mud (%)	Mean grainsize (micron)	Tests/cm^3	count	alive	dead	*A. subcatenulatus*	*A. exiguus*	*Ammobaculites spp.*	*A. becarii*
Min_115	Min-I	0.66	0.66	7.6	20.2	19	81	26	28	119	64	55			3	
Min_112	Min-I	0.702	0.71	9.3	27.0	21	79	24	82	130	43	87				
Min_110	Min-I	0.726	0.74	5.1	8.6	44	56	50	60	122	34	88				
Min_113	Min-I	0.747	0.76	10.7	15.7	33	67	38	104	167	38	129				
Min_114	Min-I	0.75	0.77	6.3	31.4	19	81	25	95	112	24	88				
Min_111	Min-I	0.706	0.71	5.6	27.9	11	89	19	76	121	59	62				
Min_108	Min-I	0.726	0.74	5.9	5.5	47	53	51	32	133	58	75				
Min_109	Min-I	0.805	0.83	8.8	7.8	40	60	46	37	122	45	77				
Min_116	Min-II	0.593	0.58	5.1	2.5	69	31	101	23	120	77	43				
Min_117	Min-II	0.609	0.60	3.8	2.7	69	31	102	22	111	89	22			1	2
Min_107	Min-II	0.619	0.61	3.8	1.6	74	26	124	19	95	69	26				
Min_105	Min-III	0.428	0.38	4.2	8.1	35	65	39	47	112	14	98		4	21	4
Min_106	Min-III	0.519	0.49	3.5	3.2	55	45	82	21	101	58	43	1	1	24	3
Min_103	Min-III	0.317	0.25	3.7	6.9	50	50	59	26	96	58	38			3	5
Min_104	Min-III	0.381	0.32	4.4	9.1	26	74	30	33	116	36	80		4	8	4
Min_201	Min-III	0.231	0.14	5.8	30.2	19	81	26	31	98	35	63			4	
Min_102	Min-III	0.294	0.22	3.0	5.1	45	55	44	14	110	65	45	2		1	
Min_101	Min-III	0.384	0.33	3.2	3.8	48	52	50	19	93	44	49			1	

Sample_ID	*A. tepida*	*Ammonia spp.*	*A. directum*	*Ammotium spp.*	*A. mexicana*	*C. excavatum*	*Elphidium* spp.	*H. wilberti*	*H. depressula*	*H. anderseni*	*E. macrescens*	*M. fusca*	*Q. seminula*	*Quinqueloculina spp.*	*Rosalina* spp.	*S. lobata*	*T. earlandi*	*T. conica*	*T. inflata*	*Trochammina* spp.
Min_115					1	17			5		22	16		1		2			31	3
Min_112								2	4		5					3			87	
Min_110								2			33	1				10			54	
Min_113								1	2		22	3		1		7			62	2
Min_114			1					4			13	3				22			57	
Min_111			2				1	39			4	9				10			35	
Min_108						2		8	3	2	9	24				14			36	3
Min_109								12			10	16	2			7			49	3
Min_116					1	71					9	1							18	
Min_117						77					3	2	11			2			3	
Min_107						77					3	5	3			3			8	
Min_105						7			1			54	5						4	
Min_106					1	50						9	7						4	
Min_103						42	2		7	1		24	14						2	
Min_104		5				21			1	2		26	28						1	
Min_201					4	31		2		4	2	22	12			6	4		6	2
Min_102	3					41		1	5	1		38			1	2		2	4	
Min_101		2		2		3		11	1		1	44	7	1	1	1	3		14	6

Appendix 4.2: Data table of surficial samples from Comerong Island (species data is represented as relative abundance in each surface sample).

Sample_ID	Spatial cluster	Elevation (m AHD)	STPI	Salinity (ppt)	LOI (%)	Sand (%)	Mud (%)	Mean grainsize (micron)	Tests/cm^3	count	alive	dead
Cm_209	Cm-Ia	0.494	0.57	1.6	4.0	57	43	84	47	110	79	31
Cm_302	Cm-Ia	0.559	0.66	2.3	2.5	61	39	87	8	122	83	39
Cm_113	Cm-Ia	0.532	0.62	1.6	2.0	68	32	105	9	105	70	35
Cm_301	Cm-Ia	0.499	0.58	2.3	1.8	70	30	105	11	108	36	72
Cm_303	Cm-Ia	0.601	0.71	2.4	1.4	69	31	100	16	115	27	88
Cm_108	Cm-Ib	0.521	0.61	2.1	3.2	65	35	96	70	141	41	100
Cm_114	Cm-Ib	1.038	1.27	1.1	8.8	67	33	137	271	74	20	54
Cm_109	Cm-Ib	0.787	0.95	0.2	0.3	100	0	268	1	51	13	38
Cm_210	Cm-Ib	0.585	0.69	3.3	12.8	23	77	24	32	81	29	52
Cm_111	Cm-Ib	0.694	0.83	1.6	2.3	75	25	137	25	83	30	53
Cm_110	Cm-Ib	0.808	0.98	0.2	4.2	81	19	188	91	127	8	119
Cm_102	Cm-II	0.278	0.30	1.9	1.5	69	31	81	20	97	22	75
Cm_112	Cm-II	0.488	0.57	2.9	3.1	61	39	93	13	116	103	13
Cm_201	Cm-II	-0.417	-0.59	2.8	6.3	32	68	27	18	83	53	30
Cm_304	Cm-II	0.522	0.61	2.2	1.9	63	37	99	10	78	63	15
Cm_106	Cm-II	0.163	0.15	2.4	5.4	52	48	58	88	105	71	34
Cm_104	Cm-II	0.165	0.15	3.2	3.5	62	38	82	26	82	56	26
Cm_103	Cm-II	0.193	0.19	4.2	3.6	60	40	66	57	95	71	24
Cm_107	Cm-II	0.256	0.27	2.5	2.5	63	37	91	11	85	66	19
Cm_105	Cm-II	0.261	0.28	2.5	20.6	57	43	69	15	60	42	18
Cm_101	Cm-II	-0.026	-0.09	3.1	5.5	39	61	34	216	112	42	70
Cm_203	Cm-III	0.226	0.23	3.1	7.4	31	69	31	20	112	88	24
Cm_204	Cm-III	0.344	0.38	2.8	7.1	28	72	29	22	75	49	26
Cm_202	Cm-III	0.233	0.24	3.0	7.5	17	83	16	22	104	61	43
Cm_205	Cm-III	0.348	0.39	4.1	10.9	17	83	17	20	94	65	29
Cm_207	Cm-III	0.376	0.42	3.1	10.6	22	78	23	24	104	52	52
Cm_206	Cm-III	0.362	0.41	3.0	6.2	37	63	34	47	128	72	56
Cm_208	Cm-III	0.418	0.48	2.8	3.6	53	47	71	18	110	44	66

Sample_ID	*A. agglutinans*	*Ammobaculites spp.*	*A. subcatenulatus*	*Ammodiscus spp.*	*A. beccarii*	*A. tepida*	*Ammonia spp.*	*A. directum*	*A. morenoi*	*Ammotium spp.*	*B. pseudoplicata*	*Bolivina spp.*	*B. striatula*	*E. australis*	*Elphidium spp.*	*C. excavatum*
Cm_209																46
Cm_302																52
Cm_113								1	8							34
Cm_301					1	5										15
Cm_303															2	19
Cm_108								3	2							9
Cm_114																
Cm_109		2			4											
Cm_210																14
Cm_111																1
Cm_110										2						
Cm_102	2	7												1		14
Cm_112					1											69
Cm_201				1	1			1						2	1	54
Cm_304																76
Cm_106	3	6	2		1			7								42
Cm_104		2			1			6						2	1	52
Cm_103					2			2			1			1	2	63
Cm_107					11											49
Cm_105					2			18		2				2		47
Cm_101	2					1		1			1	1	1	1	6	25
Cm_203					8											7
Cm_204					4		1			1						
Cm_202				1	2		3									1
Cm_205			3		9	3										2
Cm_207	1				5											10
Cm_206					1				1							7
Cm_208					7											12

Sample_ID	*Glomospira spp.*	*H. wilberti*	*H. depressula*	*H. anderseni*	*E. macrescens*	*M. fusca*	*M. obliqua*	*Q. seminula*	*Quinqueloculina spp.*	*S. lobata*	*S. vivipara*	*T. earlandi*	*T. oblonga*	*T. conica*	*T. inflata*	*Trochammina spp.*
Cm_209		2			1	13		4		5					29	
Cm_302					2	6			1	4					36	
Cm_113			1	2		24			2	7					21	1
Cm_301					6	5		4		10	1				54	
Cm_303					44	2				3					30	
Cm_108		2			6	1		1		3		1			70	1
Cm_114		3			11	1				1					84	
Cm_109			12		4	2									76	
Cm_210		10			2		22			10					42	
Cm_111		19			11					17			1		51	
Cm_110	3	20			4	11	2			9					49	
Cm_102	2		2	6	4	44				2		4		7	3	
Cm_112						3		21							6	
Cm_201				6	1	2		25							4	
Cm_304					12			3	1	1			1		6	
Cm_106			10			14			1	2	9	1		1	2	
Cm_104	1		4	5	2	16				2	1	1			1	
Cm_103			4	3	2	13		3		1		1		1		
Cm_107			5			20		6			1				8	
Cm_105			3	2		5		7			5				8	
Cm_101			4	35	2	9		7				1		4		
Cm_203			1			17		56			2				9	
Cm_204						29		53					1		9	
Cm_202		6		1		12		44							31	
Cm_205						52		21							10	
Cm_207						44		17		2					21	
Cm_206		1		1	1	62		9					2		17	
Cm_208		5			1	24		13					1		38	

Appendix 4.3: Data table of surficial samples from Cararma Inlet (species data is represented as relative abundance in each surface sample).

Sample_ID	Spatial cluster	Elevation (m AHD)	STPI	Salinity (ppt)	LOI (%)	Sand (%)	Mud (%)	Mean grainsize (micron)	Tests/cm³	count	alive	dead	*Ammobaculites spp.*	*A. subcatenulatus*	*A. becarii*	*A. tepida*
Ca_102	Ca-Ia	0.422	0.40	10.5	38.7	34	66	41	38	193	38	155	14	1	2	1
Ca_103	Ca-Ia	0.426	0.41	8.0	47.2	34	66	41	10	112	34	78	43	1	3	2
Ca_301	Ca-Ib	-0.279	-0.31	9.6	0.5	94	6	284	11	96	26	70	19		13	
Ca_302	Ca-Ib	-0.356	-0.39	9.5	0.7	94	6	286	9	93	31	62	17		23	
Ca_101	Ca-IIa	0.373	0.35	11.0	34.6	42	58	50	29	158	65	93	1		1	
Ca_106	Ca-IIa	0.513	0.49	5.4	5.7	58	42	81	45	105	27	78	7			
Ca_105	Ca-IIa	0.529	0.51	4.6	5.7	67	33	114	19	101	26	75	16			
Ca_107	Ca-IIa	0.556	0.54	4.9	5.4	69	31	112	38	101	27	74				
Ca_116	Ca-IIa	0.711	0.69	14.5	6.4	56	44	76	4	98	2	96				
Ca_120	Ca-IIa	0.763	0.75	2.1	46.3	52	48	74	5	92	10	82				
Ca_118	Ca-IIa	0.734	0.72	5.2	40.1	69	31	132	15	88	29	59				
Ca_122	Ca-IIa	0.788	0.77	1.5	12.1	61	39	102	5	88	69	19				
Ca_104	Ca-IIa	0.474	0.45	7.3	7.9	57	43	83	17	137	17	120	19	1		
Ca_110	Ca-IIb	0.591	0.57	8.5	36.8	35	65	40	50	94	12	82	33			
Ca_108	Ca-IIb	0.602	0.58	5.2	5.0	75	25	142	74	127	17	110				
Ca_113	Ca-IIb	0.632	0.61	6.1	9.5	57	43	83	19	89	27	62				
Ca_112	Ca-IIb	0.626	0.61	7.8	8.5	60	40	87	23	97	12	85				
Ca_114	Ca-IIb	0.657	0.64	9.6	15.1	44	56	54	7	80	34	46				
Ca_109	Ca-IIb	0.603	0.58	5.3	5.6	68	32	104	11	92	19	73	1			
Ca_115	Ca-IIb	0.708	0.69	11.0	14.6	55	45	76	8	108	4	104				
Ca_111	Ca-IIb	0.604	0.59	6.5	9.8	60	40	89	28	90	21	69	2			
Ca_117	Ca-IIb	0.693	0.68	16.1	14.7	52	48	73	2	89	4	85				

Sample_ID	*Ammonia spp.*	*B. robusta*	*E. advenum*	*C. excavatum*	*Elphidium spp.*	*Glomospira spp.*	*H. depressula*	*H. anderseni*	*E. macrescens*	*M. fusca*	*M. obliqua*	*Miliolinella spp.*	*Q. seminula*	*Quinqueloculina spp.*	*Rosalina spp.*	*S. lobata*	*T. inflata*	*Trochammina spp.*
Ca_102	1				1	1	2	3	1	54					2		18	
Ca_103	1			6			1	1		27			1		4		12	
Ca_301	2	2	1	33				5	2	4		1			4	1	5	7
Ca_302	2		4	25			2	4		8		2	3				9	1
Ca_101				1			1	9	1	1			13				72	
Ca_106									24	1	1			1			67	
Ca_105				2					12	1							69	
Ca_107									18					1			81	
Ca_116									22								78	
Ca_120									13							9	70	9
Ca_118									8								92	
Ca_122									2							7	91	
Ca_104				9			1		1	4	1						64	
Ca_110									46								21	
Ca_108									87								13	
Ca_113									90								10	
Ca_112									75								25	
Ca_114									80								20	
Ca_109									67								32	
Ca_115									61								39	
Ca_111									47								51	
Ca_117				3					49								47	

Appendix 4.4: Data table of surficial samples from Currambene Creek (species data is represented as relative abundance in each surface sample).

Sample_ID	Spatial Cluster	Elevation (m AHD)	STPI	Salinity (ppt)	LOI (%)	Sand (%)	Mud (%)	Mean grainsize (micron)	Tests/cm³	count	alive	dead
Cb_Spo	Cb-I	0.47	0.45	2.5	2.9	58	42	75	50	176	41	135
Cb_204	Cb-I	0.233	0.21	2.6	5.5	36	64	39	1	107	51	56
Cb_206	Cb-I	0.357	0.34	2.5	7.6	34	66	35	22	110	69	41
Cb_JucSpo	Cb-I	0.509	0.49	1.7	2.2	67	33	90	13	153	31	122
Cb_205	Cb-I	0.295	0.27	1.4	2.1	67	33	102	87	117	32	85
Cb_203	Cb-I	0.188	0.16	2.7	3.7	53	47	70	19	120	61	59
Cb_101	Cb-IIa	0.325	0.30	1.6	2.0	65	35	80	32	149	28	121
Cb_102	Cb-IIa	0.446	0.43	2.0	8.1	67	33	93	21	120	56	64
Cb_202	Cb-IIa	0.293	0.27	4.2	11.8	47	53	62	18	127	68	59
Cb_201	Cb-IIa	-0.396	-0.43	3.6	3.1	70	30	96	15	93	46	47
Cb_Mn1	Cb-IIb	0.302	0.28	6.5	9.8	44	56	49	12	122	40	82
Cb_Avi-t	Cb-IIb	0.319	0.30	9.6	10.9	38	62	43	29	154	18	136
Cb_218	Cb-IIb	0.335	0.31	7.1	36.8	18	82	28	7	116	33	83
Cb_221	Cb-IIb	0.388	0.37	7.0	22.5	50	50	62	27	108	15	93
Cb_222	Cb-IIb	0.519	0.50	2.0	3.5	63	37	103	19	108	0	108
Cb_105	Cb-IIb	0.527	0.51	19.8	31.0	43	57	50	23	100	18	82
Cb_104	Cb-IIb	0.548	0.53	3.5	8.3	38	62	43	47	205	50	155
Cb_217	Cb-IIb	0.375	0.35	6.5	40.2	42	58	50	4	114	39	75
Cb_219	Cb-IIb	0.388	0.37	3.8	9.9	30	70	38	12	107	28	79
Cb_207	Cb-IIb	0.381	0.36	3.1	9.8	24	76	29	10	113	35	78
Cb_209	Cb-IIb	0.409	0.39	3.0	9.0	30	70	37	11	89	15	74
Cb_210	Cb-IIb	0.43	0.41	2.6	10.7	27	73	30	13	97	26	71
Cb_Agi	Cb-IIb	0.491	0.47	2.3	10.4	21	79	21	30	130	21	109
Cb_208	Cb-IIb	0.392	0.37	3.5	7.0	26	74	31	24	155	53	102
Cb_106	Cb-IIb	0.538	0.52	1.8	1.7	69	31	98	10	103	32	71
Cb_220	Cb-IIIa	0.35	0.33	6.9	35.7	52	48	65	17	115	33	82
Cb_103	Cb-IIIa	0.576	0.56	1.5	0.9	80	20	133	1	58	9	49
Cb_216	Cb-IIIa	0.435	0.41	6.5	28.0	43	57	51	4	103	23	80
Cb_214	Cb-IIIa	0.447	0.43	4.7	24.1	35	65	40	102	109	34	75
Cb_Sm3	Cb-IIIa	0.795	0.78	3.2	6.9	47	53	53	31	201	7	194
Cb_108	Cb-IIIa	0.725	0.71	4.8	3.9	48	52	53	139	232	4	228
Cb_215	Cb-IIIa	0.453	0.43	4.2	11.4	47	53	57	12	96	13	83
Cb_AviSar	Cb-IIIa	0.653	0.64	26.3	31.5	19	81	24	26	157	12	145
Cb_107	Cb-IIIa	0.694	0.68	2.6	1.2	78	22	133	3	97	6	91

Sample_ID	Spatial Cluster	Elevation (m AHD)	STPI	Salinity (ppt)	LOI (%)	Sand (%)	Mud (%)	Mean grainsize (micron)	Tests/cm^3	count	alive	dead
Cb_SarSpo	Cb-IIIa	0.511	0.49	6.8	15.3	36	64	41	13	103	11	92
Cb_Juc	Cb-IIIa	0.646	0.63	4.2	17.4	16	84	18	110	202	22	180
Cb_213	Cb-IIIb	0.454	0.43	1.4	1.8	60	40	92	4	98	60	38
Cb_212	Cb-IIIb	0.463	0.44	1.7	0.9	81	19	138	5	106	4	102
Cb_109	Cb-IIIb	0.669	0.65	15.3	33.1	25	75	30	65	173	5	168
Cb_Mix2	Cb-IIIb	0.648	0.63	17.3	36.3	50	50	69	8	113	4	109
Cb_Sm2	Cb-IIIb	0.656	0.64	3.7	2.7	51	49	59	99	332	5	327
Cb_Sar	Cb-IIIb	0.707	0.69	2.4	1.0	77	23	130	9	262	10	252
Cb_211	Cb-IIIb	0.462	0.44	2.8	4.9	32	68	40	7	100	49	51

Sample_ID	*A. exiguus*	*E. foliaceus*	*Ammobaculites spp.*	*A. subcatenulatus*	*A. becarii*	*A. tepida*	*A. morenoi*	*Ammotium spp.*	*A. mexicana*	*C. excavatum*	*Elphidium spp.*	*H. wilberti*	*H. depressula*	*H. anderseni*
Cb_Spo							10		23	3		5		
Cb_204					1	1			44	1		2		
Cb_206			2					2	41			1		
Cb_JucSpo							2	3	43	1		4		1
Cb_205			2						73	3		1		
Cb_203			2						30	2		10		
Cb_101					1	1				6		11		
Cb_102				1	7	3				15		1		
Cb_202					5				1	1	3	6	2	
Cb_201			3		2		3		1	1				
Cb_Mn1			31	2	13					2				
Cb_Avi-t			41	3	2	2	2							
Cb_218			69							5			2	
Cb_221	3	2	81							2	2			
Cb_222			85							2				
Cb_105			67		4					4				
Cb_104		4	50	2						1				
Cb_217			35							11				
Cb_219		1	36						3	5			1	
Cb_207		1	27	5				2		6				
Cb_209			34							2			1	
Cb_210			23	2						2			3	
Cb_Agi			35							7			1	

Sample_ID	*A. exiguus*	*E. foliaceus*	*Ammobaculites spp.*	*A. subcatenulatus*	*A. becarii*	*A. tepida*	*A. morenoi*	*Ammotium spp.*	*A. mexicana*	*C. excavatum*	*Elphidium spp.*	*H. wilberti*	*H. depressula*	*H. anderseni*
Cb_208		3	31	7	1					5		1	1	
Cb_106		4	17		1					6				
Cb_220			2					1		1	1	1		1
Cb_103									2	10				
Cb_216			25	2						6			1	
Cb_214														
Cb_Sm3												3		
Cb_108												1		
Cb_215										2				
Cb_AviSar			1											
Cb_107			6							2				
Cb_SarSpo							7		1					
Cb_Juc							1		1			4		1
Cb_213										15	3			
Cb_212										1				
Cb_109			2										1	
Cb_Mix2			4											
Cb_Sm2														
Cb_Sar														
Cb_211			3	2						7				

Sample_ID	*E. macrescens*	*M. fusca*	*M. obliqua*	*P. stoeni*	*P. ipohalina*	*Q. seminula*	*Quinqueloculina spp.*	*S. lobata*	*S. vivipara*	*T. earlandi*	*T. conica*	*T. inflata*	*Trochammina spp.*
Cb_Spo	7	11				1		1				39	
Cb_204	1	5				12		1				27	6
Cb_206	1	4				14		2				29	5
Cb_JucSpo	1	8	2			2		3	1			31	
Cb_205	1	3				5						12	
Cb_203		12				21		2				11	8
Cb_101	6	41				2						30	2
Cb_102	5	22				18						30	
Cb_202	2	18				20		2			15	9	6
Cb_201	2	36						1	1	1	23	17	8
Cb_Mn1	2	39				2				1	1	2	1
Cb_Avi-t	1	47										3	

Sample_ID	*E. macrescens*	*M. fusca*	*M. obliqua*	*P. stoeni*	*P. ipohalina*	*Q. seminula*	*Quinqueloculina spp.*	*S. lobata*	*S. vivipara*	*T. earlandi*	*T. conica*	*T. inflata*	*Trochammina spp.*
Cb_218		22					2						
Cb_221	3	1										6	
Cb_222		9										4	
Cb_105	9	6										10	
Cb_104	6	25										10	
Cb_217	5	16										33	
Cb_219	1	25					5					23	
Cb_207	14	20				5						17	3
Cb_209	19	20				4						19	
Cb_210	15	31				5						19	
Cb_Agi	18	18	1				1					20	
Cb_208	8	26				6						11	
Cb_106	2	45				16		1				9	
Cb_220	3	1	4				1	3				76	6
Cb_103	17	5										66	
Cb_216	10						1	1				50	5
Cb_214	52	1						2				43	2
Cb_Sm3	46		5					3				42	
Cb_108	58		9					2				29	
Cb_215	43	1		2								52	
Cb_AviSar	39							1				59	
Cb_107	36	2	9					1				43	
Cb_SarSpo	26			1			1	5				59	
Cb_Juc	19		9					10				43	9
Cb_213	65	3					2					11	
Cb_212	79	2				3						15	
Cb_109	82	1										15	
Cb_Mix2	90	1			1							4	
Cb_Sm2	93											6	
Cb_Sar	98											2	
Cb_211	45	9				16						18	

Appendix 5: Stratigraphic log of sediment cores

Core number: Min_Mg2	Location: Minnamurra River	Vegetation: *Avicennia marina*	Date collected: 25/09/2016
Latitude: -34° 37' 29.64826"	Longitude: 150° 50' 35.60811"	Elevation: 0.255 m AHD	Core length: 134 cm

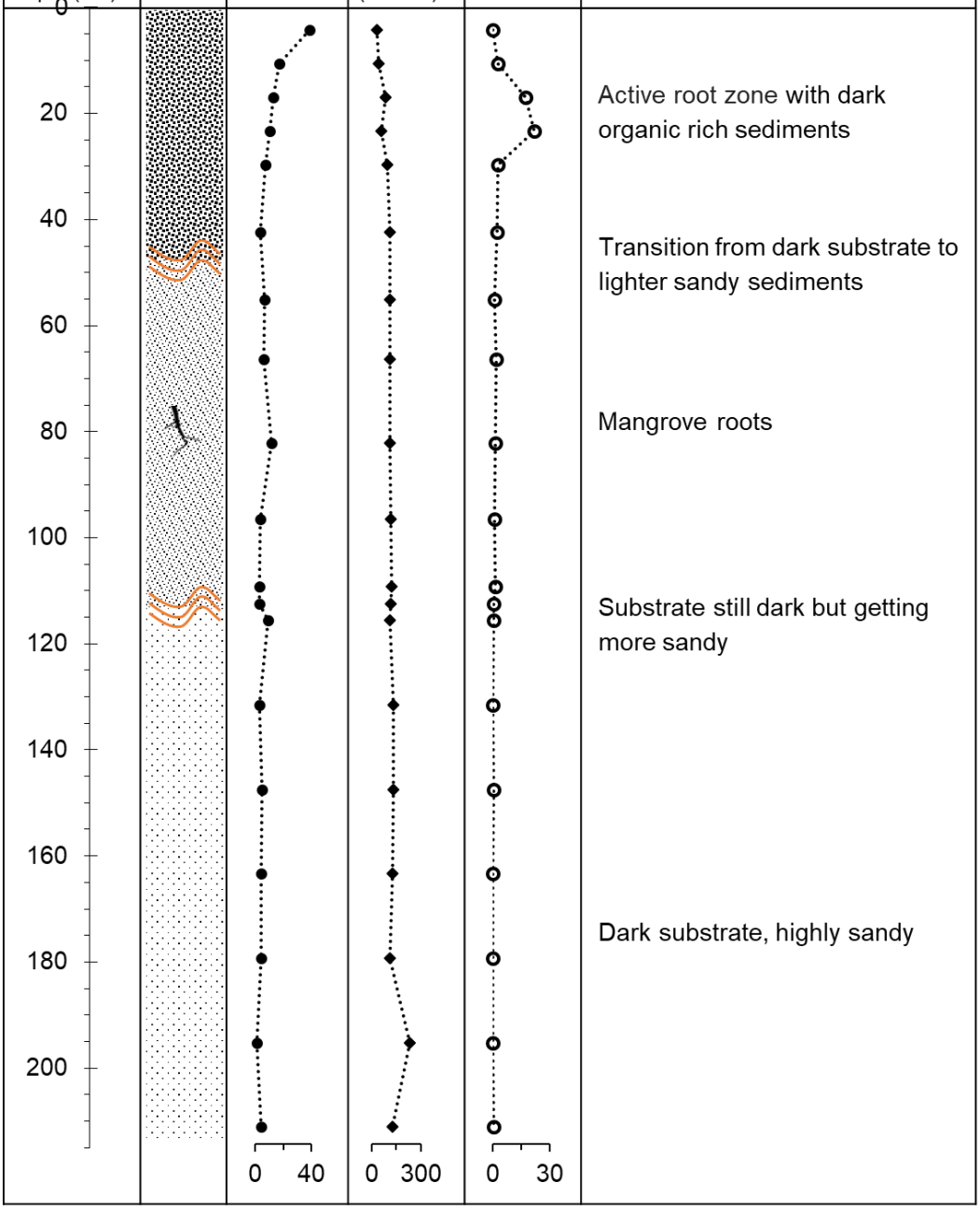

Core number: Min_Spo2	Location: Minnamurra River	Vegetation: *Sporobolus virginicus*	Date collected: 7/04/2015
Latitude: -34° 37' 41.01710"	Longitude: 150° 50' 47.71864"	Elevation: 0.719 m AHD	Core length: 137 cm

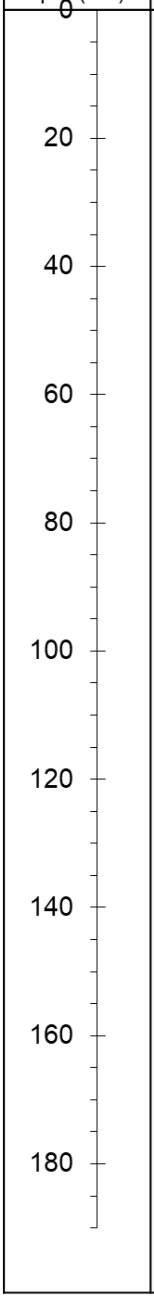

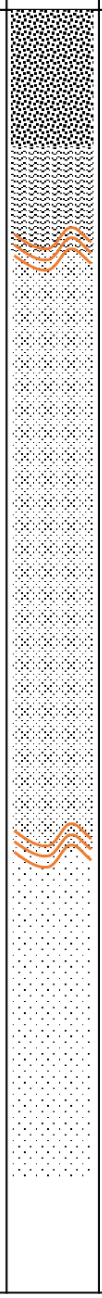

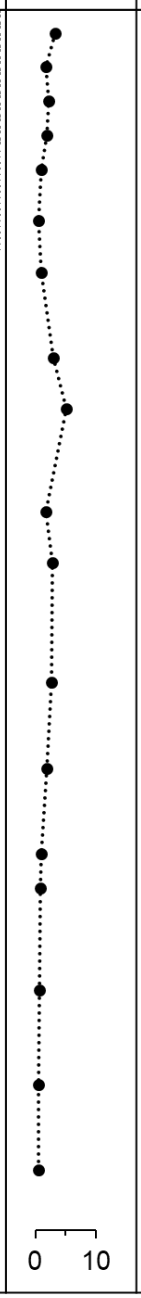

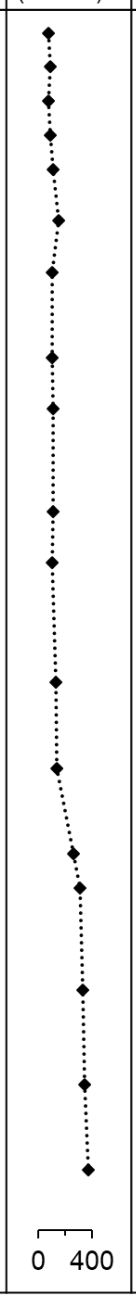

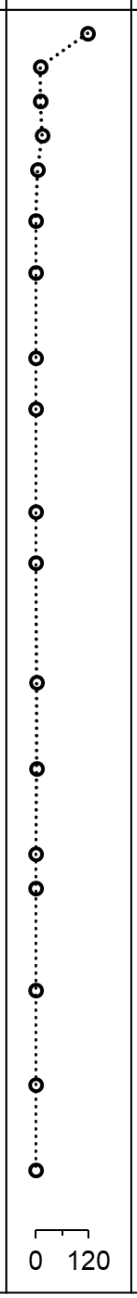

Active root zone with dark organic rich sediments

Lighter coloured substrate with patches and bands of orange (oxidation)

Transition from light to dark substrate

Dark substrate, highly sandy

Transition from dark to light substrate

Grey substrate, highly sandy

Core number: Cm_Mg1	Location: Comerong Island	Vegetation: *Avicennia marina*	Date collected: 21/04/2016
Latitude: -34° 53' 56.26328"	Longitude: 150° 45' 8.57648"	Elevation: 0.373 m AHD	Core length: 152 cm

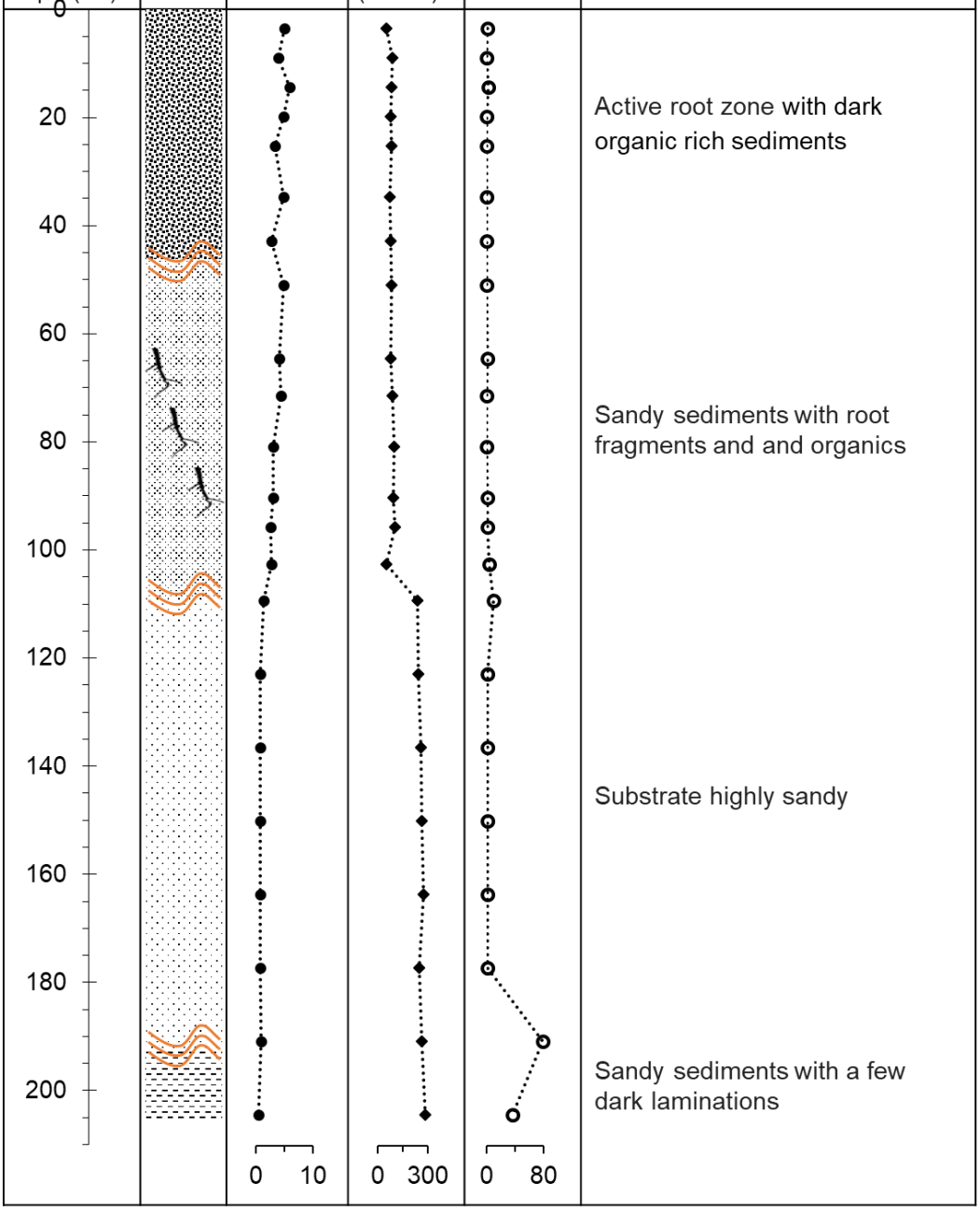

Core number: Cm_Spo	Location: Comerong Island	Vegetation: *Sporobolus virginicus/ Avicennia marina*	Date collected: 21/04/2016
Latitude: -34° 52' 55.59729"	Longitude: 150° 44' 23.33260"	Elevation: 0.388 m AHD	Core length: 137 cm

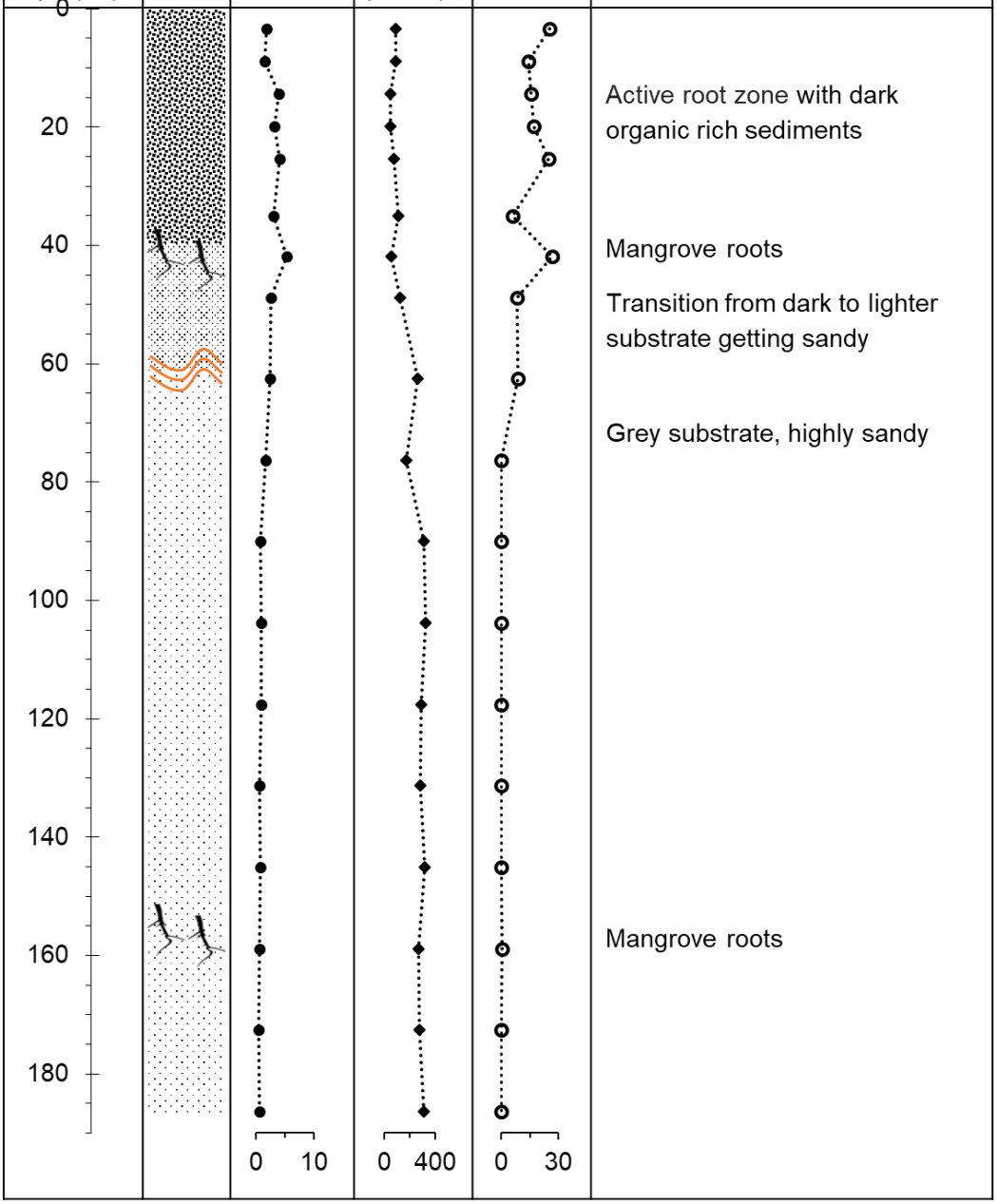

Core number: Cm_Dm	Location: Comerong Island	Vegetation: *Avicennia marinal Sarcocornia quinqueflora*	Date collected: 21/04/2016
Latitude: -34° 52' 18.98794"	Longitude: 150° 44' 35.10658"	Elevation: 0.463 m AHD	Core length: 165 cm

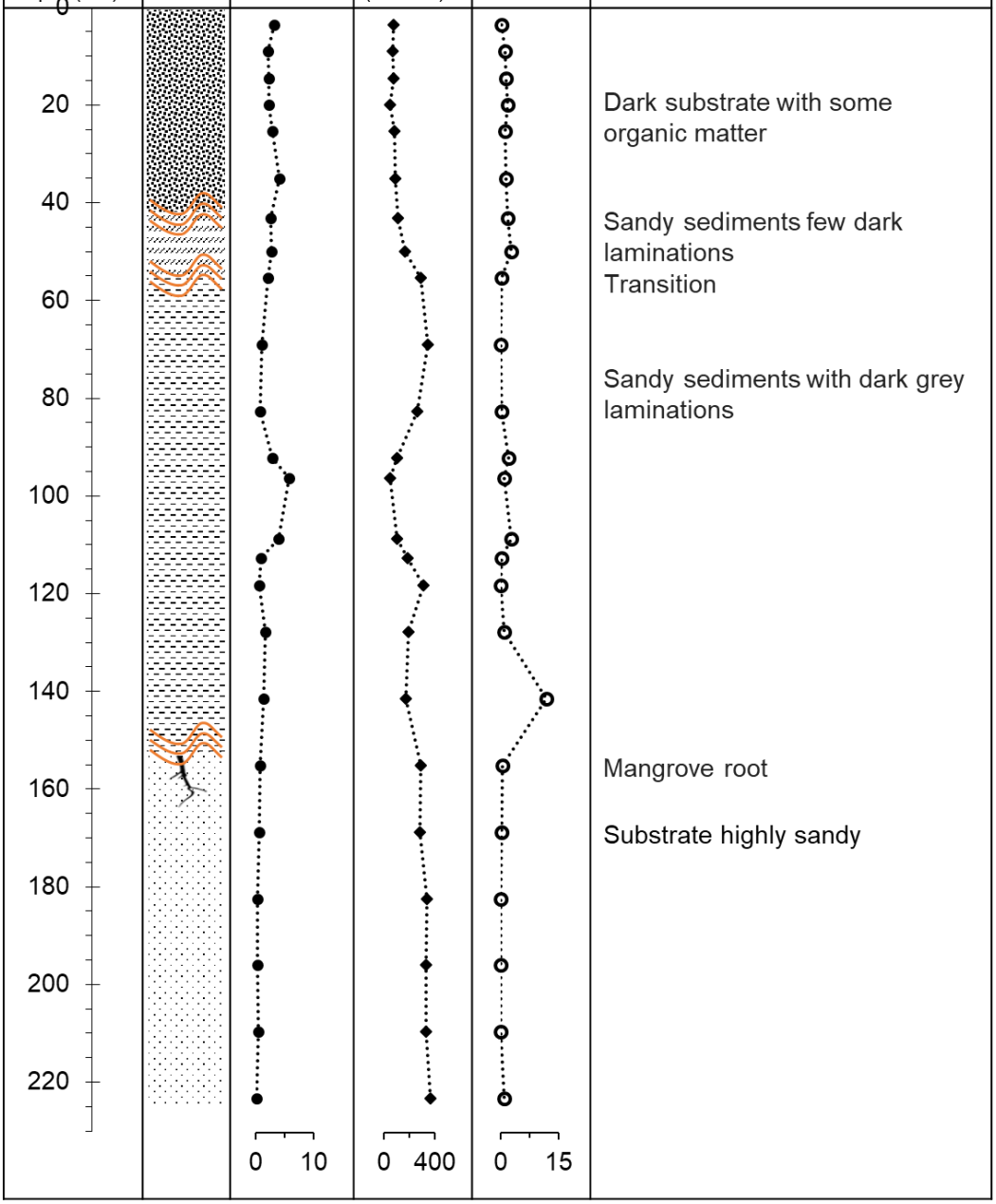

Core number: Ca_Mg2	Location: Cararma Inlet	Vegetation: *Avicennia marina*	Date collected: 10/09/2015
Latitude: -34° 59' 14.44436"	Longitude: 150° 46' 15.42640"	Elevation: 0.475 m AHD	Core length: 87 cm

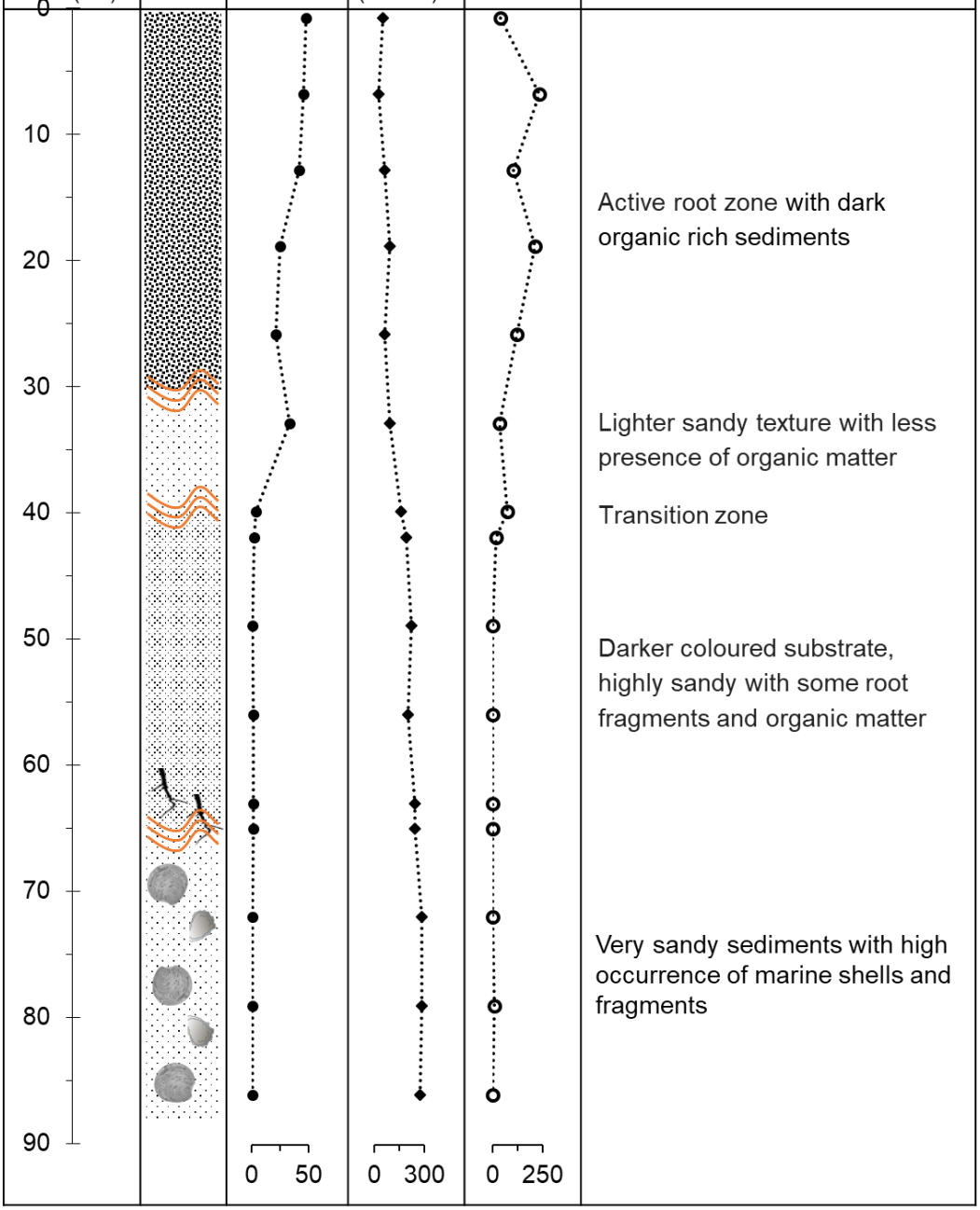

Core number: Ca_Tect	Location: Cararma Inlet	Vegetation: *Tecticornia arbuscula*	Date collected: 03/09/2015
Latitude: -34° 59' 11.90732"	Longitude: 150° 46' 19.02223"	Elevation: 0.692 m AHD	Core length: 111 cm

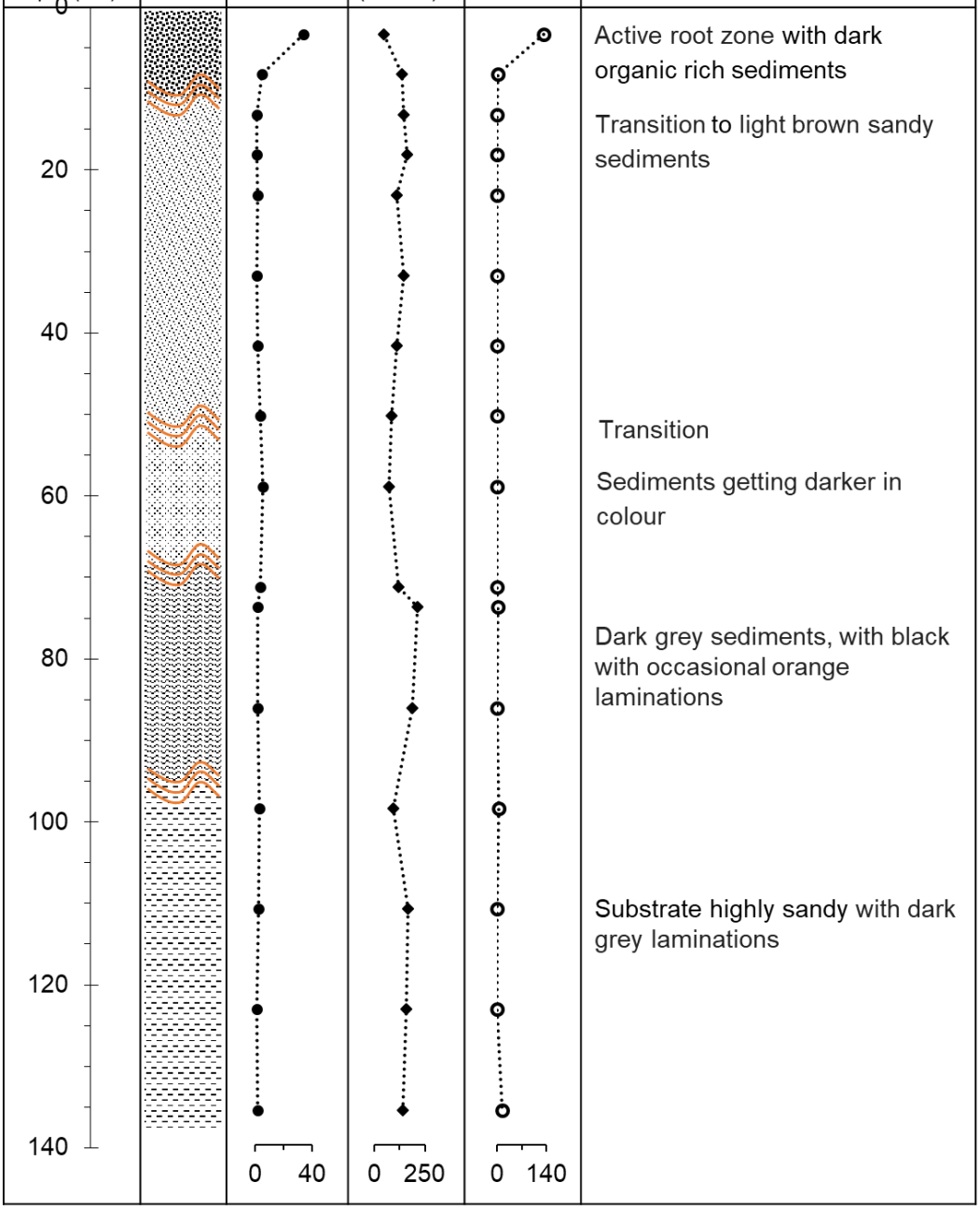

Core number: Ca_Sar2	Location: Cararma Inlet	Vegetation: *Sarcocornia quinqueflora*	Date collected: 03/09/2015
Latitude: -34° 59' 7.09394"	Longitude: 150° 46' 31.36660"	Elevation: 0.794 m AHD	Core length: 114 cm

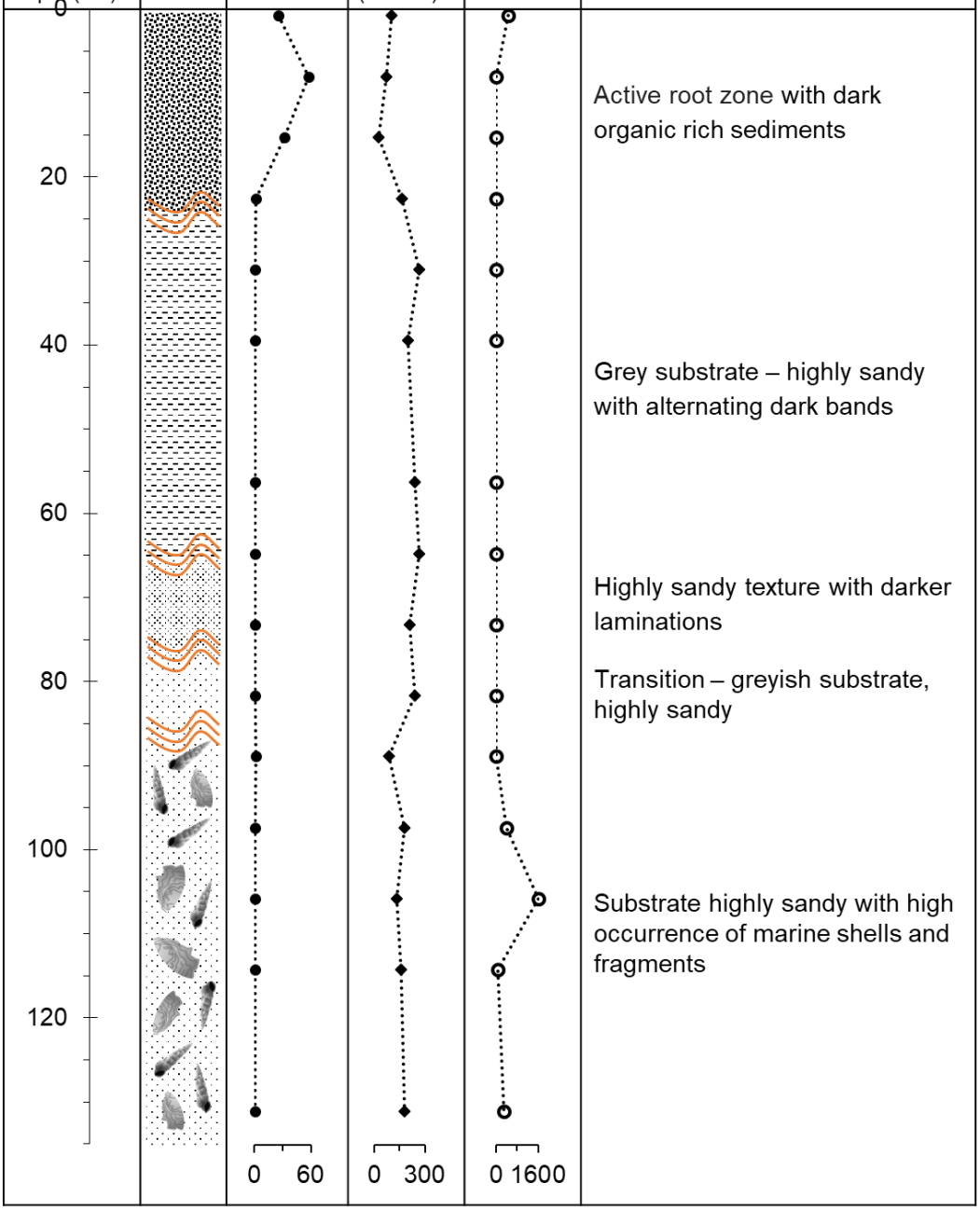

Core number: Cb_Mg1	Location: Currambene Creek	Vegetation: *Avicennia marina*	Date collected: 13/04/2015
Latitude: -35° 1' 9.43912"	Longitude: 150° 40' 1.61461"	Elevation: 0.319 m AHD	Core length: 149 cm

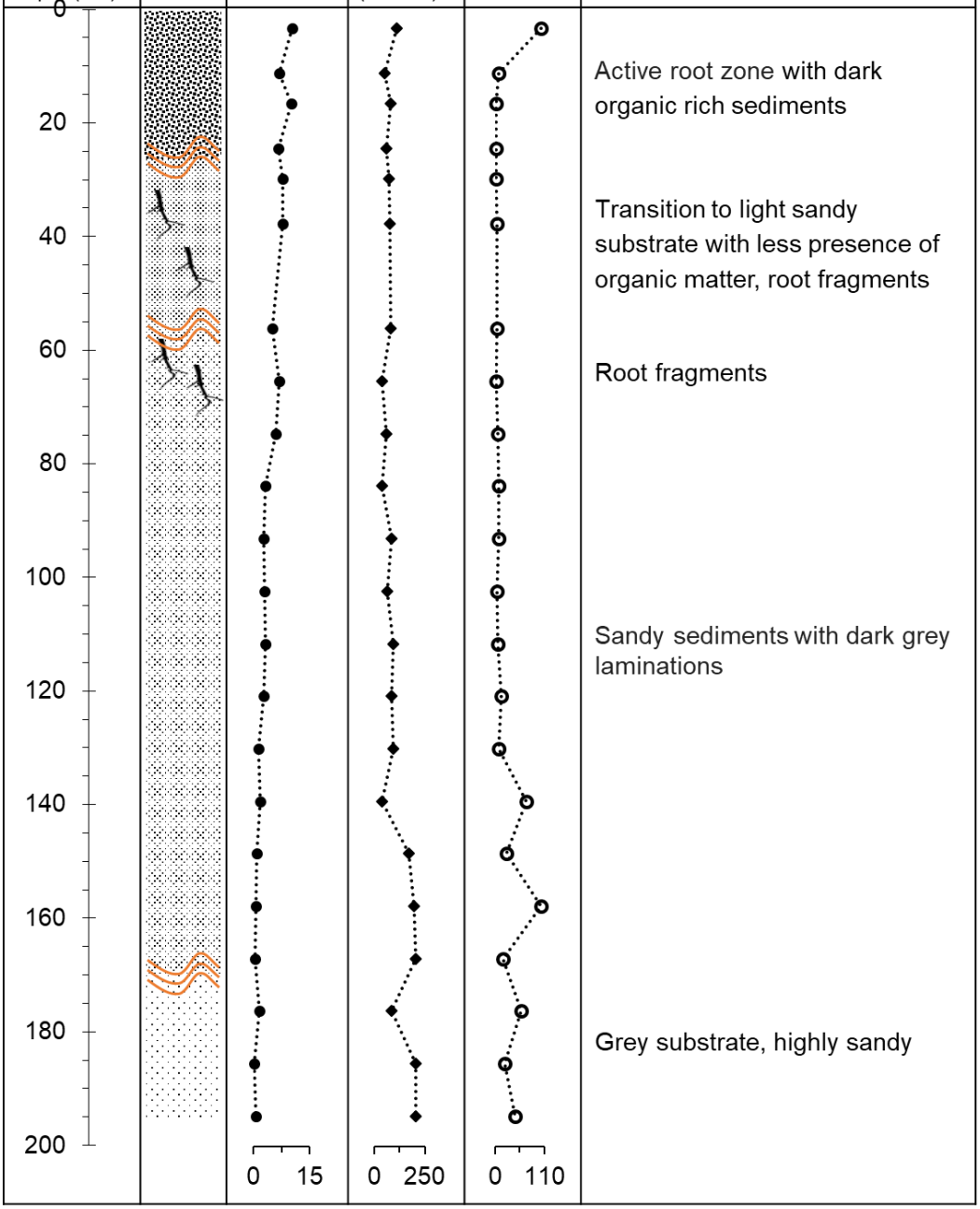

Core number: Cb_Spo	Location: Currambene Creek	Vegetation: *Sporobolus virginicus*	Date collected: 13/04/2015
Latitude: -35° 0' 56.16607"	Longitude: 150° 40' 13.64072"	Elevation: 0.470 m AHD	Core length: 145 cm

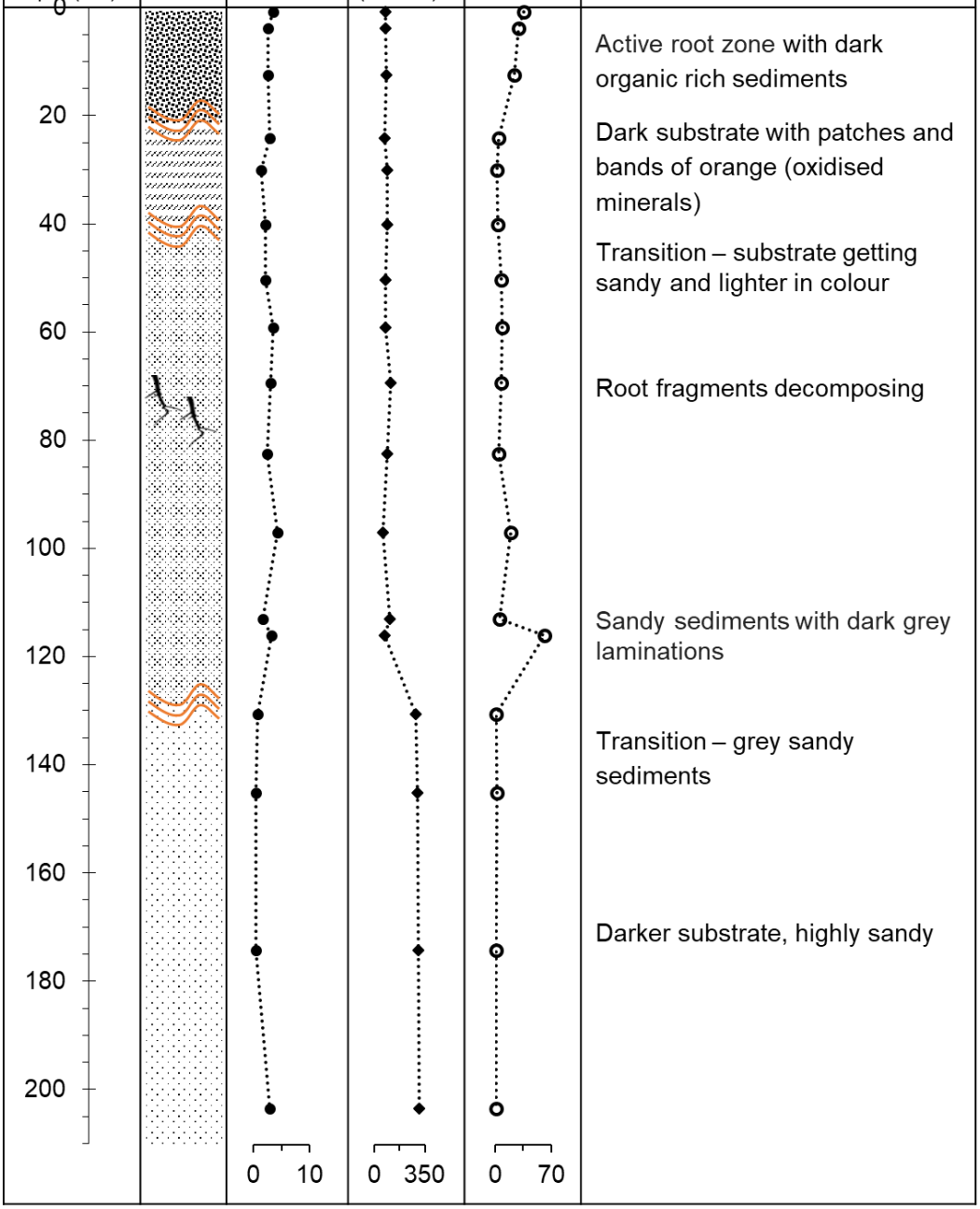

Core number: Cb_Sar2	Location: Currambene Creek	Vegetation: *Sarcocornia quinqueflora*	Date collected: 15/05/2015
Latitude: -35° 0' 53.37548"	Longitude: 150° 40' 1.61942"	Elevation: 0.707 m AHD	Core length: 152 cm